

MSFC MPR-SAT-FE-73-3

cg3



# SATURN

MPR-SAT-FE-73-3

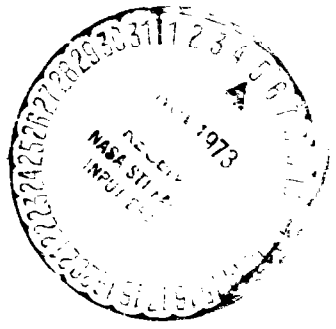
JULY 23, 1973

N73-33820

(NASA-TM-X-69538) SATURN 1B LAUNCH  
VEHICLE FLIGHT EVALUATION REPORT, SA-206,  
SKYLAB-2 (NASA) 230 p HC \$13.50 CSCI 22C

Unclas.  
G3/30 19842

## SATURN 1B LAUNCH VEHICLE FLIGHT EVALUATION REPORT-SA-206 SKYLAB-2



PREPARED BY  
SATURN FLIGHT EVALUATION WORKING GROUP



NATIONAL AERONAUTICS AND SPACE ADMINISTRATION



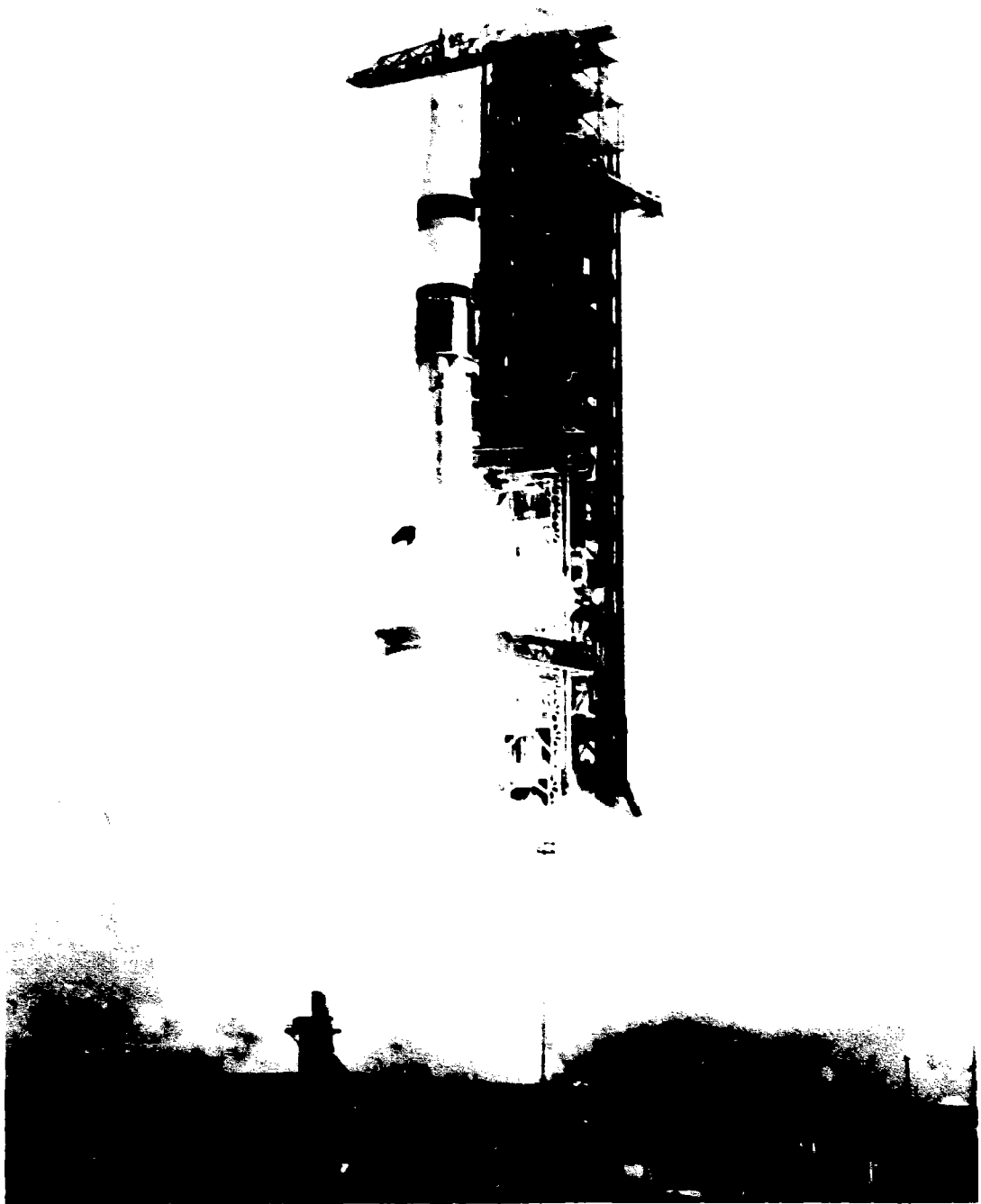
**GEORGE C. MARSHALL SPACE FLIGHT CENTER**

**MPR-SAT-FE-73-3**

**JULY 23, 1973**

**SATURN IB LAUNCH VEHICLE  
FLIGHT EVALUATION  
REPORT-SA-206  
SKYLAB-2**

**PREPARED BY  
SATURN FLIGHT EVALUATION  
WORKING GROUP**



MPR-SAT-FE-73-3

SATURN IB LAUNCH VEHICLE FLIGHT EVALUATION REPORT - SA-206

SKYLAB-2

BY

Saturn Flight Evaluation Working Group

George C. Marshall Space Flight Center

ABSTRACT

The Saturn IB, SA-206 launch vehicle was launched on May 25, 1973, from Kennedy Space Center and placed the Command Service Module containing three crew members into an 81 x 190 n mi. earth orbit. No anomalies occurred that seriously affected the mission.

Any questions or comments pertaining to the information contained in this report should be directed to:

Director, George C. Marshall Space Flight Center  
Huntsville, Alabama 35812  
Attention: Chairman, Saturn Flight Evaluation Working  
Group, SAT-E (Phone 205-453-1030)

PRECEDING PAGE BLANK NOT FILMED

TABLE OF CONTENTS

	Page		Page
TABLE OF CONTENTS		5.4 Impact Footprint	5-2
LIST OF ILLUSTRATIONS		SECTION 6 - S-IB PROPULSION	6-1
LIST OF TABLES		6.1 Summary	6-1
ACKNOWLEDGEMENT		6.2 S-IB Ignition Transient Performance	6-1
ABBREVIATIONS		6.3 S-IB Mainstage Performance	6-1
MISSION PLAN		6.4 S-IB Shutdown Transient Performance	6-7
FLIGHT SUMMARY		6.5 S-IB Stage Propellant Management	6-7
MISSION OBJECTIVES ACCOMPLISHMENT		6.6 S-IB Pressurization	6-11
FAILURES AND ANOMALIES		6.6.1 Fuel Pressurization System	6-11
SECTION 1 - INTRODUCTION	1-1	6.6.2 LOX Tank Pressurization System	6-11
1.1 Purpose	1-1	6.7 S-IB Pneumatic Control Pressure System	6-13
1.2 Scope	1-1	6.8 S-IB Hydraulic System	6-13
SECTION 2 - EVENT TIMES	2-1	SECTION 7 - S-IVB PROPULSION	7-1
2.1 Summary of Events	2-1	7.1 Summary	7-1
2.2 Variable Time and Commanded Switch Selector Events	2-1	7.2 S-IVB Shutdown and Buildup Transient Performance	7-2
SECTION 3 - LAUNCH OPERATIONS	3-1	7.3 S-IVB Mainstage Performance	7-2
3.1 Summary	3-1	7.4 S-IVB Shutdown Transient Performance	7-5
3.2 Prelaunch Milestones	3-1	7.5 S-IVB Stage Propellant Management	7-5
3.3 Terminal Countdown	3-1	7.6 S-IVB Pressurization System	7-6
3.4 Propellant Loading	3-1	7.6.1 S-IVB Fuel Pressurization System	7-6
3.4.1 RP-1 Loading	3-1	7.6.2 S-IVB LOX Pressurization System	7-7
3.4.2 LOX Loading	3-3	7.7 S-IVB Pneumatic Control Pressure System	7-9
3.4.3 LM <sub>2</sub> Loading	3-3	7.8 S-IVB Auxiliary Propulsion System	7-12
3.5 Ground Support Equipment	3-3	7.9 S-IVB/IU Stage Deorbit Propellant Dump	7-12
3.5.1 Ground/Vehicle Interface	3-3	7.10 S-IVB Orbital Safing Operation	7-17
3.5.2 MSFC Furnished Ground Support Equipment	3-4	7.10.1 Fuel Tank Safing	7-17
SECTION 4 - TRAJECTORY	4-1	7.10.2 LOX Tank Safing	7-19
4.1 Summary	4-1	7.10.3 Cold Helium Dump	7-20
4.2 Trajectory Evaluation	4-1		
4.2.1 Ascent Phase	4-1		
4.2.2 Parking Orbit Phase	4-7		
SECTION 5 - S-IVB/IU DEORBIT ANALYSIS	5-1		
5.1 Summary	5-1		
5.2 Deorbit Maneuvers	5-1		
5.3 Deorbit Trajectory Evaluation	5-2		

## TABLE OF CONTENTS (CONTINUED)

	Page		Page		
7.10.4	Stage Pneumatic Control and Engine Control Sphere Safing	7-20	SECTION 13 - VEHICLE THERMAL ENVIRONMENT	13-1	
7.10.5	Engine Control Sphere Safing	7-20	13.1	S-IB Base Heating	13-1
7.11	S-IVB Hydraulic System	7-21	SECTION 14 - ENVIRONMENTAL CONTROL SUMMARY	14-1	
SECTION P - STRUCTURES		8-1	14.1	Summary	14-1
8.1	Summary	8-1	14.2	S-IB Environmental Control	14-1
8.2	Total Vehicle Structures Evaluation	8-1	14.3	IU Environmental Control	14-3
8.2.1	Longitudinal Loads	8-1	14.3.1	Thermal Conditioning System (TCS)	14-3
8.2.2	Bending Moments	8-1	14.3.2	Gas Bearing Subsystem Performance	14-3
8.2.3	Combined Loads	8-3	SECTION 15 - DATA SYSTEMS	15-1	
8.2.4	Vehicle Dynamic Characteristics	8-8	15.1	Summary	15-1
SECTION 9 - GUIDANCE AND NAVIGATION		9-1	15.2	Vehicle Measurement Evaluation	15-1
9.1	Summary	9-1	15.2.1	Gyro Summation Current and Accelerometer Summation Current Measurement Level Shift	15-1
9.2	Guidance Comparisons	9-1	15.3	Airborne VHF Telemetry System Evaluation	15-3
9.3	Navigation and Guidance Scheme Evaluation	9-3	15.3.1	S-IB Telemetry System Loss of Synchronization	15-5
9.3.1	First Stage Boost	9-5	15.3.2	IU Telemetry System Reduction in RF Radiated Power	15-5
9.3.2	Second Stage Boost	9-5	15.4	C-Band Radar System Evaluation	15-10
9.3.3	Orbital Phase	9-5	15.5	Secure Range Safety Command Systems Evaluation	15-10
9.3.4	Deorbit Phase	9-9	15.6	Digital Command System Evaluation	15-12
9.4	Navigation and Guidance System Components	9-9	15.7	Ground Engineering Cameras	15-14
9.4.1	ST-124M Stabilized Platform System	9-9	SECTION 16 - MASS CHARACTERISTICS	16-1	
9.4.2	Guidance and Navigation Computer	9-10	16.1	Summary	16-1
SECTION 10 - CONTROL AND SEPARATION		10-1	16.2	Mass Evaluation	16-1
10.1	Summary	10-1	SECTION 17 - SPACECRAFT SUMMARY	17-1	
10.2	S-IB Control System Evaluation	10-1	SECTION 18 - MSFC INFLIGHT EXPERIMENT	18-1	
10.3	S-IVB Control System Evaluation	10-2	APPENDIX A - ATMOSPHERE	A-1	
10.3.1	S-IVB Control System Evaluation During Burn	10-2	APPENDIX B - SA-206 VEHICLE DESCRIPTION	B-1	
10.3.2	S-IVB Control System Evaluation During Orbit	10-7			
10.3.3	S-IVB Control System Evaluation During Deorbit	10-14			
10.4	Instrument Unit Control Components Evaluation	10-18			
10.5	Separation	10-18			
10.5.1	S-IB/S-IVB Separation	10-18			
10.5.2	S-IVB/CSM Separation	10-18			
SECTION 11 - ELECTRICAL NETWORKS AND EMERGENCY DETECTION SYSTEM		11-1			
11.1	Summary	11-1			
11.2	S-IB Stage Electrical System	11-1			
11.3	S-IVB Stage Electrical System	11-2			
11.4	Instrument Unit Electrical System	11-2			
11.5	Saturn IB Emergency Detection System	11-11			
SECTION 12 - VEHICLE PRESSURE ENVIRONMENT		12-1			
12.1	S-IB Base Pressure	12-1			

## LIST OF ILLUSTRATIONS

Figure	Page	Figure	Page
2-1	LVDC Clock/Ground Time Difference	2-2	
3-1	Cutoff Anomaly - Simplified ESE Circuitry	3-5	
3-2	ESE Cutoff Anomaly - Test Results	3-6	
4-1	Ascent Trajectory Position Comparison	4-3	
4-2	Ascent Trajectory Space-Fixed Velocity and Flight Path Angle Comparison	4-4	
4-3	Ascent Trajectory Acceleration Comparison	4-5	
4-4	Comparison of Separation Events	4-8	
4-5	Launch Vehicle Ground Track	4-11	
5-1	S-IVB/IU Deorbit Trajectory Altitude (No Breakup Assumed)	5-2	
5-2	S-IVB/IU Impact Footprint	5-3	
6-1	S-IB Engines Thrust Buildup	6-7	
6-2	S-IB Stage Propulsion Performance	6-3	
6-3	H-1 Engine Position #1 Gearcase Lubricant Pressure	6-6	
6-4	S-IB Inboard Engine Total Thrust Decay	6-8	
6-5	S-IB Total Outboard Engine Total Thrust Decay	6-8	
6-6	S-IB Stage LOX Mass Above Main LOX Valve	6-10	
6-7	S-IB Stage Fuel Mass Above Main Fuel Valve	6-10	
6-8	S-IB Fuel Tank Ullage Pressure	6-12	
6-9	S-IB Fuel Tank Helium Pressurization Sphere Pressure	6-12	
6-10	S-IB Center LOX Tank Ullage Pressure	6-14	
6-11	GOX Flow Control Valve Position	6-14	
6-12	S-IB Pneumatic Control Pressure	6-15	
7-1	S-IVB Start Box and Run Requirements - Burn	7-3	
7-2	S-IVB Steady-State Performance	7-4	
7-3	S-IVB LH <sub>2</sub> Ullage Pressure - Preliftoff, Boost and Burn	7-7	
7-4	S-IVB Fuel Pump Inlet Conditions	7-8	
7-5	S-IVB LOX Tank Ullage Pressure - Burn	7-9	
7-6	S-IVB LOX Pump Inlet Conditions - Burn	7-10	
7-7	S-IVB Cold Helium Supply History	7-11	
7-8	S-IVB Deorbit Propellant Dump and Safing Sequence	7-14	
7-9	S-IVB LOX Dump Parameter Histories	7-15	
7-10	S-IVB LH <sub>2</sub> Dump	7-16	
7-11	S-IVB LH <sub>2</sub> Ullage Pressure - Orbital Coast	7-18	
7-12	S-IVB LOX Tank Ullage Pressure - Orbit, Dump, and Safing	7-19	
8-1	SA-206 Longitudinal Accelerations at IU and CM During Thrust Build-Up and Launch	8-2	
8-2	SA-206 Longitudinal Acceleration at the IU and CM During S-IB Cutoff	8-3	
8-3	S-IB-6 Longitudinal Load from Strain Data at Station 942 vs. Time	8-3	
8-4	SA-206 Longitudinal Load Distribution at Time of Maximum Bending Moment and IEKO	8-4	
8-5	SA-206 Bending Moment Distributions at Time of Maximum Resultant Moment, T = 65.8	8-5	
8-6	SA-206 Bending Moment Distributions at Time of Maximum Resultant Moment, T = 65.8 Yaw	8-6	
8-7	SA-206 Bending Moment Distributions at Time of Maximum Resultant Moment, T = 65.8 Pitch	8-7	
8-8	Combined Loads Producing Minimum Safety Margins During SA-206 Flight	8-9	
8-9	Vehicle Bending Frequencies	8-10	
8-10	Vehicle Bending Amplitudes	8-11	
8-11	Vibration Measured During S-IVB Stage Burn	8-12	
8-12	LOX Pump Inlet Pressure Oscillations During S-IVB Stage Burn	8-13	

## LIST OF ILLUSTRATIONS (CONTINUED)

Figure	Page	Figure	Page
8-13	Thrust Chamber Pressure Oscillations During S-IVB Stage Burn	8-14	
8-14	S-IVB Low Frequency Analysis of Vibration and Engine Pressures	8-15	
9-1	Trajectory and ST-124M Platform Velocity Comparisons (Trajectory Minus LVDC)	9-2	
9-2	Theta Y (Pitch) Attitude Angle	9-6	
9-3	Theta Z (Yaw) Attitude Angle	9-7	
9-4	Theta X (Roll) Attitude Angle	9-8	
9-5	SA-206 ST-124M Platform System Block Diagram	9-10	
10-1	Pitch Plane Dynamics During S-IB Burn	10-3	
10-2	Yaw Plane Dynamics During S-IB Burn	10-4	
10-3	Roll Plane Dynamics During S-IB Burn	10-5	
10-4	Pitch and Yaw Plane Free Stream Angle of Attack During S-IB Burn	10-6	
10-5	Pitch Plane Dynamics - S-IVB Burn	10-8	
10-6	Yaw Plane Dynamics - S-IVB Burn	10-9	
10-7	Pitch Plane Dynamics During Orbit (Sheet 1 of 3)	10-11	
10-8	Vehicle Dynamics During Deorbit (Sheet 1 of 2)	10-15	
10-9	S-IB/S-IVB Longitudinal Acceleration	10-19	
10-10	Angular Velocities During S-IB/S-IVB Separation	10-20	
11-1	S-IVB Stage Forward No. 1 Battery Voltage, Current, and Temperature	11-3	
11-2	S-IVB Stage Forward No. 2 Battery Voltage, Current, and Temperature	11-4	
11-3	S-IVB Stage Aft No. 1 Battery Voltage, Current, and Temperature	11-5	
11-4	S-IVB Stage Aft No. 2 Battery Voltage, Current, and Temperature	11-6	
11-5	IU 6D10 Battery Parameters	11-8	
11-6	IU 6D30 Battery Parameters	11-9	
11-7	IU 6D40 Battery Parameters	11-10	
12-1	S-IB Stage Heat Shield Pressure	12-2	
12-2	S-IB Stage Flame Shield Pressure	12-3	
12-3	S-IB Stage Heat Shield Loading	12-4	
12-4	S-IB Stage Base Drag Coefficient	12-5	
13-1	S-IB Stage Heat Shield Inner Region Total Heating Rates	13-2	
13-2	S-IB Stage Heat Shield Inner Region Radiation Heating Rate	13-3	
13-3	S-IB Stage Heat Shield Inner Region Gas Temperature	13-4	
13-4	S-IB Stage Heat Shield Outer Region Gas Temperature	13-6	
13-5	S-IB Stage Flame Shield Total Heating Rates	13-7	
13-6	S-IB Stage Flame Shield Radiation Heating Rate	13-8	
13-7	S-IB Stage Flame Shield Gas Temperature	13-9	
14-1	S-IB Engine Compartment Pre-launch	14-2	
14-2	IU Sublimator Start Up Parameters for Initial Cycle	14-4	
14-3	IU TCS Coolant Control Parameters	14-5	
14-4	IU TCS Hydraulic Performance	14-6	
14-5	IU TCS GN <sub>2</sub> Sphere Pressure (D25-601)	14-7	
14-6	Inertial Platform GN <sub>2</sub> Pressures	14-8	
14-7	IU GRS GN <sub>2</sub> Sphere Pressure (D10-603)	14-9	
14-8	IU Selected Component Temperatures	14-10	
14-9	IU Selected Component Temperatures	14-11	
15-1	S-IVB VHF Telemetry Ground Station Coverage	15-4	
15-2	S-IVB VHF Telemetry Ground Station Coverage	15-4	
15-3	IU Telemetry Signal Strength and Power Output Plots Before and After Anomaly	15-6	
15-4	PCM Telemetry RF Power Output (Measurement J29-602)	15-6	
15-5	SA-206 IU Telemetry RF Subsystem	15-7	



## LIST OF ILLUSTRATIONS (CONTINUED)

Figure		Page
15-6	Mated RF Connectors	15-8
15-7	RF Connector Pins	15-9
15-8	C-Band Acquisition and Loss Times	15-11
A-1	Surface Weather Map Approximately 1 Hour Before Launch of SA-206/SL-2	A-2
A-2	500 Millibar Map Approximately 1 Hour Before Launch of SA-206/SL-2	A-4
A-3	Scalar Wind Speed at Launch Time of SA-206/SL-2	A-7
A-4	Wind Direction at Launch Time of SA-206/SL-2	A-8
A-5	Pitch Wind Velocity Component ( $W_x$ ) at Launch Time of SA-206/SL-2	A-9
A-6	Yaw Wind Velocity Component ( $W_y$ ) at Launch Time of SA-206/SL-2	A-10
A-7	Pitch ( $S_x$ ) and Yaw ( $S_y$ ) Component Wind Shears at Launch Time of SA-206/SL-2	A-11
A-8	Relative Deviation of Temperature and Pressure from the PRA-63 Reference Atmosphere, SA-206/SL-2	A-13
A-9	Relative Deviation of Density and Absolute Deviation of the Index of Refraction from the PRA-63 Reference Atmosphere, SA-206/SL-2	A-14
B-1	SL-2 Space Vehicle	B-2
B-2	S-1B Stage Configuration	B-3
B-3	S-1B Stage Structure	B-4
B-4	S-1VB Stage Configuration	B-8
B-5	Instrument Unit Configuration	B-11
B-6	Apollo Spacecraft	B-14

## LIST OF TABLES

Table	Page	Table	Page		
1	Mission Objective Accomplishment	9-4	Orbital Phase Flight Program Steering Commands	9-9	
2	Summary of Failures and Anomalies	10-1	Misalignment and Liftoff Conditions Summary	10-1	
2-1	Time Base Summary	2-2			
2-2	Significant Event Times Summary	2-3	10-2	Maximum Control Parameters During S-IB Burn	10-7
2-3	Variable Time and Commanded Switch Selector Events	2-10	10-3	Maximum Control Parameters During S-IVB Burn	10-10
3-1	SA-206/SL-2 Prelaunch Milestones	3-2	11-1	S-IB Stage Battery Power Consumption	11-1
4-1	Summary of Available Tracking Data	4-2	11-2	S-IVB Stage Battery Power Consumption	11-7
4-2	Comparison of Cutoff Events	4-6	11-3	IU Battery Power Consumption	11-11
4-3	Comparison of Significant Trajectory Events	4-6	15-1	SA-206 Measurement Summary	15-2
4-4	Comparison of Separation Events	4-7	15-2	SA-206 Flight Measurements Waived Prior to Flight	15-2
4-5	Comparison of S-IB Spent Stage Impact	4-9	15-3	SA-206 Measurement Malfunctions	15-2
4-6	S-IB Spent Stage Impact Envelope	4-9	15-4	SA-206 Launch Vehicle Telemetry Links Performance Summary	15-3
4-7	Comparison of Orbit Insertion Conditions	4-10	15-5	SA-206 IU Commands	15-13
5-1	S-IVB/IU Deorbit Velocity Comparisons	5-1	16-1	Vehicle Masses (Kilograms)	16-3
6-1	S-IB Engine Start Characteristics	6-2	16-2	Vehicle Masses (Pounds)	16-3
6-2	S-IB Individual Engine Propulsion Performance	6-5	16-3	Vehicle Masses (Kilograms)	16-4
6-3	Propellant Usage	6-9	16-4	Vehicle Masses (Pounds)	16-4
6-4	S-IB Propellant Mass History	6-11	16-5	Flight Sequence Mass Summary	16-5
7-1	S-IVB Steady State Performance (STDV Open +60 Second Time Slice at Standard Altitude Conditions)	7-5	16-6	Mass Characteristics Comparison	16-7
7-2	S-IVB Stage Propellant Mass History	7-6	A-1	Surface Observations at SA-206 Launch Time	A-3
7-3	S-IVB APS Propellant Consumption	7-13	A-2	Systems Used to Measure Upper Air Wind Data for SA-206	A-5
9-1	Inertial Platform Velocity Comparisons	9-3	A-3	Maximum Wind Speed in High Dynamic Pressure Region for Apollo/Saturn 201 through Saturn 206 Vehicles	A-12
9-2	Navigation Position and Velocity Comparisons (PACSS-13)	9-4	A-4	Extreme Wind Shear Values in the High Dynamic Pressure Region for Apollo/Saturn 201 through 206 Vehicles	A-12
9-3	SA-206 Guidance Terminal Conditions	9-5	A-5	Selected Atmospheric Observations for Apollo/Saturn 201 through Saturn 206 Vehicle Launches at Kennedy Space Center, Florida	A-16

## LIST OF TABLES (CONTINUED)

Table		Page
B-1	Summary of S-IB Stage Data	B-5
B-2	Significant S-IB Stage Configuration Changes	B-7
B-3	S-IVB Significant Configuration Changes	B-10
B-4	IU Significant Configuration Changes	B-12

## ACKNOWLEDGEMENT

This report is published by the Saturn Flight Evaluation Working Group, composed of representatives of Marshall Space Flight Center, Kennedy Space Center, and MSFC's prime contractors, and in cooperation with the Johnson Space Center. Significant contributions to the evaluation have been made by:

George C. Marshall Space Flight Center

Science and Engineering

Aero-Astroynamics Laboratory  
Astrionics Laboratory  
Computation Laboratory  
Astronautics Laboratory

Saturn Program Office

John F. Kennedy Space Center

Lyndon B. Johnson Space Center

Chrysler Corporation Space Division

McDonnell Douglas Astronautics Company

International Business Machines Corporation

Rockwell International/Rocketdyne Division

General Electric Company

The Boeing Company

## ABBREVIATIONS

AOS	Acquisition of Signal	FCC	Flight Control Computer
APS	Auxiliary Propulsion System	FM	Frequency Modulation
ARIA	Apollo Range Instrumented Aircraft	FRT	Flight Readiness Test
BDA	Bermuda	GBI	Grand Bahama Island
CDDT	Countdown Demonstration Test	GBS	Gas Bearing System
CG	Center of Gravity	GCS	Guidance Cutoff Signal
CIF	Central Instrumentation Facility	GDS	Goldstone
CM	Command Module	GFCV	GOX Flow Control Valve
CNV	Cape Kennedy	GN <sub>2</sub>	Gaseous Nitrogen
CRO	Carnarvon	GRR	Guidance Reference Release
CRP	Computer Reset Pulse	GSCU	Ground Support Cooling Unit
CSM	Command and Service Module	GSE	Ground Support Equipment
CYI	Canary Island	HAW	Hawaii
DEE	Digital Events Evaluator	HE	Helium
EBW	Explosive Bridge Wire	HSK	Honeysuckle
ECO	Engine Cutoff	IBM	International Business Machines
ECS	Environmental Control System	ICD	Interface Control Document
EDS	Emergency Detection System	IECO	Inboard Engine Cutoff
EDT	Eastern Daylight Time	IGM	Iterative Guidance Mode
EMR	Engine Mixture Ratio	IU	Instrument Unit
ESC	Engine Start Command	JSC	Johnson Space Center
ESE	Electrical Support Equipment	KSC	Kennedy Space Center
		KWJ	Kwajalein

## ABBREVIATIONS (CONTINUED)

LH <sub>2</sub>	Liquid Hydrogen	NFL	Newfoundland
LOS	Loss of Signal	NPSP	Net Positive Suction Pressure
LOX	Liquid Oxygen	NPV	Non-Propulsive Vent
LUT	Launch Umbilical Tower	OAT	Overall Test
LV	Launch Vehicle	OECO	Outboard Engine Cutoff
LVDA	Launch Vehicle Data Adapter	OMPT	Observed Mass Point Trajectory
LVDC	Launch Vehicle Digital Computer	OT	Operational Trajectory
LVGSE	Launch Vehicle Ground Support Equipment	OWS	Orbital Workshop (Modified S-IVB Stage)
MAD	Madrid	PACSS	Project Apollo Coordinate System Standard
MAP	Message Acceptance Pulse	PAFB	Patrick Air Force Base
MCC-H	Mission Control Center - Houston	PCM	Pulse Code Modulation
MDAC	McDonnell Douglas Astronautics Company	PEA	Platform Electronics Assembly
MFV	Main Fuel Valve	PLAST	Propellant Load and All System Test
MILA	Merritt Island Launch Area	PSD	Power Spectral Density
ML	Mobile Launcher	PTCS	Propellant Tanking Computer System
MOV	Main Oxidizer Valve	PU	Propellant Utilization
MR	Mixture Ratio	RCA	Radio Corporation of America
MRCV	Mixture Ratio Control Valve	RF	Radio Frequency
MSFC	Marshall Space Flight Center	RLH	Retrograde Local Horizontal
MSS	Mobile Service Structure	S/A	Service Arm
MUX	Multiplexer	SACS	Service Arm Control Switches

ABBREVIATIONS (CONTINUED)

SAS	Solar Array System
SC	Spacecraft
SDF	System Development Facility
SL	Skylab
SLA	Spacecraft Lunar Module Adapter
SM	Service Module
SOX	Solid Oxygen
SRSCS	Secure Range Safety Command System
STDV	Start Tank Discharge Valve
SV	Space Vehicle
SWS	Saturn Workshop
TAN	Tananarive
TB	Time Base
TCC	Thermal Control Coating
TCS	Terminal Countdown Sequencer
TEX	Corpus Christi
TM	Telemetry
TVC	Thrust Vector Control
US	United States
UT	Universal Time
VAB	Vertical Assembly Building
VHF	Very High Frequency (30-300 MHz)
WLP	Wallops Island

## MISSION PLAN

The Saturn IB SA-206 (SL-2 Launch) is to place the Command Service Module (CSM-116) in a 150 x 346 km (81 x 187 n. mi.) orbit. SA-206 is comprised of the S-IB-6, S-IVB-206, and the Instrument Unit (IU)-206. This is the first manned flight in the Skylab Program.

Launch is scheduled to occur on the 25th of May 1973 from Launch Complex 39, Pad B of the Kennedy Space Center (KSC) at 9:00 a.m., EDT. Flight will be along a launch-time-dependent azimuth within a flight azimuth range of 51.7 degrees to 37.8 degrees measured east of north. The launch window duration is 15.5 minutes. Vehicle weight at ignition is nominally 592,888 kg (1,307,095 lbm).

S-IB stage powered flight lasts approximately 141 seconds. The S-IVB stage provides powered flight for approximately 436.3 seconds inserting the CSM into its planned orbit. The CSM Service Propulsion System and Reaction Control System will be used to complete the CSM rendezvous maneuvers and dock axially with the orbiting Saturn Work Shop. In the same time frame the S-IVB/IU will be maneuvered to, and maintained in, an attitude for conducting the M-415 Thermal Control Coating experiment.

Deorbit of the S-IVB/IU will commence on the fourth revolution with the spent vehicle oriented in a retrograde attitude. Residual propellants in the S-IVB stage tanks will be dumped through the J-2 engine to produce the impulse required for deorbit. By controlling the vehicle attitude and the time and duration of propellant dump the spent vehicle is directed towards a designated impact region. Impact is planned to occur in an island-free area of the Pacific Ocean approximately 6 hours after liftoff.



## FLIGHT SUMMARY

The Saturn Space Vehicle, SA-206, was launched on May 25, 1973, from Kennedy Space Center. The SA-206 vehicle supported the Skylab mission by placing a Command Service Module containing three crew members into an earth orbit for rendezvous with the orbiting Saturn Work Shop.

The performance of ground systems supporting countdown and launch was satisfactory except for one anomaly. This anomaly occurred after launch commit and could have transferred vehicle power from internal to external resulting in launch without vehicle electrical power. The erroneous cutoff signal, however, was not sustained long enough to energize the cutoff relay.

The space vehicle was launched at 9:00:00 Eastern Daylight Time (EDT) on May 25, 1973, from Pad 39B of the Kennedy Space Center, Saturn Complex. The countdown was scrubbed from the original May 15, 1973 launch date to accommodate Skylab-1 Orbital Work Shop problem resolutions and work-arounds (refer to MPR-SAT-FE-73-4 for SA-513/Skylab-1 Flight Report). Damage to the pad, Launch Umbilical Tower (LUT) and support equipment was considered minimal.

SA-206 was launched as planned on an azimuth of 90 degrees east of north. A roll maneuver was initiated at approximately 10 seconds that placed the vehicle on a flight azimuth of 47.580 degrees east of north. The down range pitch program was also initiated at this time. The reconstructed trajectory was generated by merging the ascent phase and the parking orbit phase. Available C-Band radar and Unified S-Band tracking data, together with telemetered guidance velocity data were used in the trajectory reconstruction. The reconstructed flight trajectory (actual) was very close to the Post-Launch Predicted Operational Trajectory (nominal). The S-IB stage Outboard Engine Cutoff (OECO) was 1.36 seconds later than nominal. The total space-fixed velocity at this time was 7.07 m/s greater than nominal. After separation, the S-IB stage continued on a ballistic trajectory to earth impact. The S-IVB burn terminated with guidance cutoff signal and parking orbit insertion; both approximately 3.7 seconds later than nominal. A velocity of 1.82 m/s greater than nominal at insertion resulted in an apogee 6.32 km higher than nominal. The parking orbit portion of the trajectory from insertion to CSM/S-IVB separation was close to nominal. However, separation of the CSM from the S-IVB stage occurred 17.6 seconds later than nominal, which is not considered significant because it is an astronaut initiated event.

All aspects of the S-IVB/IU deorbit were accomplished successfully. The deorbit trajectory altitude was slightly higher than the real time predicted value resulting in an impact slightly downrange of nominal. These dispersions were small enough that impact actually did occur within the real time predicted footprint. Impact occurred at approximately 21,607 seconds.

The S-IB stage propulsion system performed satisfactorily throughout flight. Stage longitudinal site thrust and specific impulse averaged 1.04 percent and 0.3 percent lower than predicted, respectively. Stage LOX, fuel and total propellant flowrate averaged 0.78 percent, 0.70 percent, and 0.76 percent lower than predicted, respectively. IECO occurred 0.75 seconds later than predicted. OECO was initiated 3.69 seconds after IECO by the deactuation of the thrust OK pressure switches, as planned, of Engine #1. At OECO, the LOX residual was 2916 lbm compared to the predicted 3297 lbm and fuel residual was 6127 lbm compared to the predicted 5986 lbm. The S-IB stage hydraulic system performed satisfactorily.

The S-IVB propulsion system performed satisfactorily throughout the operational phase of burn and had normal start and cutoff transients. S-IVB burn time was 440.4 seconds, 2.5 seconds longer than predicted for the actual flight azimuth of 47.6 degrees. This difference is composed of -0.15 seconds due to higher than expected S-IB/S-IVB separation velocity and +2.65 seconds due to lower than predicted S-IVB performance. The engine performance during burn, as determined from standard altitude reconstruction analysis, deviated from the predicted Start Tank Discharge Valve (STDV) open +60 second time slice by -0.64 percent for thrust and +0.05 percent for specific impulse. The S-IVB stage Engine Cutoff (ECO) was initiated by the Launch Vehicle Digital Computer (LVDC) at 586.3 seconds. The S-IVB residuals at engine cutoff were near nominal. The best estimate of the engine cutoff residuals is 2873 lbm for LOX and 2223 lbm for LH<sub>2</sub> as compared to the predicted values of 3314 lbm for LOX and 2046 lbm for LH<sub>2</sub>. Subsequent to burn, the stage propellant tanks were vented satisfactorily. The impulse derived from the LOX and fuel dumps was sufficient to satisfactorily deorbit the S-IVB/IU. The total impulse provided was 88,360 lbf-sec with a LOX dump impulse contribution of 75,610 lbf-sec and a fuel dump impulse contribution of 12,750 lbf-sec. A disturbing force on the S-IVB/IU, coincident with LOX tank venting in T<sub>5</sub> (following propellant dumps), caused unplanned firings of Auxiliary Propulsion System (APS) module engines and subsequent propellant depletion in APS Module No. 2. Analysis indicates nearly complete blockage of LOX Nonpropulsive Vent (NPV) Nozzle No. 1. The blockage has been attributed to solid oxygen formation at the nozzle inlet during T<sub>4</sub> cyclic LOX relief venting when liquid remaining in the duct was subjected to a freezing environment. No impact due to this anomaly is expected on the Skylab-3 or Skylab-4. Propellant tank safing after fuel dump was satisfactory. The APS operation was nominal throughout flight. No helium

or propellant leaks were observed and the regulators functioned nominally. Hydraulic system performance was nominal throughout powered flight, orbital coast, and deorbit.

The structural loads experienced during the flight were well below design values. The maximum bending moment was  $14.8 \times 10^6$  in-lbf (approximately 27 percent of design) at vehicle station 942. Thrust cutoff transients experienced by SA-206 were similar to those of previous flights. The maximum longitudinal dynamic responses measured in the IU were  $+0.20$  g and  $+0.30$  g at S-IB IECO and OECO, respectively. POGO did not occur. The maximum ground wind experienced by the Saturn IB SA-206 during the prelaunch period was 22 knots (55 knots, allowable with damper). The ground winds at launch were 12 knots from the Southwest (34 knots allowable).

The Stabilized Platform and the Guidance Computer successfully supported the accomplishment of the mission objectives. Targeted conditions at orbit insertion were attained with insignificant error. The one anomaly which occurred in the guidance and navigation system was a large change in the gyro summation current and a small change in the accelerometer summation current in the ST-124M Platform Electronics Assembly. Operation of the ST-124M subsystem was not affected by these current changes. There was a pitch axis gimbal resolver switchover accomplished at 20,558 seconds, following completion of propellant dumps. However, this switchover was caused by a loss of attitude control when the S-IVB APS propellants depleted.

The control and separation systems functioned correctly throughout the powered and coast flight. Control was terminated earlier than predicted during deorbit by the depletion of S-IVB APS Module 2 propellants. Engine gimbal deflections were nominal and APS firings predictable. Bending and slosh dynamics were adequately stabilized. No undue dynamics accompanied any separation.

The electrical systems and Emergency Detection System (EDS) performed satisfactorily during the flight. Battery performance (including voltages, currents, and temperatures) was satisfactory and remained within acceptable limits. Operation of all power supplies, inverters, Exploding Bridge Wire (EBW) firing units, and switch selectors were nominal.

Base pressure data obtained from SA-206 have been compared with preflight predictions and/or previous flight data and show good agreement. Base drag coefficients were also calculated using the measured pressures and actual flight trajectory parameters.

Comparisons of SA-206 base region thermal data with corresponding data from SA-203, SA-204 and SA-205 show generally good agreement with slight differences being attributed to the H-1 engine uprating on the SA-206 vehicle. Measured heating rates in the base region were all below the S-IB stage design level.

The S-IB stage engine compartment and instrument compartment require environmental control during prelaunch operations, but are not actively controlled during S-IB boost. The desired temperatures were maintained at both areas during the prelaunch operations. The IU stage Environmental Control System (ECS) exhibited satisfactory performance for the duration of the IU mission. Coolant temperatures, pressures, and flow-rates were continuously maintained within the required ranges and design limits.

Total vehicle mass, determined from post-flight analysis, was within 1.15 percent of predicted from ground ignition through S-IVB stage cutoff signal with the exception of a longer than predicted S-IVB stage burn, resulting in a less than expected residual. Hardware weights, propellant loads and propellant utilization were close to predicted values during flight.

All data systems performed satisfactorily with the exception of the IU telemetry system during orbital operation. Flight measurements from onboard telemetry were 100 percent reliable.

Telemetry performance was normal except for a momentary loss of synchronization of the S-IB telemetry signal at liftoff due to burst of electrical noise. A reduction in Radio Frequency (RF) radiated power from the IU telemetry links was experienced during the first orbital revolution. The usual interference due to flame effects and staging were experienced. Usable telemetry data were received until 20,800 seconds (05:43:48). Good tracking data were received from the C-Band radar, with Kwajalein (KWJ) indicating final Loss of Signal (LOX) at 21,475 seconds (5:57:55).

Skylab Experiment M-415, a MSFC Thermal Control Coating experiment was performed during the flight of SA-206. The object of the experiment was to determine the effects of preflight and flight environments on various thermal control coatings. The experiment contained 48 coatings that were uncovered and exposed to the environment at different times. Preliminary data indicates that:

- a. All 24 coatings were uncovered as planned.
- b. Temperature measurements were received as planned.
- c. Coatings which were exposed continuously from prelaunch exhibited no significant difference in absorptivity/emissivity (a/e) or temperature.
- d. Two of the three coatings sealed until first stage separation as planned, but exposed to retro motor plumes, indicated approximately the same a/e and temperatures but the third sample operated about 9°C cooler.

- e. At orbital insertion, all coatings which were exposed continuously from prelaunch were running 8 to 10°C hotter than the coatings which were sealed but exposed just prior to the retro motor firing.

## MISSION OBJECTIVES ACCOMPLISHMENT

Table 1 presents the MSFC launch vehicle objectives for Skylab-2 as defined in the "Saturn Mission Implementation Plan SL-2/SA-206," MSFC Document PM-SAT-8010.22, Revision C, dated March 30, 1973, and updated by MSFC letter SAT-MGR (SAT-E-171-73) dated June 1, 1973. An assessment of the degree of accomplishment can be found in other sections of this report as shown in Table 1.

Table 1. Mission Objective Accomplishment

NO.	LAUNCH VEHICLE OBJECTIVE	DEGREE OF ACCOMPLISHMENT	DISCREPANCIES	SECTION IN WHICH DISCUSSED
1	Launch and insert a manned CSM into the earth orbit targeted for during the final launch countdown. SL-2 was targeted for an 81 x 187 n mi. (150 x 346 KM) orbit during final launch countdown.	Complete	None	4.2

## FAILURES AND ANOMALIES

Evaluation of the launch vehicle and launch vehicle ground support equipment data revealed the following four anomalies, one of which is considered significant.

**Table 2. Summary of Failures and Anomalies**

ITEM	VEHICLE SYSTEM	ANOMALY (CAUSE)	SIGNIFICANCE	CORRECTIVE ACTION	SECTION REFERENCE
1	LVGSE/ESE	AT APPROXIMATELY 102 MILLISECONDS AFTER LAUNCH COMMIT, THE THRUST FAILURE CUTOFF CIRCUIT WAS MOMENTARILY ENERGIZED. (MEMAKE OF LAUNCH BUS POWER CONTACTOR BECAUSE OF "SNEAK" DIODE SUPPRESSION CIRCUIT.)	NONE ON THIS MISSION. VEHICLE LOSS IF TRANSIENT PULSE HAD BEEN LONG ENOUGH TO ACTUATE THE CUTOFF RELAY. (APD 19C SIGNIFICANT ANOMALY, APD 44 NON-COMFORMANCE CRITICALITY CATEGORY [NCC] 1)	MODIFIED SA-207 ESE TO: 1. INHIBIT THRUST FAILURE CUTOFF CIRCUIT AFTER LAUNCH COMMIT. 2. PREVENT VEHICLE POWER TRANSFER FROM INTERNAL TO EXTERNAL AFTER COMMIT UNTIL ISSUANCE OF ENGINE CUTOFF COMMAND.	3.5.2
2	IU TELEMETRY SYSTEM	DROP IN RF RADIATED POWER STARTING AT ABOUT 970 SECONDS. (SHORTED CONNECTOR AT EITHER TM RF COUPLER OUTPUT OR TM POWER DIVIDER INPUT.)	MISSION MONITORING AND COMMAND VERIFICATION DATA NOT AVAILABLE TO GROUND CONTROLLERS FOR LONG PERIODS DURING ORBIT. (APD 19C ANOMALY, APD 44 NCC 4)	VISUAL INSPECTION OF TYPE-N CONNECTORS AND REPLACEMENT OF THOSE FOUND DEFECTIVE.	15.3.2 15.6
3	S-1VB LOX TANK VENT	BLOCKAGE OF RPV NOZZLE NO. 1 CAUSING ASYMMETRICAL VENTING BEGINNING AT 20.077 SECONDS AND RESULTING IN PREMATURE DEPLETION OF APS MODULE NO. 2 PROPELLANTS SHORTLY AFTER DEORBIT DUMP. (FORMATION OF SOLID OXYGEN (SOX) IN THE NOZZLE.)	NONE. ATTITUDE CONTROL NOT REQUIRED AFTER DEORBIT DUMP. (APD 19C ANOMALY, APD 44 NCC 4)	SA-207 AND -208 NOT AS SUSCEPTIBLE TO SOX FORMATION IN THE NOZZLE. HOWEVER, FLIGHT CONTROL PERSONNEL WILL BE BRIEFED TO TAKE APPROPRIATE ACTION IN REAL TIME IF NECESSARY TO AVOID CONDITIONS CONDUCTIVE TO SOX FORMATION.	7.10.2 10.3.3
4	ST-120M STABILIZED PLATFORM	GYRO SUMMATION CURRENT AND ACCELEROMETER SUMMATION CURRENT DROPPED AT SOME TIME BETWEEN 3500 AND 5600 SECONDS. (CHARACTERISTIC RESPONSE OF HYSTERESIS MOTORS TO UNEXPLAINED TRANSIENT ON 400 HZ POWER LINE.)	NONE. (APD 19C ANOMALY, APD 44 NCC 4)	NONE.	9.4.1

# SECTION 1

## INTRODUCTION

### 1.1 PURPOSE

This report provides the National Aeronautics and Space Administration (NASA) Headquarters, and other interested agencies, with the launch vehicle evaluation results of the SA-206 flight (Skylab-2 Launch). The basic objective of flight evaluation is to acquire, reduce, analyze, evaluate and report on flight data to the extent required to assure future mission success and vehicle reliability. To accomplish this objective, actual flight problems are identified, their causes determined, and recommendations made for appropriate corrective action.

### 1.2 SCOPE

This report contains the performance evaluation of the major launch vehicle systems with special emphasis on problems. Summaries of launch operations and spacecraft performance are included.

The official George C. Marshall Space Flight Center (MSFC) position at this time is represented by this report. It will not be followed by a similar report unless continued analysis or new information should prove the conclusions presented herein to be significantly incorrect.

### 1.3 PERFORMANCE PREDICTIONS BASELINE

Unless otherwise noted, all performance predictions quoted herein for comparison purposes are those used in or generated by the SA-206 Post Launch Predicted Operational Trajectory.



## SECTION 2

### EVENT TIMES

#### 2.1 SUMMARY OF EVENTS

Range zero occurred at 09:00:00 Eastern Daylight Time (EDT) (13:00:00 Universal Time [UT]) May 25, 1973. Range time is the elapsed time from range zero, which, by definition, is the nearest whole second prior to liftoff signal, and is the time used throughout this report unless otherwise noted. Time from base time is the elapsed time from the start of the indicated time base. Table 2-1 presents the time bases used in the flight sequence program.

The start of Time Bases  $T_0$  and  $T_1$  were nominal.  $T_2$ ,  $T_3$  and  $T_4$  were initiated approximately 0.8 seconds, 1.4 seconds and 3.7 seconds late, respectively. These variations are discussed in Sections 6 and 7 of this document. Start of  $T_5$  was initiated by the receipt of a ground command, 193.4 seconds earlier than scheduled as discussed in Section 5.2.

Figure 2-1 shows the difference between telemetry signal receipt at a ground station and vehicle [Launch Vehicle Digital Computer (LVDC) clock] time. This difference between ground and vehicle time is a function of LVDC clock speed.

A summary of significant event times for SA-206 is given in Table 2-2. The preflight predicted times were adjusted to match the actual first motion time. The predicted times for establishing actual minus predicted times in Table 2-2 were taken from 68M00001B, "Interface Control Document Definition of Saturn SA-206 and Subs Flight Sequence Program" and from the Skylab-2 (SA-206) Post-Launch Predicted Operational Trajectory (OT) S&E-AERO-MFP-85-73, dated June 12, 1973.

#### 2.2 VARIABLE TIME AND COMMANDED SWITCH SELECTOR EVENTS

Table 2-3 lists the switch selector events which were issued during the flight, but were not programmed for specific times.

Table 2-1. Time Base Summary

TIME BASE	RANGE TIME SECONDS	SIGNAL START
T <sub>0</sub>	-16.95	Guidance Reference Release
T <sub>1</sub>	0.53	IU Umbilical Disconnect Sensed by LVDC
T <sub>2</sub>	135.68	S-IB Low Level Sensors Dry Sensed by LVDC
T <sub>3</sub>	142.26	S-IB OECD Sensed by LVDC
T <sub>4</sub>	586.44	S-IVB ECD (Velocity) Sensed by LVDC
T <sub>5</sub>	19,426.79	Initiated by Receipt of Ground Command

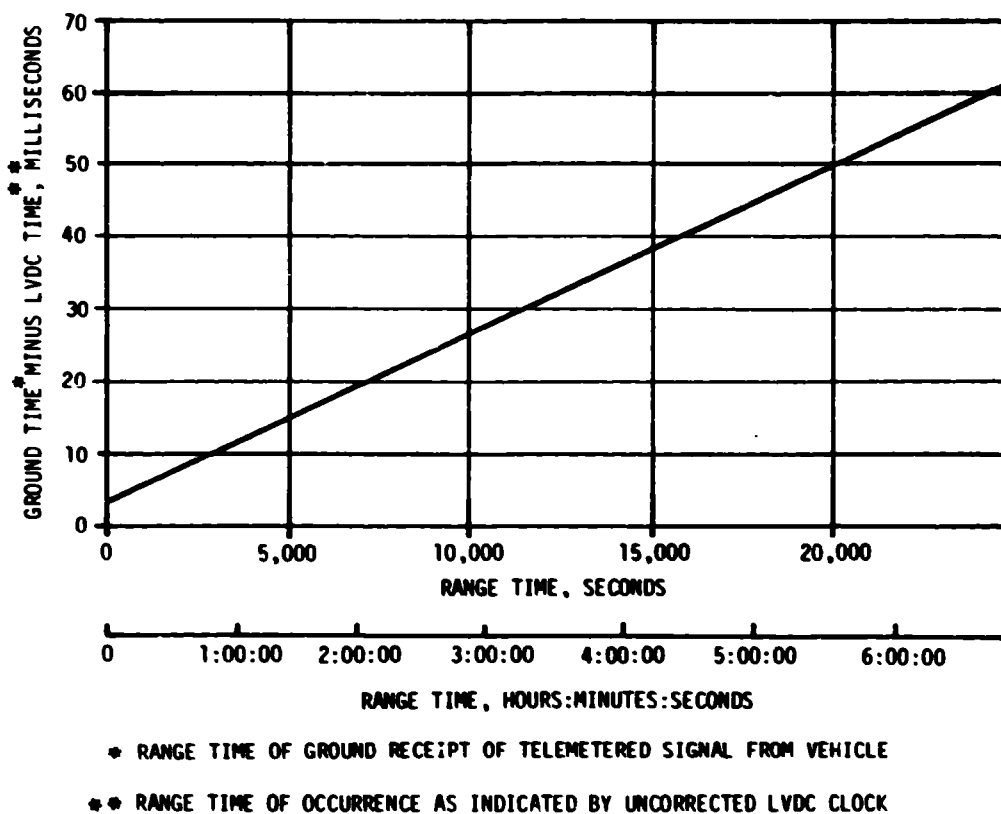


Figure 2-1. LVDC Clock/Ground Time Difference

Table 2-2. Significant Event Times Summary

ITEM	EVENT DESCRIPTION	RANGE TIME		TIME FROM BASE	
		ACTUAL SEC	ACT-PRED SEC	ACTUAL SEC	ACT-PRED SEC
1	GUIDANCE REFERENCE RELEASE (GRR)	-17.0	0.0	-17.5	-0.1
2	S-1B ENGINE START COMMAND	-3.1	0.0	-3.6	-0.1
3	S-1B START SIGNAL ENGINE NO. 7	-3.0	0.0	-3.5	-0.1
4	S-1B START SIGNAL ENGINE NO. 5	-3.0	0.0	-3.5	-0.1
5	S-1B START SIGNAL ENGINE NO. 6	-2.9	0.0	-3.4	-0.1
6	S-1B START SIGNAL ENGINE NO. 8	-2.9	0.0	-3.4	-0.1
7	S-1B START SIGNAL ENGINE NO. 2	-2.8	0.0	-3.3	-0.1
8	S-1B START SIGNAL ENGINE NO. 4	-2.8	0.0	-3.3	-0.1
9	S-1B START SIGNAL ENGINE NO. 3	-2.7	0.0	-3.2	-0.1
10	S-1B START SIGNAL ENGINE NO. 1	-2.7	0.0	-3.2	-0.1
11	RANGE ZERO	0.0	0.3	-0.5	0.2
12	FIRST MOTION	0.2	0.0	-0.3	-0.1
13	TO UMBILICAL DISCONNECT, START OF TIME BASE 1 (T1) LIFTOFF	0.5	0.1	0.0	0.0
14	SINGLE ENGINE CUTOFF ENABLE	3.5	0.1	3.0	0.0
15	LOX TANK PRESSURIZATION SHUTOFF VALVES CLOSE	6.5	0.1	6.0	0.0
16	BEGIN PITCH AND ROLL MANEUVER	10.0	-0.4	9.5	-0.5
17	MULTIPLE ENGINE CUTOFF ENABLE #1	10.5	0.1	10.0	0.0
18	MULTIPLE ENGINE CUTOFF ENABLE #2	10.6	0.1	10.1	0.0
19	TELEMETER CALIBRATE ON	20.5	0.1	20.0	0.0
20	TELEMETER CALIBRATE OFF	25.5	0.1	25.0	0.0
21	TELEMETRY CALIBRATOR IN-FLIGHT CALIBRATE ON	26.5	-0.9	26.0	-1.0
22	TELEMETRY CALIBRATOR IN-FLIGHT CALIBRATE OFF	31.5	-0.9	31.0	-1.0
23	LAUNCH VEHICLE ENGINES EOS CUTOFF ENABLE	39.5	-0.9	39.0	-1.0
24	END ROLL MANEUVER	54.8	4.0	54.3	3.9

Table 2-2. Significant Event Times Summary (Continued)

ITEM	EVENT DESCRIPTION	RANGE TIME		TIME FROM BASE	
		ACTUAL SEC	ACT-PRED SEC	ACTUAL SEC	ACT-PRED SEC
25	MACH 1	60.5	1.5	60.0	1.4
26	MAXIMUM DYNAMIC PRESSURE (MAX Q)	75.5	1.9	75.0	1.8
27	TELEMETRY CALIBRATOR IN-FLIGHT CALIBRATE ON	90.7	0.1	90.2	0.0
28	TELEMETRY CALIBRATOR IN-FLIGHT CALIBRATE OFF	95.7	0.1	95.2	0.0
29	FLIGHT CONTROL COMPUTER SWITCH POINT NO. 1	99.5	-0.9	99.0	-1.0
30	FLIGHT CONTROL COMPUTER SWITCH POINT NO. 2	100.7	0.1	100.2	0.0
31	TELEMETER CALIBRATION ON	120.3	0.1	119.8	0.0
32	FLIGHT CONTROL COMPUTER SWITCH POINT NO. 3	120.5	0.1	120.0	0.0
33	TH CONTROL ACCEL. PWR OFF	120.7	0.1	120.2	0.0
34	TELEMETER CALIBRATION OFF	125.3	0.1	124.8	0.0
35	TELEMETER CALIBRATE ON	128.0	0.1	127.5	0.0
36	EXCESS RATE (P,Y,R) AUTO-ABORT INHIBIT ENABLE	128.1	-1.0	127.6	-1.1
37	EXCESS RATE (P,Y,R) AUTO-ABORT INHIBIT AND SWITCH RATE GYROS SC INDICATION 'A'	128.3	-1.0	127.8	-1.1
38	TELEMETER CALIBRATE OFF	129.0	0.1	128.5	0.0
39	S-18 TWO ENGINES OUT AUTO- ABORT INHIBIT ENABLE	129.6	0.1	129.1	0.0
40	S-18 TWO ENGINES OUT AUTO- ABORT INHIBIT	129.8	0.1	129.3	0.0
41	PROPELLANT LEVEL SENSORS ENABLE	130.0	0.1	129.5	0.0
42	TILT ARREST	132.0	0.6	131.5	0.5
43	S-15 PROPELLANT LEVEL SENSOR ACTIVATION	135.7	0.8	135.2	0.7
44	START OF TIME BASE 2 (T2)	135.7	0.8	0.0	0.0
45	EXCESS RATE (ROLL) AUTO-ABORT INHIBIT ENABLE	135.8	0.7	0.2	0.0

Table 2-2. Significant Event Times Summary (Continued)

ITEM	EVENT DESCRIPTION	RANGE TIME		TIME FROM BASE	
		ACTUAL SEC	ACT-PRED SEC	ACTUAL SEC	ACT-PRED SEC
46	EXCESS RATE (ROLL) AUTO-ABORT INHIBIT AND SWITCH RATE GYROS SC INDICATION 'B'	136.0	0.7	0.4	0.0
47	INBOARD ENGINES CUTOFF (IECO)	138.66	0.76	2.98	-0.02
48	AUTO-ABORT ENABLE RELAY'S RESET	139.0	0.7	3.4	0.0
49	CHARGE ULLAGE IGNITION EBW FIRING UNITS	139.3	0.8	3.6	0.0
50	PREVALVES OPEN	139.9	0.7	4.2	-0.1
51	LOX DEPLETION CUTOFF ENABLE	140.2	0.8	4.5	0.0
52	FUEL DEPLETION CUTOFF ENABLE	140.6	0.7	5.0	0.0
53	S-18 OUTBOARD ENGINES CUTOFF (OECO)	142.26	1.36	6.58	0.58
54	START OF TIME BASE 3 (T3)	142.3	1.4	0.0	0.0
55	S-18 OUTBOARD ENGINES CUTOFF	142.3	1.3	0.1	0.0
56	LOX TANK PRESSURIZATION SHUTOFF VALVES OPEN	142.4	1.3	0.2	0.0
57	LOX TANK FLIGHT PRESSURE SYSTEM ON	142.5	1.3	0.3	0.0
58	S-1VB ENGINE CUTOFF NO. 1 OFF	142.6	1.3	0.4	0.0
59	S-1VB ENGINE CUTOFF NO. 2 OFF	142.7	1.3	0.5	0.0
60	SENSOR PANEL NO 1 AND PANEL 2 COVER NO. 4 EXPULSION	142.8	1.3	0.6	0.0
61	SENSOR PANEL NO 1 AND PANEL 2 COVER NO 4 EXPULSION RESET	142.9	1.3	0.7	0.0
62	MIXTURE RATIO CONTROL VALVE OPEN	143.0	1.3	0.8	0.0
63	MIXTURE RATIO CONTROL VALVE BACKUP OPEN	143.1	1.3	0.9	0.0
64	ULLAGE ROCKETS IGNITION	143.3	1.3	1.1	0.0
65	S-18/S-1VB SEPARATION SIGNAL ON	143.5	1.3	1.3	0.0
66	S-18/S-1VB PHYSICAL SEPARATION	143.7	1.4	1.4	0.0
67	S-1VB ENGINE IGNITION SEQUENCE START COMMAND	144.9	1.3	2.6	-0.1

Table 2-2. Significant Event Times Summary (Continued)

ITEM	EVENT DESCRIPTION	RANGE TIME		TIME FROM BASE	
		ACTUAL SEC	ACT-PRED SEC	ACTUAL SEC	ACT-PRED SEC
68	S-IVB MRCV OPEN (4.8:1 EMR)	145.4	1.3	3.1	-0.1
69	S-IVB STEV OPEN	145.9	1.3	3.6	-0.1
70	MAINSTAGE ENABLE ON	145.9	1.3	3.7	0.0
71	LINE 2 TANK PRESSURIZATION CONTROL SWITCH ENABLE	147.5	1.3	5.3	0.0
72	S-IVB MAINSTAGE OK PRESSURE SWITCH 1	147.9	1.4	5.5	0.0
73	S-IVB MAINSTAGE	148.2	1.3	5.9	-0.1
74	MIXTURE RATIO CONTROL VALVE CLOSE	150.9	1.3	8.7	0.0
75	MIXTURE RATIO CONTROL VALVE CLOSE (5.5:1 EMR)	151.3	1.2	9.0	-0.2
76	CHARGE ULLAGE JETTISON EBW FIRING UNITS	152.4	1.3	10.2	0.0
77	ULLAGE ROCKET JETTISON	155.5	1.3	13.3	0.0
78	ENGINE MAINSTAGE ENABLE OFF	156.0	1.4	13.7	0.0
79	SENSOR PANEL NO 1 AND PANEL 2 COVER NO. 2 EXPULSION	160.2	1.3	18.0	0.0
80	SENSOR PANEL NO 1 AND PANEL 2 COVER NO. 2 EXPULSION RESET	160.3	1.3	18.1	0.0
81	ULLAGE EBW FIRING UNITS RESET	161.5	1.3	19.3	0.0
82	ULLAGE ROCKETS IGNITION AND JETTISON RELAYS RESET	161.7	1.3	19.5	0.0
83	HEAT-EXCHANGER BYPASS VALVE CONTROL ENABLE	166.2	1.3	24.0	0.0
84	TELEMETRY CALIBRATOR IN-FLIGHT CALIBRATE ON	166.6	0.3	24.4	-1.0
85	TELEMETRY CALIBRATOR IN-FLIGHT CALIBRATE OFF	172.6	1.3	30.4	0.0
86	REGIN IGM PHASE 1	178.2	1.8	36.0	0.5
87	FLIGHT CONTROL COMPUTER SWITCH POINT NO. 4	184.2	1.3	42.0	0.0
88	FLIGHT CONTROL COMPUTER SWITCH POINT NO. 5	345.9	1.3	203.7	0.0
89	TELEMETRY CALIBRATOR IN-FLIGHT CALIBRATE ON	347.6	1.3	205.4	0.0

Table 2-2. Significant Event Times Summary (Continued)

ITEM	EVENT DESCRIPTION	RANGE TIME		TIME FROM BASE	
		ACTUAL SEC	ACT-PRED SEC	ACTUAL SEC	ACT-PRED SEC
90	TELEMETRY CALIBRATOR IN-FLIGHT CALIBRATE OFF	352.6	1.3	210.4	0.0
91	LH2 TANK PRESSURIZATION CONTROL SWITCH DISABLE	445.1	1.3	302.9	0.0
92	S-IVB MIXTURE RATIO CONTROL VALVE OPEN	470.3	1.3	328.1	0.0
93	MIXTURE RATIO CONTROL VALVE OPEN (4.8:1 EMRI)	470.4	0.0	328.1	-0.5
94	BEGIN IGM PHASE 2	471.8	0.9	329.5	-0.5
95	PROPELLANT DEPLETION CUTOFF ARM	542.2	1.3	400.0	0.0
96	BEGIN TERMINAL GUIDANCE	564.3	9.9	422.0	8.5
97	GUIDANCE CUTOFF SIGNAL (GCS)	596.19	3.69	443.93	2.33
98	S-IVB SOLENOID ACTIVATION SIGNAL	586.3	3.8	444.0	4.5
99	S-IVB MAINSTAGE OK PRESSURE SWITCH 1	586.4	3.8	444.2	4.6
100	S-IVB MAINSTAGE OK PRESSURE SWITCH 2	586.4	3.8	444.2	4.6
101	INERTIAL ATTITUDE FREEZE	586.4	3.7	0.0	0.0
102	START OF TIME BASE 4 (T4)	596.4	3.7	0.0	0.0
103	S-IVB ENGINE CUTOFF NO. 1 ON	586.5	6.3	0.1	0.0
104	S-IVB ENGINE CUTOFF NO. 2 ON	586.6	6.3	0.2	0.0
105	PREVALVES CLOSE	586.7	3.7	0.3	0.0
106	LOX TANK NPV VALVE OPEN ON	597.0	6.3	0.6	0.0
107	LOX TANK PRESSURIZATION SHUT- OFF VALVES CLOSE ON	597.2	6.3	0.8	0.0
108	LOX TANK FLIGHT PRESS SYSTEM OFF	597.4	6.3	1.0	0.0
109	PROPELLANT DEPLETION CUTOFF DISARM	588.2	6.3	1.8	0.0
110	S-IVB MIXTURE RATIO CONTROL VALVE CLOSE	588.6	6.3	2.2	0.0
111	S-IVB MIXTURE RATIO CONTROL VALVE BACKUP CLOSE	588.8	6.3	2.4	0.0

Table 2-2. Significant Event Times Summary (Continued)

ITEM	EVENT DESCRIPTION	RANGE TIME		TIME FROM BASE	
		ACTUAL SEC	ACT-PRED SEC	ACTUAL SEC	ACT-PRED SEC
112	FLIGHT CONTROL COMPUTER S-1VB BURN MODE OFF 'A'	599.9	6.3	3.5	0.0
113	FLIGHT CONTROL COMPUTER S-1VB BURN MODE OFF 'B'	590.1	6.3	3.7	0.0
114	AUX HYDRAULIC PUMP FLIGHT MODE OFF	590.3	6.3	3.9	0.0
115	S/C CONTROL OF SATURN ENABLE	591.4	6.3	5.0	0.0
116	RATE MEASUREMENTS SWITCH	592.4	6.3	6.0	0.0
117	ORBIT INSERTION	596.2	3.7	9.8	-2.6
118	S-1VB ENGINE EDS CUTOFF DISABLE	596.4	6.3	10.0	0.0
119	LH2 TANK LATCHING RELIEF VALVE OPEN ON	596.8	6.3	10.4	0.0
120	LH2 TANK LATCHING RELIEF VALVE LATCH ON	598.8	6.3	12.4	0.0
121	LH2 TANK LATCHING RELIEF VALVE OPEN OFF	600.0	6.3	13.6	0.0
122	LH2 TANK LATCHING RELIEF VALVE LATCH OFF	601.2	6.3	14.8	0.0
123	CHILLDOWN SHUTOFF VALVES CLOSE	606.4	6.3	20.0	0.0
124	PITCH MANEUVER TO LOCAL HORIZ	607.6	4.9	21.2	1.2
125	P.U. INVERTER AND DC POWER OFF	616.4	6.3	30.0	0.0
126	LOX TANK NPV VALVE OPEN OFF	617.0	3.7	30.6	0.0
127	LOX TANK VENT AND NPV VALVES BOOST CLOSE ON	620.0	6.3	33.6	0.0
128	LOX TANK VENT AND NPV VALVES BOOST CLOSE OFF	622.0	6.3	35.6	0.0
129	CSM SEPARATION SLA PANEL JETTISON	950.3	17.6	373.9	13.9
130	PREVALVES OPEN	1267.0	6.9	680.6	0.6
131	CHILLDOWN SHUTOFF VALVES OPEN	1267.2	6.9	680.8	0.6
132	LH2 TANK LATCHING RELIEF VALVE OPEN ON	1267.4	6.9	681.0	0.6
133	LH2 TANK LATCHING RELIEF VALVE OPEN OFF	1268.4	6.9	682.0	0.6



Table 2-2. Significant Event Times Summary (Continued)

ITEM	EVENT DESCRIPTION	RANGE TIME		TIME FROM BASE	
		ACTUAL SEC	ACT-PRED SEC	ACTUAL SEC	ACT-PRED SEC
134	LH2 TANK VENT AND LATCHING RELIEF VALVES BOOST CLOSE ON	1271.4	6.9	685.0	0.6
135	LH2 TANK VENT AND LATCHING RE- LIEF VALVES BOOST CLOSE OFF	1273.4	6.9	687.0	0.6
136	INITIATE THERMAL COATING EXPERIMENT M415	3300.0	-32.1	2713.5	-38.5
137	PASSIVATION ENABLE	5596.4	6.2	5000.0	0.0
138	DCS COMMAND EXECUTE LOCAL REFERENCE MANEUVER	7007.0	-5273.2	6420.5	-5279.5
139	DCS DEORBIT COMMAND	16168.0	-3442.2	15581.5	-3448.5
140	START OF TIME BASE 5 (T5)	19426.8	-193.4	0.0	0.0
141	START LOX DUMP	19460.0	-194.2	33.2	-0.8
142	END LOX DUMP	19920.9	-193.5	494.1	-0.1
143	START H2 DUMP	19951.0	-193.2	524.2	0.2
144	END H2 DUMP	20075.9	-193.3	649.1	0.1
145	S-IVB/IU IMPACT	21607.0	786.8	21020.5	780.5

Table 2-3. Variable Time and Commanded Switch Selector Events

FUNCTION	STAGE	RANGE TIME (SEC)	TIME FROM BASE (SEC)	REMARKS
Telemetry Calibrator In-Flight Calibrate ON	IU	669.9	T <sub>4</sub> +83.4	Newfoundland Revolution 1
TM Calibrate ON	S-IVB	672.9	T <sub>4</sub> +86.4	Newfoundland Revolution 1
TM Calibrate OFF	S-IVB	673.9	T <sub>4</sub> +87.4	Newfoundland Revolution 1
Telemetry Calibrator In-Flight Calibrate OFF	IU	674.9	T <sub>4</sub> +88.4	Newfoundland Revolution 1
Water Coolant Valve CLOSED	IU	780.1	T <sub>4</sub> +193.7	LVDC Function
Telemetry Calibrator In-Flight Calibrate ON	IU	3253.8	T <sub>4</sub> +2667.2	Carnarvon Revolution 1
TM Calibrate ON	S-IVB	3256.8	T <sub>4</sub> +2670.3	Carnarvon Revolution 1
TM Calibrate OFF	S-IVB	3257.8	T <sub>4</sub> +2671.3	Carnarvon Revolution 1
Telemetry Calibrator In-Flight Calibrate ON	IU	14,933.8	T <sub>4</sub> +14,347.4	Honeysuckle Revolution 3
TM Calibrate ON	S-IVB	14,936.8	T <sub>4</sub> +14,350.4	Honeysuckle Revolution 3
TM Calibrate OFF	S-IVB	14,937.8	T <sub>4</sub> +14,351.4	Honeysuckle Revolution 3
Telemetry Calibrator In-Flight Calibrate OFF	IU	14,938.8	T <sub>4</sub> +14,352.4	Honeysuckle Revolution 3
Telemetry Calibrator In-Flight Calibrate ON	IU	16,173.89	T <sub>4</sub> +15,587.4	Hawaii Revolution 3
TM Calibrate ON	S-IVB	16,176.8	T <sub>4</sub> +15,590.4	Hawaii Revolution 3
TM Calibrate OFF	S-IVB	16,177.8	T <sub>4</sub> +15,591.4	Hawaii Revolution 3
Telemetry Calibrator In-Flight Calibrate OFF	IU	16,178.8	T <sub>4</sub> +15,592.4	Hawaii Revolution 3

## SECTION 3

### LAUNCH OPERATIONS

#### 3.1 SUMMARY

The performance of ground systems supporting the SA-206/Skylab-2 count-down and launch was satisfactory except for the Launch Vehicle Ground Support Equipment (LVGSE) cutoff anomaly discussed in Paragraph 3.5.2. This malfunction occurred after launch commit and could have transferred vehicle power from internal to external resulting in launch without vehicle electrical power. The erroneous cutoff signal, however, was not sustained long enough to energize the cutoff relay.

The space vehicle was launched at 9:00:00 Eastern Daylight Time (EDT) on May 25, 1973, from Pad 39P of the Kennedy Space Center, Saturn Complex. The SA-206/Skylab-2 countdown was scrubbed from the original May 15, 1973 launch date to accommodate Skylab-1 Orbital Work Shop problem resolutions and work-arounds (refer to MPR-SAT-FE-73-4 for SA-513/Skylab-1 Flight Report). Damage to the pad, Launch Umbilical Tower (LUT) and support equipment was considered minimal.

#### 3.2 PRELAUNCH MILESTONES

A chronological summary of prelaunch milestones is contained in Table 3-1. All stages, S-IB, S-IVB and Instrument Unit (IU) performed satisfactorily and no anomalies were experienced during the countdown.

#### 3.3 TERMINAL COUNTDOWN

The SA-206/Skylab-2 terminal countdown was picked up at T-59 hours (countdown clock time) on May 23, 1973. Scheduled holds were initiated at T-3 hours 30 minutes for a duration of 73 minutes and at T-15 minutes for a duration of 2 minutes. The space vehicle was launched at 9:00:00 EDT on May 25, 1973. Launch commit occurred at 0.020 seconds range time.

Postlaunch review of the Digital Events Evaluator (DEE-6) printout revealed that at 102 milliseconds after launch commit the LVGSE issued a momentary cutoff signal. This signal was present during only one scan of the DEE-6 and was not of sufficient duration to energize the cutoff relay. This anomaly is discussed in Paragraph 3.5.2.

#### 3.4 PROPELLANT LOADING

##### 3.4.1 RP-1 Loading

The RP-1 system successfully supported countdown and launch without incident. Tail Service Mast fill and replenish was accomplished at

Table 3-1. SA-206/Skylab-2 Prelaunch Milestones

DATE	ACTIVITY OR EVENT
August 1, 1972	Command Service Module (CSM) 116 Arrival
August 19, 1972	S-IVB-206 Stage Arrival
August 22, 1972	S-IB-6 Stage Arrival
August 24, 1972	Instrument Unit (IU) S-IU-206 Arrival
August 31, 1972	S-IB Erection on Mobile Launcher (ML)-1
September 5, 1972	S-IVB Erection
September 7, 1972	IU Erection
October 6, 1972	Launch Vehicle (LV) Electrical Systems Test Complete
January 9, 1973	LV Moved to Pad B for First Time
January 30, 1973	Propellant Load and All System Test (PLAST) Complete
February 5, 1973	LV Returned to Vertical Assembly Building (VAB)
February 21, 1973	Spacecraft (SC) Erection
February 26, 1973	LV Returned to Pad B
March 14, 1973	LV Propellant Dispersion/Malfunction Overall Test (OAT)
March 29, 1973	Space Vehicle (SV) Electrical Mate
April 2, 1973	SV OAT 1 (Plugs In)
April 10, 1973	SV Flight Readiness Test (FRT) Complete
April 23, 1973	RP-1 Loaded
May 3, 1973	Countdown Demonstration Test (CDDT) Completed (Wet)
May 4, 1973	CDDT Complete (Dry)
May 14, 1973	SL-2 Scrubbed
May 23, 1973	SL-2 Scrub Turnaround Preparation Started
May 25, 1973	SL-2 Launch

T-8 hours and level adjust/line inert at about T-60 minutes. Both operations were completed satisfactorily as planned. Launch countdown support consumed 41,616 gallons of RP-1.

#### 3.4.2 LOX Loading

The LOX system successfully supported countdown and launch without incident. The fill sequence began with S-IB chilldown at 2145 EDT, May 24, 1973, and was completed 2 hours 3 minutes later with all stage replenish at 2348 EDT. Replenish was automatic through the Terminal Countdown Sequencer (TCS) without incident. LOX consumption during launch countdown was 160,000 gallons.

#### 3.4.3 LH<sub>2</sub> Loading

The LH<sub>2</sub> system successfully supported countdown and launch. The fill sequence began at 2347 EDT, May 24, 1973, and was completed 53 minutes later when normal S-IVB replenish was established manually at 0040 EDT, May 25, 1973. Replenish was nominal and was terminated at the start of TCS. Launch countdown support consumed about 150,000 gallons of LH<sub>2</sub>.

### 3.5 GROUND SUPPORT EQUIPMENT

#### 3.5.1 Ground/Vehicle Interface

In general, performance of the ground service systems supporting all stages of the launch vehicle was satisfactory. Overall damage to the pad, LUT, and support equipment from blast and flame impingement was considered minimal.

The Propellant Tanking Computer Systems (PTCS) adequately supported all countdown operations and there was no damage.

The Environmental Control System (ECS) performed satisfactorily throughout the countdown and launch. Changeover from air to GN<sub>2</sub> occurred at 2041 EDT on May 24, 1973.

The Service Arm Control Switches (SACS) satisfactorily supported SL-2 launch and countdown. The SAC No. 3 primary switch closed at 289 milliseconds and SAC No. 7 primary switch closed at 268 milliseconds after commit. There were no problems and only a minimal amount of heat and blast damage to the SACS.

The Hydraulic Charging Unit and Service Arms (S/A's 1A, 6, 7, and 8) satisfactorily supported the SL-2 countdown and launch. Performance was nominal during terminal count and liftoff.

During CDDT primary damper disconnect from the Spacecraft in support of

Mobile Service Structure (MSS) emplacement on May 4, 1973, a hydraulic hose ruptured (Retract Damping Cylinder Hose, PN 11M00718-13). The failed hose was replaced. Subsequently, the primary damper hydraulic hoses were proof tested in place to 1000 psig, and the system was functionally tested.

Because of this hose rupture during CDDT it was decided that the Primary Damper would not be connected during launch countdown unless high winds endangered the launch vehicle. Primary damper operation was not required. The auxiliary damper performed normally.

The DEE-3 and DEE-6 systems satisfactorily supported all countdown operation. There was no system damage.

### 3.5.2 MSFC Furnished Ground Support Equipment

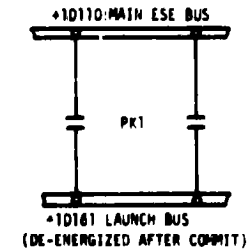
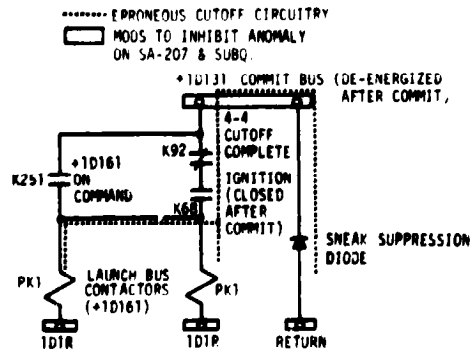
All Ground Power and Battery Equipment supported the prelaunch operations satisfactorily. All systems performed within acceptable limits. The Hazardous Gas Detection System successfully supported SL-2 countdown on May 24, 1973.

Postlaunch review of the DEE-6 print out revealed that at 102 milliseconds after commit, the Saturn IB ESE issued a momentary cutoff signal. This signal was substantiated by the recording of a thrust failure indication and cutoff start indication during one scan of the DEE-6. The cutoff signal was not of sufficient duration to energize the cutoff relay (K-72). See Figure 3-1.

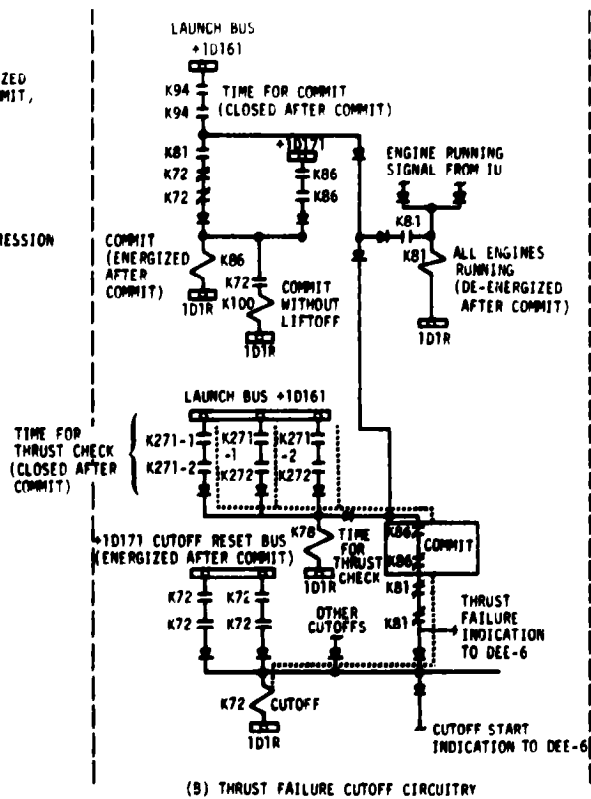
If the erroneous cutoff signal had been sustained long enough to energize the cutoff relay, an improper automatic cutoff sequence would have been initiated. Vehicle power would have been transferred from internal to external without engine cutoff resulting in launch without vehicle electrical power and mission or vehicle loss (see Figure 3-1).

Circuit analysis has revealed the source of these indications to be a momentary re-energization of the Launch Bus (+1D161), caused by remake of the launch bus contactors. This resulted in a circuit through the thrust failure cutoff circuitry to the cutoff relay (K72) and issuance to the DEE-6 of a thrust failure and initiation of a cutoff sequence (Figure 3-1). Test results confirmed that the contactor remake resulted from diode suppression of the launch bus contactor coils (See Figure 3-2).

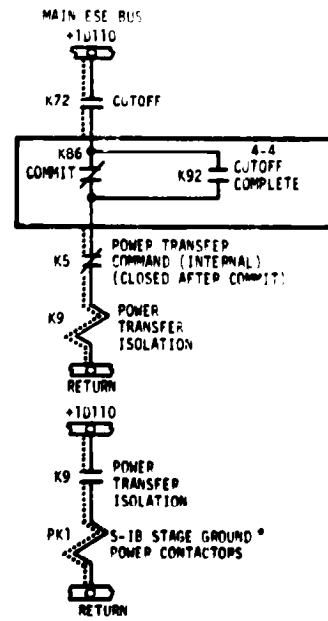
Diode suppression for these coils was not intentionally provided but was inherent in the ESE circuitry through a diode in a discrete input signal conditioner of the RCA 110A ground computer (see Figure 3-1). Diode suppression dampens voltage transients, but also extends the inductive time constant of the collapsing electrical circuit through the contactor coil. This delays the decay of the coils magnetic force so that as the contactor's contacts break the magnetic force exceeds the mechanical spring force which is attempting to open the contacts and causes a momentary remake.



(A) LAUNCH BUS REMAKE CIRCUITRY



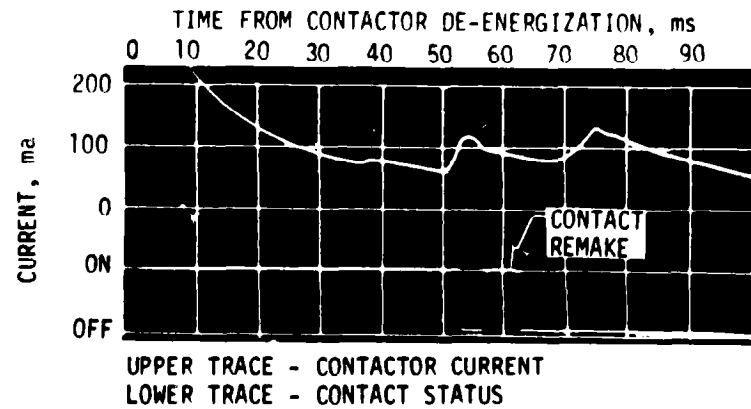
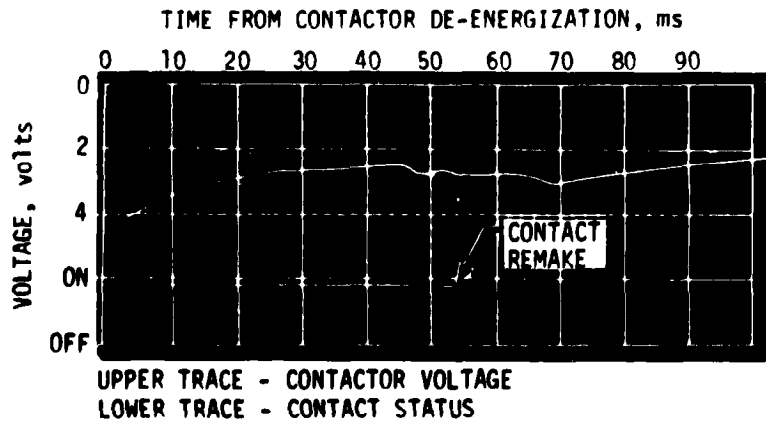
(B) THRUST FAILURE CUTOFF CIRCUITRY



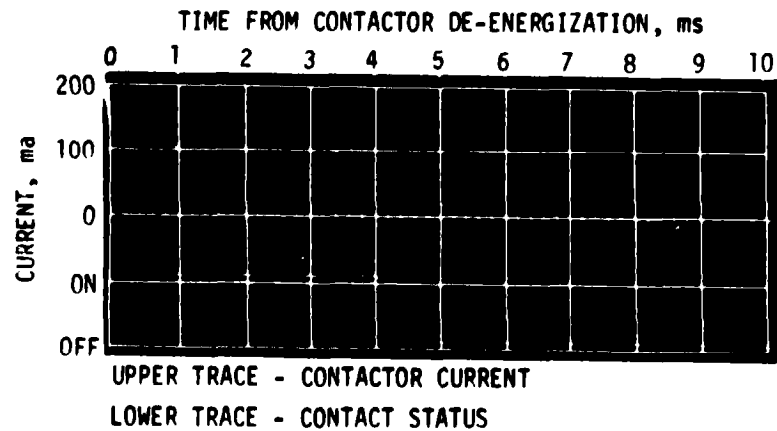
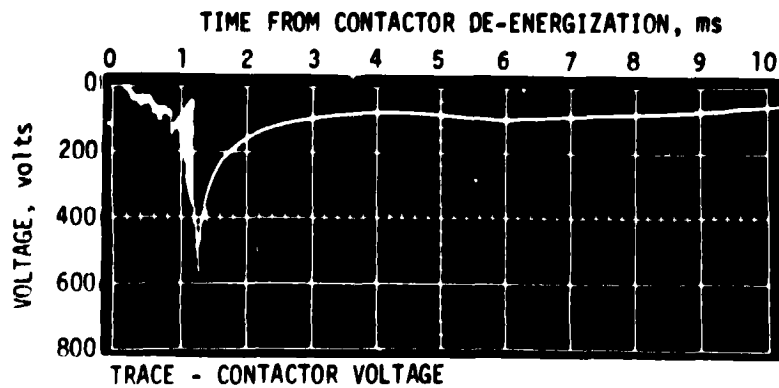
(C) POWER TRANSFER CIRCUITRY

\* ENERGIZING OF S1B STAGE GROUND POWER CONTACTORS RESULTS IN POWER TRANSFER FROM INTERNAL TO EXTERNAL ON ALL STAGES

Figure 3-1. ESE Cutoff Anomaly - Simplified ESE Circuitry



(A) CONTACTOR WITH DIODE SUPPRESSION AND RESULTING REMAKE



(B) CONTACTOR WITHOUT DIODE SUPPRESSION AND ABSENCE OF REMAKE

Figure 3-2. ESE Cutoff Anomaly - Test Results



Two normally closed commit (K86) relay contacts shown on the Figure 3-1 have been added to inhibit the thrust failure cutoff circuit after commit. Additionally, the automated power transfer circuitry has been modified to prevent a power transfer to external after commit until an actual command to cutoff the S-IB stage engines has been given (see Figure 3-1). This makes the ESE power transfer logic consistent with the cutoff logic. These modifications have been verified at the MSFC Saturn IB Systems Development Breadboard Facility and are installed in the ESE for SA-207. This anomaly is considered closed relative to the power transfer circuitry. Additional tests and analysis were conducted to verify proper operation of all launch vehicle and ESE relay applications from "time for ignition" through the last umbilical disconnect.

## SECTION 4

### TRAJECTORY

#### 4.1 SUMMARY

SA-206 was launched as planned on an azimuth of 90 degrees east of north. A roll maneuver was initiated at approximately 10 seconds that placed the vehicle on a flight azimuth of 47.580 degrees east of north. The down range pitch program was also initiated at this time.

The reconstructed trajectory was generated by merging the ascent phase and the parking orbit phase. Available C-Band radar and Unified S-Band tracking data, together with telemetered guidance velocity data were used in the trajectory reconstruction.

The reconstructed flight trajectory (actual) was very close to the Post Launch Predicted Operational Trajectory (nominal). The S-IB stage Outboard Engine Cutoff (OECO) was 1.36 seconds later than nominal. The total space-fixed velocity at this time was 7.07 m/s greater than nominal. After separation, the S-IB stage continued on a ballistic trajectory to earth impact. The S-IVB burn terminated with guidance cutoff signal and parking orbit insertion; both approximately 3.7 seconds later than nominal. A velocity of 1.82 m/s greater than nominal at insertion resulted in an apogee 6.32 km higher than nominal.

The parking orbit portion of the trajectory from insertion to CSM/S-IVB separation was close to nominal. However, separation of the CSM from the S-IVB stage occurred 17.6 seconds later than nominal, which is not considered significant because it is an astronaut initiated event.

#### 4.2 TRAJECTORY EVALUATION

##### 4.2.1 Ascent Phase

The ascent phase spans the interval from guidance reference release to parking orbit insertion. The ascent trajectory was established from telemetered guidance velocity data, the tracking data from five C-Band stations described in Table 4-1, and an 18 term guidance error model.

The initial launch phase (from first motion to 22 seconds) was established by a least squares curve fit of the initial portion of the ascent trajectory developed above. Comparisons between the resultant best estimate trajectory and the available tracking data shows consistency and good agreement.

Table 4-1. Summary of Available Tracking Data

DATA SOURCE, TYPE	PHASE	INTERVAL (SEC)
Bermuda, C-Band	Ascent	295-708
Bermuda, C-Band	Orbital	258-708
Bermuda, S-Band	Orbital	400-690
Cape Kennedy, C-Band	Ascent	20-420
Merritt Island, C-Band	Ascent	22-503
Patrick, C-Band	Ascent	32-504
Wallops Island, C-Band	Ascent/Orbital	190-656

Telemetered guidance data were used as a model for obtaining proper velocity and acceleration profiles through the transient areas of Mach 1, maximum dynamic pressure, S-IB thrust decay, and S-IVB thrust decay.

Actual and nominal altitude, cross range, and surface range for the boost phase are presented in Figure 4-1. Figure 4-2 presents similar comparisons of space fixed velocity and flight path angle. Comparisons of actual and nominal total inertial accelerations are displayed in Figure 4-3. Inspection shows the actual was very close to the nominal values.

The S-IB stage OECO was a result of LOX depletion and the S-IVB Guidance Cutoff Signal (GCS) was issued by the guidance computer when end conditions were satisfied.

The accumulated difference between actual and nominal burn time of the S-IB and S-IVB stages was 3.71 seconds. The S-IB stage contributed 1.36 seconds of this deviation and the S-IVB burn contributed 2.35 seconds as shown in Table 4-2. Trajectory parameters at significant events are presented in Table 4-3. Table 4-4 presents significant parameters at the S-IB/S-IVB and S-IVB/CSM separation events.

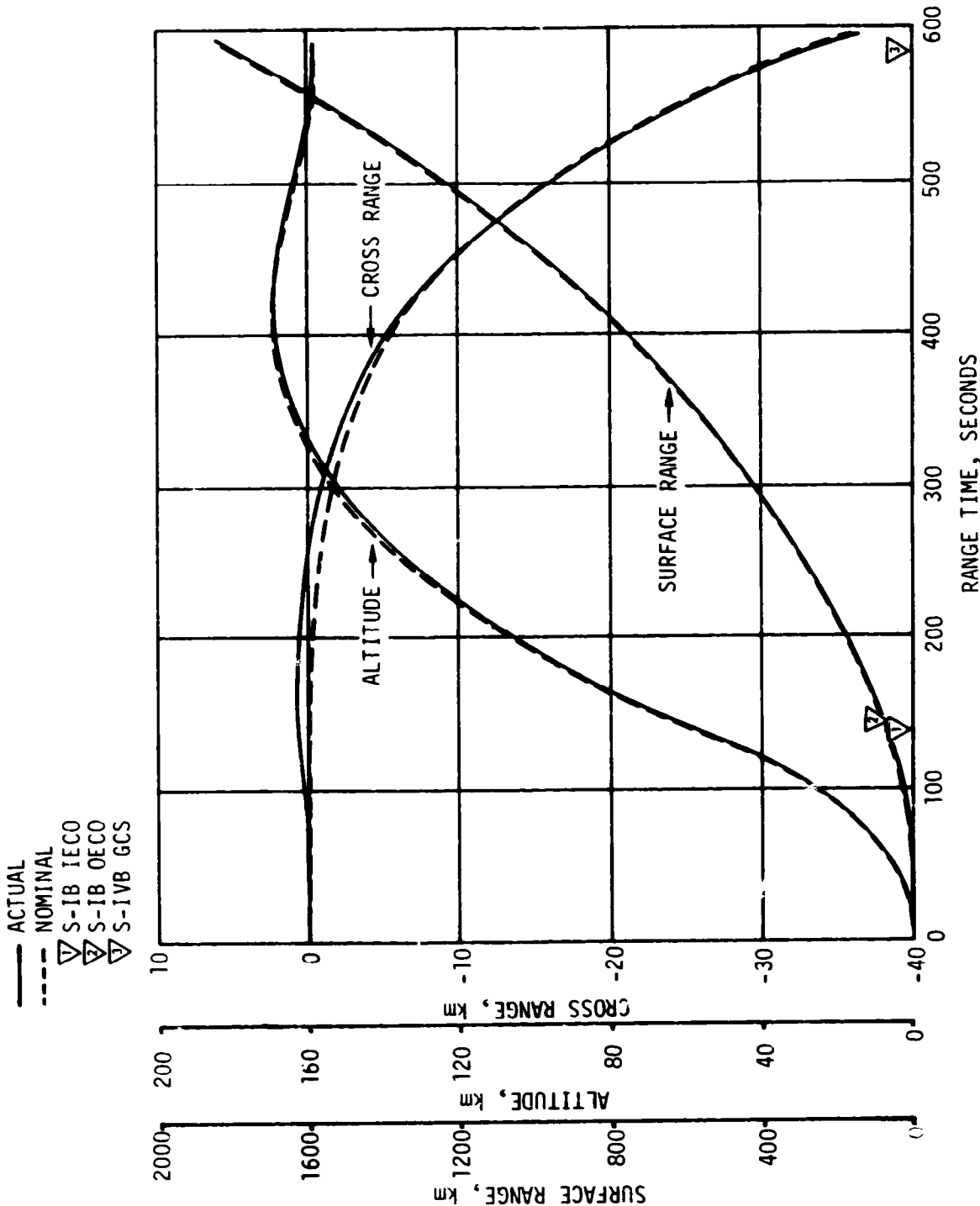


Figure 4-1. Ascent Trajectory Position Comparison

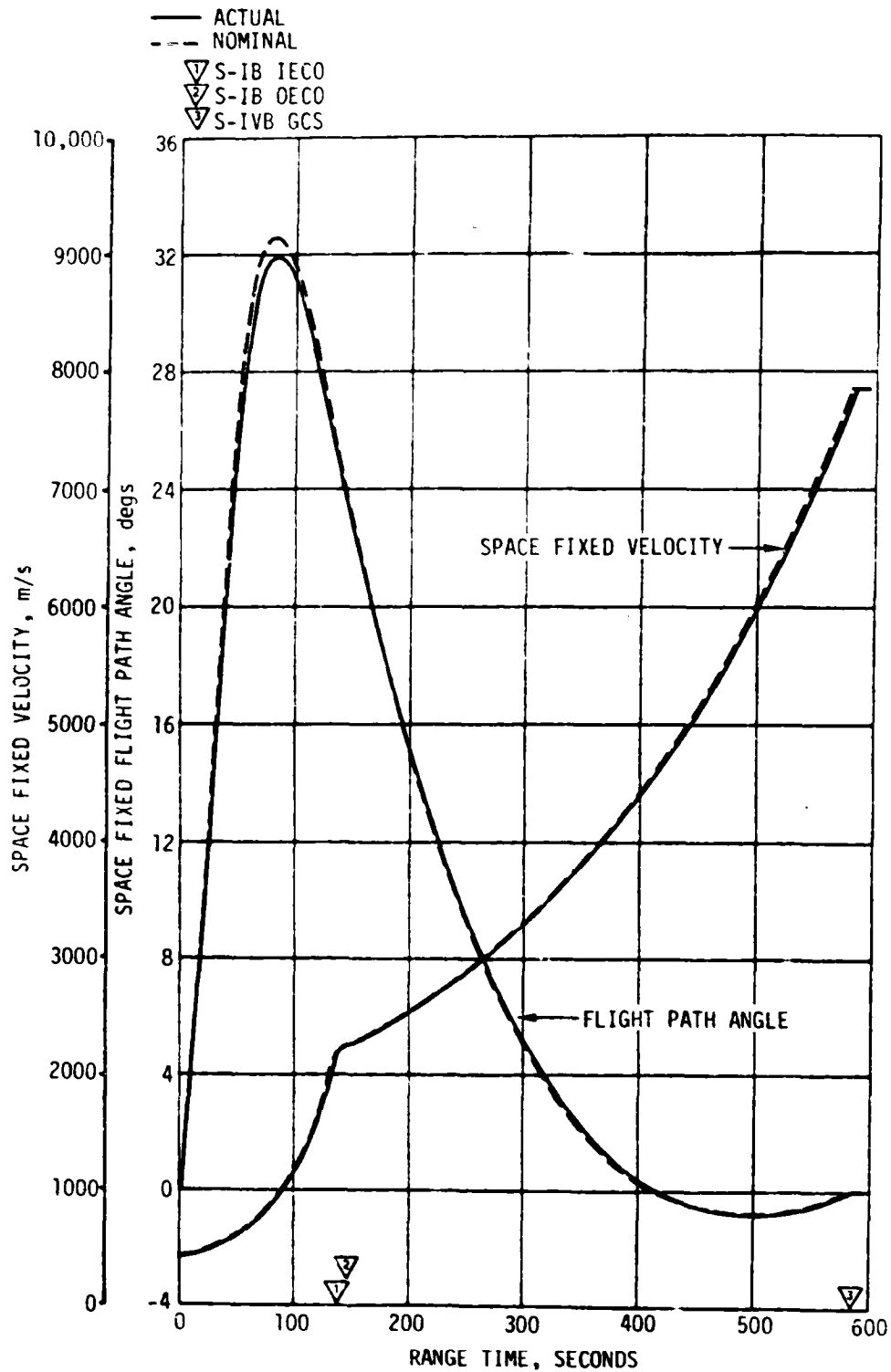


Figure 4-2. Ascent Trajectory Space-Fixed Velocity and Flight Path Angle Comparison

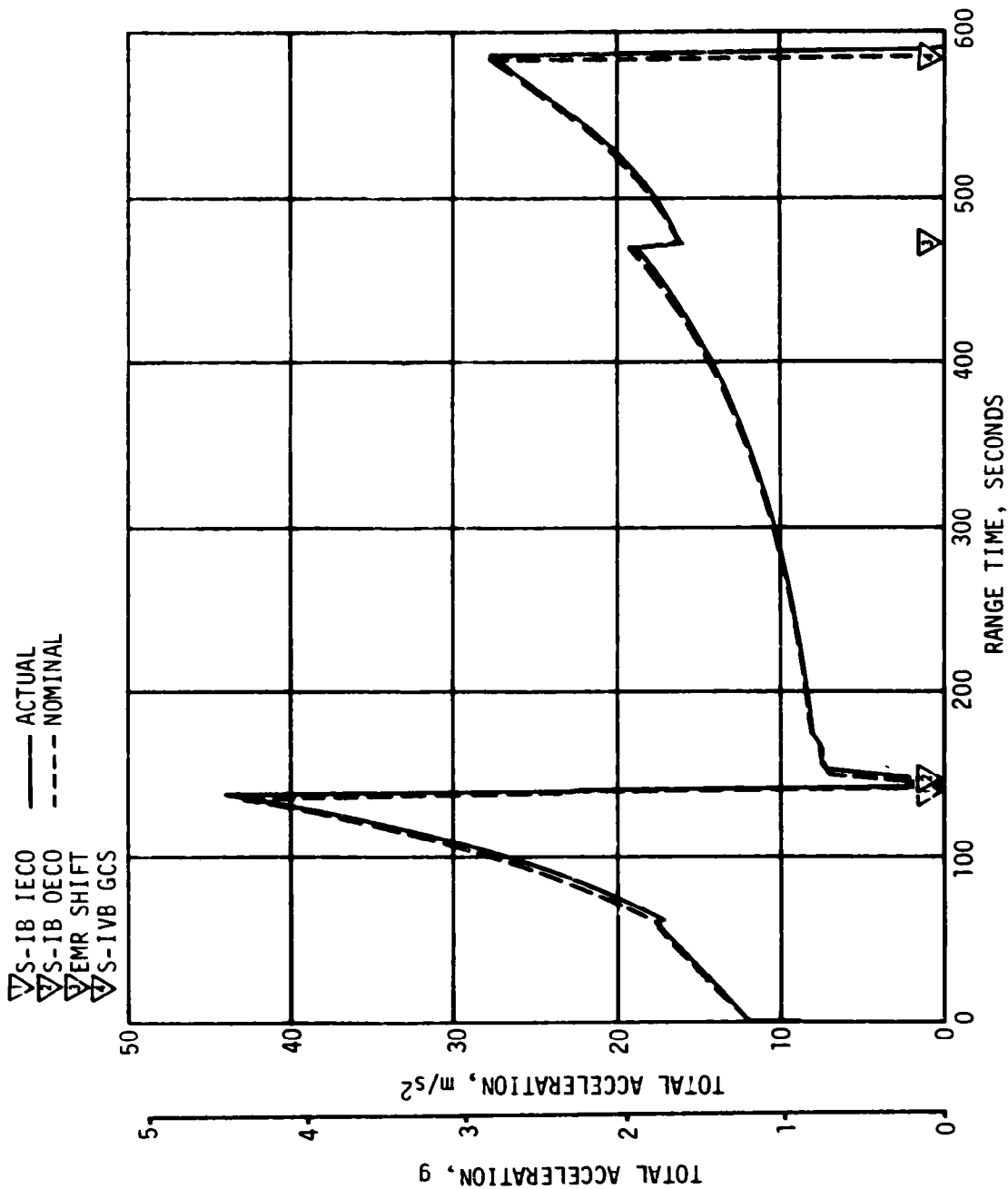


Figure 4-3. Ascent Trajectory Acceleration Comparison

Table 4-2. Comparison of Cutoff Events

PARAMETER	S-IB IECC			S-IB OECC			S-IVB GCS		
	ACTUAL	NOMINAL	ACT-NOM	ACTUAL	NOMINAL	ACT-NOM	ACTUAL	NOMINAL	ACT-NOM
Range Time (sec)	138.7	137.9	0.8	142.26	140.90	1.36	586.21	582.5	3.71
Altitude (km)	54.70	55.33	-0.63	58.14	58.22	-0.08	158.37	158.34	0.03
Space-Fixed Velocity (m/s)	2266.18	2265.54	0.64	2330.38	2323.31	7.07	7865.54	7864.87	0.67
Flight Path Angle (deg)	24.615	1.938	-0.323	23.958	24.416	-0.458	-0.007	-0.008	0.001
Heading Angle (deg)	55.473	55.360	0.113	55.237	55.157	0.080	55.398	55.330	0.068
Surface Range (km)	59.35	58.70	0.65	65.71	63.95	1.76	1782.73	1773.27	9.46
Gross Range (km)	0.54	-0.07	0.61	0.55	-0.08	0.63	-33.87	-33.20	-0.67
Gross Range Velocity (m/s)	1.31	-3.63	4.94	1.09	-3.65	4.74	-272.59	-275.83	3.24

Table 4-3. Comparison of Significant Trajectory Events

EVENT	PARAMETER	ACTUAL	NOMINAL	ACT-NOM
First Motion	Range Time, sec	0.190	0.190	0.000
	Total Inertial Acceleration, m/s <sup>2</sup>	12.090	12.234	-0.144
Mach 1	Range Time, sec	60.500	58.973	1.527
	Altitude, km	7.66	7.43	0.23
Maximum Dynamic Pressure	Range Time, sec	75.500	73.583	1.917
	Dynamic Pressure, N/cm <sup>2</sup>	3.381	3.361	0.020
	Altitude, km	12.84	12.43	0.41
*Maximum Total Inertial Acceleration: S-IB	Range Time, sec	138.640	137.902	0.738
	Acceleration, m/s <sup>2</sup>	44.277	42.906	1.371
*Maximum Earth-Fixed Velocity: S-IB	Range Time, sec	142.000	141.190	0.810
	Velocity, m/s	2040.94	2037.29	3.65
*Maximum Total Inertial Acceleration: S-IVB	Range Time, sec	586.210	582.402	3.808
	Acceleration, m/s <sup>2</sup>	27.982	28.149	-0.167
*Maximum Earth-Fixed Velocity: S-IVB	Range Time, sec	591.000	584.190	6.810
	Velocity, m/s	7570.49	7568.76	1.73
*Nearest Time Points Available				

Table 4-4. Comparison of Separation Events

PARAMETER	S-IB/S-IVB			S-IVB/CSM		
	ACTUAL	NOMINAL	ACT-NOM	ACTUAL	NOMINAL	ACT-NOM
Range Time (sec)	143.7	142.3	1.4	960.28	942.70	17.58
Altitude (km)	59.34	59.47	-0.13	172.32	171.13	1.19
Space-Fixed Velocity (m/s)	2326.16	2323.49	2.67	7859.32	7858.79	0.53
Flight Path Angle (deg)	23.680	24.166	-0.486	0.387	0.361	0.026
Heading Angle (deg)	55.244	55.152	0.092	78.860	77.681	1.179
Geodetic Latitude (deg)	29.036	29.031	0.005	49.265	49.068	0.197
Longitude (deg)	-80.102	-80.120	0.018	-34.125	-35.615	1.490
Surface Range (km)	67.98	66.26	1.72	--	--	--
Cross Range (km)	0.55	-0.09	0.64	--	--	--
Cross Range Velocity (m/s)	1.12	-3.60	4.72	--	--	--

Mach number and dynamic pressure history comparisons are shown in Figure 4-4. These parameters were calculated using measured meteorological data to an altitude of 66 km; above this altitude the U. S. Standard Reference Atmosphere was used. The variations seen in the actual dynamic pressure near its peak are attributable to the high wind gusts which were measured but that did not appear in the monthly average wind used in developing the nominal case.

A theoretical free flight trajectory was computed for the spent S-IB stage, using initial conditions from the actual trajectory at S-IB/S-IVB separation signal. Three trajectories were integrated from that point to impact using nominal retro motor performance and outboard engine decay data. The three trajectories incorporate three different drag conditions for 1) stabilized at zero angle of attack (nose forward), 2) tumbling stage, and 3) stabilized at 90 degree angle of attack (broadside). Tables 4-5 and 4-6 summarize the results of these simulations and present the impact envelope. Tracking data were not available, but previous flight data indicate the tumbling drag trajectory to be a close approximation to actual flight. The impact point for this case was 31.547 degrees north latitude, 76.756 degrees west longitude.

#### 4.2.2 Orbit Phase

The orbit documented herein originates at orbit insertion and terminates at S-IVB/CSM separation.



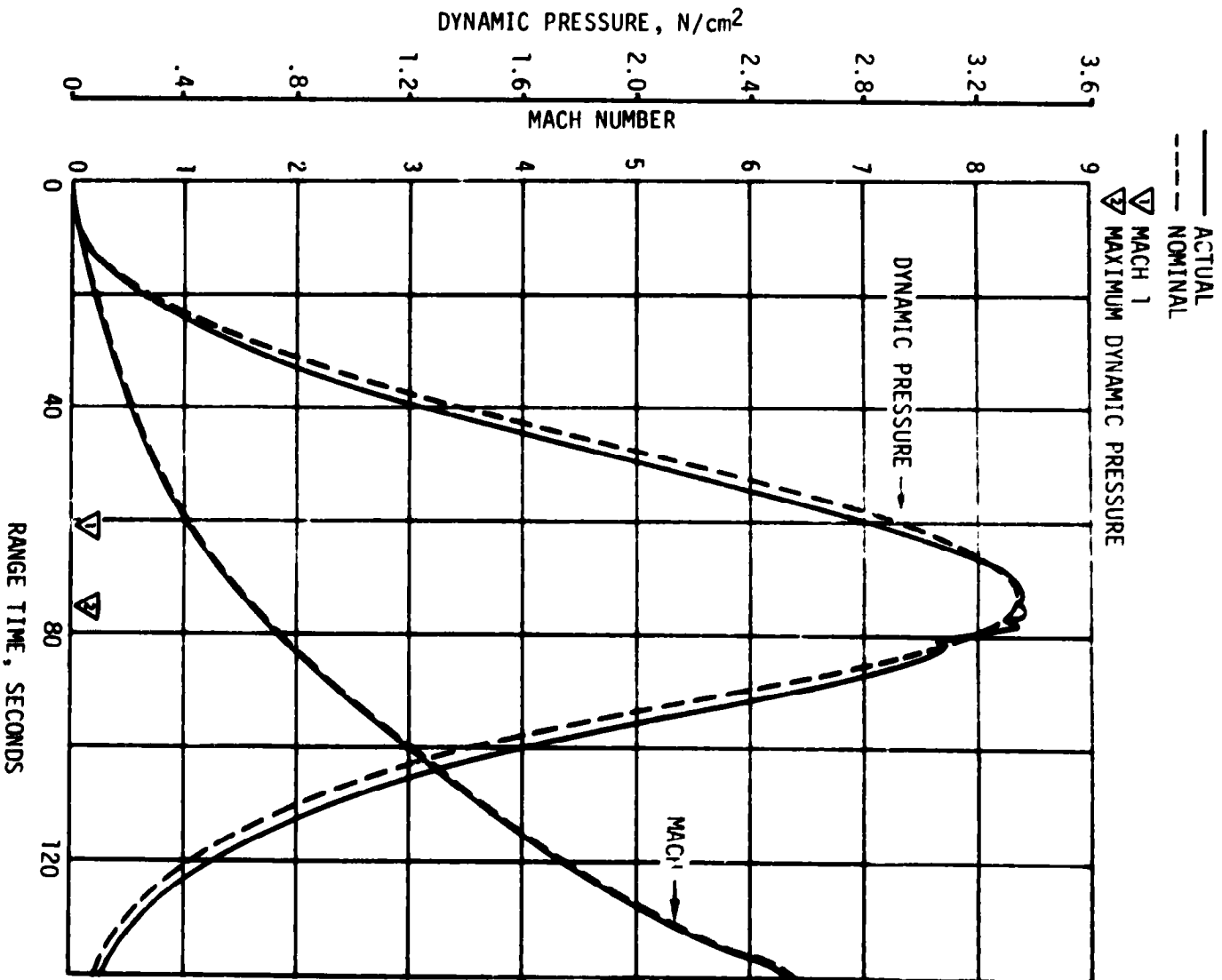


Figure 4-4. Dynamic Pressure and Mach No. Comparisons

Table 4-5. Comparison of S-IB Spent Stage Impact Point

PARAMETER	ACTUAL	NOMINAL	ACT-NOM
Range Time (sec)	535.34	536.76	-1.42
Surface Range (km)	493.44	496.83	-3.39
Cross Range (km)	4.17	3.07	1.10
Geodetic Latitude (deg)	31.547	31.574	-0.027
Longitude (deg)	-76.756	-76.736	-0.020

NOTE: Data reflects simulation of tumbling stage.

Table 4-6. S-IB Spent Stage Impact Envelope

PARAMETER	DRAG SIMULATION		
	NOSE FORWARD	TUMBLING	BROADSIDE
Range Time (sec)	473.76	535.34	576.64
Surface Range (km)	506.21	493.44	484.49
Cross Range (km)	4.40	4.17	4.03
Geodetic Latitude (deg)	31.620	31.547	31.495
Longitude (deg)	-76.652	-76.756	-76.829

Orbital tracking was conducted by the NASA Space Tracking and Data Network. One C-Band (Bermuda) and one S-Band station (Bermuda) were available for tracking coverage during the first revolution. Some high speed tracking data beyond insertion were available from Wallops Island. These high speed data were edited to provide additional useful orbital tracking information. The trajectory parameters at orbital insertion were established by a differential correction procedure in the Orbital Correction Program which adjusts the preliminary estimate of the insertion conditions to final values in accordance with relative weight assigned to the tracking data. A comparison of the actual and nominal parking orbit insertion parameters are delineated in Table 4-7. Figure 4-5 presents the SA-206 ground track from liftoff through CSM separation.

Table 4-7. Comparison of Orbit Insertion Conditions

PARAMETER	ACTUAL	NOMINAL	ACT-NOM
Range Time (sec)	596.21	592.50	3.71
Altitude (km)	158.52	158.49	0.03
Space-Fixed Velocity (m/s)	7873.35	7871.53	1.82
Flight Path Angle (deg)	0.011	0.009	0.002
Heading Angle (deg)	55.855	55.785	0.070
Cross Range (km)	-36.56	-35.92	-0.64
Cross Range Velocity (m/s)	-265.81	-269.02	3.21
Inclination (deg)	50.030	50.032	-0.002
Descending Node (deg)	155.213	155.222	-0.009
Eccentricity	0.0152	0.0148	0.0004
Apogee Altitude (km)	352.07	345.75	6.32
Perigee Altitude (km)	149.99	149.97	0.02
Period (min)	89.53	89.46	0.07
Geodetic Latitude (deg)	39.271	39.220	0.051
Longitude (deg)	-65.053	-65.141	0.088

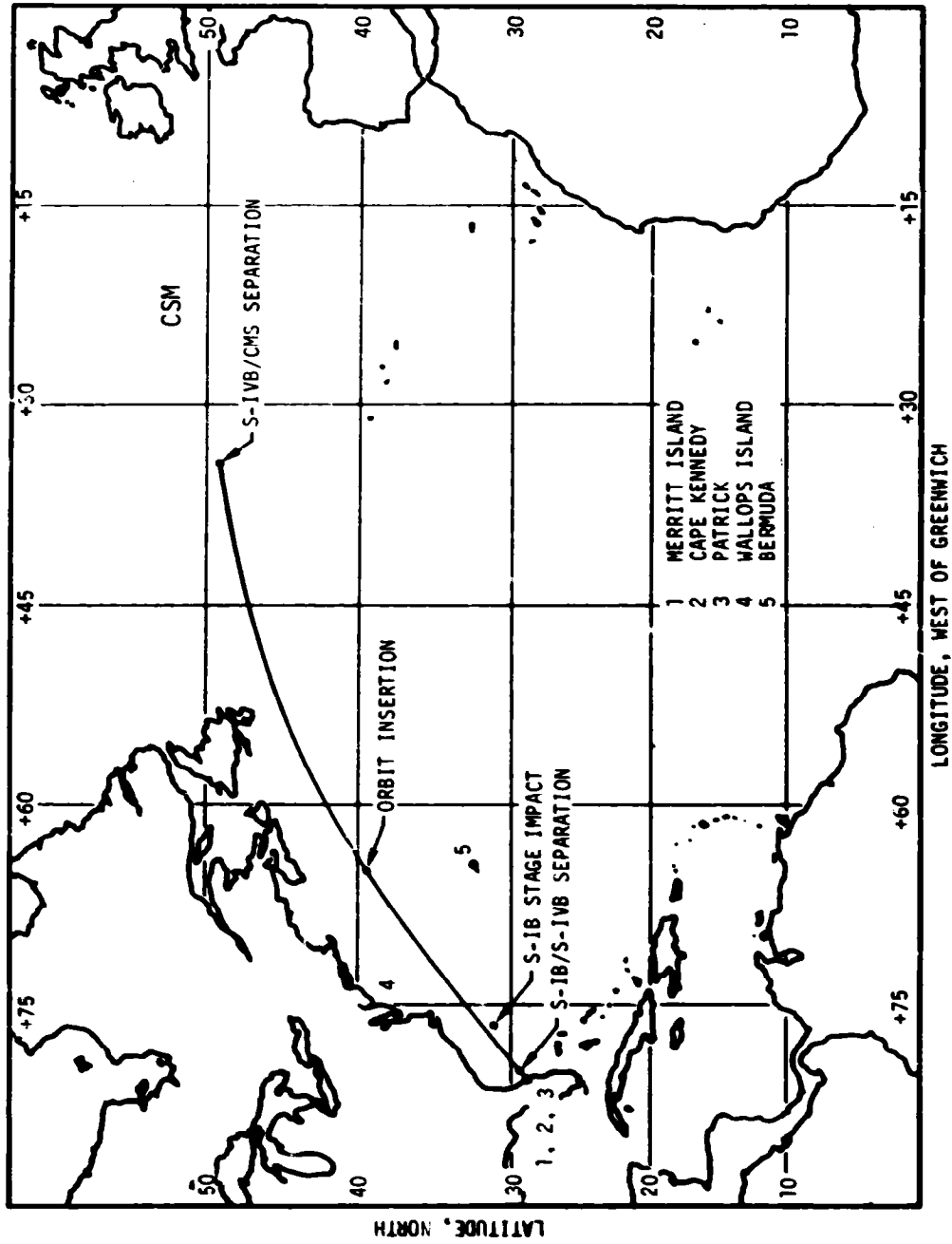


Figure 4-5. Launch Vehicle Ground Track

## SECTION 5

### S-IVB/IU DEORBIT ANALYSIS

#### 5.1 SUMMARY

All aspects of the S-IVB/IU deorbit were accomplished successfully. The deorbit trajectory altitude was slightly higher than the real time predicted value resulting in an impact slightly downrange of nominal. These dispersions were small enough that impact actually did occur within the real time predicted footprint. Impact occurred at approximately 21,607 seconds.

#### 5.2 DEORBIT MANEUVERS

Timebase 5 (start of S-IVB/IU deorbit events) was initiated 193.5 seconds earlier than nominal to free communication equipment needed in working Orbital Work Shop problems. During the fourth revolution, with the S-IVB/IU oriented in a retrograde attitude, deorbit was initiated with a LOX dump at approximately 19,460 seconds for a duration of 460 seconds. This was followed 30 seconds later with a schedule LH<sub>2</sub> dump having a duration of 125 seconds. Attitude control was adequately provided by the thrust vector control system of the J-2 engine and the APS during the dumps.

The velocities for the deorbit sequence are presented in Table 5-1, as real time predictions, propulsion reconstructions, and the accumulated telemetered acceleration data from Apollo Range Instrument Aircraft (ARIA). The data presented show that the total retrograde velocity imparted to the S-IVB/IU was within the real time estimated dispersions, although the velocity from the commanded LH<sub>2</sub> dump was outside the real time estimate, see paragraph 7.9.

Table 5-1. S-IVB/IU Deorbit Velocity Comparisons

	LOX ΔV (M/SEC)	LH <sub>2</sub> ΔV (M/SEC)	TOTAL ΔV (M/SEC)
Real time Prediction: Maximum	29.73	6.27	36.00
Nominal	24.55	5.91	30.46
Minimum	19.05	5.37	24.42
Propulsion Reconstructed	23.03	4.63	27.06
Telemetered Accelerometer Data	23.09	4.01	27.10

### 5.3 DEORBIT TRAJECTORY EVALUATION

The deorbit trajectory reconstruction was based on a tracking vector. The LOX and LH<sub>2</sub> dump data used in the reconstruction were taken from the propulsion parameters.

The deorbit trajectory altitude was slightly higher than the real time nominal, as seen in Figure 5-1. This is attributable to the retrograde velocities being slightly lower than nominal. The accumulated effect was that the impact occurred slightly downrange of nominal. This was noted in real time by the Kwajalein radar which tracked the vehicle after the deorbit maneuver and provided a positive confirmation of deorbit.

Attitude control was lost approximately 418 seconds after the LH<sub>2</sub> dump terminated due to depletion of APS Module No. 2 propellants (paragraph 7.10.2). Though the S-IVB/IU tumbled prior to reentry, this did not have a significant effect on the deorbit trajectory or impact location.

### 5.4 IMPACT FOOTPRINT

The actual and real time predicted footprints, including dispersions, are shown in Figure 5-2 for the SA-206 S-IVB/IU impact. Impact occurred in the Pacific Ocean at approximately 21,607 seconds, 787 seconds later than predicted. The delay and downrange aspect of impact are both attributable to the less than predicted retrograde velocities acquired in the scheduled LOX and LH<sub>2</sub> dumps. See Paragraph 7.9.

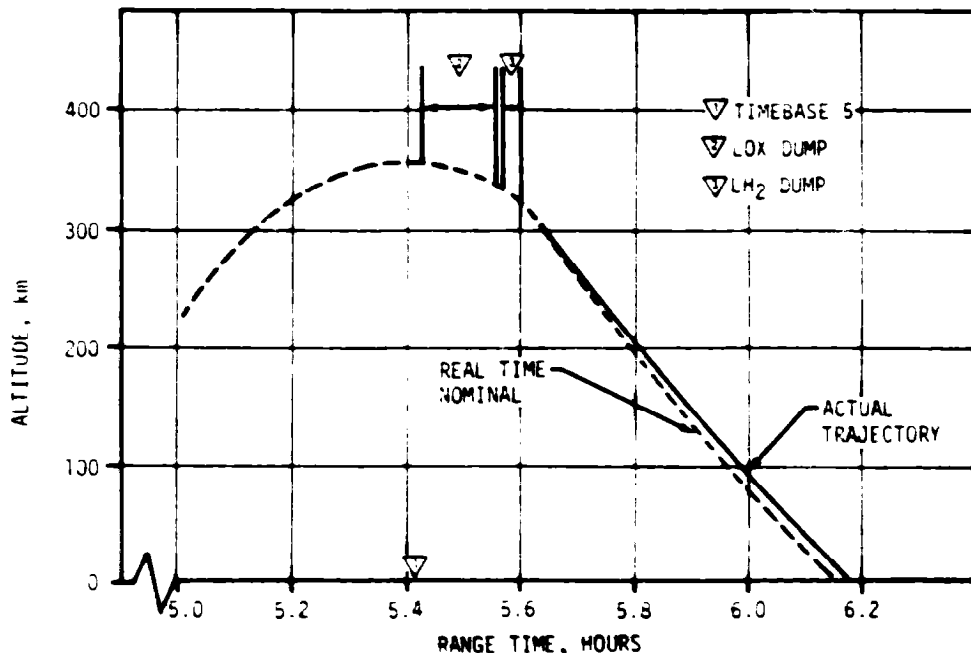


Figure 5-1. S-IVB/IU Deorbit Trajectory Altitude (No Breakup Assumed)

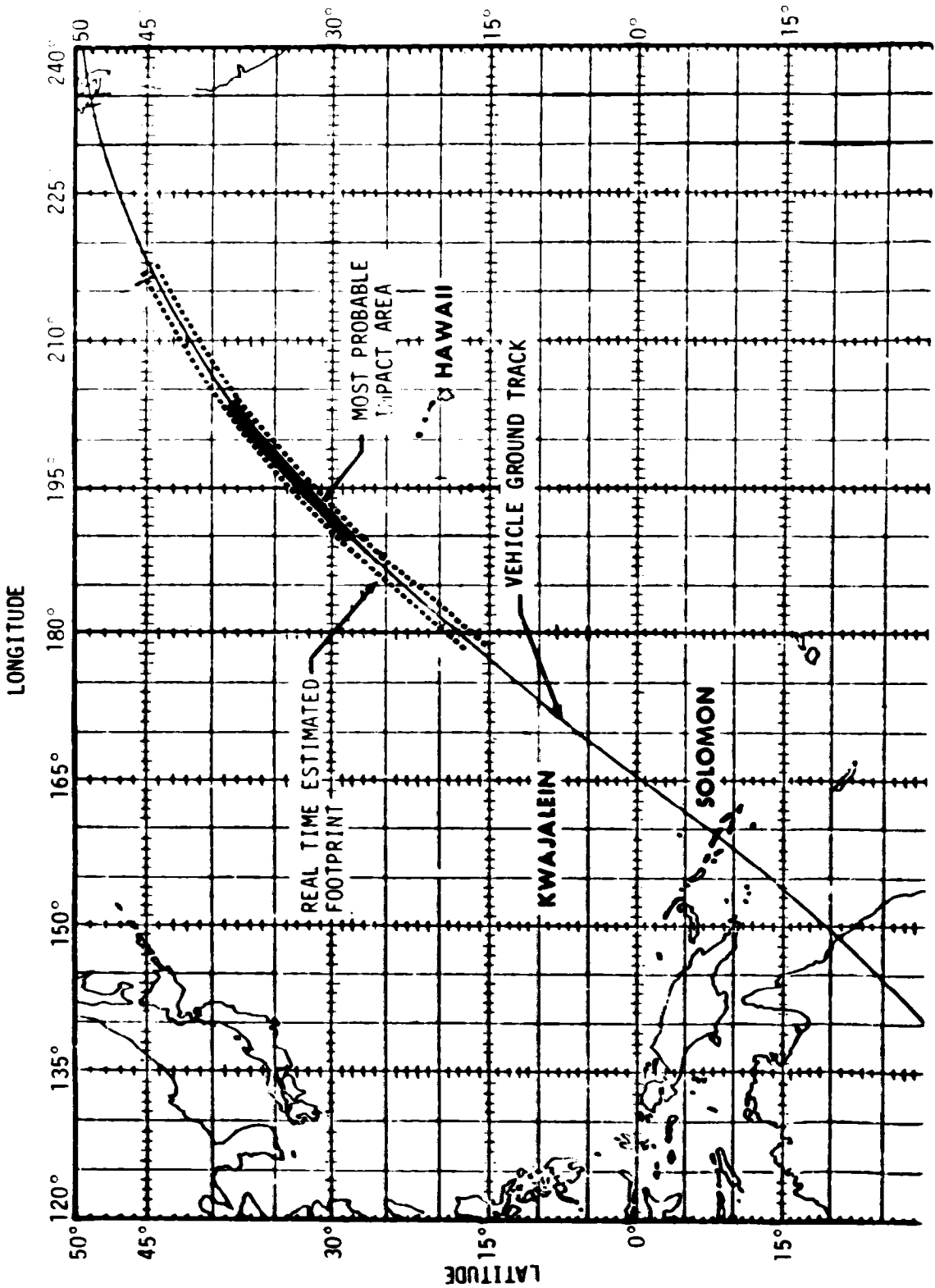


Figure 5-2. S-IVB/IU Impact Footprint

## SECTION 6

### S-IB PROPULSION

#### 6.1 SUMMARY

The S-IB stage propulsion system performed satisfactorily throughout flight. Stage longitudinal site thrust and specific impulse averaged 1.04 percent and 0.3 percent lower than predicted, respectively. Stage LOX, fuel and total propellant flowrate averaged 0.78 percent, 0.70 percent, and 0.76 percent lower than predicted, respectively. Inboard Engine Cutoff (IECO) occurred 0.76 seconds later than predicted. Outboard Engine Cutoff (OECO) was initiated 3.68 seconds after IECO by the deactuation of the thrust OK pressure switches, as planned, of Engine #1. At OECO, the LOX residual was 2916 lbm compared to the predicted 3297 lbm and fuel residual was 6127 lbm compared to the predicted 5986 lbm. The S-IB stage hydraulic system performed satisfactorily.

#### 6.2 S-IB IGNITION TRANSIENT PERFORMANCE

All eight H-1 engines ignited satisfactorily. The automatic ignition sequence, which schedules the engines to start in pairs with a 0.100 second delay between each pair, began with ignition command at -3.055 seconds range time. The start sequence that occurred, while not optimum, was satisfactory. The maximum spread in the start times of engines within a pair was 0.037 seconds and was between Engines 2 and 4 (third pair of engines). The maximum deviation in the planned 0.100 second sequence between pairs was 0.133 seconds and was between the second and third pair. The start sequence of eight engines in four pairs with 0.100 seconds between pairs, while optimum, is not a likely occurrence. Past S-IB start sequences have all been satisfactory but none exactly optimum.

Table 6-1 compares predicted and actual start event times. The individual engine thrust buildup curves are shown in Figure 6-1. The thrust values shown are the total engine thrusts and do not account for cant angles.

#### 6.3 S-IB MAINSTAGE PERFORMANCE

S-IB stage performance was satisfactory although lower than predicted as shown in Figure 6-2. Stage longitudinal site thrust averaged 18,670 pounds (1.04 percent) lower than predicted. Stage specific impulse averaged 0.83 seconds (0.30 percent) lower than predicted. The stage mixture ratio averaged 0.0017 (0.074 percent) lower than predicted. Total propellant flowrate averaged 47.9 lbm/sec (0.76 percent) lower than predicted. These averages were taken between range time zero and IECO.



Table 6-1. S-IB Engine Start Characteristics

ENGINE POSITION AND SERIAL NUMBER	TIME, IGNITION COMMAND TO ENGINE IGNITION SIGNAL (msec)		TIME, ENGINE IGNITION SIGNAL TO THRUST CHAMBER IGNITION (msec)		TIME, ENGINE IGNITION SIGNAL TO P <sub>c</sub> PRIME (msec)	
	ACTUAL (1)	PROGRAMMED	ACTUAL	NOMINAL	ACTUAL	NOMINAL
5 H-406R	105	100	522	584 (2)	857	875 (2)
7 H-4070	105	100	572		882	
6 H-4069	204	200	576		863	
8 H-4072	204	200	557		862	
2 H-7072	303	300	592		934	
4 H-7075	303	300	589		897	
1 H-7071	405	400	554		880	
3 H-7073	405	400	552		859	

(1) Values referenced to event "Time for Ignition Command."  
 (2) Values presented are mean values S-IB-6 through S-IB-12 static test.

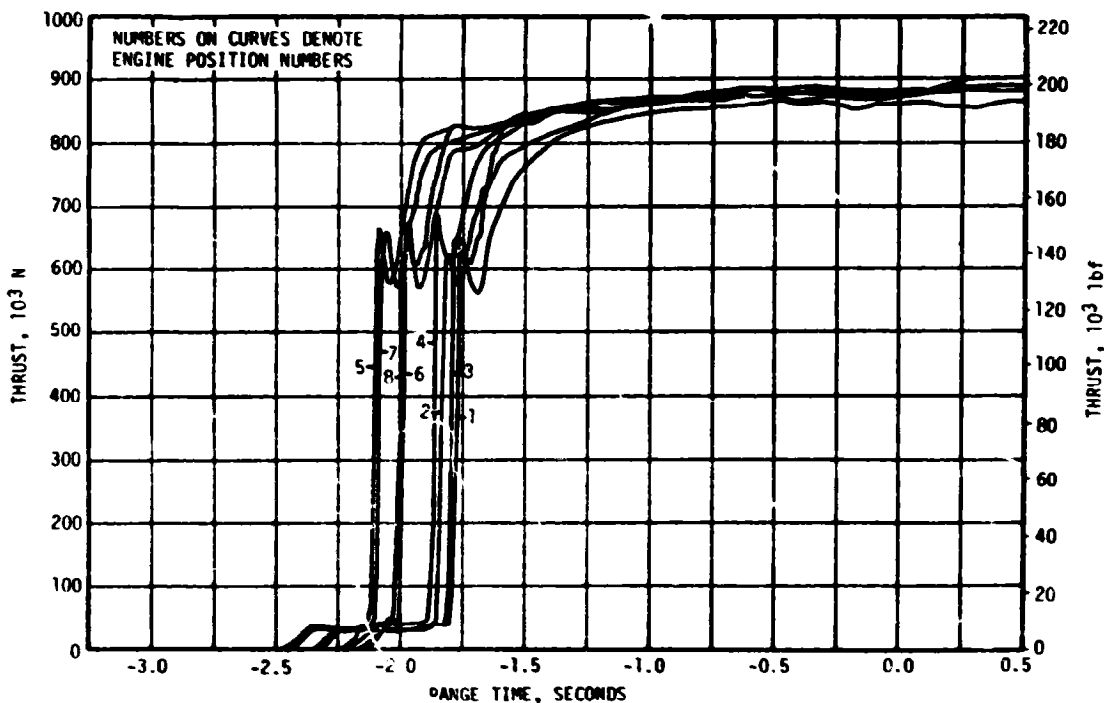


Figure 6-1. S-IB Engines Thrust Buildup

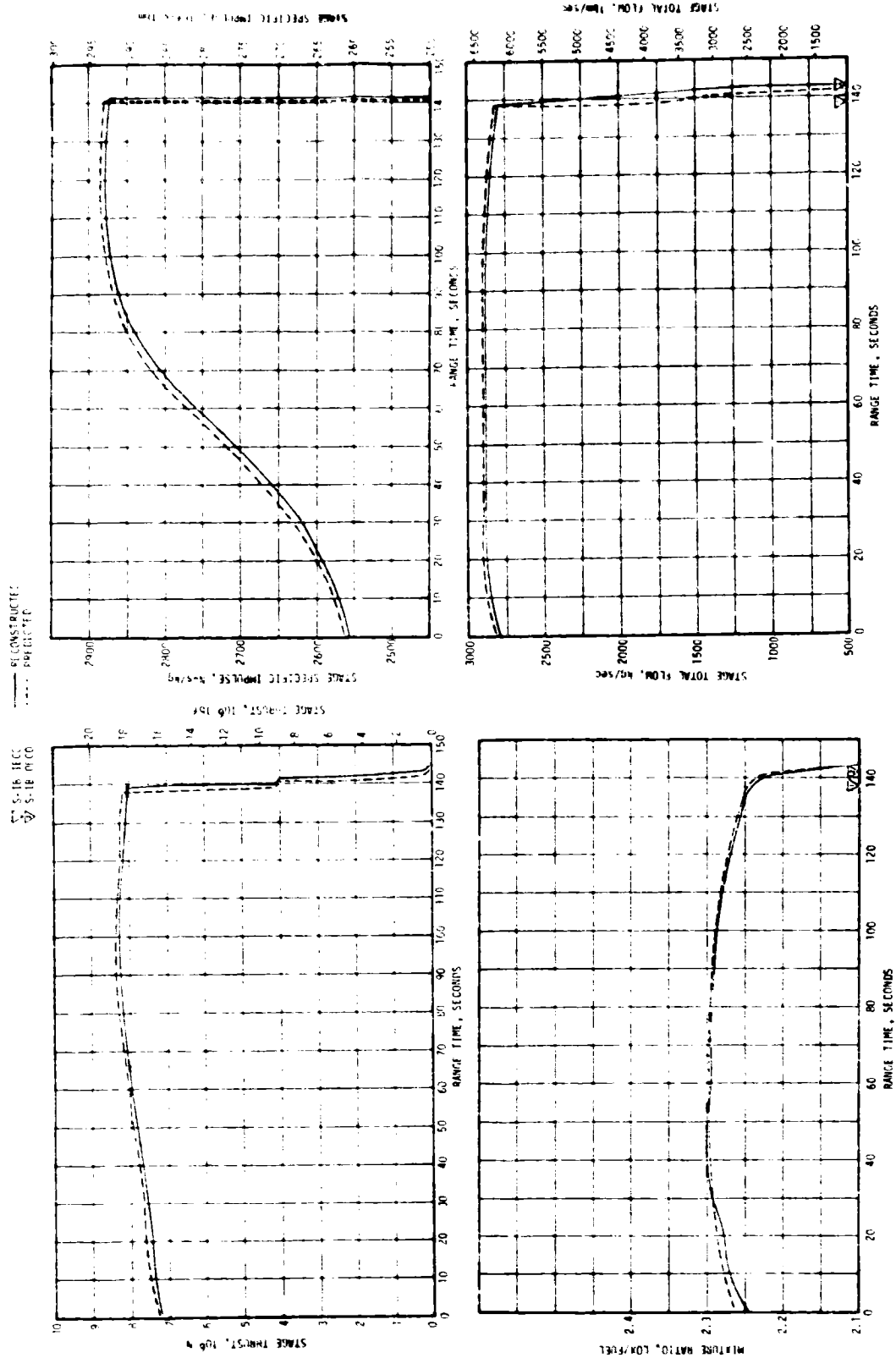


Figure 6-2. S-1B Stage Propulsion Performance

S-IB propulsion system flight performance was determined by reconstructing the flight with the Mark IV computer program: a mathematical model of the Saturn first stage propulsion system which utilizes a table of influence coefficients to determine engine performance. Input data was obtained from telemetry flight measurements and calculated propellant residuals.

The lower than predicted site thrust and specific impulse were primarily the result of the engines performing at lower power levels than expected for rated operating conditions, although colder fuel and hotter LOX than predicted also contributed to the lower site values.

Table 6-2 summarizes the S-IB engines propulsion performance, reduced to standard sea level conditions and compared to the predicted performance and also reduced to standard conditions.

Postflight evaluation of previous Saturn IB flights had shown that the 200 Klbf thrust engines exhibited significantly higher (1.0 percent) thrust and flowrates at rated conditions than those obtained during single engine and stage acceptance tests (ground), although the specific impulse was slightly lower during flight. Therefore, the uprated S-IB-6 engines (205 Klbf thrust) were predicted to have higher sea level thrust values than indicated by the acceptance tests because similar trends were expected. However, sea level thrust values derived from the S-IB-6 flight data, given in Table 6-2, were lower than acceptance test data. Stage static tests for S-IB-6 also showed sea level data lower than the Engine Contractor tests.

Targeting performance for this stage was complicated due to inconsistencies in the different ground tests. Thus, the lower flight performance may be a result of the same inconsistencies and not the unique flight performance of 205 Klbf H-1 engines.

Engine #1 gearcase lubricant pressure experienced unexpected inflight pressure shifts of approximately +8, +13, and -8 psi at 2, 28, and 93 seconds range time (Figure 6-3). The fourth step (at 138 seconds) is a normal response to Inboard Engine Cutoff.

The first three pressure steps are not completely unusual, the same type having been observed during flight on Engine Position 2 of SA-205. Also, at least 14 prior cases of abrupt change in gearcase lubricant pressure have been observed during static testing at the Engine Contractor site. All such perturbations were determined to have been caused by partial restriction of individual bearing jets by particles remaining in the lube system passages from the casting process or introduced during turbopump assembly. Improved procedures for flushing these passages and maintaining them in a clean condition have been implemented to correct this condition. No evidence of damage due to jet restriction has been experienced because redundancy is provided by multiple lubrication jets in addition to splash lubrication from the gears to the bearings. No corrective action is considered necessary because no evidence of damage has been experienced with

Table 6-2. S-IB Individual Engine Propulsion Performance\*

ENGINE NO.	THRUST (LBF)			SPECIFIC IMPULSE (LBF-SEC/LBM)			LOX FLOWRATE (LBM/SEC)			FUEL FLOWRATE (LBM/SEC)			MIXTURE RATIO O/F		
	PRED	ACTUAL	% DIFF	PRED	ACTUAL	% DIFF	PRED	ACTUAL	% DIFF	PRED	ACTUAL	% DIFF	PRED	ACTUAL	% DIFF
1	206,061	202,292	-1.829	262.474	261.58	-0.341	542.68	534.66	-1.478	242.39	238.67	-1.535	2.2388	2.2401	+0.058
2	204,186	204,233	+0.023	262.901	262.09	-0.308	536.09	539.16	+0.573	240.58	240.07	-0.212	2.2284	2.2458	+0.781
3	205,554	202,728	-1.375	262.580	261.85	-0.278	542.56	536.74	-1.073	240.62	237.46	-1.313	2.2582	2.2603	+0.093
4	204,539	203,897	-0.314	262.469	261.55	-0.350	537.78	539.24	+0.271	241.51	240.33	-0.489	2.2268	2.2437	+0.759
5	206,334	203,781	-1.237	263.005	262.32	-0.260	543.71	538.55	-0.949	240.82	238.30	-1.046	2.2577	2.2599	+0.097
6	205,533	203,908	-0.791	262.598	262.05	-0.209	542.43	539.45	-0.549	240.28	238.66	-0.674	2.2576	2.2603	+0.120
7	205,552	203,839	-0.833	263.299	262.74	-0.212	542.20	539.02	-0.586	238.48	236.79	-0.709	2.2736	2.2802	+0.290
8	205,236	203,828	-0.686	263.030	262.52	-0.194	540.93	538.47	-0.455	239.35	237.95	-0.585	2.2599	2.2629	+0.133
Avg	205,374	203,563	-0.881	262.794	262.08	-0.272	541.04	538.15	-0.534	240.50	238.53	-0.819	2.2501	2.2566	+0.289

\*Performance levels reduced to standard sea level conditions. Data taken at 30 seconds.

Standard sea level conditions:

LOX density (970.79 lbm/ft<sup>3</sup>)  
 Fuel density (50.45 lbm/ft<sup>3</sup>)  
 Ambient pressure (14.67 psia)  
 Fuel pump inlet pressure (57.00 psia)  
 LOX pump inlet pressure (6500 psia)  
 Fuel temperature (60.0°F)

6-3

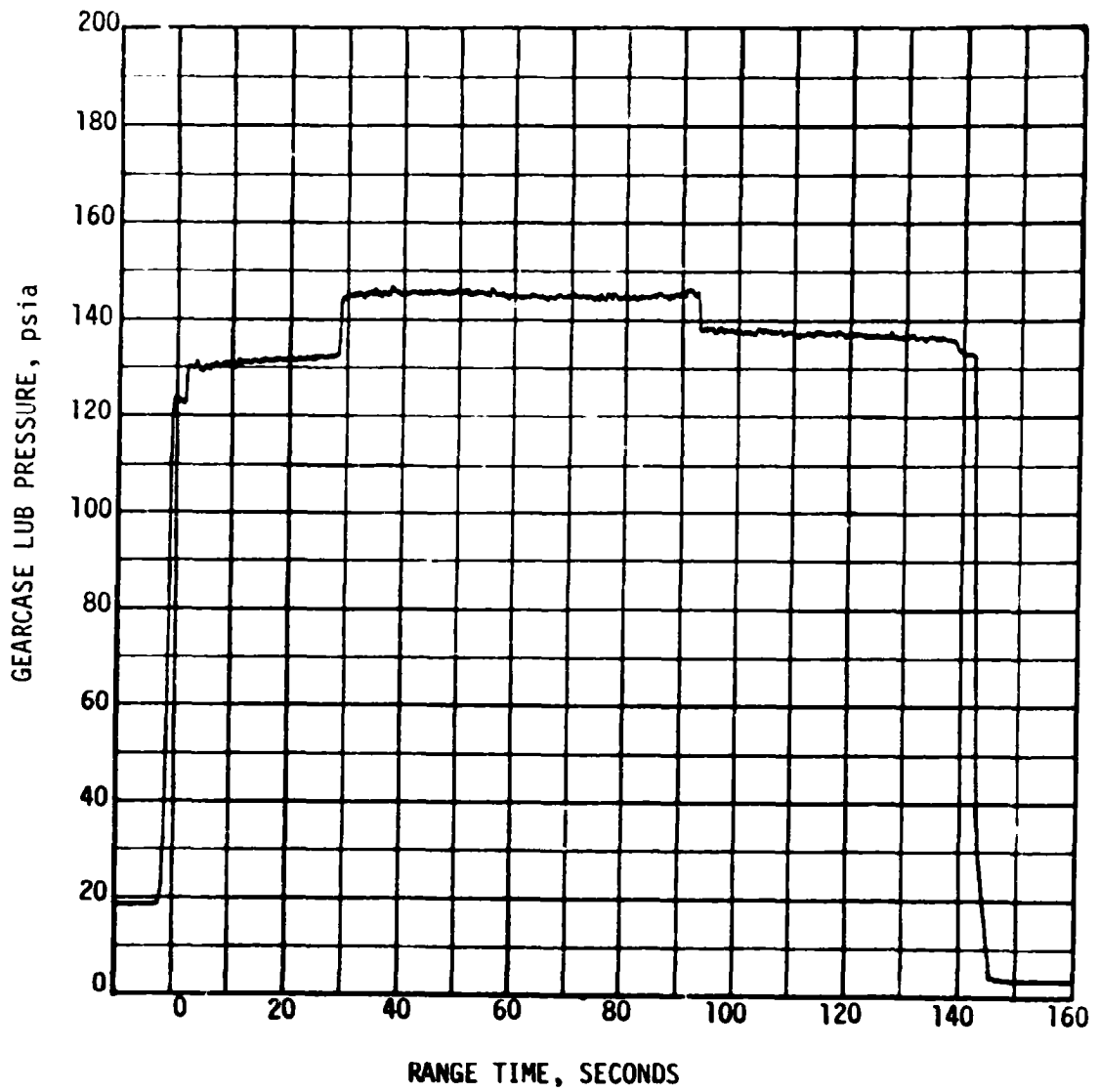


Figure 6-3. H-1 Engine Position #1 Gearcase Lubricant

partially and even completely blocked bearing lube jets. The other seven gearcase lubricant pressures were normal throughout the flight.

Although contamination in this system is apparently not an unsafe condition, any contamination is a significant concern. The Engine Contractor will review the cleaning, assembly, and test histories for the engines assigned to the remaining Saturn IB missions to provide assurance that contamination will not exceed acceptable levels.

#### 6.4 S-IB SHUTDOWN TRANSIENT PERFORMANCE

The cutoff sequence on the S-IB-6 stage began at 135.34 seconds with the actuation of the low-level sensor in LOX tank 02. IECO was initiated 3.32 seconds later by the LVDC at 138.66 seconds. IECO was 0.76 second later than predicted. The longer than predicted burn time to IECO was the result of engine rated power levels lower than predicted, LOX warmer than predicted, and the fuel colder than predicted.

Thrust decay on each inboard engine was normal. The total IECO impulse was 267,520 lbf-sec compared to the predicted impulse of 279,638 lbf-sec. Inboard engine total thrust decay is shown in Figure 6-4.

LOX starvation was experienced by the four outboard engines. OECO was initiated by deactuation of a thrust OK pressure switch on Engine 1 and OECO occurred at 142.34 seconds. The predicted time differential between IECO and OECO was 3.00 seconds. The actual time differential was 3.69 seconds. The 0.68 seconds greater IECO-OECO delta time was caused by the combined effects of (1) early T<sub>2</sub>-IECO timer, (2) lower LOX flowrate, lower fuel temperature, higher LOX temperature, and less LOX residual than predicted, (3) greater center-to-outer tank height differential.

Thrust decay of each outboard engine was normal. See Figure 6-5. Total cutoff impulse for the outboard engines was 184,987 lbf-sec, compared to the predicted impulse of 207,444 lbf-sec.

#### 6.5 S-IB STAGE PROPELLANT MANAGEMENT

Propellant management is the relationship of the propellant consumed to propellant loaded, and is an indication of the propulsion system performance and the capability of the propellant loading system to load the proper propellant weights. The predicted and actual (reconstructed) percentages of loaded propellants utilized during the flight are shown in Table 6-3.

The planned mode of OECO was by LOX starvation to be detected by the engines thrust OK switches. The LOX and fuel level cutoff probe heights and flight sequence settings were determined for a 3.00 second time interval between cutoff probe actuation and IECO. The planned time interval between IECO and OECO was 3.00 seconds. OECO was to be

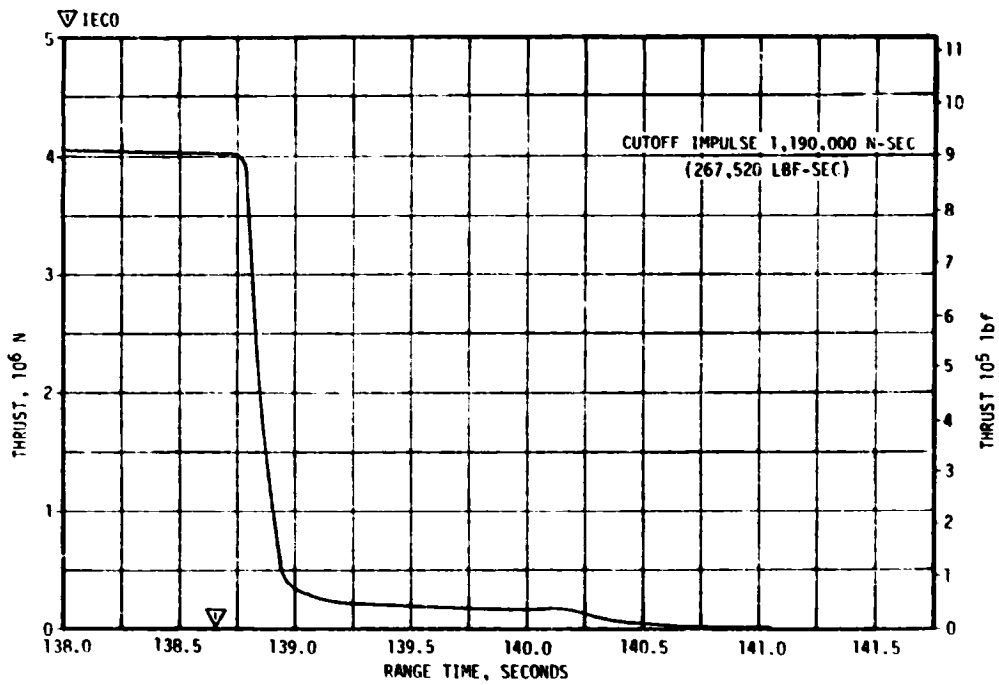


Figure 6-4. S-IB Inboard Engine Total Thrust Decay

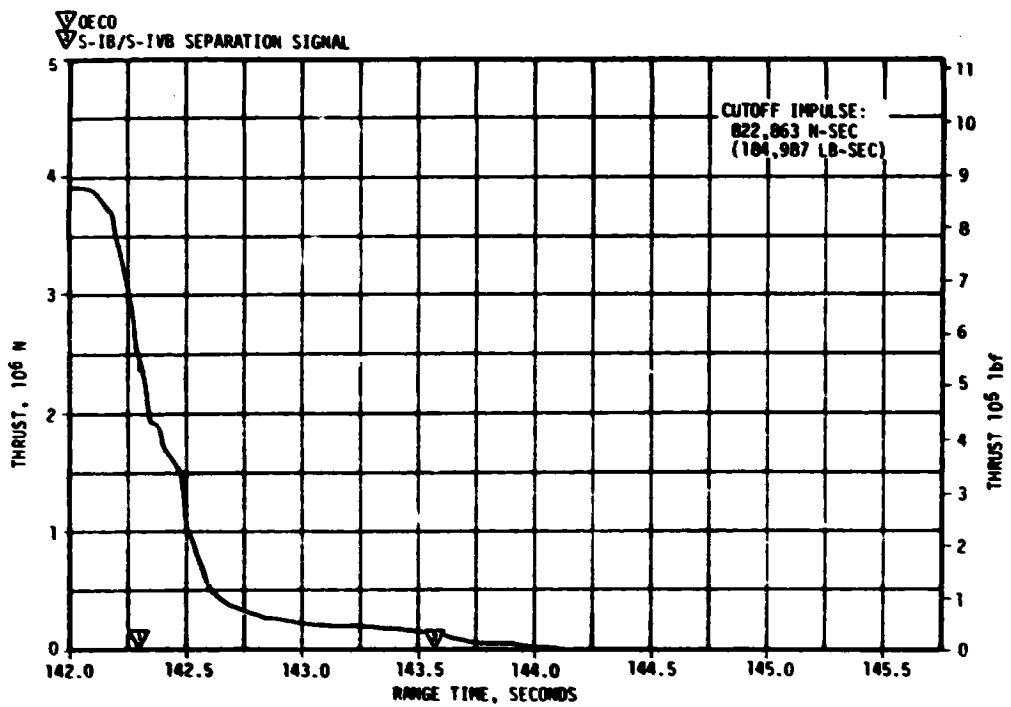


Figure 6-5. S-IB Total Outboard Engine Total Thrust Decay

Table 6-3. S-IB Propellant Usage

PROPELLANT	PREDICTED (%)	ACTUAL (%)
Total	99.20	99.21
Fuel	98.34	98.26
LOX	99.58	99.64

initiated by the deactuation of two of the three thrust OK pressure switches on any outboard engine as a result of LOX starvation. It was assumed that approximately 271 gallons of LOX in the outboard suction lines were usable. The backup timer (flight sequencer) was set to initiate OEEO 13.00 seconds after initiation of T2.

To prevent fuel starvation, fuel depletion cutoff probes were located in fuel tanks F2 and F4 container sumps. The center LOX tank sump orifice was  $19.0 \pm .005$  inches in diameter, and a liquid level height differential of approximately 3.0 inches between the center and outboard LOX tanks was predicted at IEEO (Center tank level higher).

The fuel bias for S-IB-6 was 1550 lbm. This fuel weight, included in the predicted residual, was available for consumption to minimize propellant residual due to off-nominal conditions and was not expected to be used during a nominal flight.

Data used in evaluating the S-IB stage propellant usage consisted of two discrete probe racks of fifteen probes each in tanks F1 and F3; three probes in OC, O1, and O3; cutoff level sensors in tanks O2, O4, F2, and F4; and fuel depletion probes in the F2 and F4 sumps.

The cutoff sequence on S-IB-6 was initiated by a signal from the cutoff level sensor in tank O2 at 135.34 seconds. The IEEO signal was received 3.32 seconds later at 138.66 seconds. OEEO was initiated 3.68 seconds after IEEO at 142.34 seconds by the Engine #1 thrust OK pressure switches. Fuel depletion probes were not actuated prior to retro motor ignition.

Based on discrete probe data, liquid levels in the fuel tanks were nearly equal and approximately 23.2 inches above theoretical tank bottom at IEEO. This level represents a mass of 11,012 lbm of fuel onboard. At that time 11,401 lbm of LOX remained onboard. Corresponding liquid height in the center tank was approximately 15.3 inches and average height in the outboard tanks was approximately 10.7 inches above theoretical tank bottom. Propellants remaining above the main valves after outboard engine decay were 2394 lbm of LOX and 4803 lbm of fuel. Predicted values for these quantities were 2650 lbm of LOX and 4630 lbm of fuel.

Total LOX and fuel masses above the main propellant valves beginning at ignition command are shown in Figures 6-6 and 6-7. A summary of the



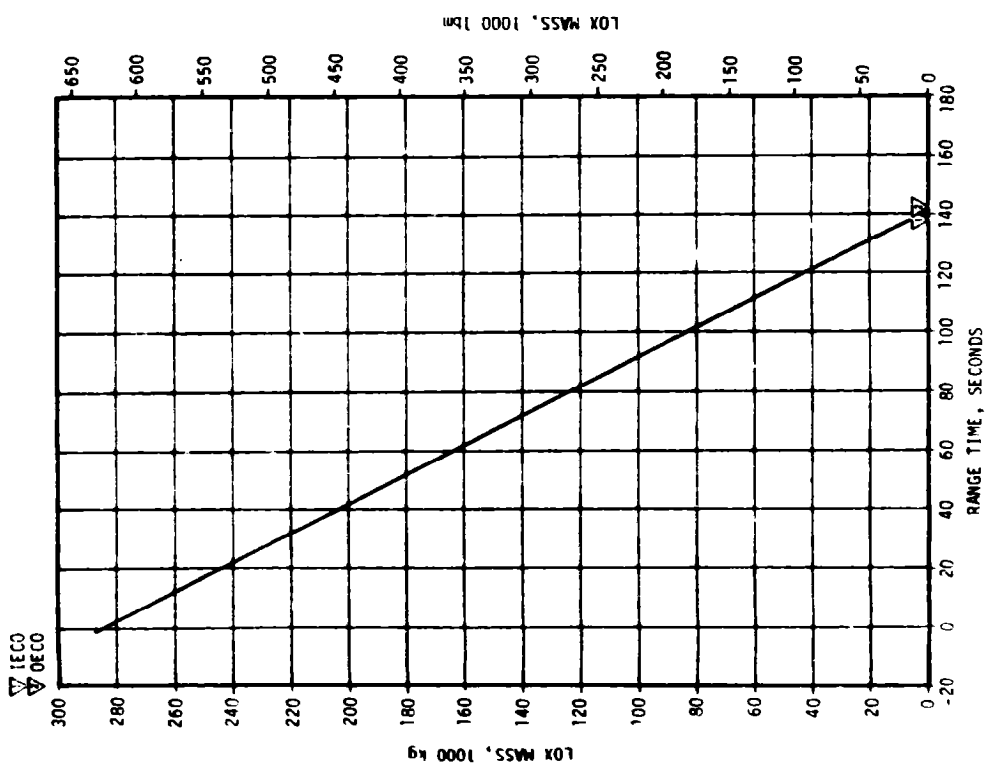
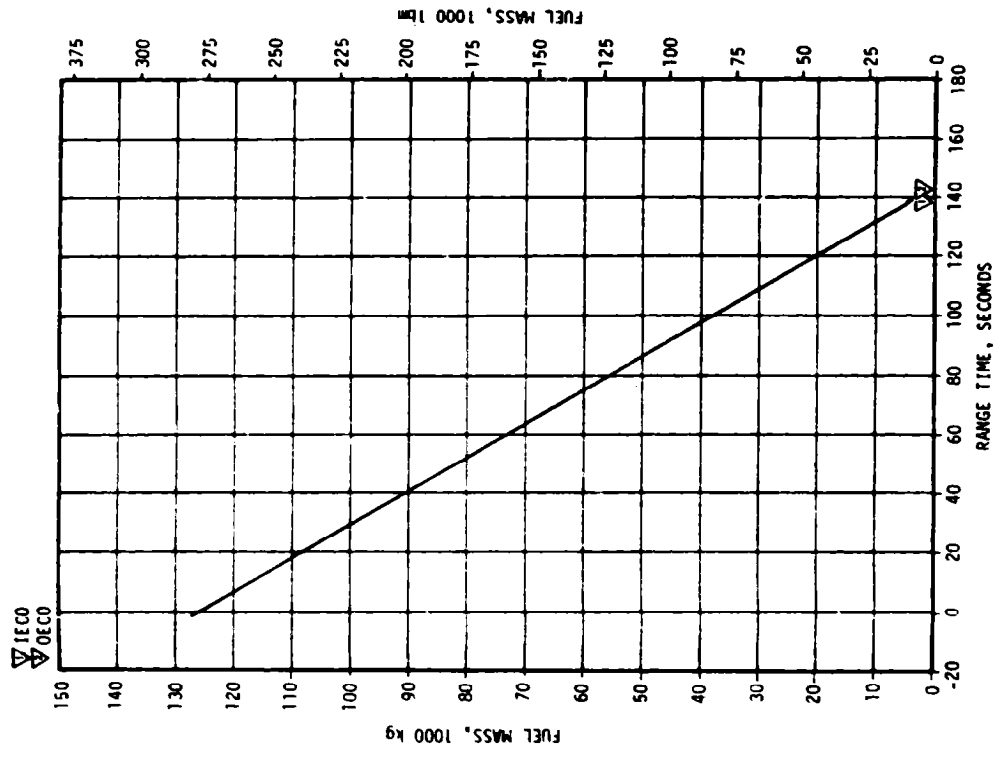


Figure 6-6. S-IB Stage LOX Mass Above Main LOX Valve Figure 6-7. S-IB Stage Fuel Mass Above Main Fuel Valve

propellants remaining at major event times is presented in Table 6-4.

Table 6-4. S-IB Propellant Mass History

EVENT	PREDICTED (LBM)			RECONSTRUCTED (LBM)		
	FUEL	LOX	TOTAL	FUEL	LOX	TOTAL
Ignition Command	279,579	632,016	911,595	280,167	632,041	912,208
IU Umbilical Disconnect	276,314	620,974	897,288	276,422	619,885	896,307
IECO	10,243	10,436	20,679	11,012	11,401	22,413
OECO	5,986	3,297	9,284	6,127	2,916	9,043
Separation	4,898	2,734	7,632	5,075	2,476	7,551
Zero Thrust	4,630	2,650	7,280	4,803	2,394	7,197

## 6.6 S-IB PRESSURIZATION SYSTEM

### 6.6.1 Fuel Pressurization System

The fuel tank pressurization system performed satisfactorily during the entire flight. With the exception of the sonic nozzle in the fuel pressurization system, the helium blowdown system was the same as that of S-IB-5 which included two 19.28 ft<sup>3</sup> spheres, light-weight tanks, and vent valves. The nozzle orifice diameter was increased from 0.210/0.211 inches to 0.220/0.221 inches to accommodate the higher fuel flow rates required from uprating the engines. The fuel pump inlet pressure met the minimum net positive suction pressure (NPSP) requirement throughout flight.

A comparison of measured ullage pressure and nominal pressure is presented in Figure 6-8. Ullage pressure compared favorably to the nominal pressure during the flight and at no time exceeded a difference of 2.3 psi from the nominal pressure. No vent cycling during flight was observed.

Fuel vent valves 1 and 2 closed at the beginning of the prepressurization sequence and they remained closed. Because of the system cooling, the pressurization valves opened three times for repressurizing. The fuel tank helium pressurization sphere pressure was 2970 psia at ignition and decayed as expected during the flight. See Figure 6-9.

### 6.6.2 LOX Tank Pressurization System

The LOX tank pressurization system performed satisfactorily during the SA-20C flight. The LOX pump inlet pressure met the minimum NPSP requirement throughout flight.

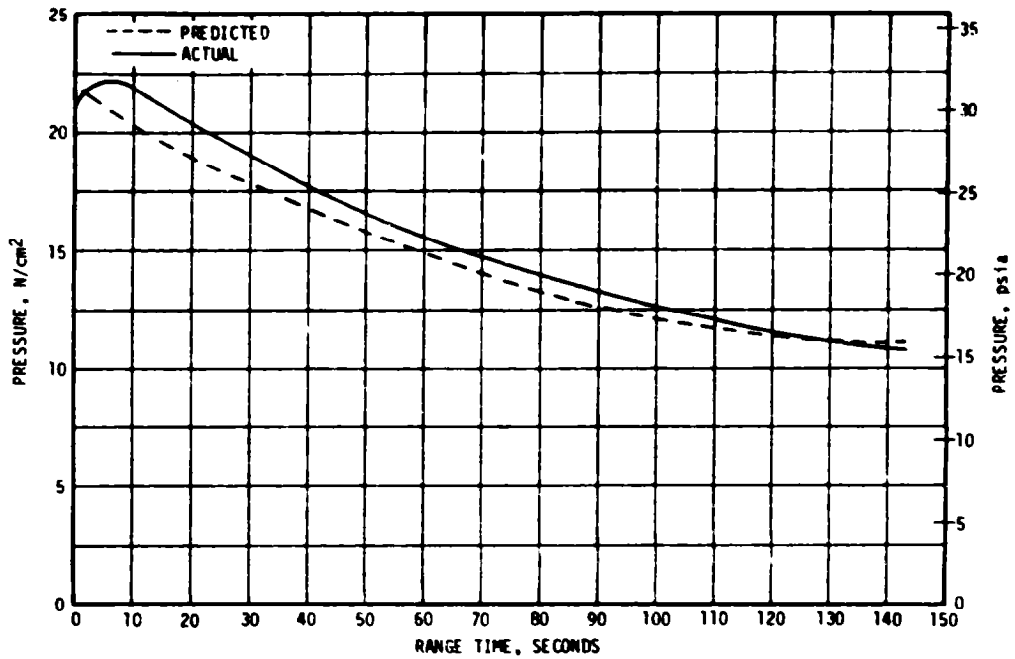


Figure 6-8. S-IB Fuel Tank Ullage Pressure

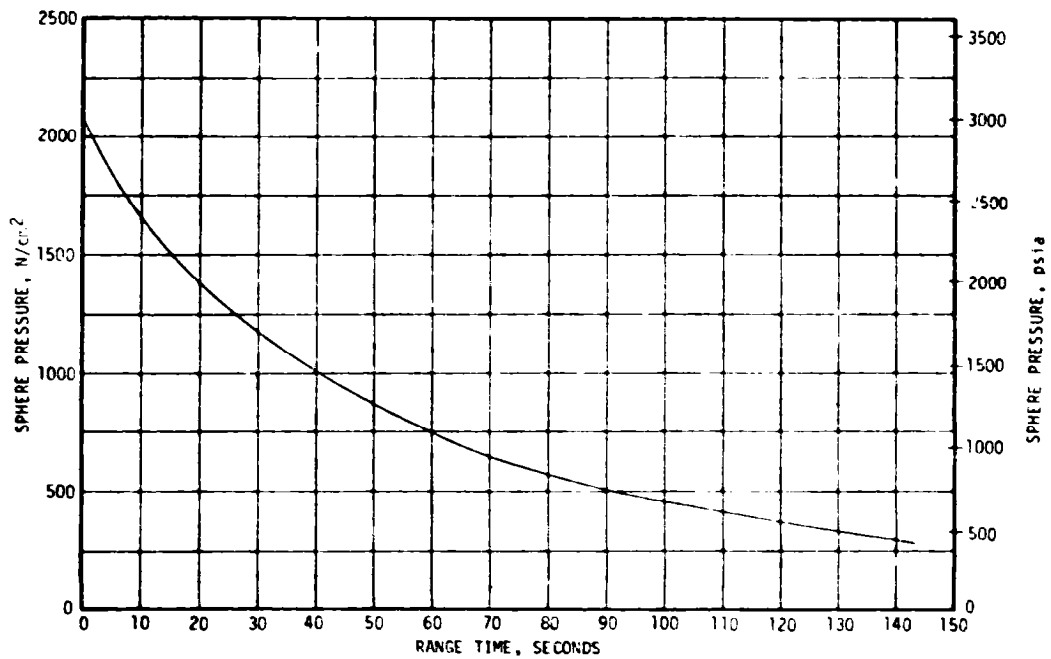


Figure 6-9. S-IB Fuel Tank Helium Pressurization Sphere Pressure

Initial pressurization started at T-103 seconds and continued for 73.3 seconds. The LOX tank pressurizing switch which has an actuation range of  $57.7 \pm 0.8$  psia actuated for 6 prepressurization cycles. The reconstructed LOX tank ullage volume prior to vent closure was 1,047 gallons (1.56 of ullage volume). Orifice bypass flow was initiated at T-2.4 seconds.

The center LOX tank pressure during flight, compared with the predicted LOX tank pressure, is shown on Figure 6-10. The predicted pressure was derived from static test data and from SA-201 through SA-205 flight results.

The lowest LOX tank ullage pressure was approximately 47 psia as a result of engine start. Maximum pressure of approximately 52.3 psia occurred at 30 seconds. Ullage pressure had decayed to 48.3 psia at IEEO. No venting was noted during powered flight.

The GFCV started to close at ignition, and after the normal hesitations during the start transient, reached the full closed position at 20 seconds and remained closed until 83 seconds, at which time the decreased LOX tank pressure caused the valve to start opening (Figure 6-11). At IEEO the valve was approximately 15 percent open. The pressure and temperature upstream of the GFCV were as expected and indicated nominal GOX flowrate.

#### 6.7 S-IB PNEUMATIC CONTROL PRESSURE SYSTEM

The S-IB pneumatic control pressure system supplied  $\text{GN}_2$  at a regulated pressure of 770-785 psia to pressurize the H-1 engine turbopump gearboxes and to purge the LOX and lube seal cavities and two radiation calorimeters. This regulated pressure was also used to close the LOX and fuel prevalves at IEEO and OEEO.

The 750 psig regulator was replaced during prelaunch checkout and system performance was satisfactory during prelaunch and flight. The actual sphere pressure remained within the acceptable band as shown in Figure 6-12.

#### 6.8 S-IB HYDRAULIC SYSTEM

The performance of the hydraulic system was satisfactory. The four outboard H-1 engines were gimbal mounted to the S-IB stage thrust structure. Controlled positioning of these engines by means of hydraulic actuators provided thrust vectoring for vehicle attitude control. The force required for actuator movement is provided by four independent closed-loop hydraulic systems.

The system pressures were satisfactory during flight and were similar to those of the SA-205 flight. At zero seconds the system pressures ranged from 3245 to 3310 psig. The pressure decreased approximately

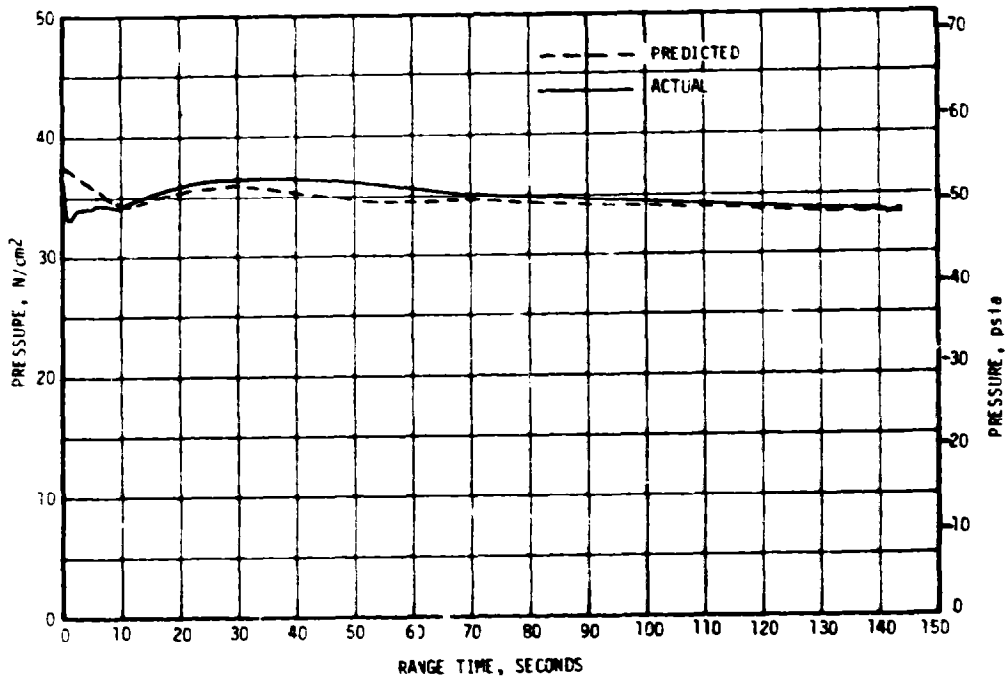


Figure 6-10. S-IB Center LOX Tank Ullage Pressure

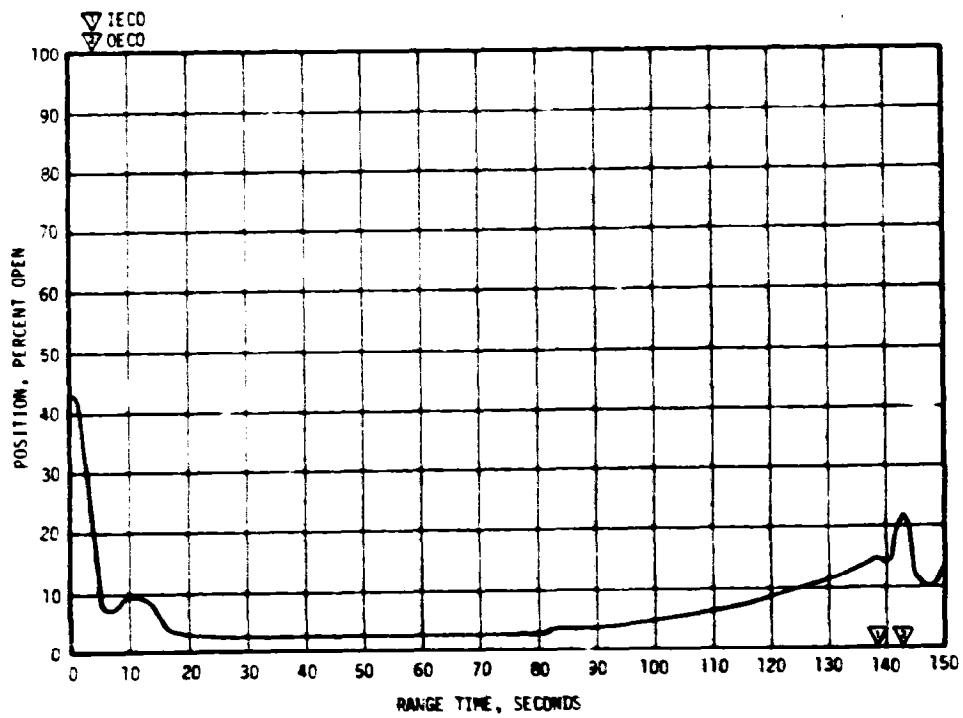


Figure 6-11. GOX Flow Control Valve Position

55 psi on each engine during flight, which is normal and is due to the main pump temperature increase during the flight.

Reservoir oil levels were also similar to those of the SA-205 flight. There was a rise of approximately 3 percent in each level during flight indicating about 20°F rise in each hydraulic system's average oil temperature (not reservoir oil temperature).

The reservoir oil temperatures were satisfactory during flight and at liftoff averaged 120°F as compared to an average of 133°F for the four S-IB-5 hydraulic systems. The average reservoir temperature decrease during the flight was 16°F as compared to a decrease of 17°F for the four S-IB-5 hydraulic systems.

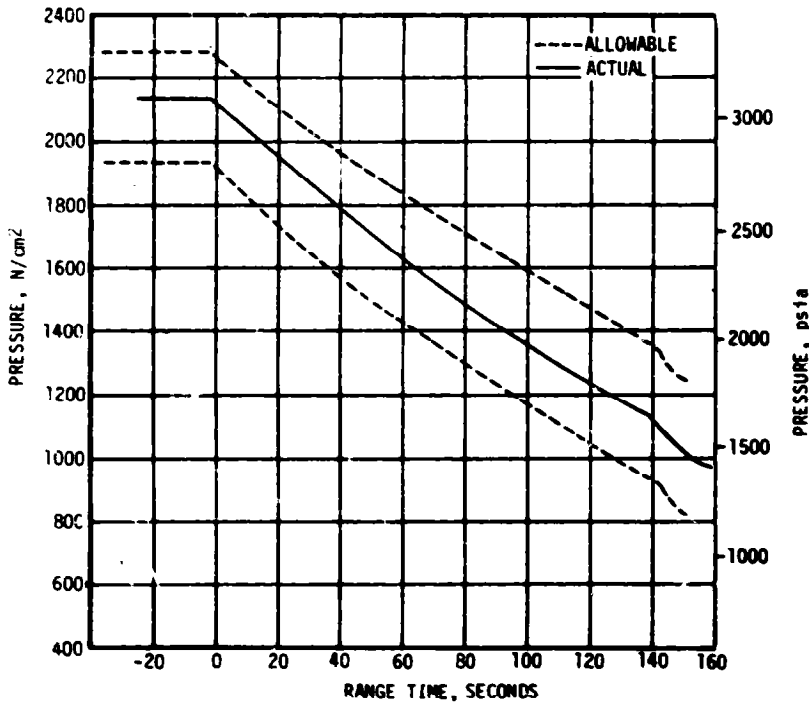


Figure 6-12. S-IB Pneumatic Control Pressure

## SECTION 7

### S-IVB PROPULSION

#### 7.1 SUMMARY

The S-IVB propulsion system performed satisfactorily throughout the operational phase of burn and had normal start and cutoff transients. S-IVB burn time was 440.4 seconds, 2.5 seconds longer than predicted for the actual flight azimuth of 47.6 degrees. This difference is composed of -0.15 seconds due to higher than expected S-IB/S-IVB separation velocity and +2.65 seconds due to lower than predicted S-IVB performance. The engine performance during burn, as determined from standard altitude reconstruction analysis, deviated from the predicted Start Tank Discharge Valve (STDV) open +60 second time slice by -0.64 percent for thrust and +0.05 percent for specific impulse. The S-IVB stage Engine Cutoff (ECO) was initiated by the Launch Vehicle Digital Computer (LVDC) at 586.3 seconds. The S-IVB residuals at engine cutoff were near nominal. The best estimate of the engine cutoff residuals is 2873 lbm for LOX and 2223 lbm for LH<sub>2</sub> as compared to the predicted values of 3314 lbm for LOX and 2046 lbm for LH<sub>2</sub>.

Subsequent to burn, the stage propellant tanks were vented satisfactorily.

The impulse derived from the LOX and fuel dumps was sufficient to satisfactorily deorbit the S-IVB/IU. The total impulse provided was 88,360 lbf-sec with a LOX dump impulse contribution of 75,610 lbf-sec and a fuel dump impulse contribution of 12,750 lbf-sec.

A disturbing force on the S-IVB/IU, coincident with LOX tank venting in T<sub>5</sub> (following propellant dumps), caused unplanned firings of APS module engines and subsequent propellant depletion in Auxiliary Propulsion System (APS) Module No. 2. Analysis indicates nearly complete blockage of LOX Nonpropulsive Vent (NPV) Nozzle No. 1. The blockage has been attributed to solid oxygen formation at the nozzle inlet during T<sub>4</sub> cyclic LOX relief venting when liquid remaining in the duct was subjected to a freezing environment. No impact due to this anomaly is expected on the Skylab-3 or Skylab-4.

Propellant tank safing after fuel dump was satisfactory.

The APS operation was nominal throughout SA-206 flight. No helium or propellant leaks were observed and the regulators functioned nominally.

Hydraulic system performance was nominal throughout powered flight, orbital coast, and deorbit.

## 7.2 S-IVB CHILLDOWN AND BUILDUP TRANSIENT PERFORMANCE

The thrust chamber temperature at liftoff was  $-215^{\circ}\text{F}$ , which was below the maximum allowable redline limit of  $-185^{\circ}\text{F}$ . At S-IVB Start Tank Discharge Valve (STDV) open signal, the temperature was  $-185^{\circ}\text{F}$ , which was within the requirements of  $-225 \pm 75^{\circ}\text{F}$ .

The chilldown and loading of the engine  $\text{GH}_2$  start tank and pneumatic control bottle prior to liftoff was satisfactory. At liftoff, the engine control sphere pressure and temperature were 3050 psia and  $-180^{\circ}\text{F}$  and the start tank pressure and temperature were 1280 psia and  $-192^{\circ}\text{F}$ . At STDV, the engine control sphere pressure and temperature were 3083 psia and  $-181.4^{\circ}\text{F}$  and the start tank conditions were 1305 psia and  $-189.2^{\circ}\text{F}$ , which was within the start box.

Propellant tank prepressurization was successful and the propellant recirculation systems operation, which was continuous from before liftoff until just prior to Engine Start Command (ESC), was satisfactory. Start and run box requirements for both fuel and LOX were met, as shown in Figure 7-1. At STDV open the LOX pump inlet temperature was  $-294.8^{\circ}\text{F}$  and the ullage pressure was 41.2 psia. At STDV open the fuel pump inlet temperature was  $-421.9^{\circ}\text{F}$  and the ullage pressure was 31.7 psia.

Fuel lead followed the expected pattern and resulted in satisfactory conditions as indicated by the fuel injector temperature.

The engine start transient was satisfactory, and the thrust buildup was within the limits set by the engine manufacturer. This buildup was similar to the thrust buildups observed during previous flights. The Mixture Ratio Control Valve (MRCV) was in the closed position (4.8 Engine Mixture Ratio) during the buildup. The total impulse from STDV open to STDV open +2.4 seconds was 160,893 lbf-s.

## 7.3 S-IVB MAINSTAGE PERFORMANCE

The propulsion reconstruction analysis showed that the stage performance during mainstage operation was satisfactory. A comparison of predicted and actual performance of thrust, specific impulse, total flowrate, and Engine Mixture Ratio (EMR) versus time is shown in Figure 7-2. Table 7-1 shows the thrust, specific impulse, flowrate, and EMR deviations from predicted at the STDV open +60 second time slice at standard altitude conditions.

Specific impulse was slightly greater than predicted. Engine burn time was 440.4 seconds which was 2.5 seconds longer than predicted for the actual flight azimuth of 47.6 degrees. This difference is composed of  $-0.15$  seconds due to higher than expected S-IB/S-IVB separation velocity and  $+2.65$  seconds due to lower than predicted S-IVB performance.



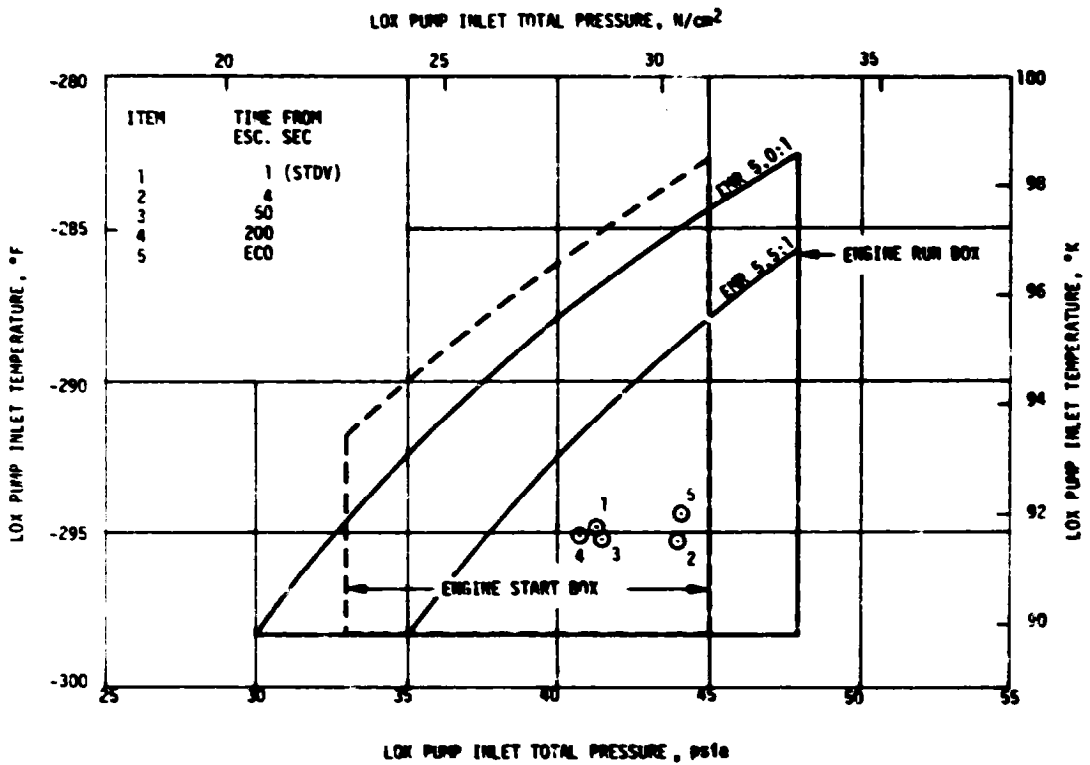
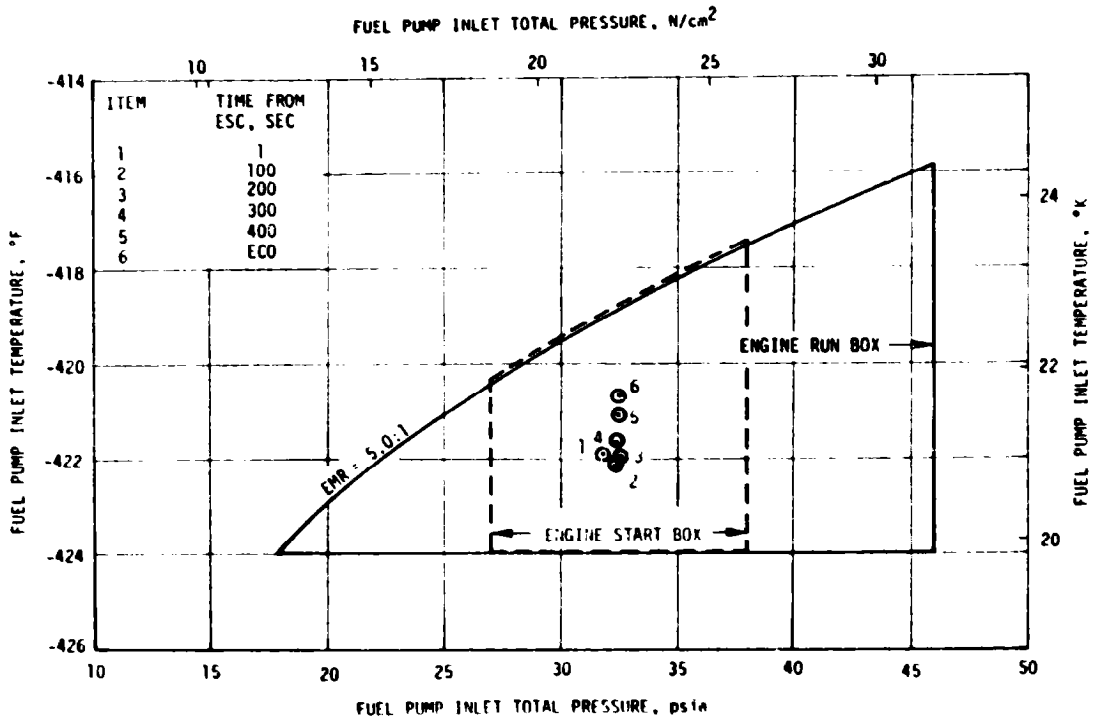


Figure 7-1. S-IV<sub>B</sub> Start Box and Run Requirements

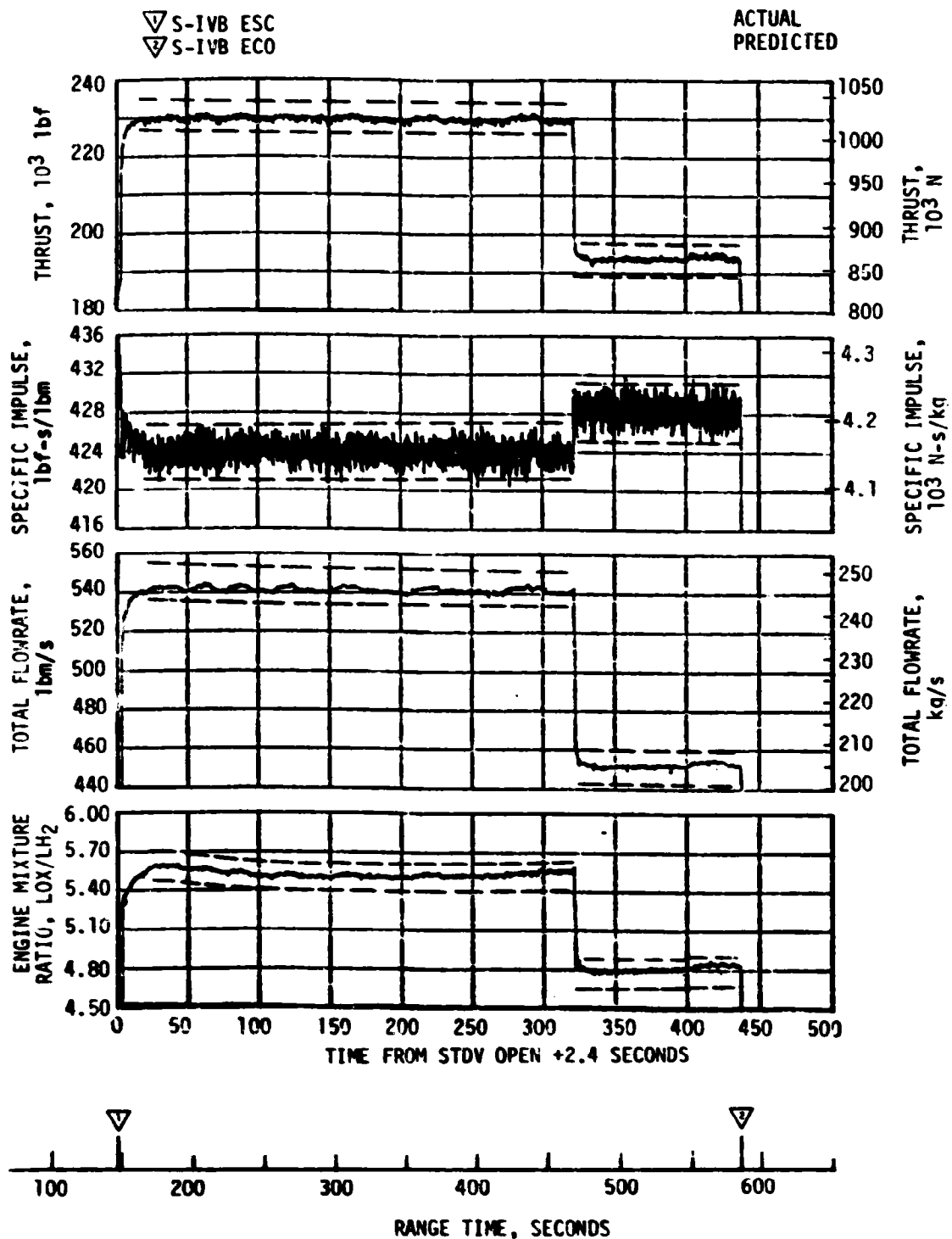


Figure 7-2. S-IVB Steady-State Performance

Table 7-1. S-IVB Steady State Performance (STDV Open +60 Second Time Slice at Standard Altitude Conditions)

PARAMETER	PREDICTED	RECON- STRUCTED	FLIGHT DEVIATION	PERCENT DEVIATION FROM PREDICTED
Thrust, lbf	229,294	227,832	-1462	-0.64
Specific Impulse, lbf-s/lbm	423.4	423.6	+0.2	+0.05
LOX Flowrate, lbm/s	458.78	455.59	-3.19	-0.70
Fuel Flowrate, lbm/s	82.78	82.23	-0.55	-0.66
Engine Mixture Ratio, LOX/fuel	5.542	5.541	-0.001	-0.02

The engine helium control system performed satisfactorily during mainstage operation. The engine control bottle was connected to the stage pneumatic supply bottle. An estimated 0.35 lbm of helium was consumed during burn.

#### 7.4 S-IVB SHUTDOWN TRANSIENT PERFORMANCE

S-IVB ECO was initiated at 586.3 seconds by guidance velocity cutoff command. The ECO transient was satisfactory. The total cutoff impulse to zero thrust was 48,150 lbf-s which was 695 lbf-s lower than the nominal predicted value of 48,845 lbf-s and within the +5320 lbf-s predicted band. Cutoff occurred with the MRCV in the 4.8 EMR position.

#### 7.5 S-IVB STAGE PROPELLANT MANAGEMENT

A comparison of propellant masses at critical flight events, as determined by various analyses, is presented in Table 7-2. At liftoff the best estimate for LOX is 193,931 +538 lbm and the best estimate for LH<sub>2</sub> is 38,307 +165 lbm. The best estimate full load propellant masses were 0.036 percent less for LOX and 0.448 percent greater for LH<sub>2</sub> than predicted. This deviation was well within the required loading accuracy.

Extrapolation of best estimate residuals data to depletion, using the propellant flowrates, indicated that LOX depletion would have occurred approximately 6.24 seconds after the velocity cutoff.

The pneumatically controlled two position Mixture Ratio Control Valve

Table 7-2. S-IVB Stage Propellant Mass History

EVENT	UNITS	PREDICTED		PU INDICATED (CORRECTED)		PU VOLUMETRIC		FLOW INTEGRAL		BEST ESTIMATE	
		LOX	LH <sub>2</sub>	LOX	LH <sub>2</sub>	LOX	LH <sub>2</sub>	LOX	LH <sub>2</sub>	LOX	LH <sub>2</sub>
S-IVB Liftoff	LBM	194000	38136	193984	38268	193941	38258	193893	38379	193931	38307
S-IVB ESC	LBM	194000	38136	193984	38268	193941	38258	193893	38379	193931	38307
S-IVB Cutoff	LBM	3314	2046	2669	2232	2668	2232	2873	2223	2873	2223

The masses shown do not include mass below the main engine valves, as presented in Section 16.

(MRCV) was positioned at the 4.8 EMR engine start position 0.5 seconds after Engine Start Command (ESC) +325.6 seconds where it was commanded to the 4.8 EMR for the remainder of the flight.

## 7.6 S-IVB PRESSURIZATION SYSTEM

### 7.6.1 S-IVB Fuel Pressurization System

The LH<sub>2</sub> pressurization system met all of its operational requirements. The LH<sub>2</sub> pressurization system indicated acceptable performance during prepressurization, boost, burn, earth orbit and deorbit.

The LH<sub>2</sub> tank prepressurization command was received at -119.3 seconds and the tank pressurized signal was received 33.0 seconds later. Following the termination of prepressurization, the ullage pressure reached relief conditions (approximately 31.6 psia) at liftoff, as shown in Figure 7-3.

The LH<sub>2</sub> ullage pressure was 31.7 psia at ESC. The average pressurization flowrate was 0.64 lbm/s until step pressurization, when it increased to 0.92 lbm/s. This provided a total flow of 317.0 lbm during burn. Throughout the burn, the ullage pressure was at relief (31.8 psia), as predicted.

The LH<sub>2</sub> pump inlet Net Positive Suction Pressure (NPSP) was calculated from the pump interface temperature and total pressure. These values

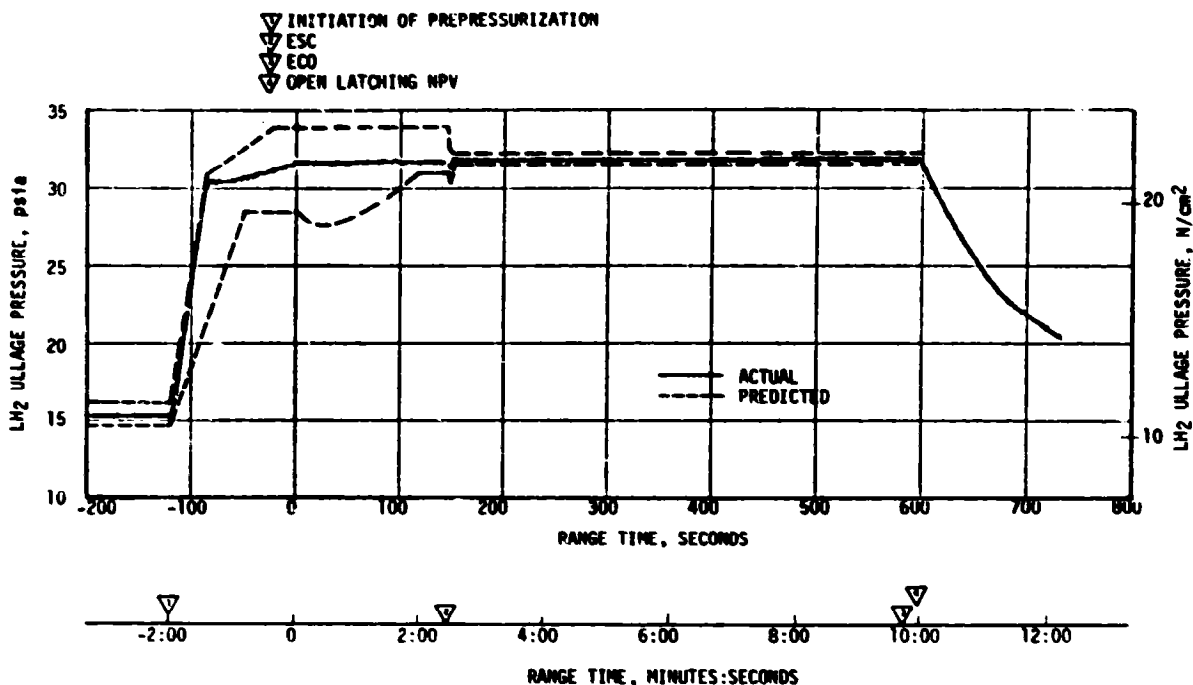


Figure 7-3. S-IVB LH<sub>2</sub> Ullage Pressure - Preliftoff, Boost and Burn

indicated that the NPSP at STDV was 13.8 psi. At the minimum point, the NPSP was 5.6 psi above the minimum required value. Throughout the burn, the NPSP had satisfactory agreement with the predicted values. Figure 7-4 summarizes the fuel pump inlet conditions during burn.

#### 7.6.2 S-IVB LOX Pressurization System

LOX tank prepressurization was initiated at -167 seconds and increased the LOX tank ullage pressure from ambient to 39.3 psia in 16.4 seconds, as shown in Figure 7-5. Two makeup cycles were required to maintain the LOX tank ullage pressure before the ullage temperature stabilized. A total of 6.35 lbm of helium were required for LOX tank prepressurization. At -119 seconds, fuel tank prepressurization and the vent valve purge caused the LOX tank pressure to increase from 38 to 40.8 psia at liftoff.

During boost there was a nominal rate of ullage pressure decay caused by tank volume increase (acceleration effect) and ullage temperature decrease. No makeup cycles could occur because of an inhibit from liftoff +6.0 seconds until ESC -2.5 seconds. LOX tank ullage pressure was 36.6 psia just prior to separation and was increasing at ESC due to a makeup cycle.

During burn, nine over-control cycles were initiated, including the programmed over-control cycle initiated prior to ESC. The LOX tank pressurization flowrate variation was 0.22 to 0.37 lbm/s during under-control and 0.30 and 0.43 lbm/s during over-control system operation. This

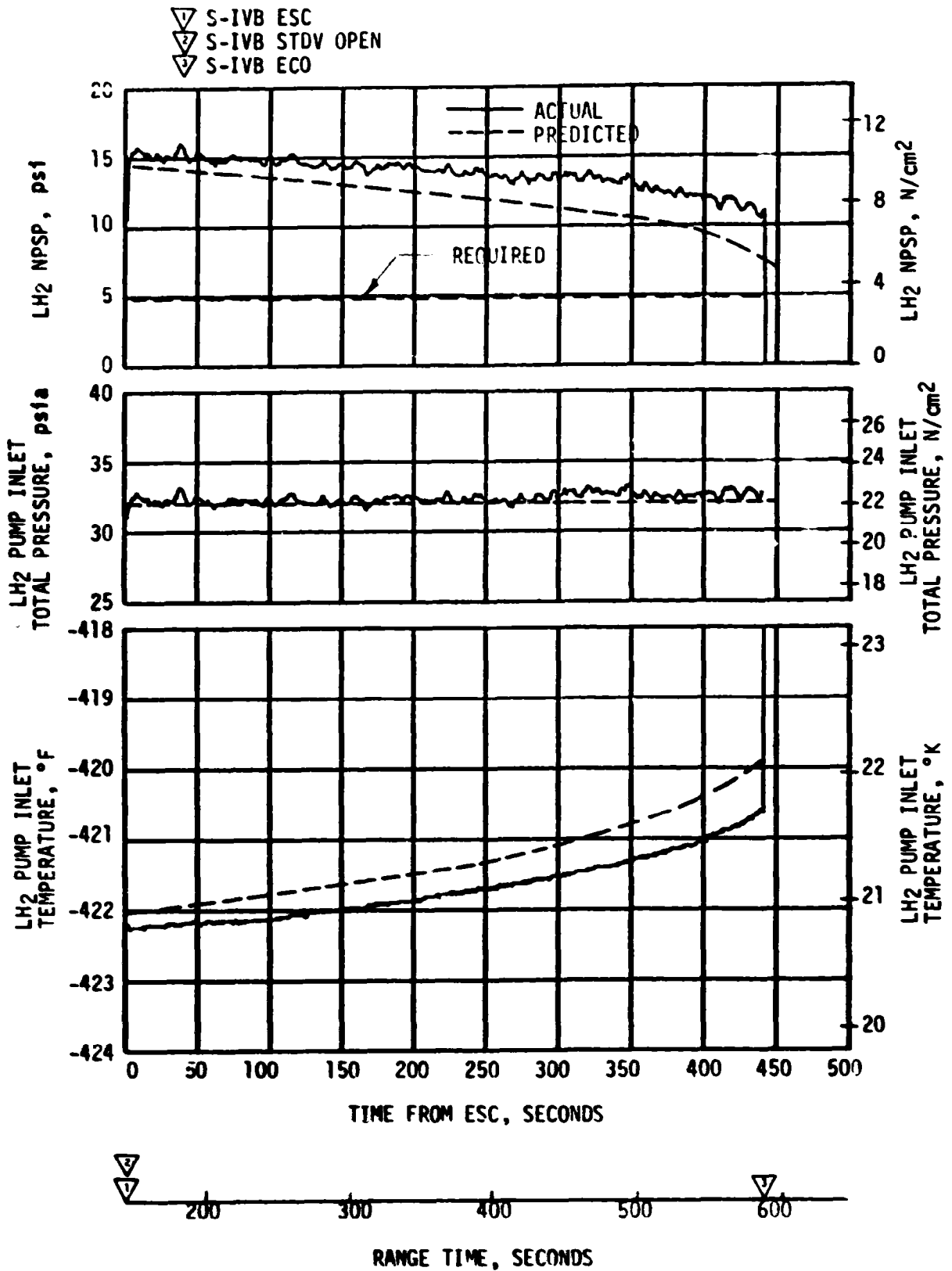


Figure 7-4. S-IVB Fuel Pump Inlet Conditions

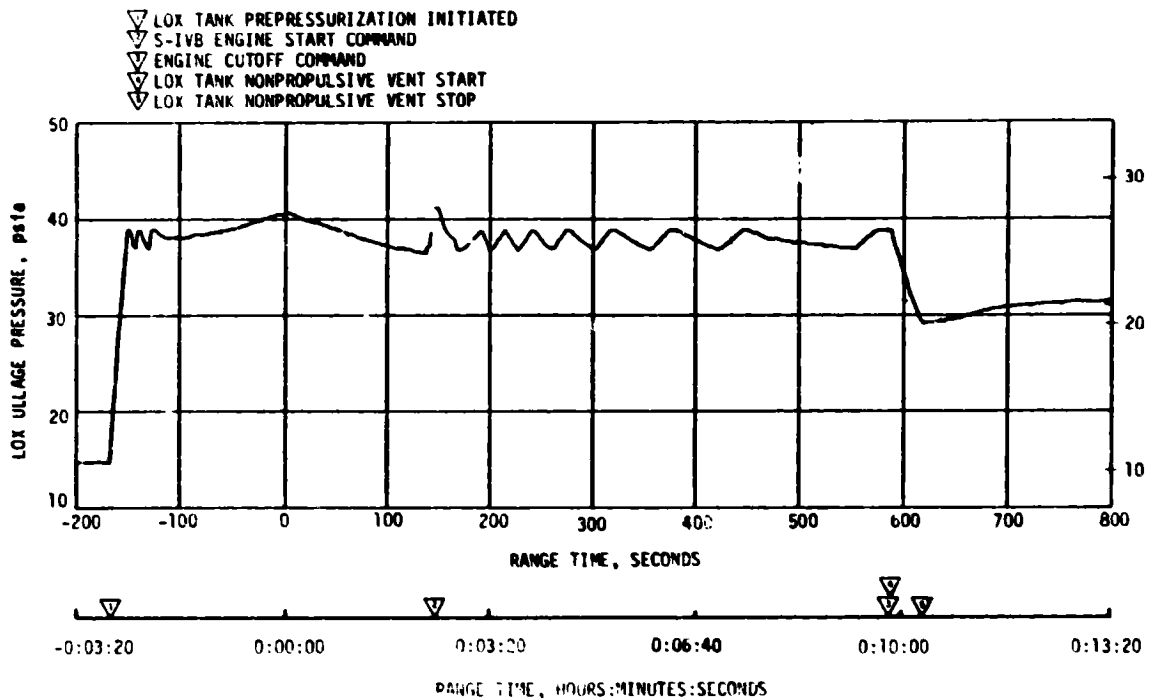


Figure 7-5. S-IVB LOX Tank Ullage Pressure

variation is normal and is caused by temperature effects. Heat exchanger performance during burn was satisfactory.

The LOX NPSP calculated at the interface was 23.0 psi at ESC. This was 10.2 psi above the NPSP minimum requirement for start. The LOX pump static interface pressure during burn follows the cyclic trends of the LOX tank ullage pressure. Figure 7-6 summarizes the LOX pump conditions for burn. The LOX pump run requirements for burn were satisfactorily met.

During orbital coast, the LOX tank ullage pressure experienced a higher rate of increase than nominally predicted, but remained within the predicted band. This higher rate of increase at approximately 10,000 seconds corresponded to complete boiloff of the liquid hydrogen. Pressure rises occurred during the solar inertial and retrograde local horizontal maneuvers due to LOX sloshing. Relief venting was initiated between 15,300 and 16,000 seconds.

The cold helium supply was adequate to meet all flight requirements. At first burn ESC, the cold helium spheres contained 257 lbm of helium. At the end of burn, the helium mass had decreased to 100 lbm. Figure 7-7 shows helium supply pressure history.

## 7.7 S-IVB PNEUMATIC CONTROL PRESSURE SYSTEM

The stage pneumatic system performed satisfactorily during all phases of

▽ S-IVB ENGINE START COMMAND

▽ S-IVB ENGINE CUTOFF

— ACTUAL

- - - PREDICTED

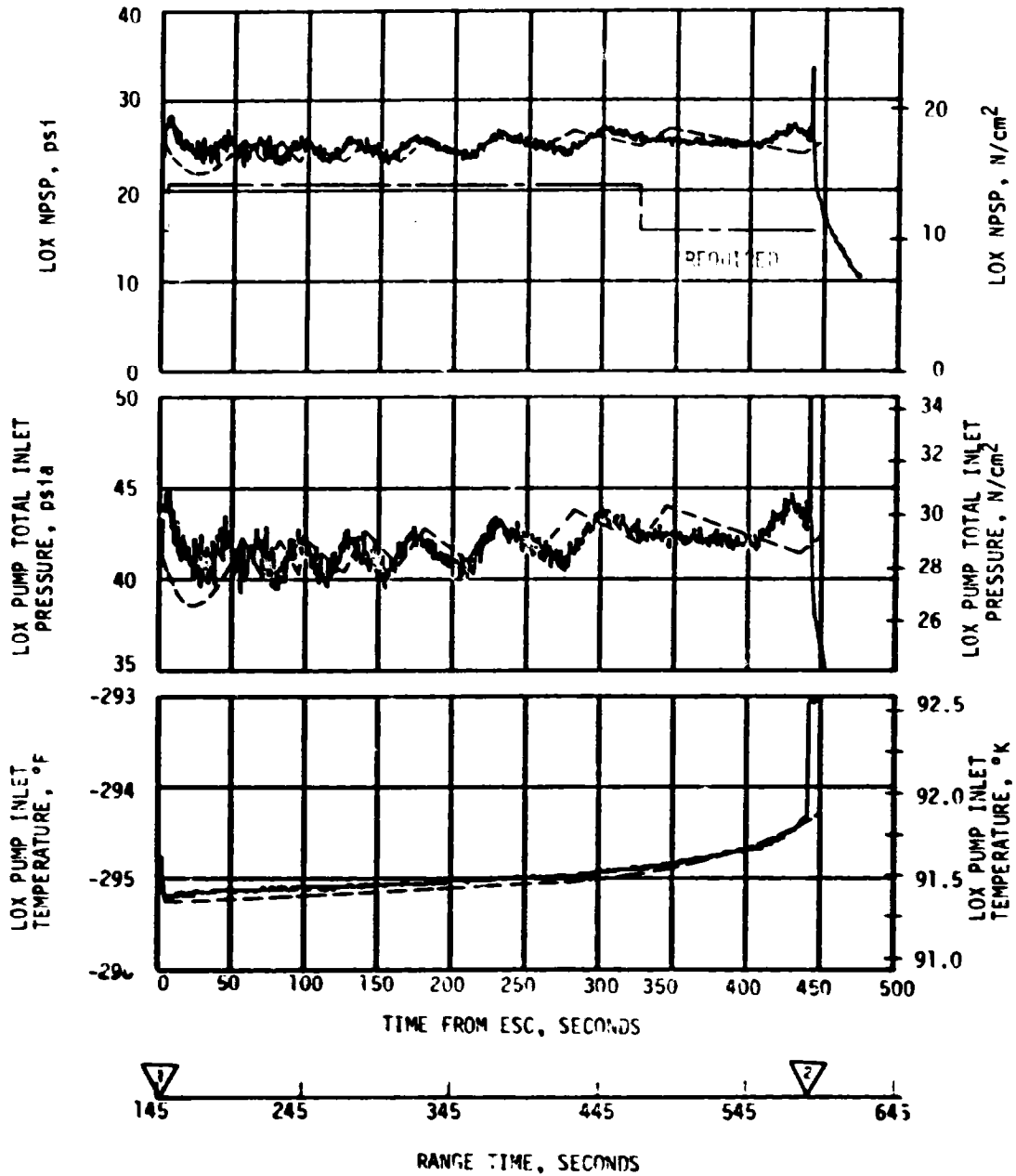


Figure 7-6. S-IVB LOX Pump Inlet Conditions - During Burn



- ▽ S-IVB FIRST ESC
- ▽ S-IVB FIRST ECO
- ▽ START COLD HELIUM DUMP
- ▽ END COLD HELIUM DUMP

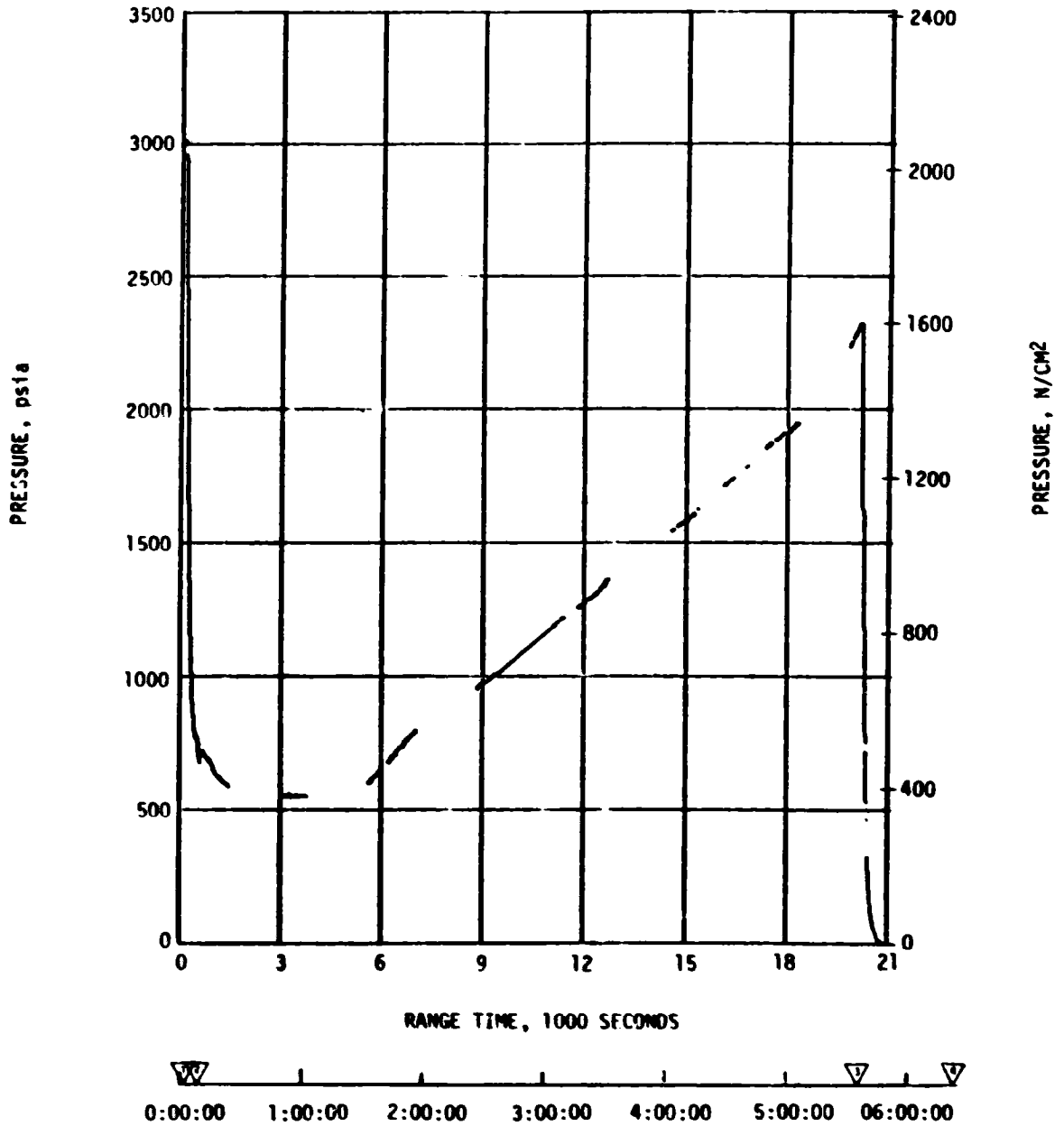


Figure 7-7. S-IVB Cold Helium Supply History

the mission. The pneumatic sphere pressure increased to 3100 psia, due to orbital heating, at initiation of propellant dump for deorbit.

The stage pneumatic regulator performance was nominal with a near constant discharge pressure of 475 psia.

This was the first flight with an interconnection between the stage pneumatic sphere and the engine control sphere. The interconnection provides additional helium to hold the engine propellant valves open during dump. System performance was satisfactory with helium being transferred to the engine system during engine burn and propellant dump. The pneumatic sphere pressure at the end of propellant dump was 600 psia.

#### 7.8 S-IVB AUXILIARY PROPULSION SYSTEM

The Auxiliary Propulsion System (APS) demonstrated close to nominal performance throughout the flight and met control system demands as required through the deorbit sequence.

The oxidizer and fuel propellant supply systems performed as expected during the flight. The propellant temperatures ranged from 68°F to 99°F. The APS propellant usage was nominal till the end of fuel dump. Following the propellant dumps and the initiation of propellant tank safing, APS propellant usage exceeded the expected usage as a result of the LOX NPV thrust unbalance. Module No. 2 propellants were depleted early with Module No. 2 fuel depleting at 20,492 seconds and the oxidizer at 20,500 seconds. Table 7-3 presents the APS propellant usage during specific portions of the mission.

The APS pressurization system also functioned nominally. Module No. 1 regulator outlet pressure ranged from 192.5 to 193 psia. Module No. 2 regulator outlet pressure ranged from 194.5 to 195.5 psia.

The performance of the attitude control thrusters was nominal. The thruster chamber pressures ranged from 90 to 100 psia. The longest engine firing recorded was 1.6 seconds on the Module No. 2 pitch engine immediately following the deorbit dumps.

Because of the many data dropouts during the mission, the impulse from many engine firings could not be calculated. Therefore, a good total impulse value could not be obtained from which to calculate the engine average specific impulse.

#### 7.9 S-IVB/IU STAGE DEORBIT PROPELLANT DUMP

All aspects of the S-IVB/IU deorbit were accomplished successfully. The impulse derived from the LOX and fuel dumps was sufficient to satisfactorily deorbit the S-IVB/IU. The total impulse provided was 88,360 lbf-sec. This is less than the real time nominal predicted value of 101,000 lbf-sec, but

Table 7-3. S-IVB APS Propellant Consumption

	MODULE NO. 1				MODULE NO. 2			
	OXIDIZER		FUEL		OXIDIZER		FUEL	
	LBM	PERCENT	LBM	PERCENT	LBM	PERCENT	LBM	PERCENT
Initial Load	39.4		24.0		39.2		23.8	
Burn (Roll Control)	0.8	2.0	0.6	2.5	.7	1.8	.5	2.1
ECO to Spacecraft Separation	2.0	5.1	1.3	5.4	2.0	5.1	1.3	5.5
Spacecraft Separation to Maneuver to Solar Inertial	2.1	5.3	1.4	5.8	1.6	4.1	1.1	4.6
Maneuver to Solar Inertial	1.1	2.8	0.7	2.9	0.9	2.3	0.7	2.9
Solar Inertial Attitude	7.2	18.3	5.0	20.8	7.8	19.9	5.5	23.1
Maneuver to Retrograde Local Horizontal	1.6	4.1	0.9	3.8	0.7	1.8	.5	2.1
Retrograde Local Horizontal	1.4	3.6	1.0	4.2	1.8	4.6	1.2	5.0
Deorbit Dump (Roll Control)	0.3	0.8	0.2	0.8	0.3	0.8	.2	.8
End of Dump to Liftoff + 20794 sec.	7.5	18.9	4.9	20.4	23.4	59.6	12.8	53.9
Total Propellant Usage	24.0	60.9	16.0	66.6	39.2	100.0	23.8	100.0

well above the real time predicted minimum of 77,400 lbf-sec. The sequence in which the propellant dumps (and safing) were accomplished is presented in Figure 7-8.

The LOX dump was initiated at approximately 19,461 seconds (05:24:21) and was satisfactorily accomplished. Reconstructed and real time predicted nominal LOX dump performance (total impulse, mass flowrate, LOX tank mass, and actual and real time predicted LOX ullage pressure) is shown in Figure 7-9. The reconstruction corresponds to the best fit on available LOX ullage pressure flight data and the calculated velocity change (determined from LVDC accelerometer data) for LOX dump.

The LOX residual at start of dump was 2215 lbm. During dump, the ullage pressure decreased from approximately 41.0 to 8.5 psia. A steady state LOX dump thrust (calculated) of 743 lbf was attained. Ullage gas ingestion (based on the reconstruction) occurred at 19,511 seconds (05:25:11). LOX dump ended at 19,921.259 seconds (05:32:01.259) by closing the Main Oxidizer Valve (MOV). The reconstructed total impulse before MOV closure was 75,610 lbf-sec, as compared to real time predicted total impulse of 82,000 lbf-sec. The lower than predicted nominal total impulse is attributed primarily to lower than nominal predicted liquid specific impulse. LVDC accelerometer data indicates the S-IVB stage velocity change due to LOX dump was 75.75 ft/sec.

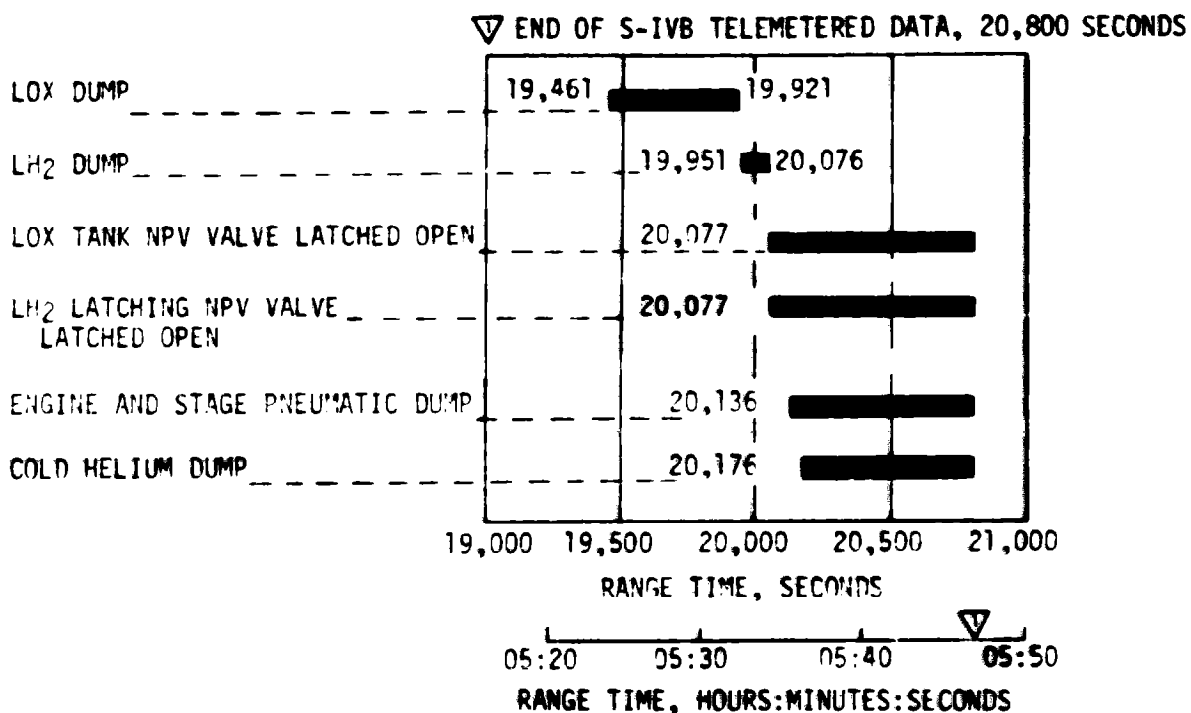


Figure 7-8. S-IVB Deorbit Propellant Dump and Safing Sequence

Fuel dump was initiated at 19,951 seconds (5:32:31) and was satisfactorily accomplished. Fuel dump impulse, flowrate, mass remaining in fuel tank, and ullage pressure are shown in Figure 7-10. Only  $GH_2$  remained in the tank at dump start. The  $LH_2$  completely boiled off during orbital coast. The ullage pressure decreased from 32.3 to 23.2 psia during the 125-second dump. The dump was terminated at 20,076 seconds (5:34:36) when the Main Fuel Valve (MFV) was closed. LVDC accelerometer data indicates the S-IVB stage velocity change due to fuel dump was 13.15 ft/sec.

A reconstruction of the dump indicates the dump impulse, 12,750 lbf-sec, was less than the real time nominal and minimum predictions, 19,000 and 16,700 lbf-sec, respectively. The impulse was lower than expected because the actual effective area of the J-2 fuel injector (established by the dump reconstruction) is 2.0 in<sup>2</sup>, much less than the 3.7 in<sup>2</sup> value used in the prediction. Prior to SA-206 no data were available for dumping gaseous hydrogen through the J-2 engine and the effective area was uncertain.

The ullage mass at the start of dump was 315 lbm, much less than the nominal predicted value of 945 lbm. The lower mass was a result of a higher than expected ullage temperature (-260°F actual vs. -390°F predicted). This indicates that the propellant and ullage heating rates were much greater than anticipated. The high ullage temperature in

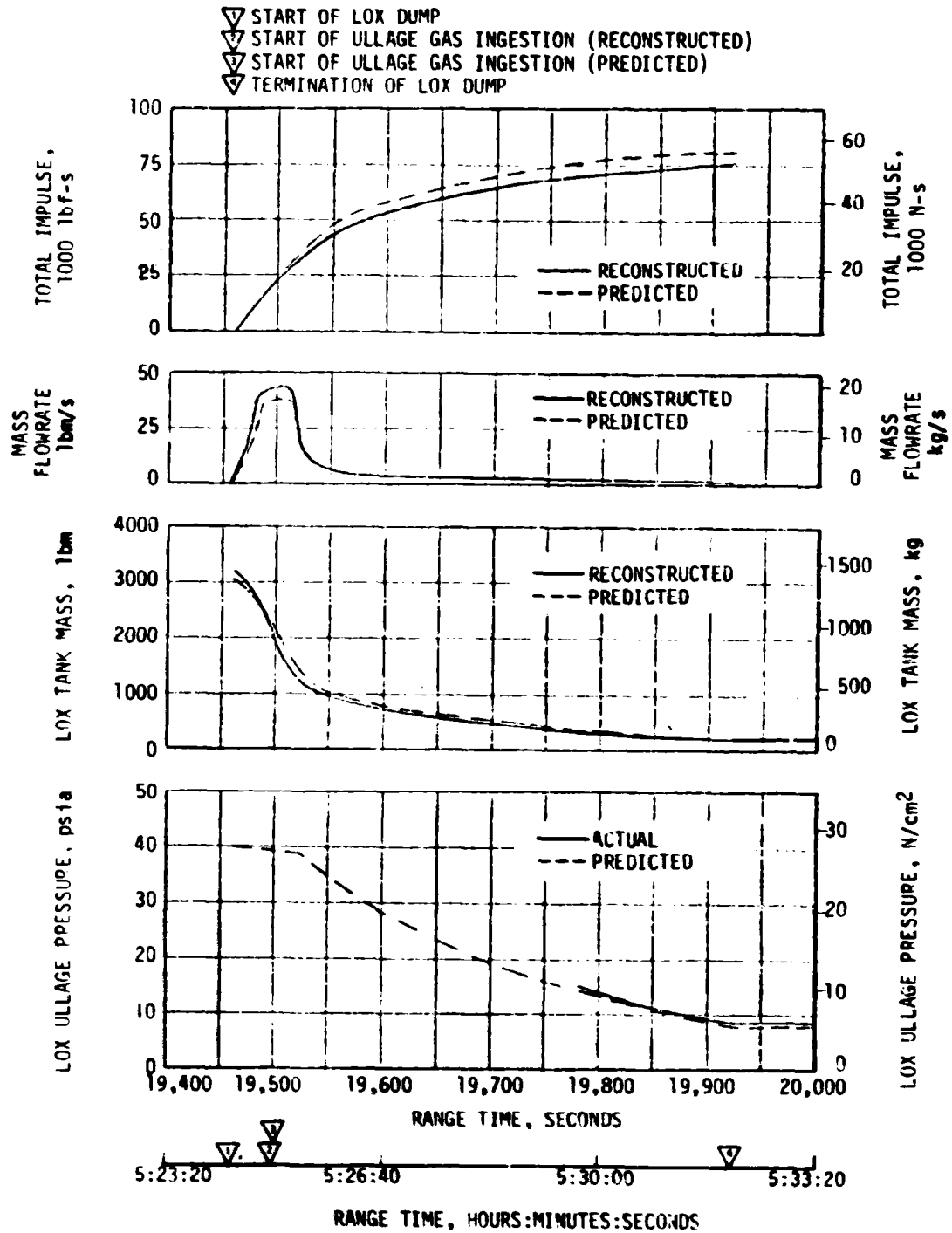


Figure 7-9. S-IVB LOX Dump Parameter Histories

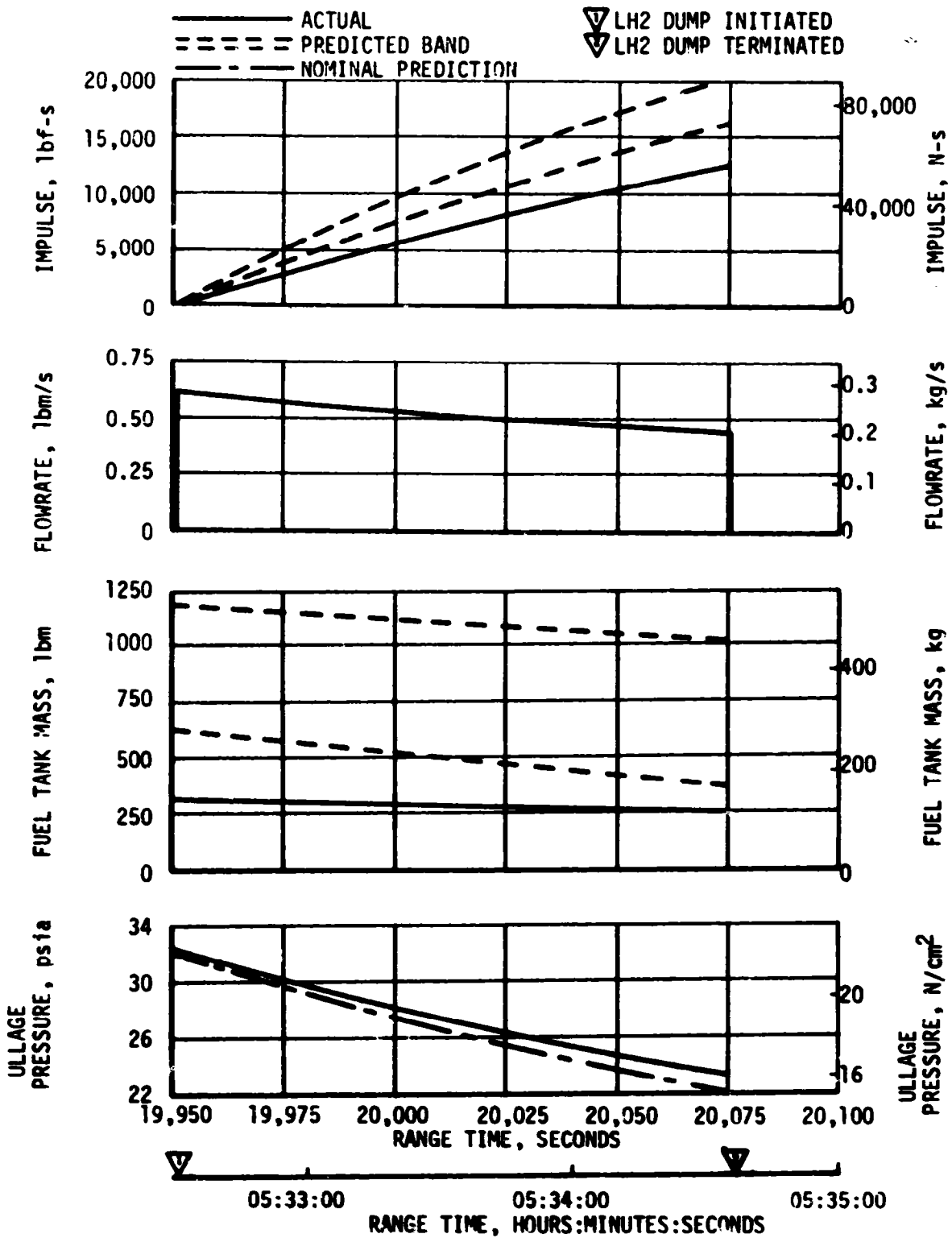


Figure 7-10. S-IVB LH<sub>2</sub> Dump

conjunction with the reduced effective area of the engine resulted in only 65 lbm of mass dumped as compared to the predicted value of 220 lbm. The ullage pressure decay prediction was in good agreement with the actual decay because the high ullage temperature and reduced effective area had compensating effects.

Data were not available at the start of deorbit dump, but the engine control bottle pressure was projected to be 3600 psia at the start of LOX dump. The engine control bottle pressure was 320 psia at the end of the dump sequence.

## 7.10 S-IVB ORBITAL SAFING OPERATION

The S-IVB high pressure systems were safed following J-2 engine cutoff. The thrust developed during LOX and fuel dumps was utilized to provide a velocity change for S-IVB deorbit. The manner and sequence in which the safing was performed is presented in Figure 7-8, and in the following paragraphs.

### 7.10.1 Fuel Tank Safing

The fuel tank was satisfactorily safed by utilizing both nonpropulsive venting and fuel dump, as indicated in Figure 7-8. The fuel tank ullage pressure during earth orbit and deorbit is shown in Figure 7-11. A 670-second fuel tank vent, initiated at ECO +10 seconds, lowered the ullage pressure from 32 to 10.5 psia. Fuel tank data from 963 seconds to about 1033 seconds show indications of liquid venting. The ullage pressure stays constant, as shown in Figure 7-11, indicating partial vent restriction. Approximately 175 lbm of liquid could have been vented during the 70-second interval (average flowrate of 2.5 lbm/sec). Analysis indicates that the thrust unbalance associated with liquid venting is within the allowable  $\pm 2\%$  range of the Nonpropulsive Vent (NPV) system. The ullage pressure reached relief at approximately 3500 seconds (00:58:20).

Data received at Texas Revolution 1, 5565 seconds (1:32:45) to 5950 seconds (1:39:10) shows 2.75 cycles of the LH<sub>2</sub> tank ullage pressure between 31.5 psia and 32.6 psia. The cycles consist of approximately 100 seconds of self pressurization followed by 40 seconds of relief venting. The pressure rise rate indicates a heat input to the liquid of about 200,000 btu/hour. This is higher than expected, but consistent with orienting the liquid along the hot sidewall of the tank due to the solar inertial attitude.

Madrid data, 6180 seconds (1:43:00) to 7100 seconds (1:58:20) shows five additional cycles of LH<sub>2</sub> tank ullage pressure. The later cycles are of decreased magnitude (approximately 31.7 psia to 32.5 psia) and eventually merge to the "feathering" relief level of 32.5 psia. This behavior indicates a reduction of the heat input to the expected levels.

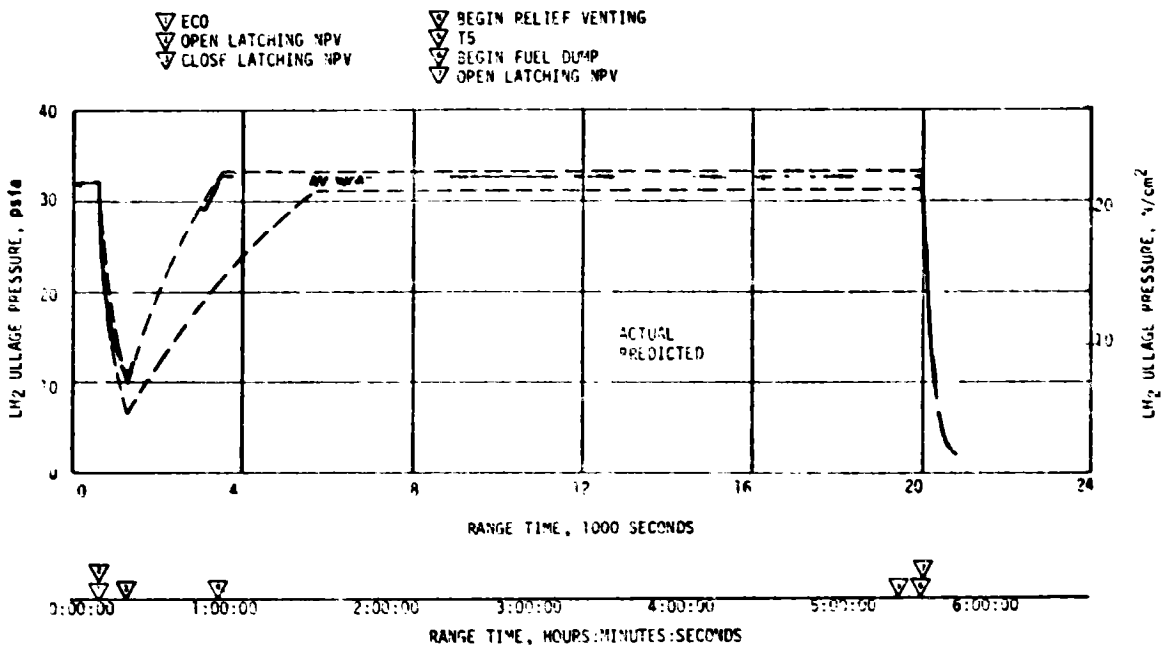


Figure 7-11. S-IVB LH<sub>2</sub> Ullage Pressure - Orbital Coast

During the relief portions of the ullage pressure cycles noted at Texas and the first three cycles at Madrid, the LH<sub>2</sub> NPV nozzle pressures show oscillations of up to +3 psia. The remaining cycles show "smooth" nozzle pressures during the first portion of the venting, but the data ends (data dropout on the DP link) just as the IU data (reference Section 10.3.2) indicates oscillations starting. The ullage pressure profile substantiates this fact in that during the "smooth" nozzle pressures, the ullage pressure remains constant and as DP data is lost, the ullage pressure starts to drop. The nozzle pressures at the end of the Madrid data indicate the return to the "feathering" relief mode with no oscillations. The valve position switch (talkback) indicates that during the oscillatory periods both the vent and latching relief valves were cycling.

The NPV pressure oscillations were similar to those occurring during step pressurization of AS-505 second burn. As a result of the oscillations, the forward skirt exhibits low level vibrations, causing oscillatory output from the IU rate gyros (reference Section 10.3.2). The oscillations had no detrimental effect on the mission and no corrective action is required. Also, no force unbalance was noted during the venting periods.

The LH<sub>2</sub> latching vent valve was opened and latched at the end of fuel dump, 20,077 seconds (5:34:37). The ullage pressure, initially 23.2 psia, decayed to 2.0 psia at end of data, 20,800 seconds (5:46:40).



## 7.10.2 LOX Tank Safing

At LOX dump termination the LOX NPV valve was opened and latched. The LOX tank ullage pressure decayed from 8.6 psia at 20,077.035 seconds (05:34:37.035) to 7.5 psia at 20,180 seconds (05:36:20). The pressure then increased to 13.0 psia at 20,305 (05:38:25) seconds as a result of cold helium dump, then decayed to 7.5 psia at loss of data. Approximately 133 lbm of helium and 180 lbm of GOX were vented overboard. The LOX tank pressure during safing is shown on Figure 7-12.

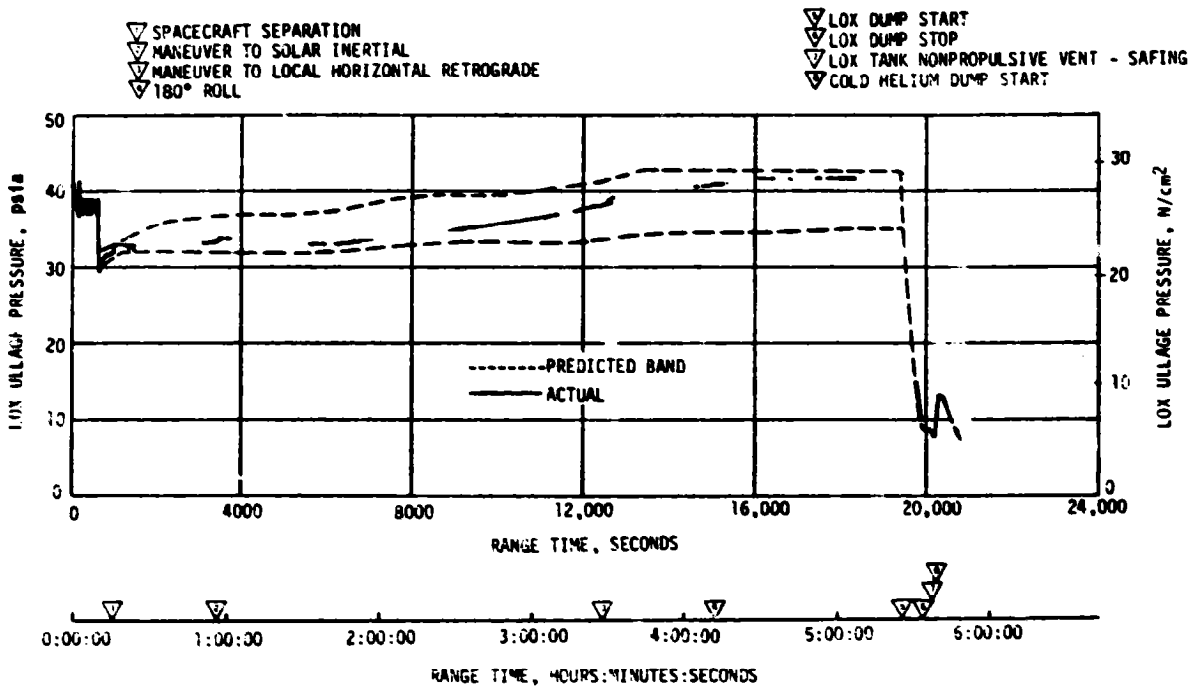


Figure 7-12. S-IVB LOX Tank Ullage Pressure - Orbit, Dump, and Safing

A disturbance force on the S-IVB/IU, coincident with LOX tank venting in TB5 (following propellant dumps), caused unplanned firings of APS module engines and subsequent propellant depletion in APS Module No. 2 (see Section 7.8). Analysis of the APS engine firing data indicated that the corrective impulse/disturbance force was in the plane of the LOX Nonpropulsive Vents (NPV). Calculations (and slow nozzle temperature response) indicate nearly complete blockage of LOX NPV Nozzle No. 1; calculated thrust for one nozzle (based on nozzle pressure data) agrees closely with calculated disturbance force, rate of LOX tank pressure decay during venting prior to cold helium dump corresponds to one-nozzle blowdown, and calculated maximum LOX tank pressure during venting prior to cold helium dump corresponds to one-nozzle blowdown, and calculated maximum LOX tank pressure during cold helium dump corresponds to one-nozzle flow.

The blockage of LOX NPV Nozzle No. 1 has been attributed to solid oxygen formation at the nozzle inlet during the TB4 cyclic LOX relief venting. The vehicle attitude immediately prior to and after relief venting resulted in the Nozzle No. 1 portion of the NPV system being subjected to a colder thermal environment. Attitude control system data indicate that the disturbance force existed (and was increasing in magnitude) during LOX relief venting, although the small magnitude and intermittent nature of the venting did not cause significant APS propellant usage. Solid oxygen in the vent system was most probably the result of cyclic liquid relief venting, where liquid remaining in the duct after the short duration relief cycles was subjected to a freezing environment (due to liquid evaporation when the duct pressure decreased below the vapor pressure corresponding to the oxygen triple point pressure). Liquid in the vent system was indicated by instrumentation, while liquid at the forward end of the tank was most probably due to liquid slosh initiated by the maneuver to retrograde local horizontal attitude.

No impact, due to the LOX NPV system anomaly, is expected on the SL-3 or SL-4 missions. The SL-2 Retrograde Local Horizontal (RLH) maneuver (ground-commanded approximately 3000 seconds prior to the first indication of LOX tank relief venting) occurred at a time when the liquid was partially settled. The resultant liquid slosh initiated by the maneuver (at a time of low settling force) resulted in liquid at the vent inlet during relief venting. The RLH maneuvers will occur early on both SL-3/SL-4 missions with long periods available for liquid slosh dampening prior to expected LOX tank relief venting. Subsequent maneuvers are not expected to result in liquid motion towards the forward end of the tank.

#### 7.10.3 Cold Helium Dump

It was planned to save the cold helium supply by dumping the helium through the LOX tank Nonpropulsive Vent system for 2800 seconds beginning at 20,176 seconds. At loss of data, the cold helium pressure was approximately zero. An estimated 100 lbm of helium was dumped.

#### 7.10.4 Stage Pneumatic Control and Engine Control Sphere Safing

The stage pneumatic sphere was safed by dumping through the interconnect to the engine control sphere.

Safing was initiated at 20,136 seconds by energizing the engine helium control solenoid. The sphere pressure was 670 psia at the start of dump. At loss of data the sphere pressure was 150 psia.

#### 7.10.5 Engine Control Sphere Safing

The safing of the engine control sphere began at 20,135.9 seconds. The

helium control solenoid was energized to dump helium through the engine purge system. The initial pressure in the sphere was approximately 620 psia. Based on the last available (20,790 seconds) data, the pressure had decreased to approximately 58 psia.

#### 7.11 S-IVB HYDRAULIC SYSTEM

The S-IVB Hydraulic System performed within the predicted limits after liftoff with no overboard venting of system fluid as a result of hydraulic fluid expansion. Prior to start of propellant loading, the accumulator was precharged to 2440 psia at 86°F. Reservoir oil level (auxiliary pump off) was 78 percent at 62°F.

The auxiliary hydraulic pump was programmed to flight mode "ON" at 11 minutes prior to liftoff. System pressure stabilized at 3645 psia and remained steady. During boost, all system fluid temperatures rose steadily when the auxiliary pump was operating and convection cooling was decreasing. At S-IVB engine start, system pressure increased to 3660 psia and remained steady through the burn period.

System internal leakage rate, 0.69 gpm/min (0.4 to 0.8 gpm allowable), was provided primarily by the auxiliary pump during engine burn as characterized by the auxiliary pump motor current draw of 41 amperes. However, at engine start aft bus 2 current indicated 27 amps for a short period before stabilizing at 41 amps. Also, at engine start, system pressure and reservoir pressure increased indicating the engine drive pump was sharing part of the internal leakage requirements.

Engine deflections were nominal throughout the boost phase. Actuator positions were offset from null during powered flight due to the displacement of the vehicle's center of gravity off the vehicle's vertical axis the J-2 engine installation tolerances, thrust misalignment, uncompensated gimbal clearances, and thrust structure compression effects.

During the orbital coast period, seven programmed auxiliary hydraulic pump thermal cycles were required to maintain system readiness for the deorbit phase. Available data during orbital coast indicated nominal system performance. During the M-415 experiment (a MSFC thermal paint experiment), system temperature trends were as predicted. Reservoir oil temperature during the first four thermal cycles ranged from 125°F to 91°F. However, at approximately 3 hours, 26 minutes, the S-IVB was maneuvered to an in-plane local horizontal retrograde position with vehicle Position I toward the earth. This maneuver occurred earlier than planned causing an increase in system temperature due to additional heating from the sun. The maximum reservoir oil temperature noted during orbital coast was 152°F.

System operation during the deorbit phase was normal. System pressure stabilized at 3645 psia and remained steady. The maximum pump inlet oil temperature noted during this period was 165°F.

## SECTION 8

### STRUCTURES

#### 8.1 SUMMARY

The structural loads experienced during the SA-206 flight were well below design values. The maximum bending moment was  $14.8 \times 10^6$  in-lbf (approximately 27 percent of design) at vehicle station 942. Thrust cutoff transients experienced by SA-206 were similar to those of previous flights. The maximum longitudinal dynamic responses measured in the Instrument Unit (IU) were +0.20 g and +0.30 g at S-IB Inboard Engine Cutoff (IECO) and Outboard Engine Cutoff (OECO), respectively. POGO did not occur.

The maximum ground wind experienced by the Saturn IB SA-206 during the prelaunch period was 22 knots (55 knots, allowable with damper). The ground winds at launch were 12 knots from the Southwest (34 knots allowable).

#### 8.2 TOTAL VEHICLE STRUCTURES EVALUATION

##### 8.2.1 Longitudinal Loads

The SA-206 vehicle liftoff steady-state acceleration was 1.25 g. Maximum longitudinal dynamic response measured during thrust buildup and release was +0.20 g in the IU and +0.60 g at the Command Module (CM) (Figure 8-1). Comparable values have been recorded on previous flights.

The SA-206 IECO and OECO transient response were equal to or less than those of previous flights. The maximum longitudinal dynamics resulting from IECO were +0.2 g at the IU and +0.5 g at the CM (Figure 8-2).

The total longitudinal load at station 942, based on strain data, is shown in Figure 8-3 as a function of range time. The envelope of previous flights (S-IB vehicles SA-202, -203, -204, and -205) is shown for comparison. The longitudinal load distributions at the time of maximum bending moment (65.8 seconds) and IECO (138.7 seconds) are shown in Figure 8-4. Steady-state longitudinal accelerations at these time slices were 1.87 g and 4.35 g, respectively. The maximum longitudinal load ( $1.35 \times 10^6$  lbf) occurred at IECO and was well within design limit capability.

##### 8.2.2 Bending Moments

The maximum bending moment of  $14.8 \times 10^6$  in-lbf at vehicle station 942 was 27 percent of design bending allowable. The distributions are calculated for the vehicle mass and flight trajectory configuration at the

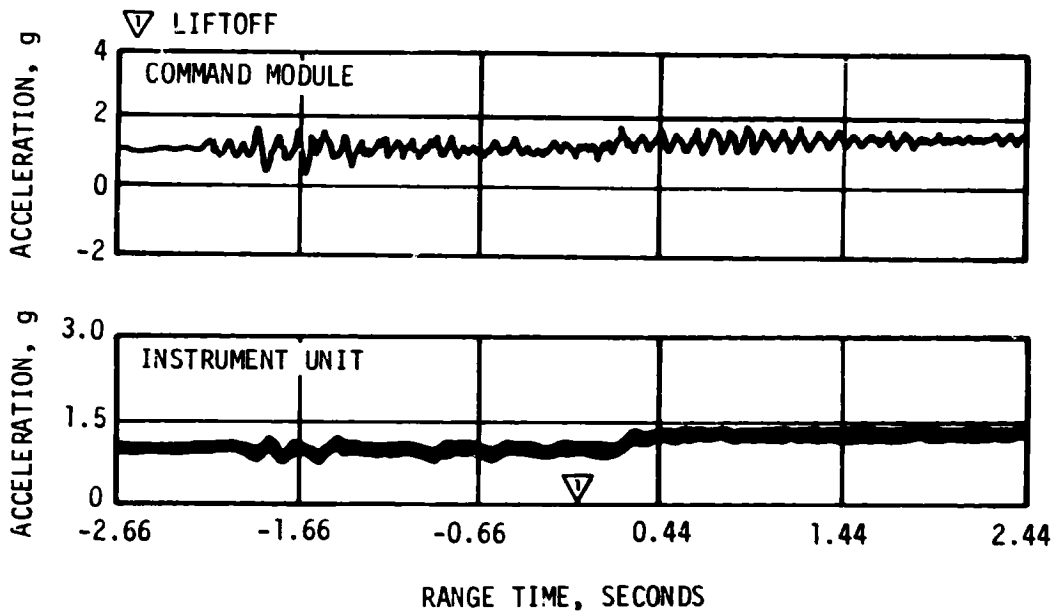


Figure 8-1. SA-206 Longitudinal Accelerations at IU and CM During Thrust Build-Up and Launch

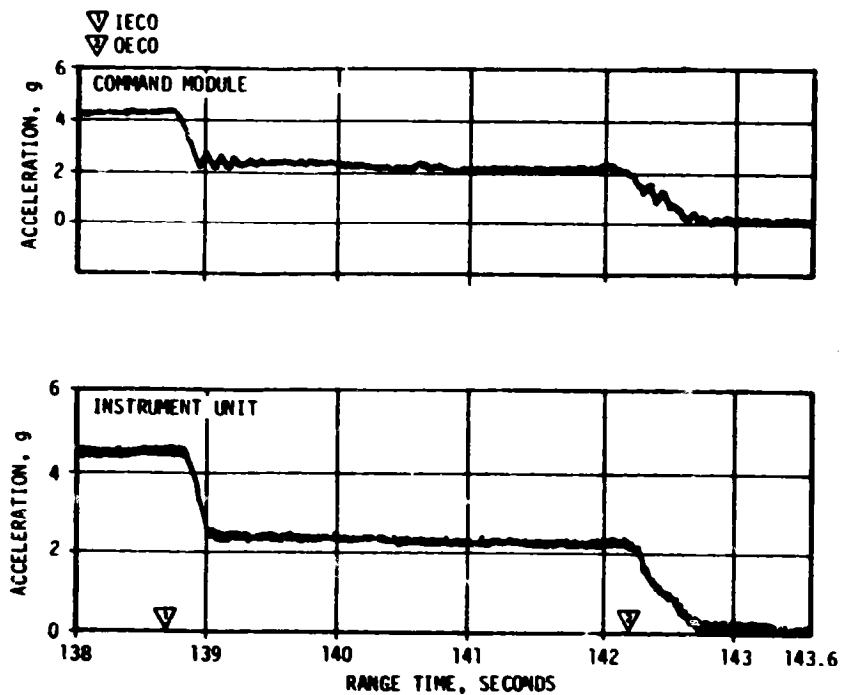


Figure 8-2. SA-206 Longitudinal Acceleration at the IU and CM During S-IB Cutoffs

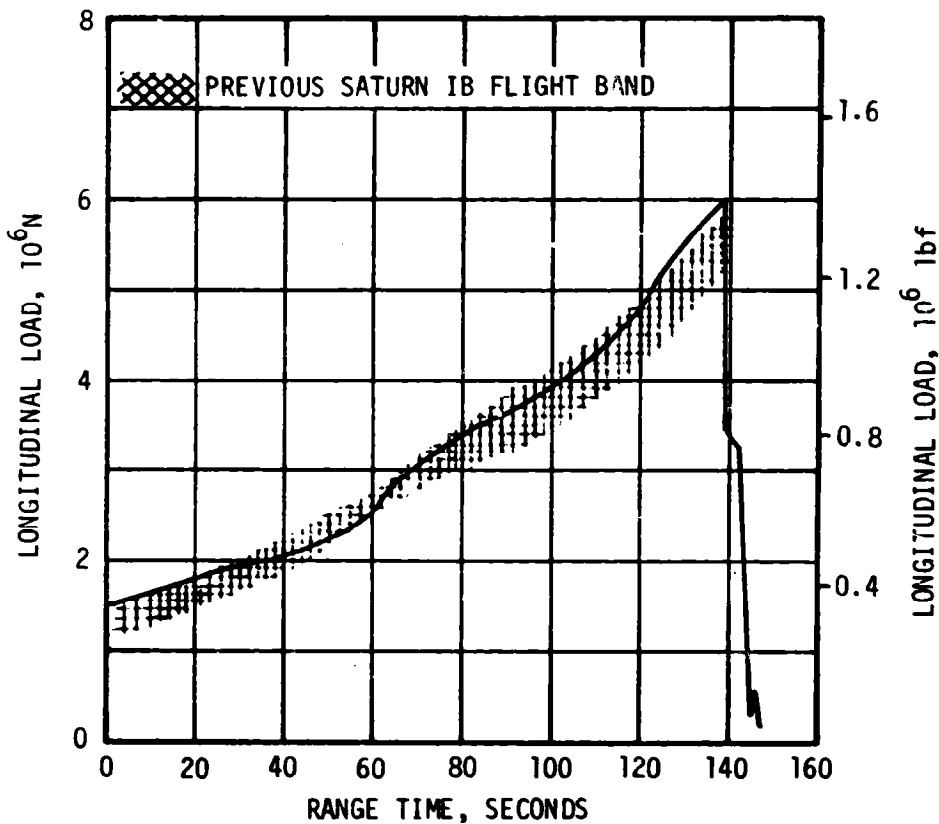


Figure 8-3. S-IB-6 Longitudinal Load from Strain Data at Station 942

indicated range time. The strain data, less 105-inch LOX tank bending moment, are those measured by the eight LOX stud strain serts and do not include the increment carried by the 105-inch LOX tank. The strain data must be increased by approximately 10 percent (based on previous flight analyses for which 105-inch LOX strain gage data were recorded) to represent total vehicle bending moment. There was no significant lateral modal dynamics during S-IB burn. The lateral acceleration distributions (normal load factors) are displayed in Figures 8-5 through 8-7.

### 8.2.3 Combined Loads

Combined compression and tension loads were computed for maximum yaw bending moment (53.3 secs.), resultant bending moment (65.8 secs.), pitch bending moment (67.8 secs.) and engine cutoff (~136.94 secs.)

⊙ STRAIN DATA

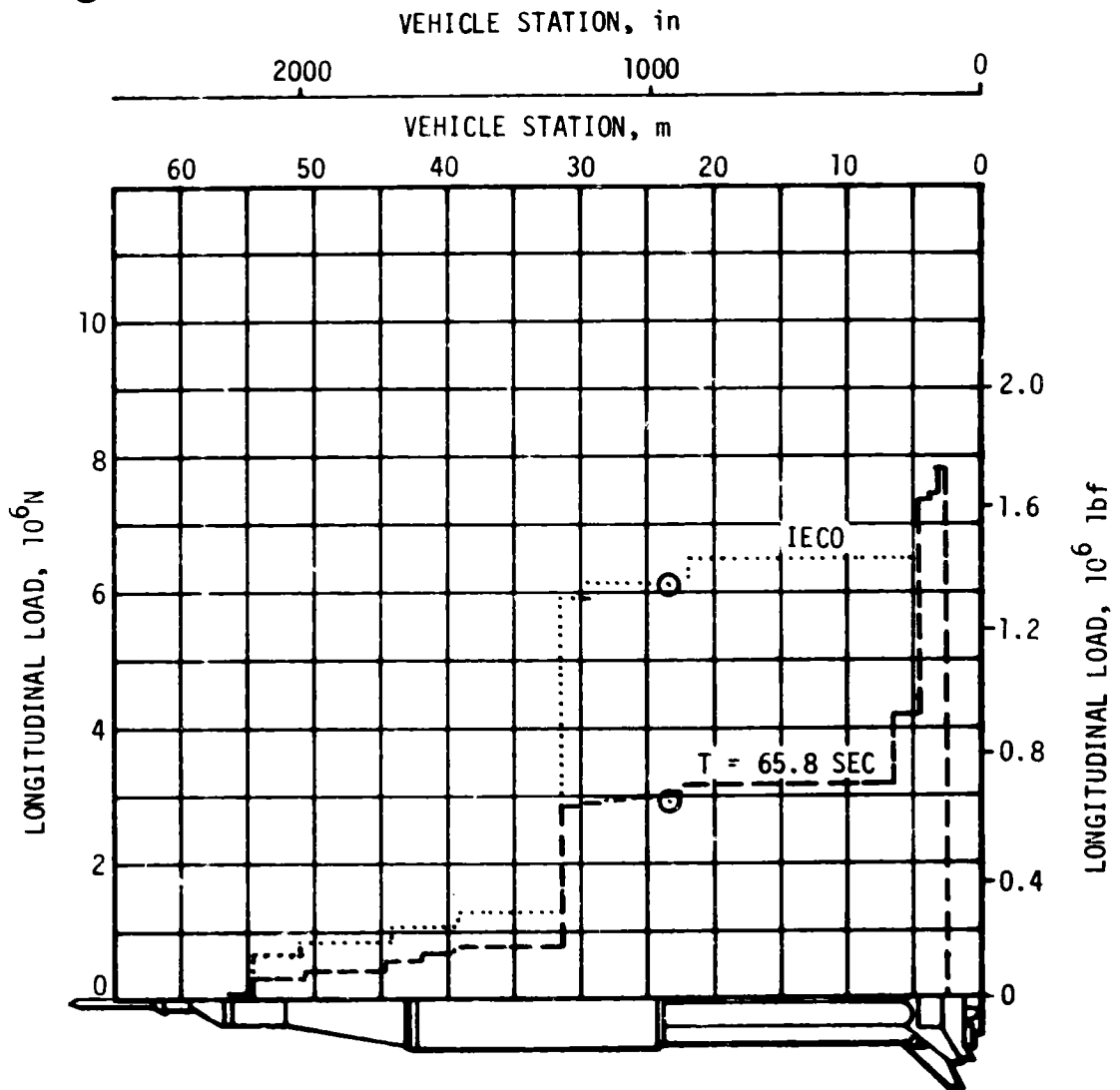


Figure 8-4. SA-206 Longitudinal Load Distribution at Time of Maximum Bending Moment and IECO

SATURN IB (SA-206)  
 T = 65.8 SECONDS  
 M = 1.248  
 q = 4.646 PSI  
 $\alpha$  = 2.28 DEGREES  
 $\beta$  = 1.45 DEGREES

⊙ STRAIN DATA

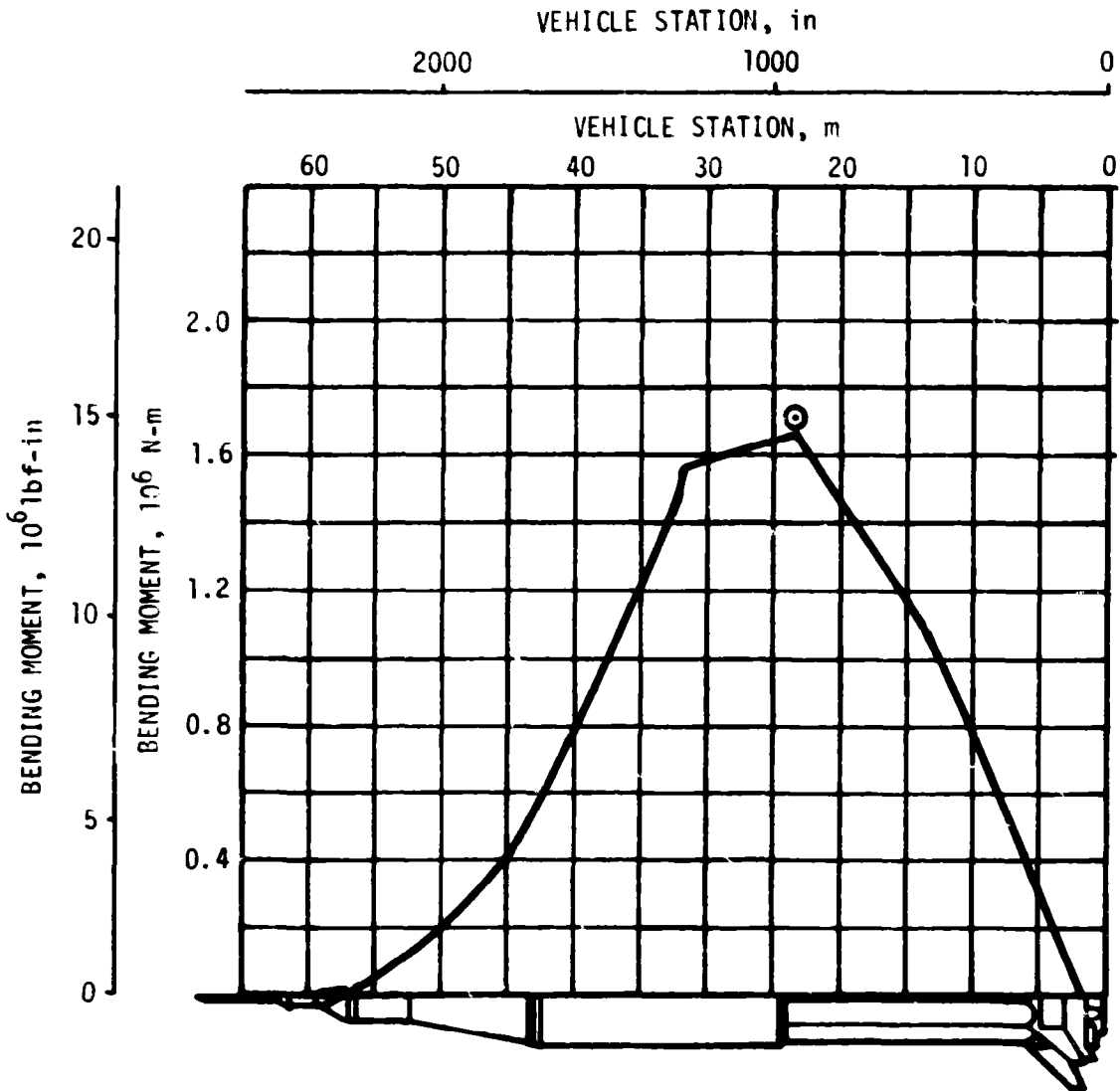


Figure 8-5. SA-206 Bending Moment Distributions at Time of Maximum Resultant Moment, T = 65.8 Resultant



SATURN IB (SA-206)  
 T = 65.8 SECONDS  
 M = 1.248  
 q = 4.646 PSI  
 $\alpha_y = 2.00$  DEGREES  
 $\beta_y = 1.20$  DEGREES

○ STRAIN DATA  
 ▽ A5-603 ACCELEROMETER DATA  
 ● CENTER OF GRAVITY

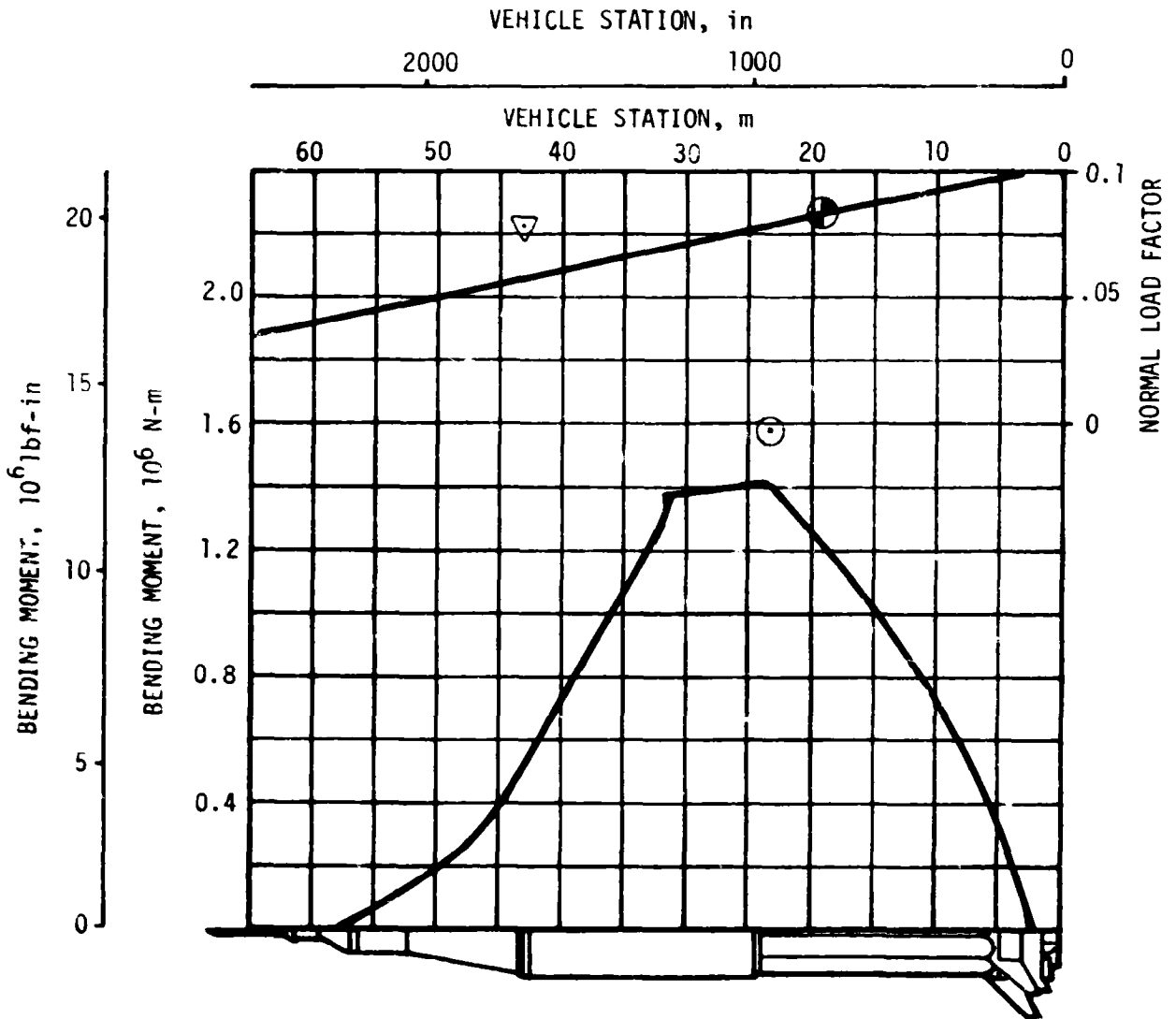


Figure 8-6. SA-206 Bending Moment Distributions at Time of Maximum Resultant Moment, T = 65.8 Yaw

SATURN IB (SA-206)  
 T = 65.8 SECONDS  
 M = 1.248  
 q = 4.646 PSI  
 $\alpha_p$  = 1.30 DEGREES  
 $\beta_p$  = 0.82 DEGREES

⊙ STRAIN DATA  
 ▼ A4-601 ACCELEROMETER DATA  
 ● CENTER OF GRAVITY

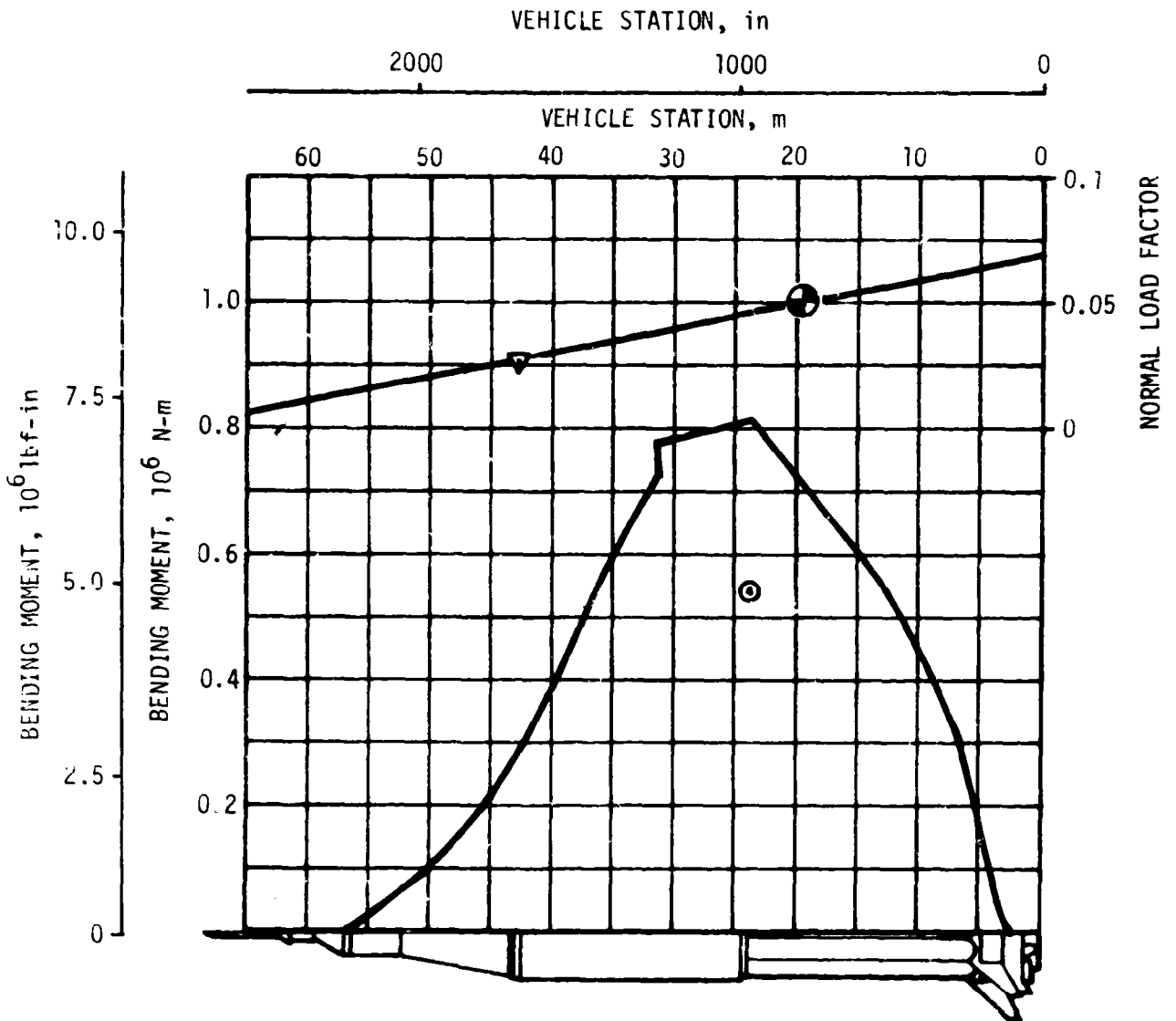


Figure 8-7. SA-206 Bending Moment Distributions at Time of Maximum Resultant Moment, T = 65.8 Pitch

using measured ullage pressures. The loads which produced minimum safety margins are plotted versus vehicle station along with the associated capabilities in Figure 8-8. The minimum factor of safety (ultimate load/limit load) of 1.51 at station 1186 was experienced at IECO.

#### 8.2.4 Vehicle Dynamic Characteristics

The longitudinal stability analysis of SA-206 showed all vibration and pressure fluctuations to be smooth and low with no POGO instability.

The first, second and third S-IB bending mode frequencies are compared to the modes predicted by analysis in Figure 8-9. Response amplitudes at these frequencies were low and similar to previous Saturn IB flights. The amplitude time histories are presented in Figure 8-10. Power spectral density analysis of selected time points of engine thrust pad vibration and LOX pump inlet and engine chamber pressure fluctuations revealed the maximum composite rms level to be 0.269 g on the Engine 6 thrust pad at liftoff with a maximum component rms amplitude of 0.688 g at a frequency of 10 Hz. The composite maximum rms LOX pump inlet and engine chamber pressure fluctuations, corresponding to the same time slice for maximum vibration, were 1.86 and 8.82 psi, respectively. These levels are considered insignificant and would not contribute to POGO.

During the S-IVB stage boost phase, 17 Hz oscillations were measured for a duration of approximately 40 seconds immediately after S-IVB stage ignition (Figure 8-11). The maximum level was +0.1 g, which is well below design values. These oscillations near engine ignition are probably caused by LOX pump self-induced oscillations and are of no concern. The SA-206 overall amplitude history is compared to those measured on the AS-505 and AS-512 flights in Figure 8-11.

The dynamic pressures measured during the S-IVB boost phase of the SA-206 flight are compared to those from the AS-511 and AS-512 flights in Figures 8-12 and 8-13. The overall amplitudes from the SA-206 flight are higher because of a generally higher Engine Mixture Ratio (EMR) (5.5 to 4.8) than those on Saturn V flights (5.0 to 4.3). The SA-206 pressure measurements show no evidence of any POGO activity.

Spectral density plots for the vibration and engine pressures at selected time periods are shown in Figure 8-14. The 17 Hz structural frequency is predominant during the 150 second time period. The 465 second time period shows the apparent "buzz" frequency noted on the Saturn V flights. The frequency during the SA-206 flight is 80 Hz (three times the LOX feedline frequency of 27 Hz) at this time period which is higher than those on Saturn V flights. The higher frequency tends to correlate with the higher Net Positive Suction Pressure (NPSP) as compared to Saturn V flights and the resultant higher LOX feedline frequency. The 550 second time period shows the structural vibration at 16 Hz. These amplitudes were considerably lower than the maximum levels measured during the Saturn V flights, and are well below design values.

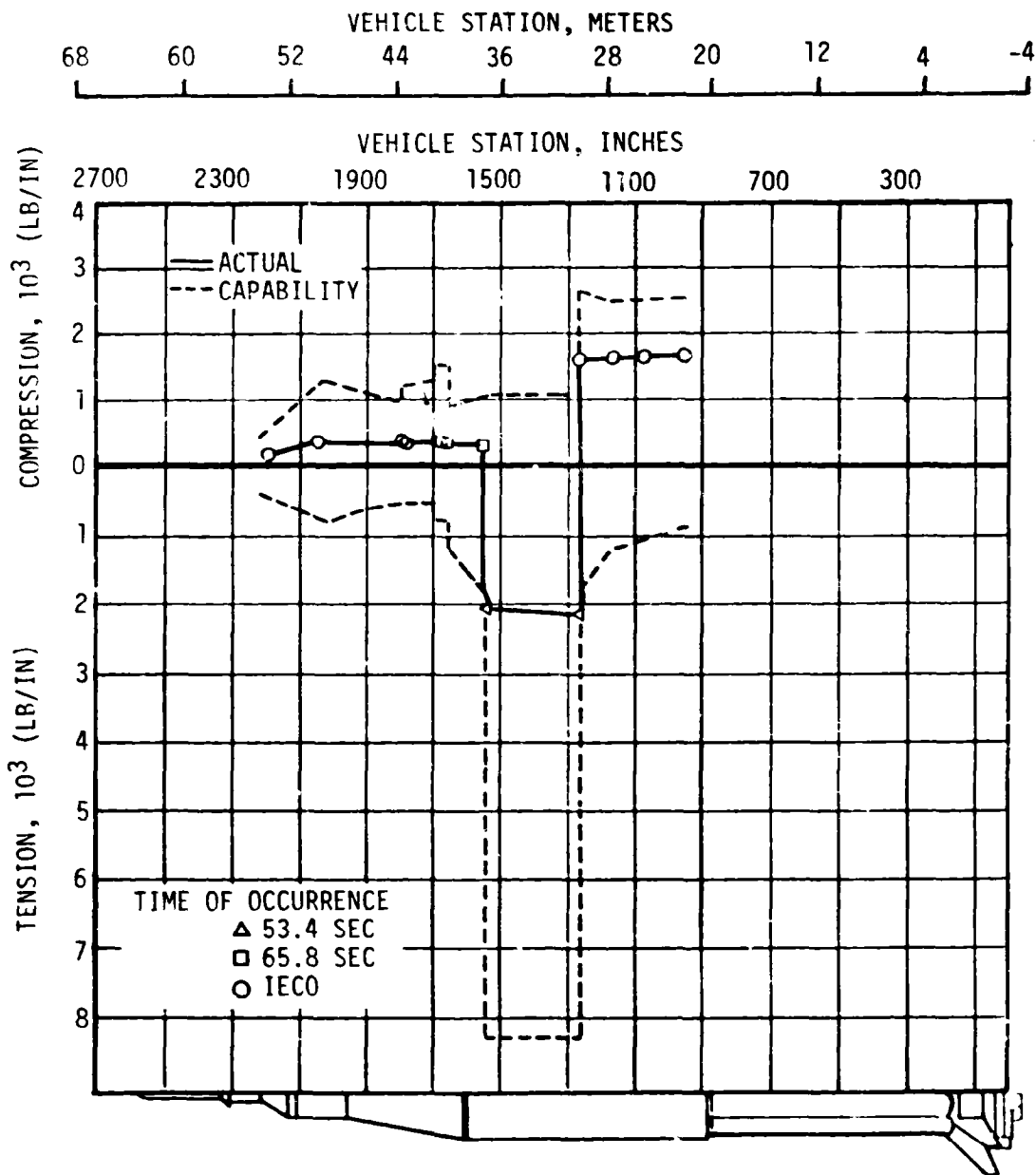


Figure 8-8. Combined Loads Producing Minimum Safety Margins During SA-206 Flight

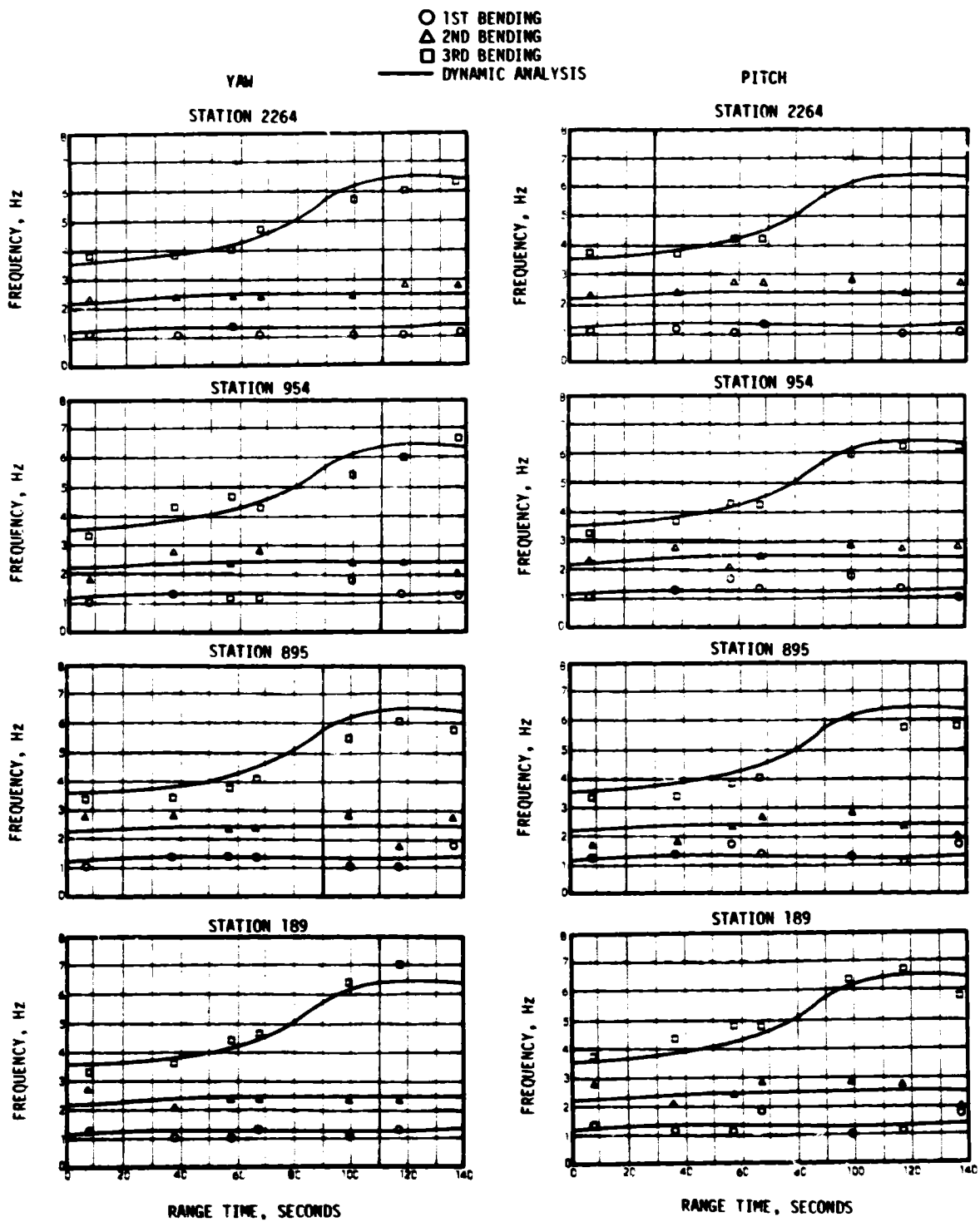


Figure 8-9. Vehicle Bending Frequencies

——— 1ST BENDING  
 - - - 2ND BENDING  
 - · - 3RD BENDING

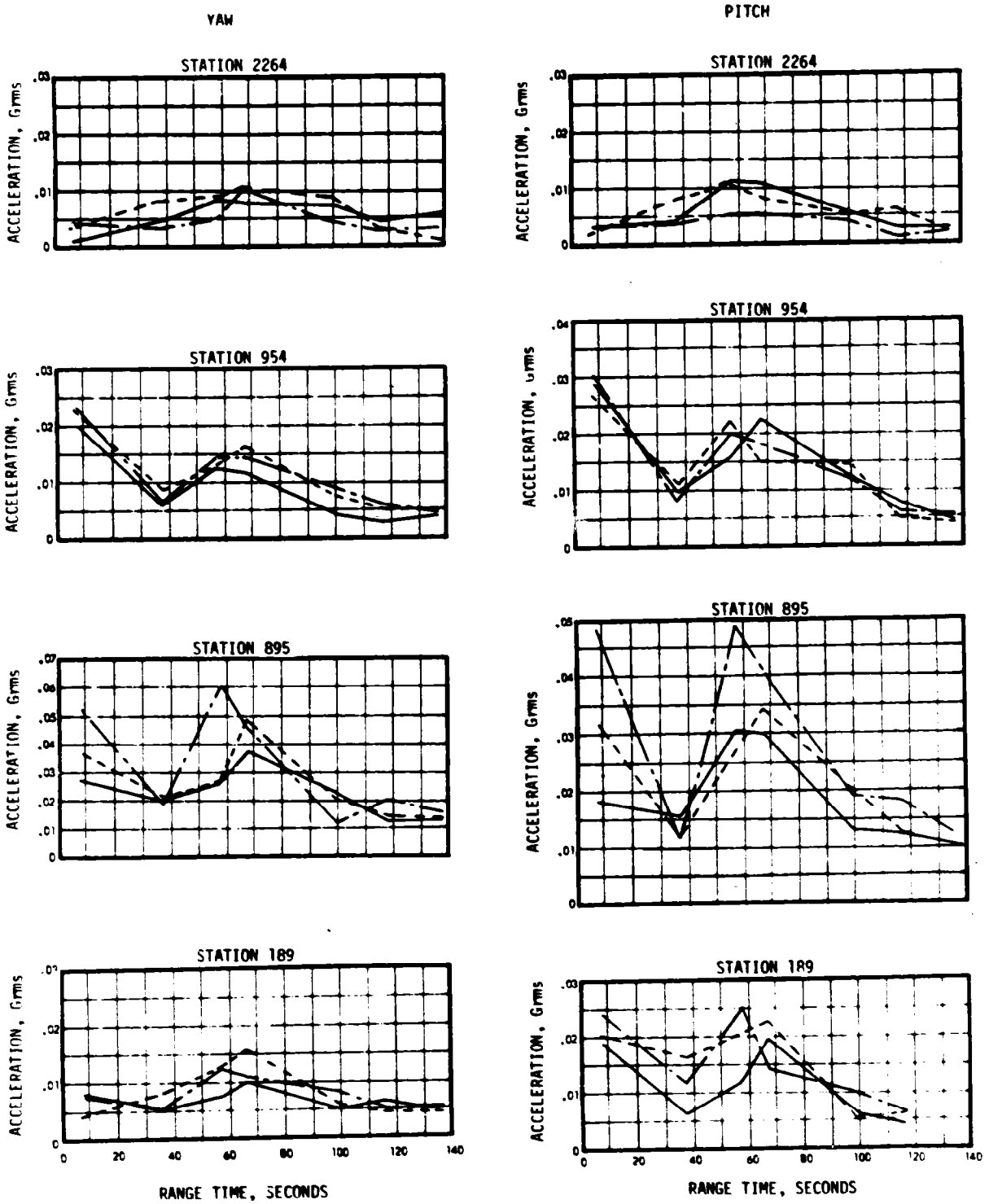


Figure 8-10. Vehicle Bending Amplitudes

Figure 8-11. LOX Pump Inlet Pressure Oscillations During S-IVB Stage Burn

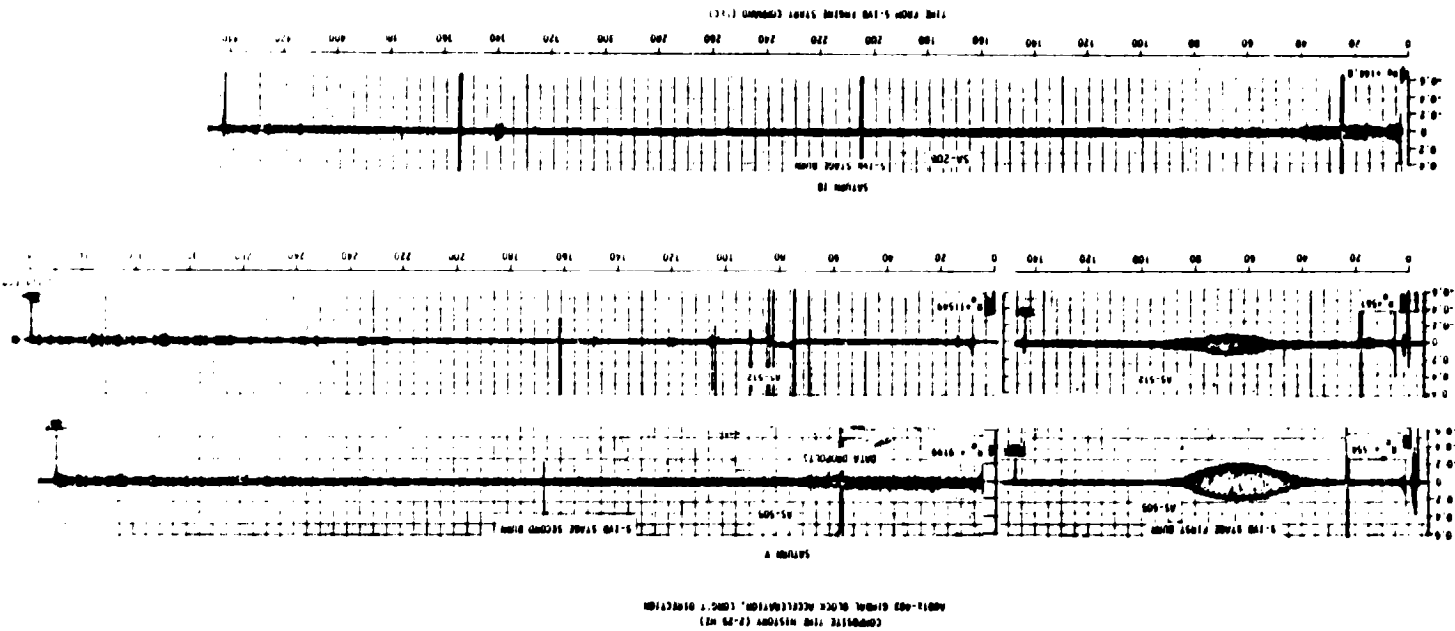
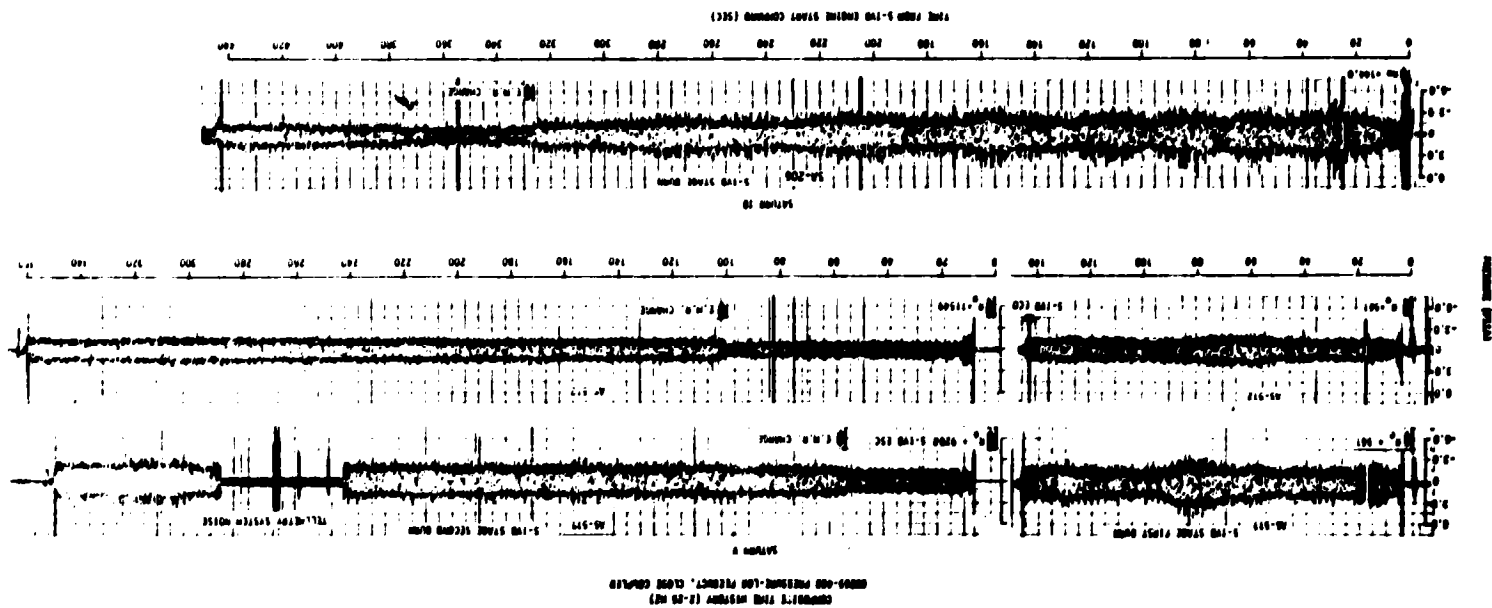


Figure 8-12. Vibration Measured During S-IVB Stage Burn





COMPOSITE TIME HISTORY (2-22-67)  
RECORD OF THRUST CHAMBER OSCILLATIONS

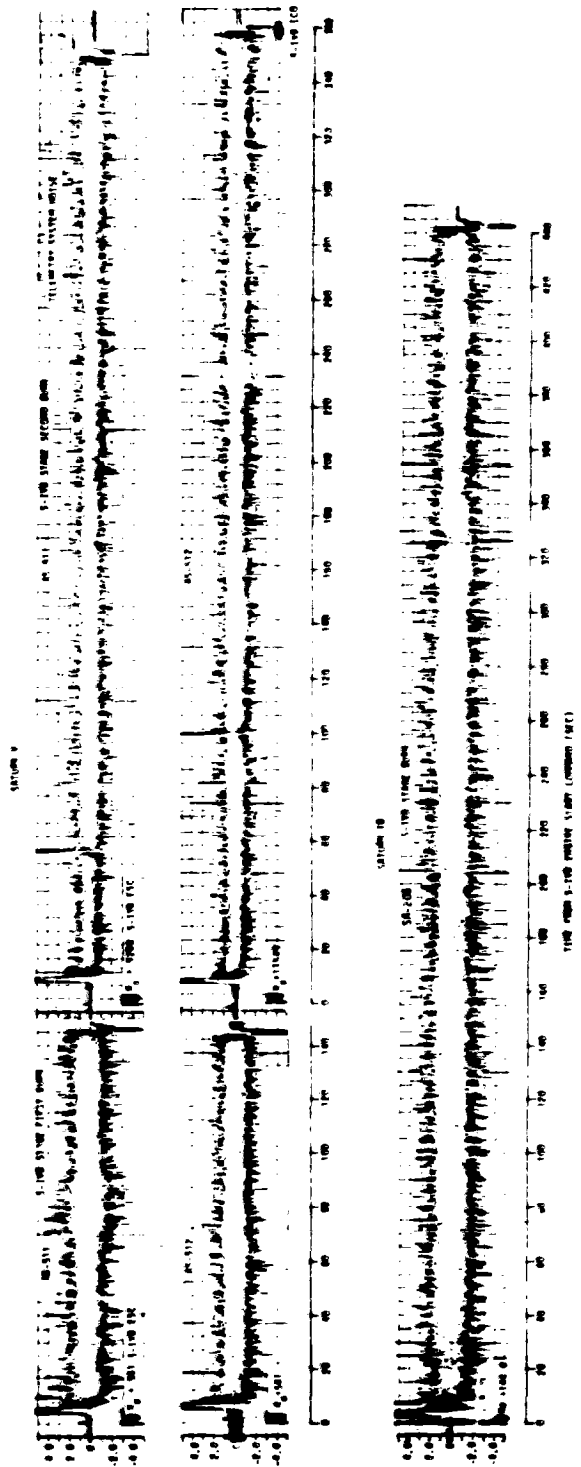


Figure 8-13. Thrust Chamber Pressure Oscillations During S-108 Stage Burn

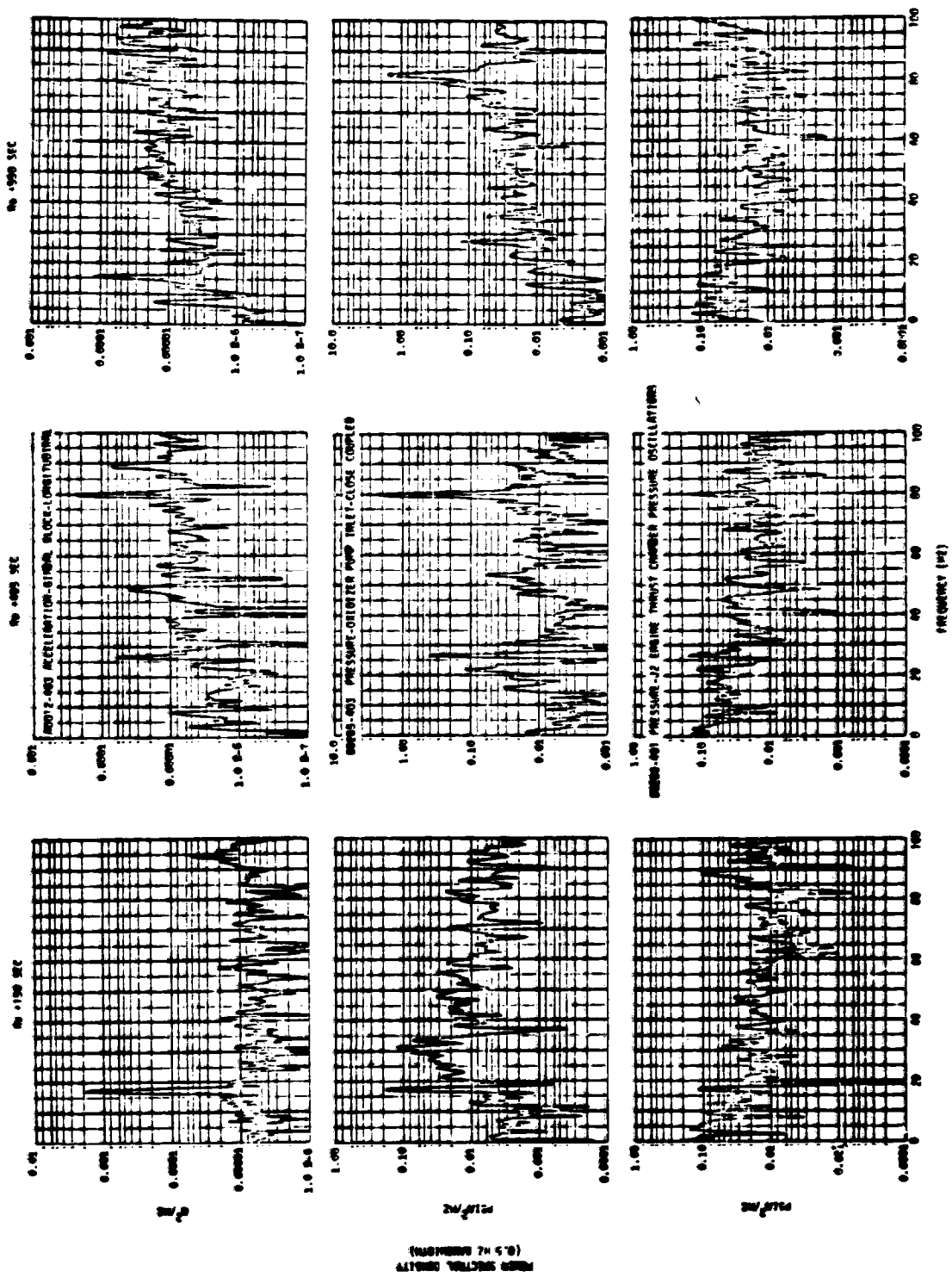


Figure 8-14. S-IVB Low Frequency Analysis of Vibration and Engine Pressures

## SECTION 9

### GUIDANCE AND NAVIGATION

#### 9.1 SUMMARY

The Stabilized Platform and the Guidance Computer successfully supported the accomplishment of the mission objectives. Targeted conditions at orbit insertion were attained with insignificant error.

The one anomaly which occurred in the guidance and navigation system was a large change in the gyro summation current and a small change in the accelerometer summation current in the ST-124M Platform Electronics Assembly. Operation of the ST-124M subsystem was not affected by these current changes.

There was a pitch axis gimbal resolver switchover accomplished at 20,558 seconds, following completion of propellant dumps. However, this switchover was caused by a loss of attitude control when the S-IVB Auxiliary Propulsion System propellants depleted.

#### 9.2 GUIDANCE COMPARISONS

The postflight guidance error analysis was based on comparisons of telemetered position and velocity data with corresponding data from the 14 day Observed Mass Point Trajectory (OMPT) which was established from external tracking and telemetered velocity data (see Section 4.0). Comparisons of the inertial platform measured velocities with the OMPT data are shown in Figure 9-1 for boost. The velocity differences are small for the entire boost phase and well within the accuracies of the onboard measuring system and the OMPT. The vertical velocity differences indicate an offset of about 0.05 m/s (0.16 ft/s). The crossrange velocity differences after Outboard Engine Cutoff (OECO) indicate some combination of small platform drifts. Since the downrange velocity differences are not characteristic of hardware errors, they are probably the result of some small time or angular error in referencing the tracking data to the launch site at time of Guidance Reference Release (GRR). The Launch Vehicle Digital Computer (LVDC) downrange component of position was within +60 meters (197 feet) of the OMPT values for the total boost phase.

The inertial platform velocity measurements at significant event times are shown in Table 9-1 along with corresponding data from the OMPT. Figure 9-1 shows a plot of the differences in velocities as seen by the LVDC and as reconstructed in the OMPT.

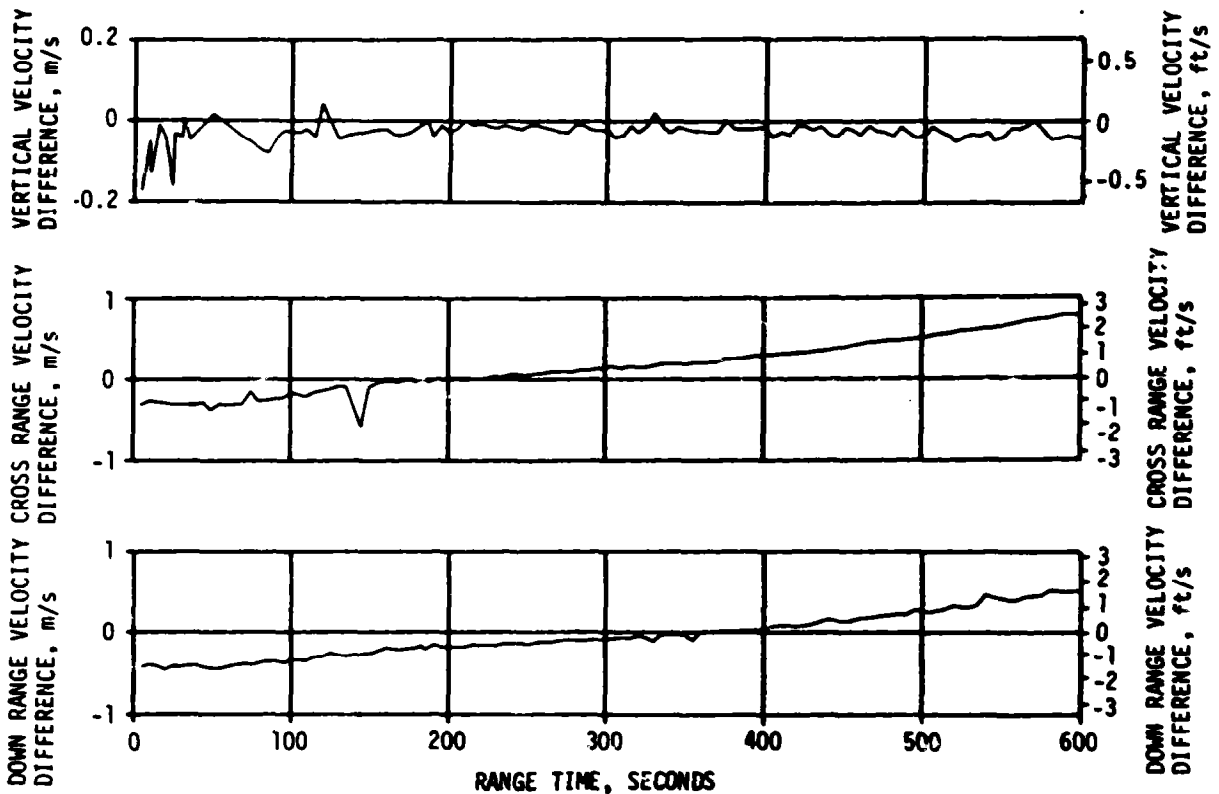


Figure 9-1. SA-206 Trajectory and ST-124M Platform Velocity Comparisons (Trajectory Minus LVDC)

The LVDC data was determined using switch selector event times and velocity pickoffs referenced to GRR and are accurate to  $\pm 0.10$  m/s (0.33 ft/s) of the actual onboard accumulated velocities. The velocity difference at S-IVB cutoff signal and at orbit insertion are consistent with the time history plots.

Velocity gain due to thrust decay after Guidance Cutoff Signal (GCS) was 8.16 m/s (26.77 ft/s) compared to 6.83 m/s (22.41 ft/s) predicted by the Post-Launch Predicted Operational Trajectory (OT). This difference is reflected in the velocity overspeed shown at orbit insertion in Table 9-2.

Comparisons of positions, velocities, and flight path angle at significant event times are presented in Table 9-2. Differences between the LVDC and OT values reflect the actual flight environment and vehicle performance. At GCS, LVDC velocity and radius values were 0.07 m/s (0.23 ft/s) and 24 meters (79 feet), respectively, greater than the OT values. At orbit insertion the LVDC total velocity was 1.37 m/s

Table 9-1. SA-206 Inertial Platform Velocity Comparisons

EVENT	DATA SOURCE	VELOCITY (PACSS 12) *		
		METERS/SECOND (FEET/SECOND)		
		$\dot{X}_m$	$\dot{Y}_m$	$\dot{Z}_m$
IECO	LVDC	2429.94 (7972.24)	3.65 (11.98)	1756.62 (5763.19)
	POSTFLIGHT TRAJECTORY	2431.98 (7978.94)	3.34 (10.96)	1761.97 (5780.74)
OECO	LVDC	2467.35 (8095.01)	3.23 (10.60)	1830.91 (6006.92)
	POSTFLIGHT TRAJECTORY	2465.60 (8089.24)	2.80 (9.19)	1833.68 (6016.01)
S-IVB GCS	LVDC	3304.31 (10840.91)	-492.51 (-1615.85)	7739.81 (25393.08)
	POSTFLIGHT TRAJECTORY	3304.22 (10840.62)	-491.78 (-1613.45)	7740.46 (25395.21)
ORBITAL INSERTION	LVDC	3302.95 (10836.45)	-493.45 (-1618.93)	7747.80 (25419.29)
	POSTFLIGHT TRAJECTORY	3302.90 (10836.29)	-492.68 (-1616.40)	7748.30 (25420.93)

\*PACSS 12 (PROJECT APOLLO COORDINATE SYSTEM STANDARD)

(4.49 ft/s) greater than the OT value. This velocity difference was due to a small difference in actual and predicted thrust decay.

The LVDC and OMPT position data were in very good agreement from launch to orbit insertion. The differences in total velocity at GCS and orbit insertion are essentially the deviations in downrange (Z) velocity. This deviation is probably the result of a small time or angular error in data transformation or a forced fit of the boost trajectory to a point determined from orbit data. In any case, the guidance system was highly successful in guiding the SA-206 launch vehicle to the prescribed end conditions and placing the spacecraft on the proper transfer orbit to rendezvous with the Skylab-1 orbital work shop.

### 9.3 NAVIGATION AND GUIDANCE SCHEME EVALUATION

The flight program performed all required functions properly. Targeted guidance cutoff conditions at orbit insertion were achieved with a high degree of accuracy. All events scheduled at preset times occurred within acceptable tolerances. Times of occurrence of major navigation and guidance events are included in Table 2-2.

Table 9-2. SA-206 Navigation Position and Velocity Comparisons (PACSS-13)

EVENT	DATA SOURCE	POSITIONS METERS (FEET)				VELOCITIES METERS/SECOND (FEET/SECOND)				FLIGHT PATH ANGLE - DEGREES
		Xs	Ys	Zs	R	Xs	Ys	Zs	Vs	
S-1B IECO	LVDC	6426924.3 (21085710.)	56631.4 (185799.)	95228.6 (312430.)	6427879.2 (21088843.)	909.14 (2982.74)	272.49 (894.00)	2051.63 (6731.07)	2260.53 (7416.44)	24.6219
	POSTFLIGHT TRAJECTORY	6426923.6 (21085707.)	56599.4 (185694.)	95181.6 (312276.)	6427877.6 (21088837.)	911.20 (2989.50)	272.19 (893.01)	2056.98 (6748.52)	2266.18 (7434.97)	24.6154
	OPERATIONAL TRAJECTORY	6427576. (21087848.)	55798. (183064.)	94226. (309140.)	6428509. (21090909.)	922.99 (3028.18)	267.39 (877.26)	2051.65 (6731.15)	2265.54 (7432.87)	24.938
S-1B OECO	LVDC	6430215.4 (21096507.)	57614.2 (189023.)	102777.6 (337197.)	6431294.8 (21100049.)	911.72 (2991.21)	271.79 (891.70)	2125.36 (6972.97)	2328.57 (7639.67)	24.0230
	POSTFLIGHT TRAJECTORY	6430224.2 (21096536.)	57580.5 (188912.)	102761.1 (337143.)	6431303.1 (21100076.)	910.00 (2985.56)	271.37 (890.32)	2128.13 (6982.05)	2330.38 (7645.60)	23.9578
	OPERATIONAL TRAJECTORY	6430352. (21096955.)	56599. (185692.)	100483. (329669.)	6431386. (21100348.)	925.12 (3036.17)	266.89 (875.62)	2114.40 (6937.01)	2323.31 (7622.41)	24.416
S-1VB GCS	LVDC	6223037.3 (20416789.)	102476.6 (336209.)	1969849.3 (6462760.)	6528169.7 (21417880.)	-2368.88 (-7771.92)	-282.50 (-926.84)	7494.39 (24587.89)	7864.94 (25803.61)	-0.00866
	POSTFLIGHT TRAJECTORY	6223012.4 (20416707.)	102564.6 (336498.)	1969877.5 (6462853.)	6528156.0 (21417835.)	-2368.94 (-7772.11)	-281.76 (-924.41)	7495.03 (24589.99)	7865.54 (25805.58)	-0.00733
	OPERATIONAL TRAJECTORY	6226337. (20427615.)	102763. (337149.)	1959301. (6428153.)	6528146. (21417802.)	-2356.06 (-7729.86)	-283.00 (-928.48)	7498.34 (24600.85)	7864.87 (25803.38)	-0.008
	LVDC	6198891.6 (20337571.)	99636.6 (326892.)	2044719.6 (6708398.)	6528174.5 (21417895.)	-2459.18 (-8068.18)	-284.77 (-934.28)	7473.55 (24519.52)	7872.90 (25829.72)	0.00976
ORBITAL INSERTION	POSTFLIGHT TRAJECTORY	6198864.6 (20337482.)	99731.5 (327203.)	2044763.2 (6708541.)	6528164.1 (21417861.)	-2459.20 (-8068.24)	-283.99 (-931.73)	7474.05 (24521.16)	7873.35 (25831.20)	0.01126
	OPERATIONAL TRAJECTORY	6202320. (20348819.)	99919. (327818.)	2034207. (6673907.)	6528151. (21417818.)	-2446.18 (-8025.52)	-285.15 (-935.53)	7476.36 (24528.74)	7871.53 (25825.23)	0.009
	TRAJECTORY									

POSTFLIGHT TRAJECTORY - DENOTES ACTUAL  
OPERATIONAL TRAJECTORY - DENOTES NOMINAL

### 9.3.1 First Stage Boost

Time Base 1 started 17.482 seconds after Guidance Reference Release (GRR) and 0.1 second after IU umbilical disconnect. A flight program time guard prevents search for the liftoff discrete for 17.4 seconds after GRR. Following satisfaction of this time guard the liftoff search is enabled but not started for another minor loop. Thus the total delay in starting the liftoff search could be 80 to 90 milliseconds after satisfaction of the 17.4 second time guard. Since the IU umbilical disconnect (liftoff discrete set) occurred approximately 18 milliseconds before satisfaction of the time guard, the total delay from disconnect to recognition by the flight program was approximately 100 milliseconds. This delay was not significant on SA-206 and present mission definitions indicate such a delay would be insignificant for SA-207 and SA-208.

The roll and time-tilt pitch maneuver was begun at 10.029 seconds. The roll maneuver was completed (roll gimbal angle within 0.5 degree of zero) 54.8 seconds. The pitch time-tilt was arrested at 131.144 seconds with Pitch Attitude Command = -63.3237 degrees. First stage guidance and navigation were normal.

### 9.3.2 Second Stage Boost

Second stage guidance was normal with no undue occurrences noted. The desired and achieved guidance terminal conditions for boost are shown in Table 9-3.

Table 9-3. SA-206 End Conditions

PARAMETER	DESIRED	ACHIEVED	ERROR (ACHIEVED- DESIRED)
Velocity, $V_T$ (m/sec)	7871.46	7871.5264	0.0664
Radius, $R_T$ (meters)	6528199.0	6528171.0	-28.0
Path Angle, $\theta_T$ (deg)	0.0	-0.001866	-0.001866
Inclination, $I$ (deg)	50.032463	50.033817	0.001354
Resonating Mode, $\lambda$ (deg)	155.22073	155.22312	0.00239

Vehicle attitude angles along with predicted values during both first and second stage boosts are shown in Figures 9-2 through 9-4.

### 9.3.3 Orbital Phase

At the start of Time Base 4 an attitude hold (Chi-freeze) was initiated, followed by a local reference maneuver scheduled 20 seconds later. These commands are shown in Table 9-4.

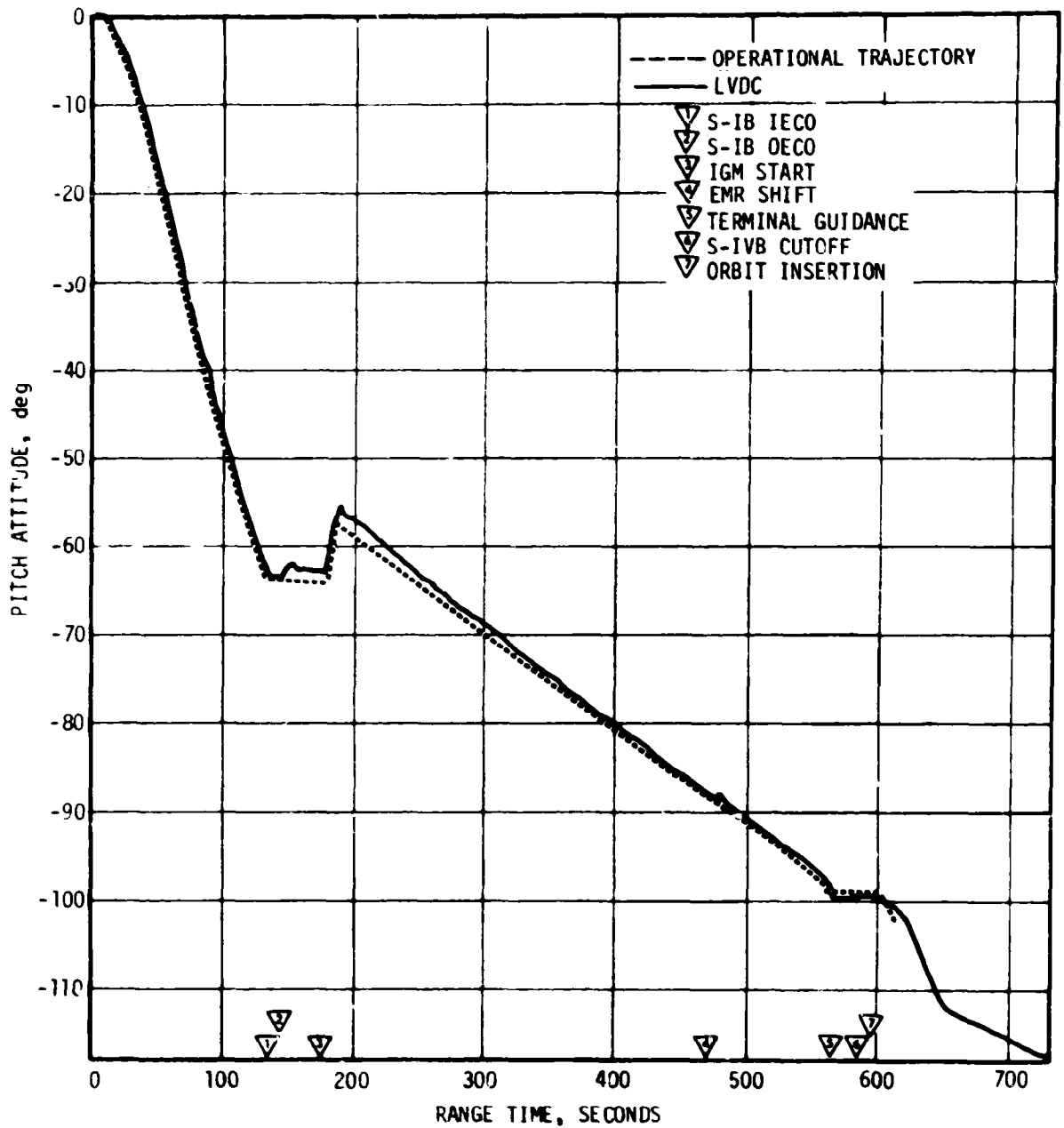


Figure 9-2. SA-206 Theta Y (Pitch) Attitude Angle During Boost



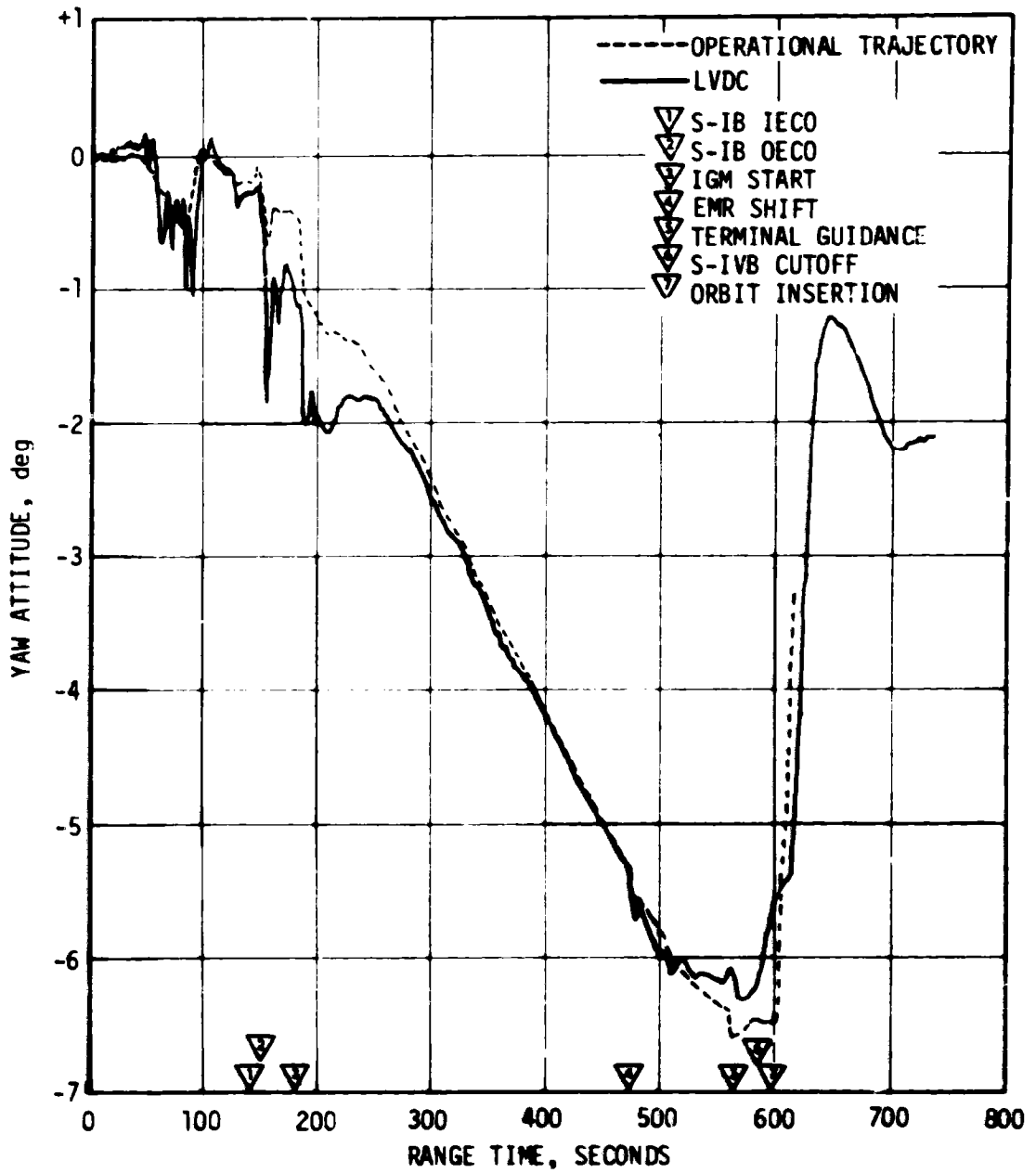


Figure 9-3. SA-206 Theta Z (Yaw) Attitude Angle During Boost

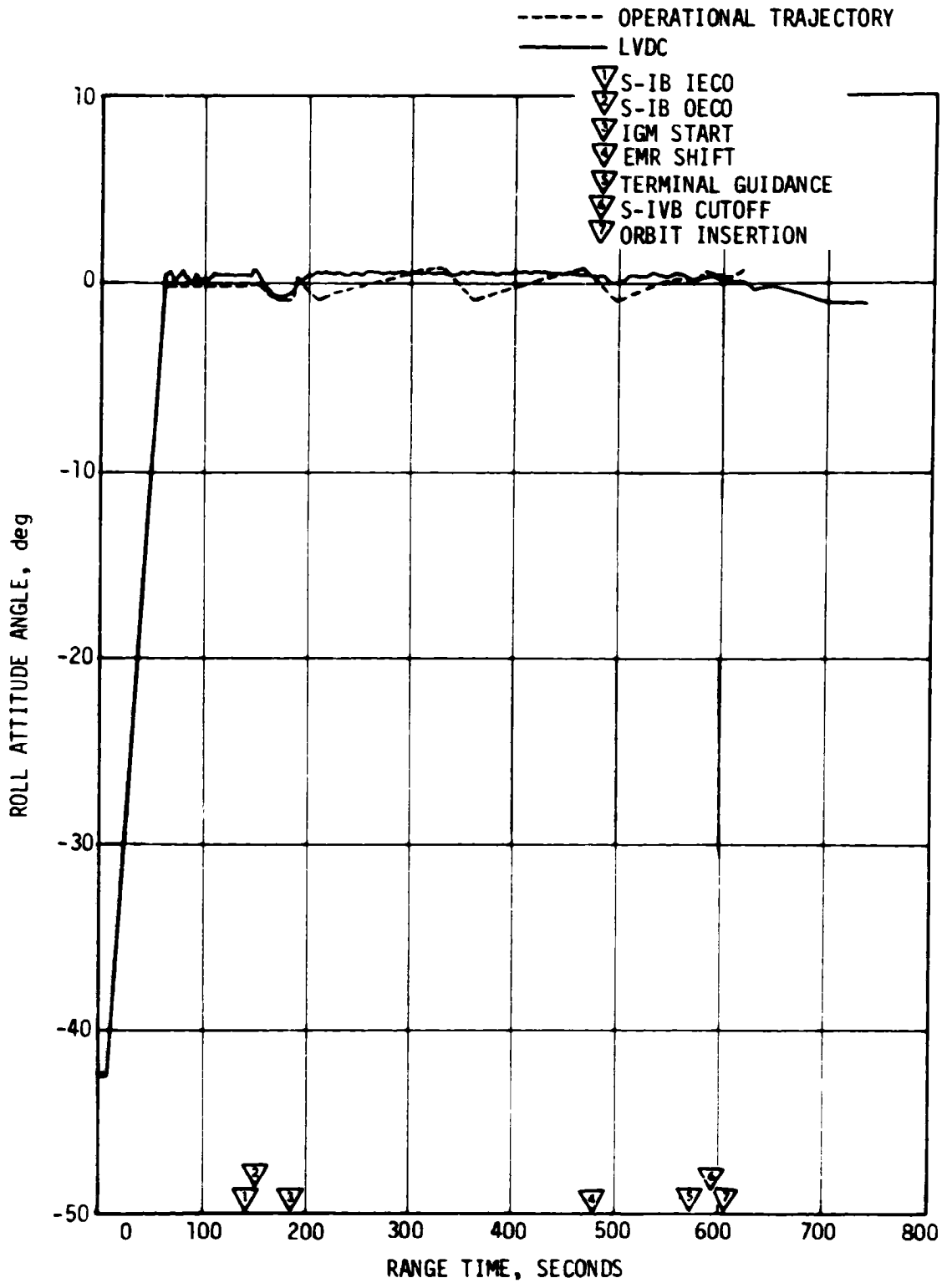


Figure 9-4. SA-206 Theta X (Roll) Attitude Angle During Boost

Table 9-4. SA-206 Orbital Phase Flight Program Steering Commands

EVENT	COMMANDED ATTITUDE (DEGREES)		
	ROLL	PITCH	YAW
Timebase 4 Chi-Freeze	0.6668	-99.663	-6.1468
Timebase 4 +21.15 sec (In-Plane Posigrade Local Horizontal Maneuver)	0.0	-108.9934	-2.0822

Subsequent ground commands were satisfactorily supported when received.

#### 9.3.4 Deorbit Phase

During the deorbit phase, a pitch axis gimbal switchover from fine to coarse resolver occurred due to the pitch rate exceeding two deg/s. Any rate sensed in excess of two deg/s is considered unreasonable. Three unreasonable values within one second cause switchover to occur. The switchover was properly executed and was the result of the vehicle being out of control due to the depletion of S-IVB Auxiliary Propulsion System (APS) propellants. Depletion of APS propellants is discussed in Section 7.10.2.

### 9.4 NAVIGATION AND GUIDANCE SYSTEM COMPONENTS

The navigation and guidance hardware satisfactorily supported the accomplishment of mission objectives.

#### 9.4.1 ST-124M Stabilized Platform System

The one anomaly which occurred in the guidance and navigation system was a large change in the gyro summation current and a small change in the accelerometer summation current in the ST-124M Platform Electronics Assembly. See Figure 9-5. The gyro summation current measurement shifted from 3.69 to 1.69 amperes. Also, the accelerometer summation current measurement shifted from 1.165 to 1.125 amperes. These shifts occurred during the period from 3500 to 5200 seconds while the vehicle was between tracking stations. It is therefore impossible to positively identify the cause. The reduced level of current was sustained throughout the remainder of the mission. The ST-124M operational performance was unaffected.

A characteristic response of the gyro and accelerometer hysteresis spin motors to interruption of transients on the 400 Hz power line is a change in the magnetomotive force components and hence a shift in input currents. Summation current shifts of the observed magnitudes have occurred in the laboratory and at the Saturn V Systems Development Breadboard Facility as the result of switching from one channel to the other in the Platform Alternating Current Power Supply. Such a shift may also result from a transient in the direct current input voltage, an inverter failure, or a perturbation in the wheel power relay (PEA K2).

Laboratory tests have been run in which a (see Figure 9-5) similar current shift was sustained in excess of 24 hours with no effect on the operational performance of the inertial components. Because this anomaly has been evidenced throughout the years in laboratory and ground testing and the motors have always maintained synchronous speed, no corrective action is deemed necessary.

#### 9.4.2 Guidance and Navigation Computer

The LVDC and LVDA performed satisfactorily. No computer anomalies were observed during any phase of the SL-2 mission. Component temperatures and internal power supply voltages were normal.

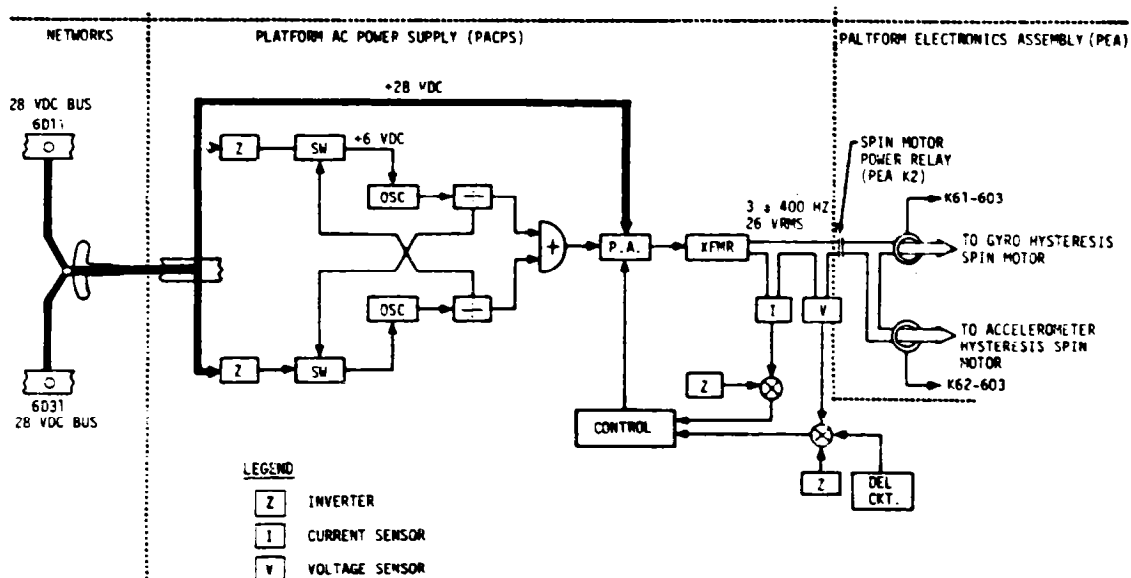


FIGURE 9-5. SA-206 ST-124M Platform System Block Diagram

SECTION 10  
CONTROL AND SEPARATION

10.1 SUMMARY

The control and separation systems functioned correctly throughout the powered and coast flight of SA-206. Control was terminated earlier than predicted during deorbit by the depletion of S-IVB Auxiliary Propulsion System (APS) Module 2 propellants. Engine gimbal deflections were nominal and APS firings predictable. Bending and slosh dynamics were adequately stabilized. No undue dynamics accompanied any separation.

10.2 S-IB CONTROL SYSTEM EVALUATION

No abnormal dynamics developed as a result of launch from the pedestal Tower clearance was adequate without a clearance maneuver (as usual for Saturn IB vehicles). Table 10-1 summarizes liftoff misalignments. Roll misalignment of the inboard engines was greater than the predicted value, but resulted in a roll error of less than 0.5 degree.

Table 10-1. SA-206 Misalignment Summary

PARAMETER	PREDICTED $3\sigma$ RANGE			LAUNCH		
	PITCH	YAW	ROLL	PITCH	YAW	ROLL
Thrust Misalignment, deg	$\pm 0.46$	$\pm 0.46$	$\pm 0.19$	0.0	0.0	-0.04
Inboard Engines Misalignment, deg	$\pm 0.25$	$\pm 0.25$	$\pm 0.25$	0.0	0.0	+0.35
Vehicle Stacking and Pad Misalignment, deg	$\pm 0.39$	$\pm 0.39$	0.0	0.0	0.0	0.0

The SA-206 control system performed as expected during S-IB boost. Jim-sphere measurements indicated wind velocities near the 95th percentile levels for May. The wind peak was 42.0 meters per second at 13.4 kilometers altitude with an azimuth of 286 degrees. In the high dynamic pressure region, the maximum angle of attack of 3.2 degrees occurred in the yaw plane in response to a wind peak. The control system adequately stabilized the vehicle response to the high altitude

winds. About 22 percent of the available yaw gimbal angle and 14 percent of the available pitch gimbal angle were used. Both deflections were due to wind speed peaks and associated shears.

Time histories of pitch and yaw and roll control parameters are shown in Figures 10-1 through 10-4. The peaks are summarized in Table 10-2. Dynamics in the region between liftoff and 56 seconds resulted primarily from guidance commands. Between 56 and 100 seconds, the vehicle responded normally to the pitch tilt program and the wind. Dynamics from 100 seconds to S-IB outboard engine cutoff were caused by Inboard Engine Cutoff (IECO), tilt arrest, separated airflow aerodynamics, and high altitude winds. Pitch and yaw plane control accelerometers were deactivated at 120 seconds.

The attitude errors indicate that the equivalent thrust vector misalignments were negligible in both pitch and yaw. Only roll plane thrust misalignments could be detected on this flight, and they averaged -0.04 degrees for all eight engines and +0.35 degrees for the four inboard engines, see Table 10-1.

The attitude errors resulting from the effects of thrust unbalance, offset center of gravity, thrust vector misalignment and control system misalignments were within predicted envelopes. The peak angles of attack in the maximum dynamic pressure region were 2.19 degrees in yaw and 1.73 degrees in pitch. The peak average engine deflections required to trim out the aerodynamic moments in this region were 1.77 and -1.12 degrees for yaw and pitch, respectively. No divergent bending or slosh dynamics were observed.

### 10.3 S-IVB CONTROL SYSTEM EVALUATION

The S-IVB thrust vector control system provided satisfactory pitch and yaw control during boost and during the deorbit propellant dumps. The APS provided satisfactory roll control while the vehicle was under thrust vector control. The APS also provided satisfactory pitch, yaw, and roll control during orbital coast. Loss of attitude control occurred approximately 418 seconds after completion of the deorbit propellant dumps due to depletion of APS Module 2 propellants.

#### 10.3.1 S-IVB Control System Evaluation During Burn

During S-IVB burn, control system transients were experienced at S-IB/S-IVB separation, Iterative Guidance Mode (IGM) initiation, Engine Mixture Ratio (EMR) shift, terminal guidance mode, and S-IVB Engine Cutoff (ECO). These transients were expected and were well within the capabilities of the control system.

The S-IVB burn pitch attitude error, angular rate, and actuator position are presented in Figure 10-5. The yaw plane burn dynamics are presented in Figure 10-6. The maximum attitude errors and rates occurred

- ▽ BEGIN PITCH/ROLL MANEUVER
- ▽ BEGIN ACCELEROMETER CONTROL
- ▽ END ROLL MANEUVER
- ▽ MACH 1
- ▽ MAX q
- ▽ 1ST GAIN SWITCH
- ▽ END ACCELEROMETER CONTROL
- ▽ 2ND GAIN SWITCH
- ▽ TILT ARREST
- ▽ INBOARD ENGINE CUTOFF
- ▽ OUTBOARD ENGINE CUTOFF
- ▽ STAGING

— MEASURED  
 - - - SIMULATED

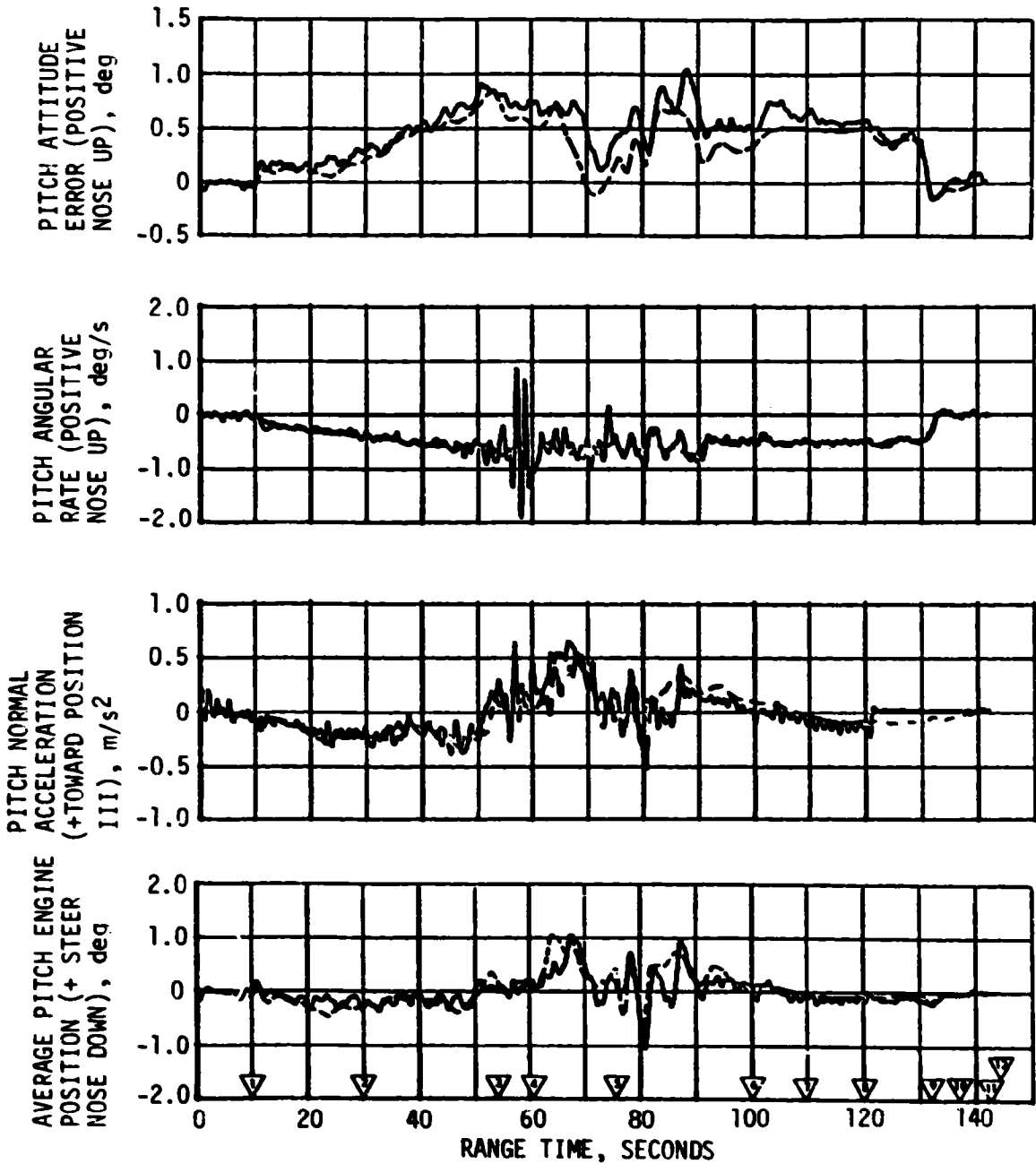


Figure 10-1. SA-206 Pitch Plane Dynamics During S-IB Burn

- ▽ BEGIN PITCH/ROLL MANEUVER
  - ▽ BEGIN ACCELEROMETER CONTROL
  - ▽ END ROLL MANEUVER
  - ▽ MACH 1
  - ▽ MAX q
  - ▽ 1ST GAIN SWITCH
  - ▽ END ACCELEROMETER CONTROL
  - ▽ 2ND GAIN SWITCH
  - ▽ TILT ARREST
  - ▽ INBOARD ENGINE CUTOFF
  - ▽ OUTBOARD ENGINE CUTOFF
  - ▽ STAGING
- MEASURED  
 - - - SIMULATED

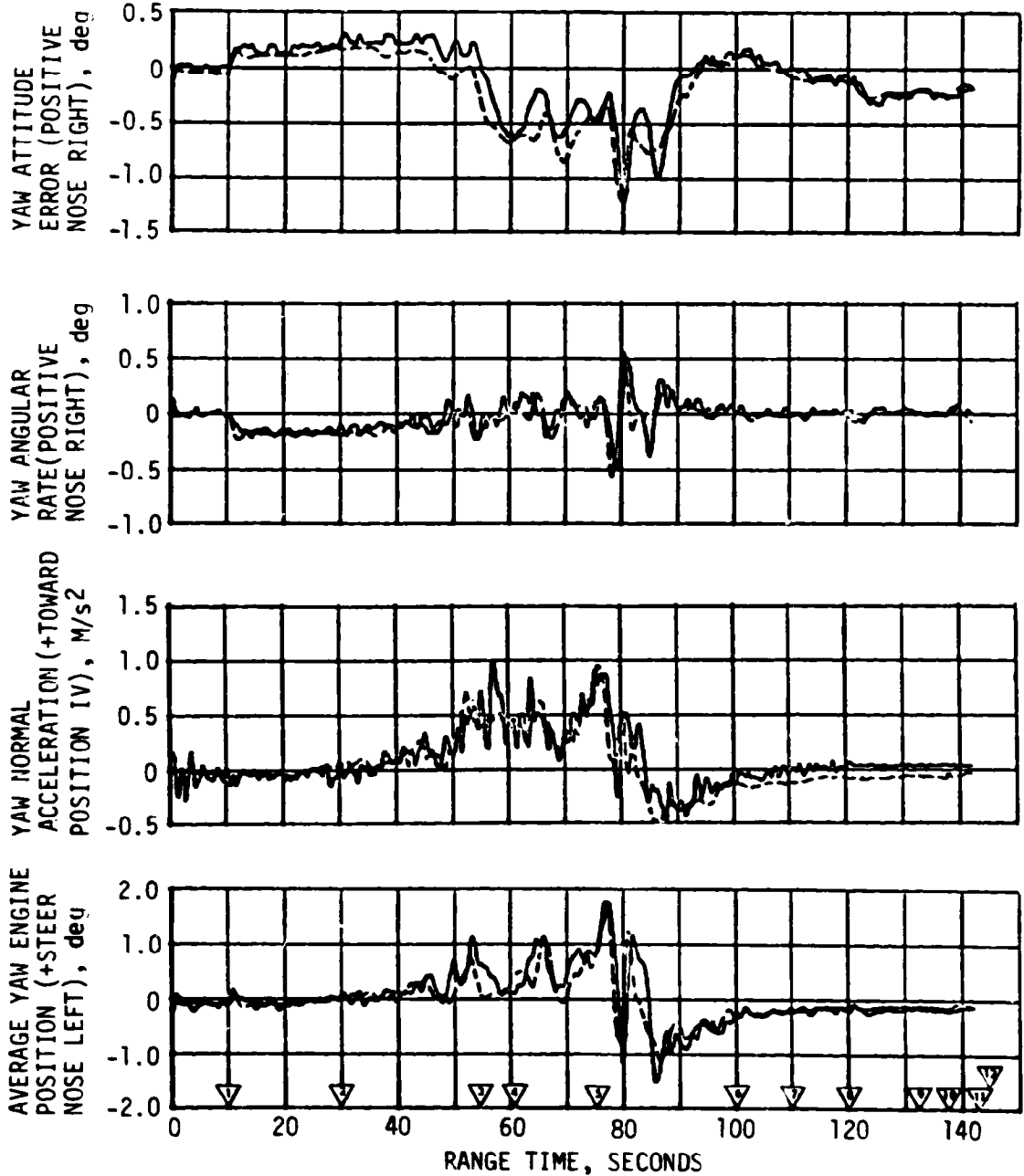


Figure 10-2. Yaw Plane Dynamics During S-IB Burn



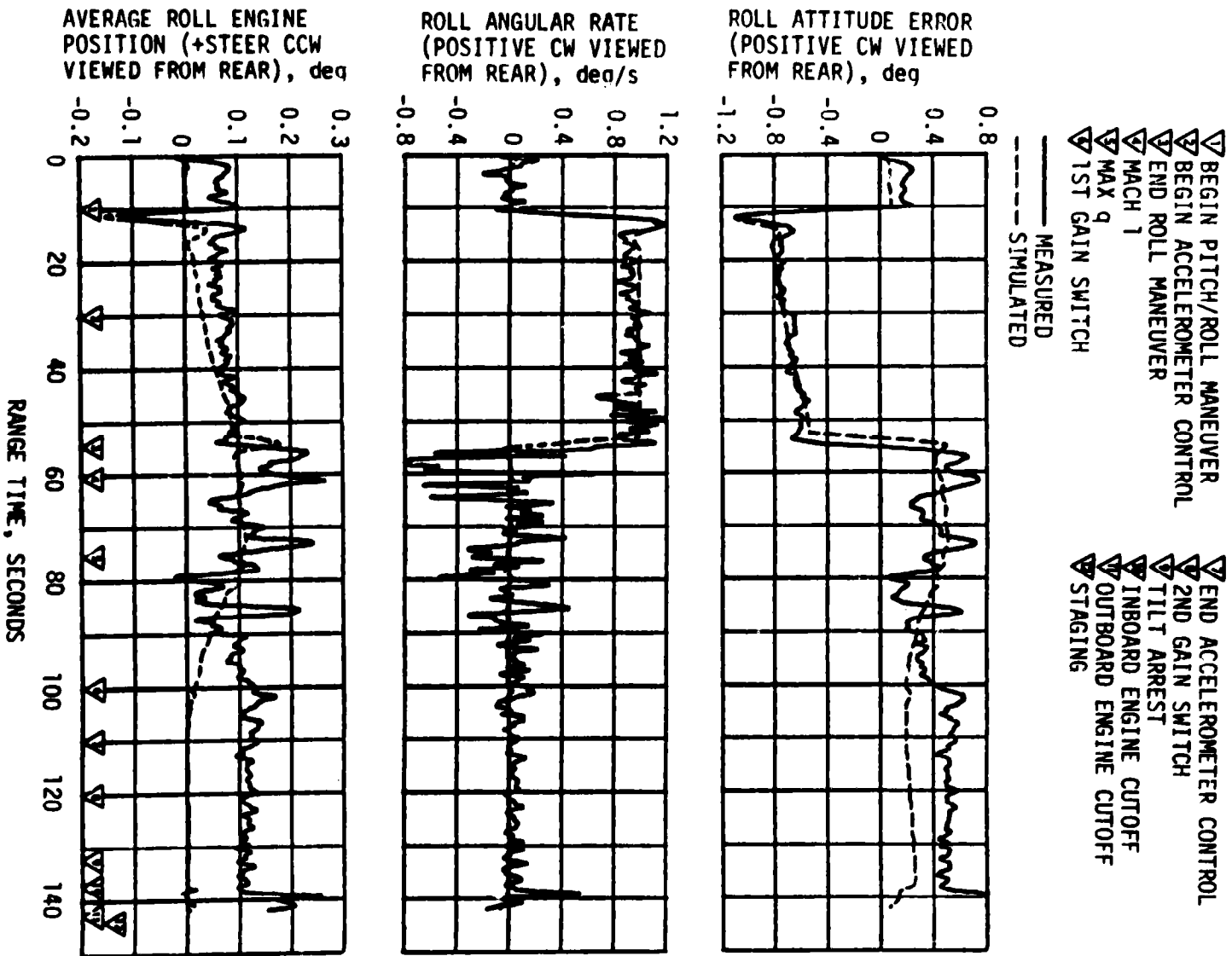


Figure 10-3. SA-206 Roll Plane Dynamics During S-1B Burn

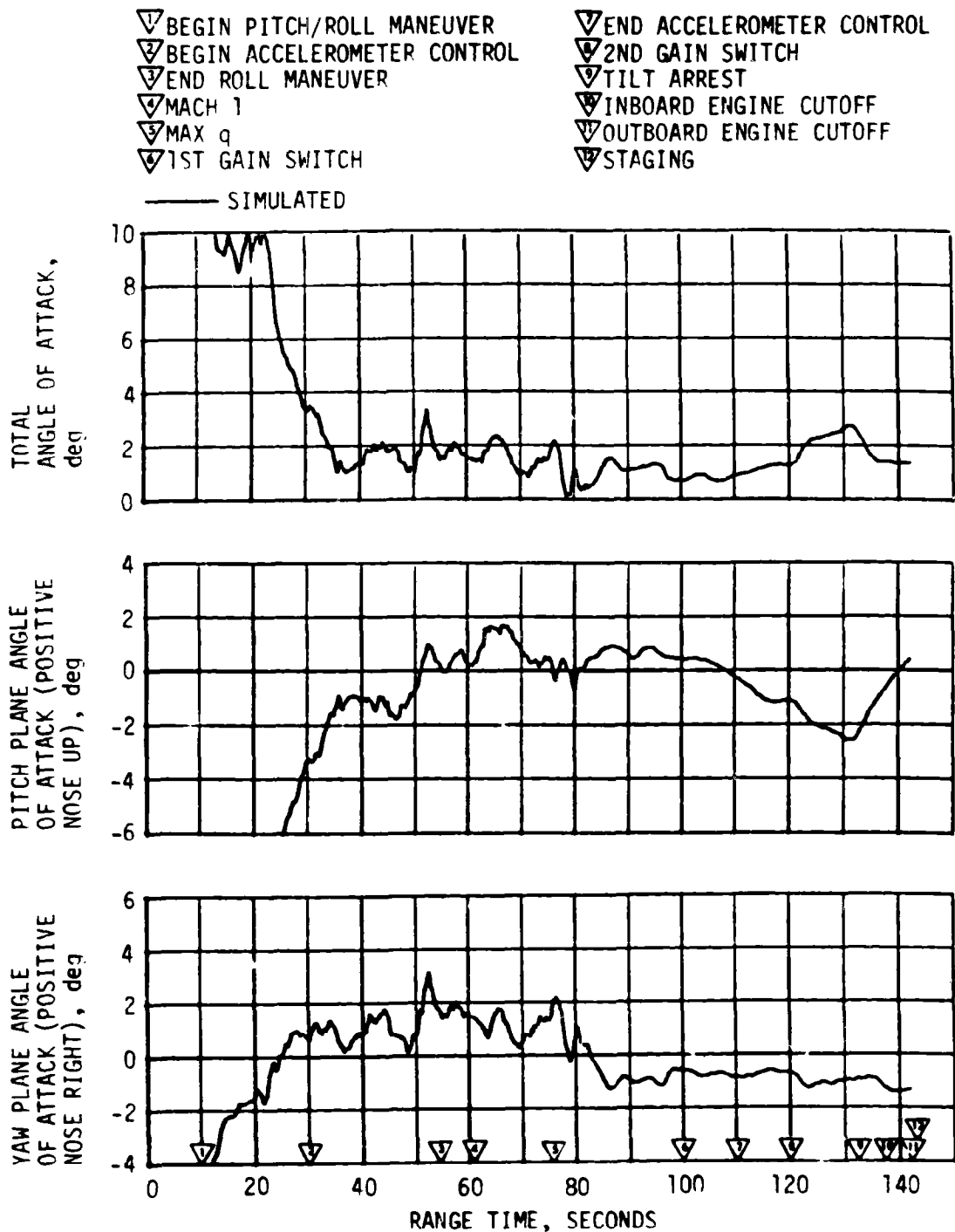


Figure 10-4. SA-206 Pitch and Yaw Plane Free Stream Angle of Attack During S-IB Burn

Table 10-2. Maximum Control Parameters During S-IB Burn

PARAMETER	PITCH PLANE		YAW PLANE		ROLL PLANE	
	AMPLITUDE	RANGE TIME (SEC)	AMPLITUDE	RANGE TIME (SEC)	AMPLITUDE	RANGE TIME (SEC)
Attitude Error, deg	1.05	88.2	-1.22	80.0	-1.05	12.0
Angular Rate, deg/s	-0.95	80.5	0.51	81.1	1.20	12.3
Average Gimbal Angle, deg	-1.12	81.0	1.77	77.5	0.27	61.1
Angle of Attack, deg	1.73	66.7	2.19	76.7	-	-
Angle of Attack Dynamic Pressure Product, deg-n/cm <sup>2</sup> (deg-lbf/ft <sup>2</sup> )	5.71 (1190)	66.7	7.40 (1540)	76.7	-	-
Normal Acceleration, m/s <sup>2</sup> (ft/s <sup>2</sup> )	0.65 (2.13)	56.8	1.01 (3.31)	57.3	-	-

\*Angular rate data questionable between 55 and 60 seconds due to noise content and low sampling rate.

at IGM initiation. A summary of the maximum values of critical flight control parameters is presented in Table 10-3.

The pitch and yaw effective thrust vector misalignments during the first part of burn (prior to EMR shift) were +0.17 and -0.22 degrees, respectively. Following the EMR shift the misalignments were +0.19 and -0.22 degrees for pitch and yaw, respectively. A steady state roll torque prior to EMR shift of 18.0 N-m (13.3 lbf-ft) clockwise looking forward required roll APS firings. The steady state roll torque following EMR shift was 8.8 N-m (6.5 lbf-ft) clockwise looking forward and required a few roll APS firings. The steady state roll torque experienced on previous flights has ranged between 61.4 N-m (45.3 lbf-ft) counterclockwise and 54.2 N-m (40.0 lbf-ft) clockwise.

Propellant sloshing during burn was observed on data obtained from the Propellant Utilization (PU) mass sensors and on the pitch and yaw actuator position and actuator valve current data. The propellant slosh had a negligible effect on the operation of the attitude control system.

### 10.3.2 S-IVB Control System Evaluation During Orbit

The APS provided satisfactory orientation and stabilization during orbit. Loss of attitude control occurred at 20,493 seconds (05:41:33) due to depletion of APS Module 2 propellant. This is discussed in paragraphs 10.3.3 and 7.10.

▽	S-IVB BURN MODE ON "B"	143.9 SECONDS
▽	IGM INITIATION	178.2 SECONDS
▽	MIXTURE RATIO SHIFT	470.3 SECONDS
▽	BEGIN TERMINAL GUIDANCE	564.3 SECONDS
▽	CHI FREEZE	581.7 SECONDS
▽	S-IVB ENGINE CUTOFF	586.2 SECONDS

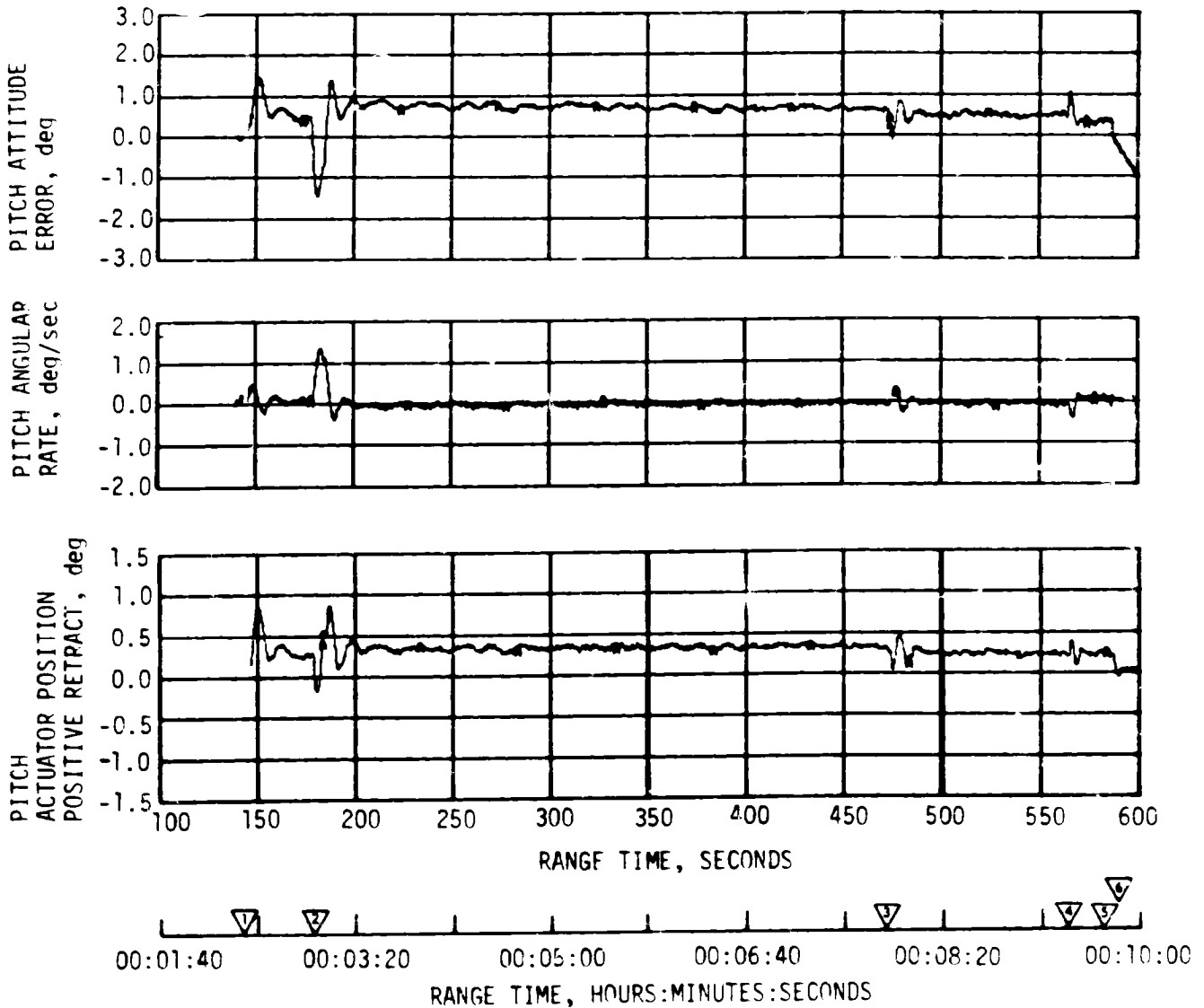


Figure 10-5. SA-206 Pitch Plane Dynamics - S-IVB Burn

▽	S-IVB BURN MODE ON "B"	143.9	SECONDS
▽	IGM INITIATION	178.2	SECONDS
▽	MIXTURE RATIO SHIFT	470.3	SECONDS
▽	BEGIN TERMINAL GUIDANCE	564.3	SECONDS
▽	CHI FREEZE	581.7	SECONDS
▽	S-IVB ENGINE CUTOFF	586.2	SECONDS

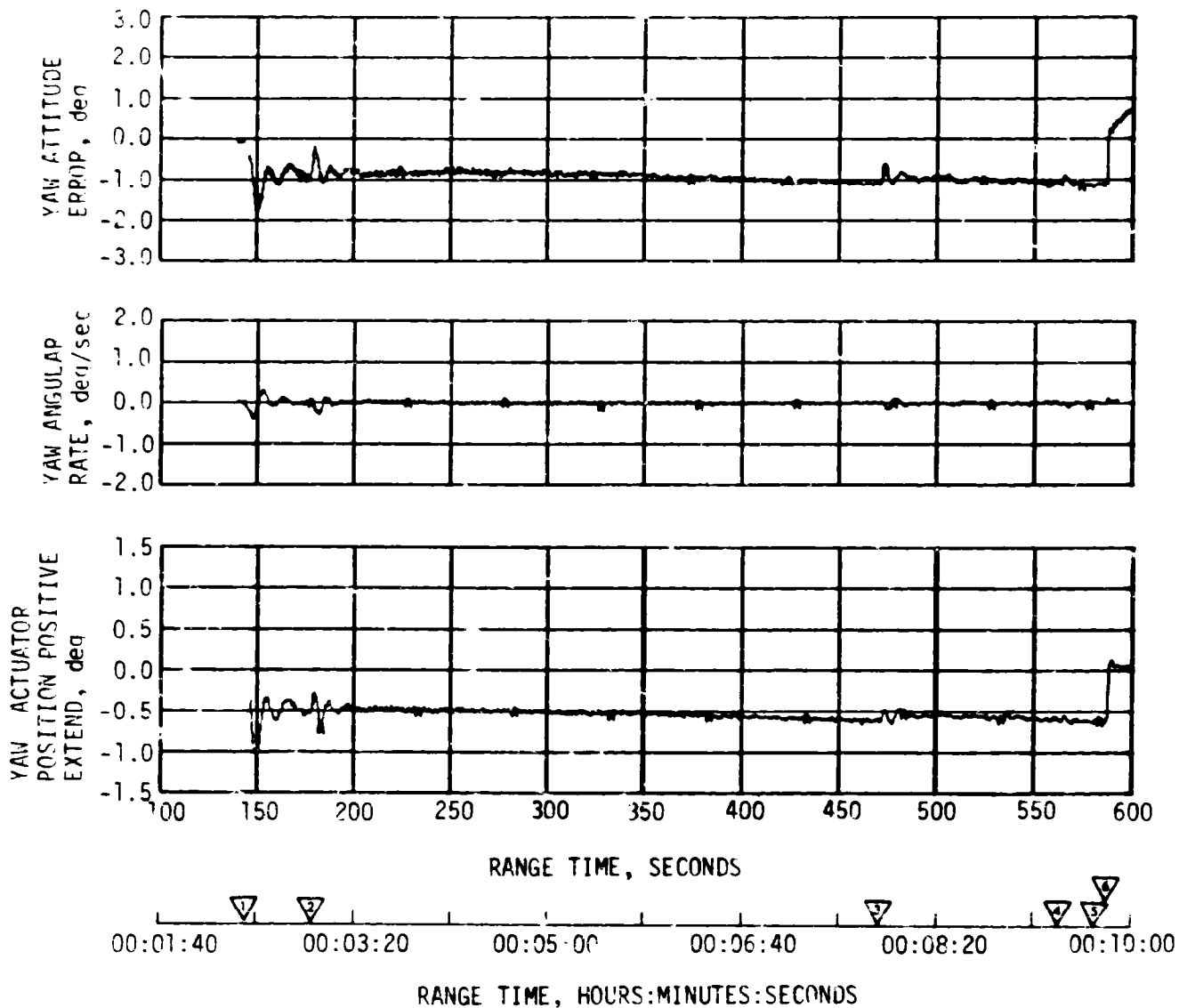


Figure 10-6. SA-206 Yaw Plane Dynamics - S-IVB Burn

Table 10-3. SA-206 Maximum Control Parameters During S-IVB Burn

PARAMETER	PITCH PLANE		YAW PLANE		ROLL PLANE	
	AMPLITUDE	RANGE TIME (SEC)	AMPLITUDE	RANGE TIME (SEC)	AMPLITUDE	RANGE TIME (SEC)
Attitude Error, deg	1.6	151.0	-2.0	150.4	-0.8	157.0
Angular Rate, deg/s	1.3	183.0	-0.4	147.5	-0.3	147.0
Maximum Gimbal Angle, deg	0.9	186.8	-1.0	150.0	-	-
* Values removed						

Significant events related to orbital coast attitude control were the maneuver to the in-plane local horizontal following S-IVB cutoff, spacecraft separation, the maneuver to the M-415 solar inertial attitude, the maneuver back to the in-plane local horizontal, and a ground commanded 180° roll maneuver. Effects of LOX and LH2 Non Propulsive Vent (NPV) operation prior to the deorbit sequence (TB5) were also noticed on attitude control system data.

The pitch attitude error and angular rate for the maneuvers and spacecraft separation are shown in Figure 10-7.

Following S-IVB cutoff and switching to the orbital control mode, the vehicle was maneuvered to the in-plane posigrade local horizontal (Position I down), and the orbital pitch rate was established. This maneuver began at 607 seconds (00:10:07) and consisted of approximately -11 degrees in pitch, +4 degrees in yaw and -0.7 degree in roll.

Spacecraft separation, which occurred at 960.3 seconds (00:16:00.3), produced vehicle disturbances slightly larger than those experienced on AS-205. See paragraph 10.5.2 for a discussion of vehicle motion during CSM separation.

At 3340 seconds (00:55:40) the maneuver to the M-415 solar inertial attitude was begun. This maneuver was a three axis maneuver and resulted in a pitch maneuver change from approximately 68.4 to 37.17 degrees, a yaw maneuver change from 2.12 to 2.20 degrees, and a roll maneuver change from 0.0 to -93.35 degrees measured in the platform coordinate system. This attitude was held for approximately 8900 seconds.

While in the M-415 solar inertial attitude the fuel tank ullage pressure was observed to be cycling between 31.5 and 32.6 psia following Acquisition of Sign (AOS) at 5625 seconds (1:33:45), reference paragraph 7.10.1. The vent cycles consist of approximately 100 seconds of self-pressurization followed by 40 seconds of relief venting. During the 40 second vent cycles high frequency oscillations were noted in the telemetered rate gyro outputs in all axes. This appears to result from high frequency local structural oscillation in the S-IVB forward skirt and Instrument

▽ INITIATE MANEUVER TO LOCAL HORIZONTAL  
 ▽ SPACECRAFT SEPARATION

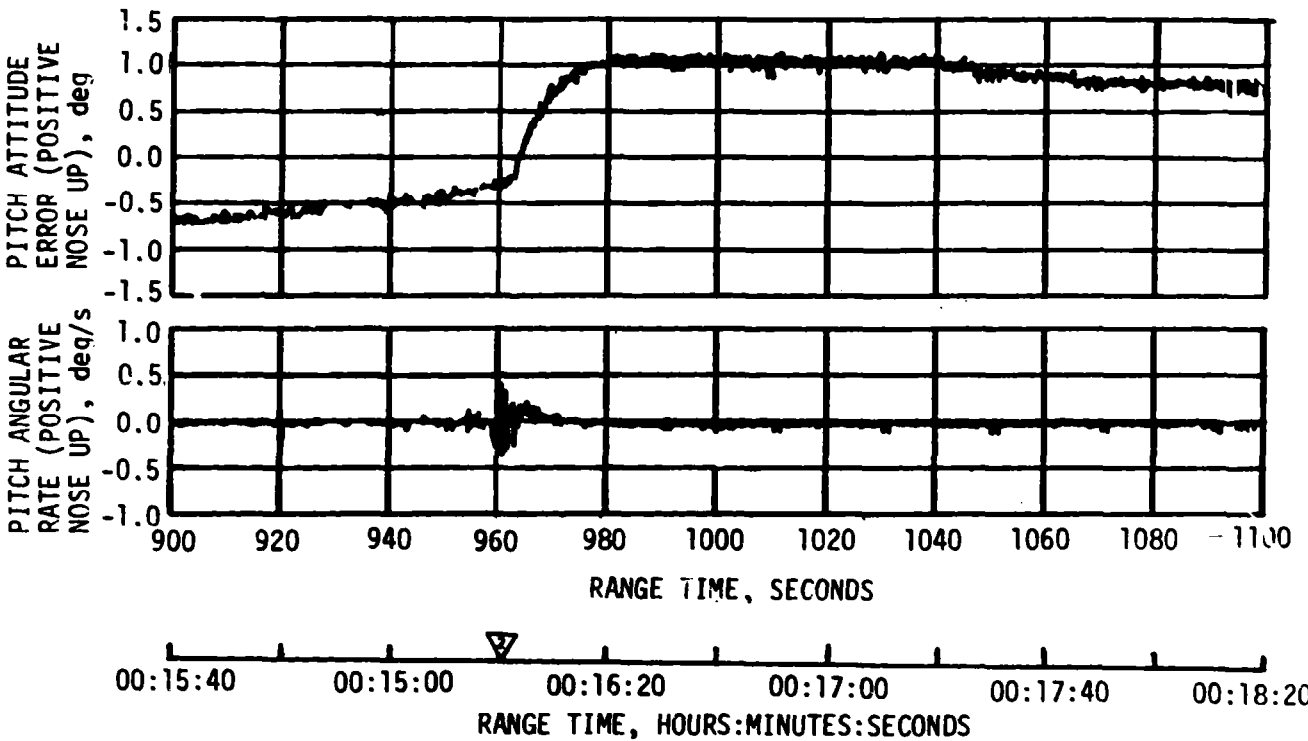
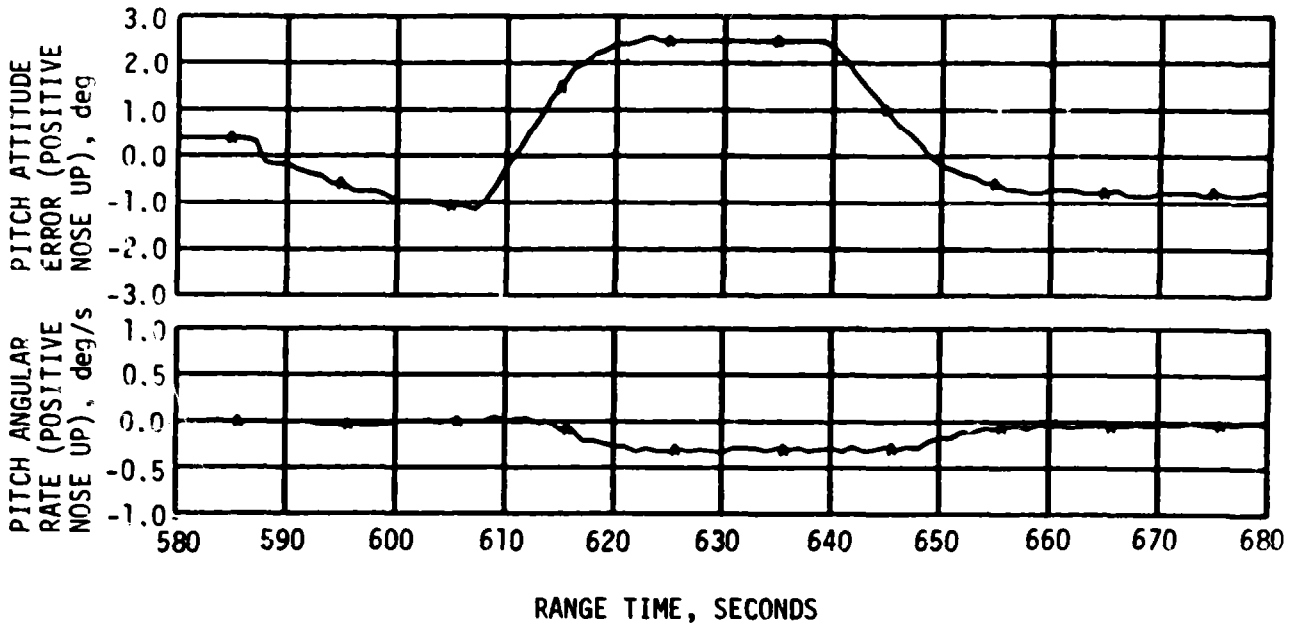


Figure 10-7. SA-206 Pitch Plane Dynamics During Orbit (Sheet 1 of 3)

▽ INITIATE MANEUVER TO M415 SOLAR INERTIAL ATTITUDE  
 ▽ INITIATE MANEUVER TO RETROGRADE LOCAL HORIZONTAL

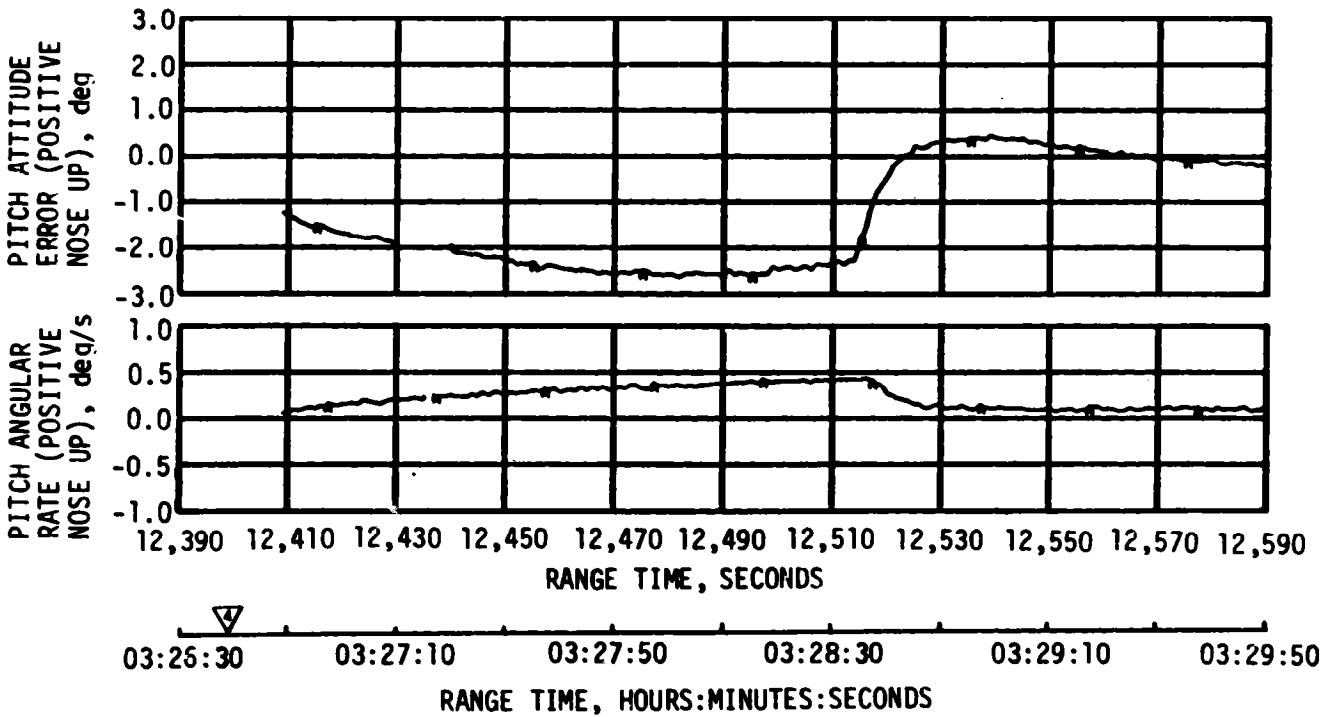
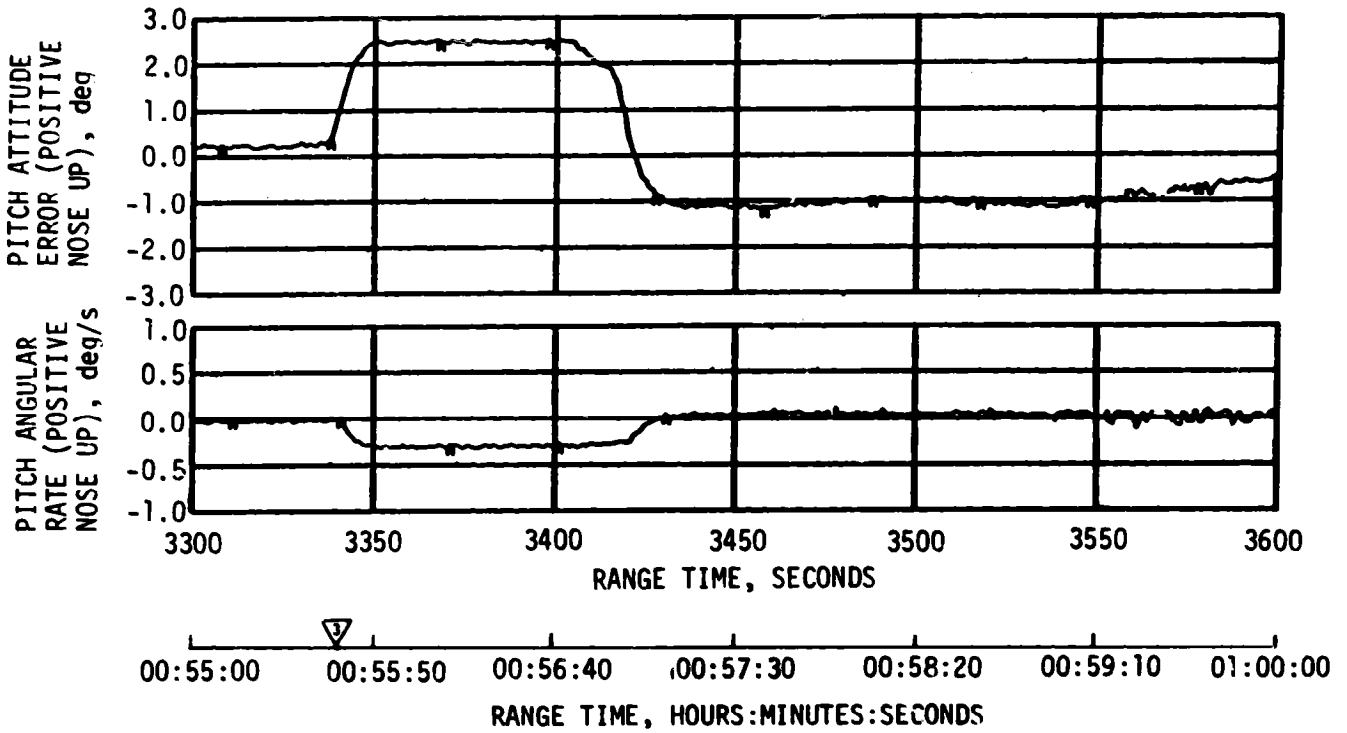


Figure 10-7. SA-206 Pitch Plane Dynamics During Orbit (Sheet 2 of 3)



▽ INITIATE MANEUVER TO ROLL -180 DEGREES

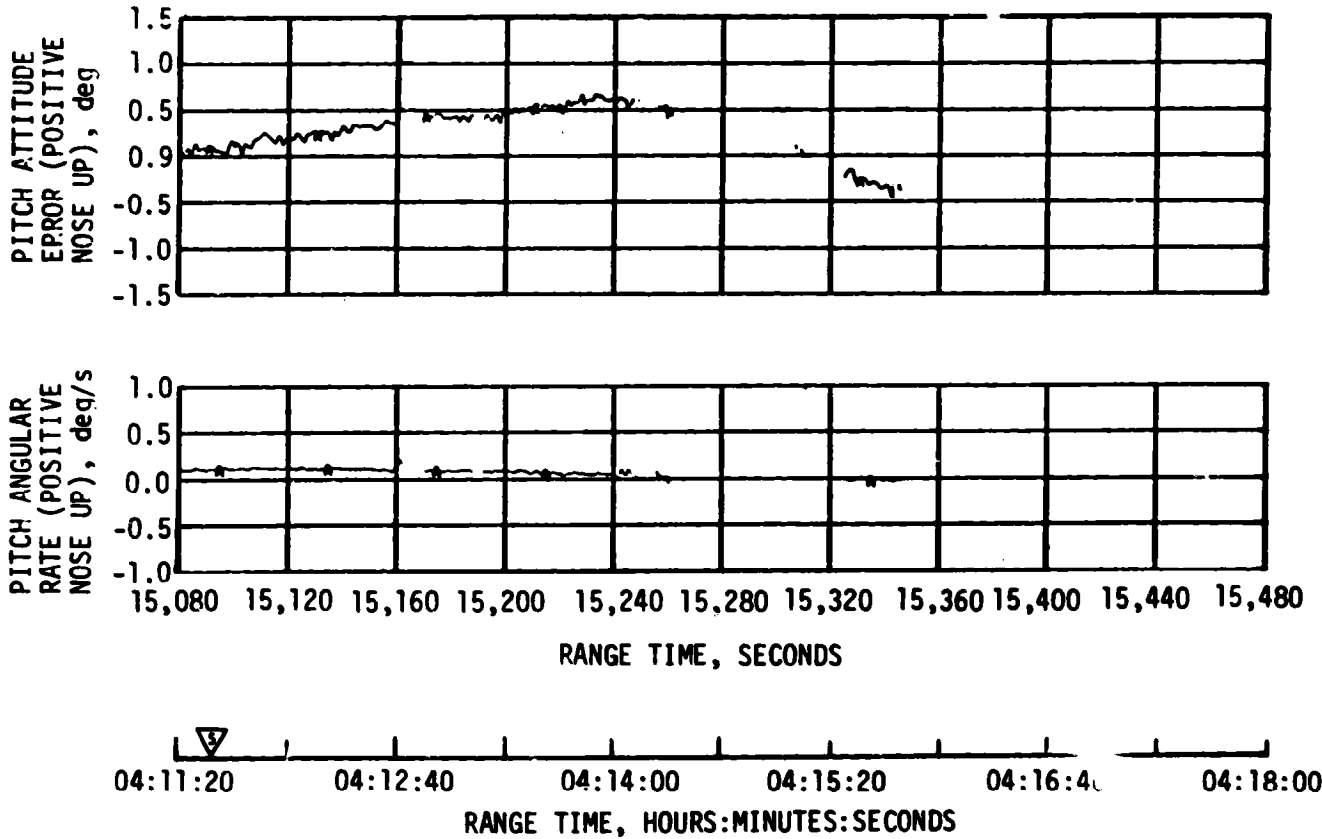


Figure 10-7. SA-206 Pitch Plane Dynamics During Orbit (Sheet 3 of 3)

Unit which results from the high frequency vent system oscillation noted in Paragraph 7.10.1. The rate signal is filtered upstream of the APS spatial amplifiers in the Flight Control Computer and based on the observed APS firing history and vehicle dynamic behavior, the rate oscillations had no effect on control system operation.

During the 40 second relief vent periods the vehicle experienced small disturbance torques opposite in polarity to the observed aerodynamic torques. The attendant vehicle motion resulted in an APS propellant usage rate which was slightly higher than that observed from data received through Goldstone one revolution later, at which time the fuel vent was operating in a continuous relief mode (cyclic fuel venting activity ceased over Madrid at 6780 seconds [1:53:00]).

At 12,399 seconds (03:26:39) a ground command was initiated to perform a maneuver to the retrograde in-plane local horizontal attitude with Position I down, and to establish an orbital pitch rate. This maneuver consisted of vehicle rotations of approximately -46 degrees in pitch, -0.9 degrees in yaw, and -86 degrees in roll.

At 15,093 seconds (04:11:33) a ground command was initiated to roll the vehicle -180° (Position III down). This maneuver took approximately 360 seconds to complete. The purpose of the maneuver was to acquire the opposite command antennas in hopes of improving command reception.

Low level disturbances were noted on attitude control data following Hawaii AOS at 16,090 seconds (04:26:20) and ARIA AOS at 17,620 seconds (04:53:40). These low level disturbances are associated with LOX NPV operation over these telemetry stations (see paragraph 7.10.2 for discussion of LOX NPV operation).

### 10.3.3 S-IVB Control System Evaluation During Deorbit

Satisfactory vehicle stability and control characteristics were observed during the deorbit propellant dump. Thrust Vector Control (TVC) was used for pitch and yaw, while the APS was used for roll control during the dump period. Attitude error data for the pitch, yaw and roll axes are presented in Figure 10-8 for the last 152 seconds of the 460 second LOX dump and the 125 second LH<sub>2</sub> dump. The figure also shows the 30 second period between LOX and LH<sub>2</sub> dump, during which no TVC control is provided.

Although telemetered data could not be obtained for the first 310 seconds of the LOX dump, a comparison of the data in the figure with predicted values shows that, in general, performance was better than expected. For example, the average pitch attitude error for worst case conditions was predicted to be approximately -3.0 degrees. Actual performance shows the average pitch attitude error to be approximately -1.4 degrees. The known center of gravity (CG) offset contributes approximately -0.8 degree leaving only -0.6 degree of attitude error

▽	END LOX DUMP	19,920	SECONDS
▽	START FUEL DUMP	19,950	SECONDS
▽	END FUEL DUMP	20,075	SECONDS
▽	FCC BURN MODE OFF "B"	20,075.6	SECONDS
▽	LOX NPV OPEN	20,076.9	SECONDS
▽	FUEL NPV OPEN	20,077.1	SECONDS

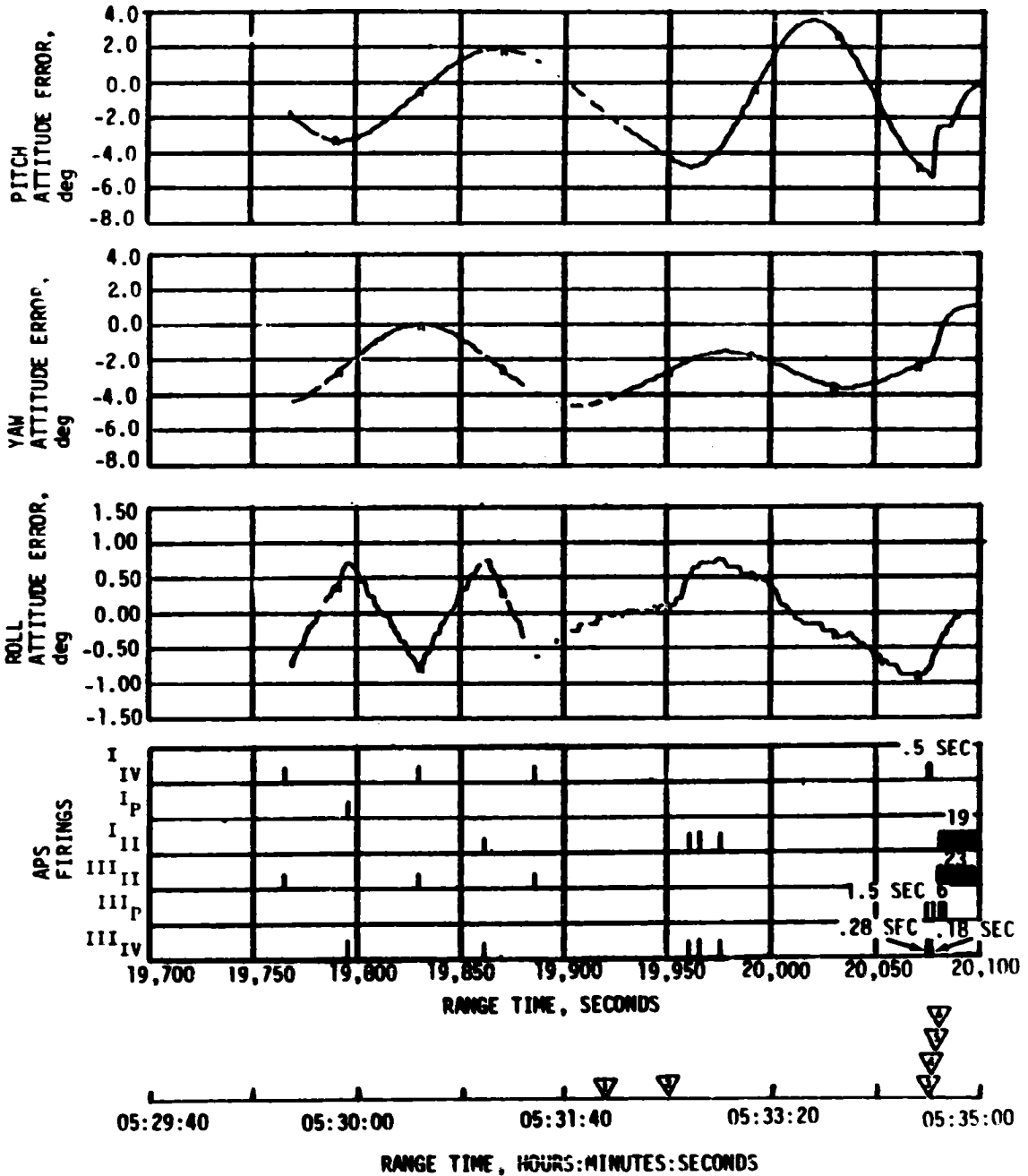


Figure 10-8. SA-206 VEHICLE DYNAMICS DURING DEORBIT (SHEET 1 OF 2)

▽ FCC BURN MODE OFF "B"	20,075.6	SECONDS
▽ LOX NPV OPEN	20,076.9	SECONDS
▽ LH <sub>2</sub> NPV OPEN	20,077.1	SECONDS
▽ START ENGINE PNEUMATIC DUMP	20,135.9	SECONDS
▽ START COLD HE DUMP	20,175	SECONDS
▽ APS MODULE 2 DEPLETION	20,493	SECONDS

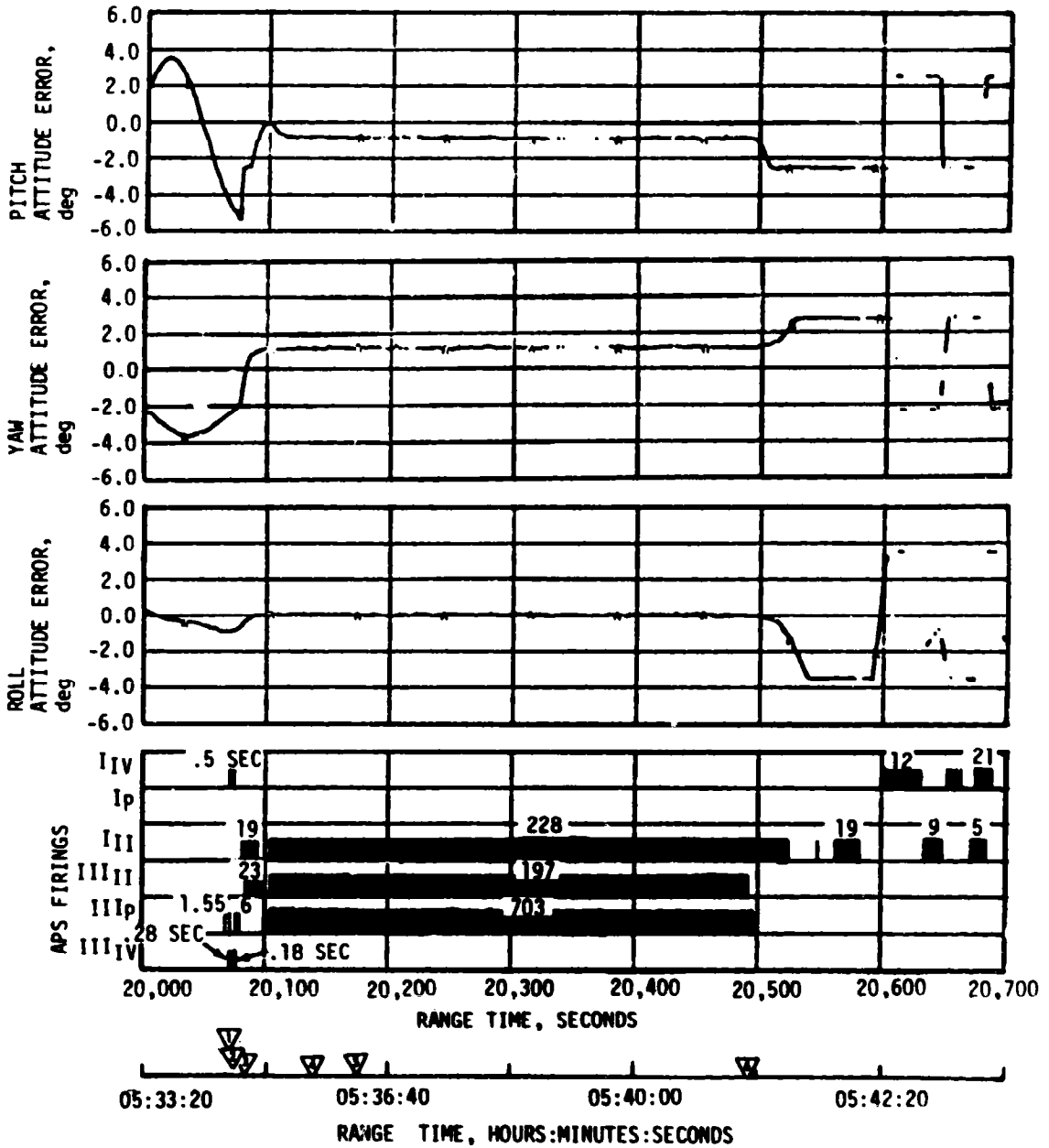


Figure 10-8. SA-206 Vehicle Dynamics During Reorhit (Sheet 2 of 2)

attributable to thrust vector misalignment.

A comparison of the average yaw attitude error shows a similar improvement over the predicted values. The predicted average yaw attitude error was approximately -4.4 degrees, while the actual was only -2.5 degrees. This difference is also directly attributable to assuming a worst case vector misalignment of -1.0 degree in obtaining the predicted value. The known CG offset accounts for -2.18 degrees and the actual thrust misalignment for -0.16 degree.

During the 30 second period between LOX and LH<sub>2</sub> dump (19,920 to 19,951 seconds), in which there is no thrust for control, it is noted from the figure that the attitude error buildup in pitch is much larger than in yaw. The reason for this is that the residual pitch rate at LOX dump termination is -0.12 degree/sec and the attitude error slope is negative, while the residual yaw rate is +0.03 degree/sec and the attitude error slope is positive. Thus, pitch attitude error becomes more negative during the uncontrolled period and yaw becomes less negative.

A comparison of the peak to peak amplitude for the predicted and observed data in pitch (near the end of the LOX dump) shows -4.3 degrees and -5.0 degrees, respectively; a similar comparison for yaw axis data shows -6.4 degrees and 4.6 degrees, respectively. The predicted and observed data here are judged to agree reasonably well and indicate that TVC provided satisfactory control.

Following the 30 second period of no TVC control, the LH<sub>2</sub> dump was initiated and the control system reacted to reduce the negative attitude errors in pitch and yaw. Since the control system is low frequency and lightly damped the attitude errors existing at LH<sub>2</sub> dump initiation tended to present a new bound on the magnitude of the oscillation. Thus, pitch attitude errors are larger than yaw during LH<sub>2</sub> dump.

The vehicle was limit cycling in roll during the LOX dump. A small roll disturbance at the start of LH<sub>2</sub> dump required three APS roll firings. No APS roll firings were required during the remainder of the fuel dump.

The programmed command for S-IVB burn mode off was initiated at 20,075.6 seconds, transferring pitch and yaw attitude control from the Thrust Vector Control system to the Coast Attitude Control system.

Initial conditions at the end of the LH<sub>2</sub> dump were as follows:

Pitch Attitude Error	-5.4°	Pitch Angular Rate	-0.07°/s
Yaw Attitude Error	-2.0°	Yaw Angular Rate	+0.05°/s
Roll Attitude Error	-0.9°	Roll Angular Rate	0.0°/s

These attitude errors and angular rates were easily nulled out by the

Coast Attitude Control system (see Figure 10-4, Sheet 2 of 2). Following termination of the LH<sub>2</sub> dump, the LOX and LH<sub>2</sub> Nonpropulsive Vents (NPV) were opened at 20,076.9 and 20,077.1 seconds, respectively. A partial blockage of the LOX NPV Nozzle 1 (see Section 7) caused APS Module 2 to deplete its propellant within 418 seconds after the LH<sub>2</sub> dump.

Control forces were present on the vehicle following termination of the fuel dump. The location of the total control force lies on or within 8 degrees of the LOX NPV nozzle plane. Accelerometer data show very little acceleration during this time period indicating a balance of forces and substantiates a disturbance force aft of the vehicle CG and coincident with an NPV nozzle.

Following depletion of APS Module 2 propellant, the vehicle diverged in all axes with APS Module 1 attempting to control in the yaw-roll axes.

#### 10.4 INSTRUMENT UNIT CONTROL COMPONENTS EVALUATION

The IU control subsystem functioned properly throughout the SA-206 mission. All planned maneuvers occurred at or near the anticipated time of flight.

#### 10.5 SEPARATION

##### 10.5.1 S-IB/S-IVB Separation

A detailed reconstruction of the separation dynamics was not possible since S-IVB telemetry data dropped out due to flame attenuation for approximately 2.5 seconds following separation. The separation analysis was done by comparing SA-205 data with the available SA-206 data. S-IB and S-IVB longitudinal acceleration and body rates showed essentially nominal separation when compared with SA-205 data.

Figure 10-9 shows the S-IB/S-IVB longitudinal acceleration, and Figure 10-10 shows pitch, yaw, and roll angular rates during S-IB/S-IVB separation. Vehicle dynamics were nominal, and well within staging limits.

##### 10.5.2 S-IVB/CSM Separation

S-IVB/CSM separation was accomplished on SA-206 with the vehicle in the in-plane local horizontal attitude with an orbital pitch rate of approximately  $-0.069$  degrees/seconds. S-IVB disturbances due to spacecraft separation began at 960.4 seconds (00:16:00.4). Maximum vehicle rates following separation were 0.176 degrees/second in pitch, 0.035 degrees/second in yaw, and  $-0.057$  degrees/second in roll. APS firings occurred following separation in response to separation-induced disturbances.

Following removal of spacecraft separation transients at approximately

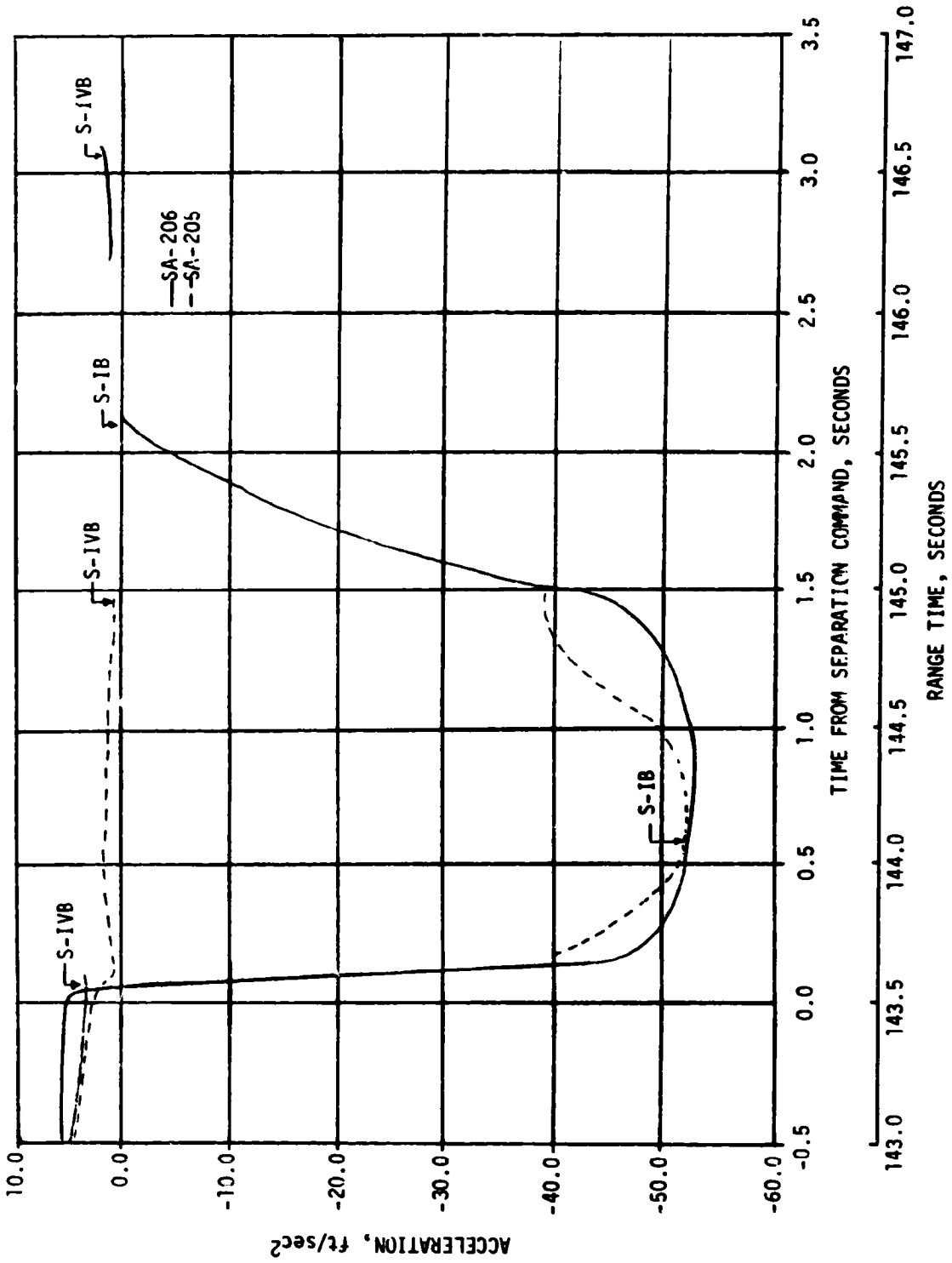


Figure 10-9. S-IB/S-IVB Longitudinal Acceleration

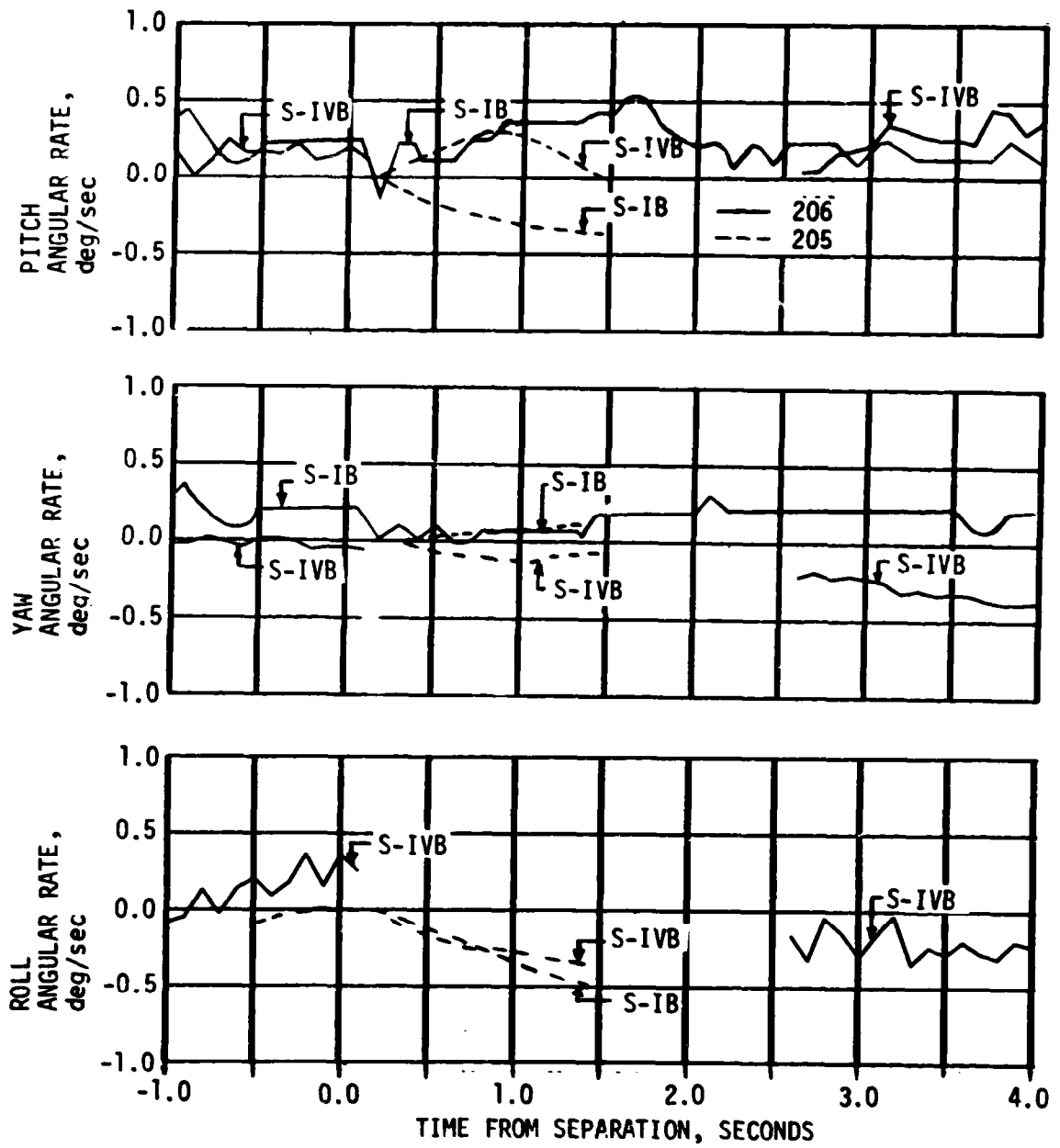


Figure 10-10. Angular Velocities During S-IB/S-IVB Separation



980 seconds (00:16:20), one sided pitch and yaw disturbances were observed on attitude error data until approximately 1030 seconds (00:17:10). This corresponds time-wise with some liquid venting from the S-IVB LH<sub>2</sub> nonpropulsive vents, see Paragraph 7.10.1.

## SECTION 11

### ELECTRICAL NETWORKS AND EMERGENCY DETECTION SYSTEM

#### 11.1 SUMMARY

The electrical systems and Emergency Detection System (EDS) of the SA-206 launch vehicle performed satisfactorily during the flight. Battery performance (including voltages, currents, and temperatures) was satisfactory and remained within acceptable limits. Operation of all power supplies, inverters, Exploding Bridge Wire (EBW) firing units, and switch selectors were nominal.

#### 11.2 S-IB STAGE ELECTRICAL SYSTEM

The S-IB-6 stage electrical system was modified to eliminate single-point relay contact failures and to incorporate redundant wiring to critical interface functions. A new type of battery with improved regulation was also utilized (reference Appendix B).

The S-IB stage electrical system operated satisfactorily. Battery voltage and current excursions during flight coincided with significant vehicle events as predicted. Voltages for the 1D10 and 1D20 batteries averaged 28.8 V and 29.0 V respectively from power transfer to S-IB/S-IVB separation. The current on batteries 1D10 and 1D20 averaged 16.9 amperes and 17.2 amperes respectively throughout the boost phase. The most pronounced power drains were caused by the H-1 engines conax valve firings and pre-act operations during S-IB stage engine cutoff. Battery power consumption was within the rated capacity of each battery as shown in Table 11-1.

Table 11-1. S-IB Stage Battery Power Consumption

BATTERY	RATED CAPACITY (AMP-HR)	POWER CONSUMPTION*	
		AMP-HR	PERCENT OF CAPACITY
1D10	33.3	5.0	14.8
1D20	33.3	4.5	13.2

\* Battery Consumptions were calculated from activation until end of telemetry (at 380 seconds).

The measuring voltage supplies performed satisfactorily and remained within the allowable tolerance of  $5.000 \pm .0125$  V.

All switch selector channels functioned as commanded by the Instrument Unit (IU) and were within the required time limits.

The separation and retro motor EBW firing units were armed and triggered as programmed. Charging time and voltage characteristics were within performance limits.

The range safety command system EBW firing units were in a state-of-readiness for vehicle destruct had it been necessary.

### 11.3 S-IVB STAGE ELECTRICAL SYSTEM

The S-IVB stage electrical system was modified to incorporate a two unit Aft No. 2 battery for increased capacity, and to add redundant low temperature thermostats to the battery heater control circuitry. The LH<sub>2</sub> depletion sensor system electrical circuitry was also modified to provide 3 out of 4 voting logic (reference Appendix B).

The S-IVB stage electrical system performed satisfactorily. The battery voltages and currents remained within the normal range.

Battery temperatures remained within specified limits and the battery heater controller malfunction experienced on AS-512 did not recur. Battery voltage, current and temperature plots are shown in Figures 11-1 through 11-4.

Battery power consumption was within the rated capacity of each battery as shown in Table 11-2. The three 5-V and five 20-V excitation modules all performed within acceptable limits. The LOX and LH<sub>2</sub> chilldown inverters performed satisfactorily and fulfilled load requirements.

All switch selector channels functioned properly, and all sequencer outputs were issued within required time limits.

Performance of the EBW circuitry for the separation system was satisfactory. Firing units charge and discharge responses were within predicted time and voltage limits. The command destruct firing units were in the required state-of-readiness if vehicle destruct had been necessary.

### 11.4 INSTRUMENT UNIT ELECTRICAL SYSTEM

The IU electrical power is supplied by three batteries. The 6D20 battery, which powered only the C-Band transponders on SA-205, was deleted because of the minimal mission requirements (see Appendix B).

The IU electrical system functioned satisfactorily. All battery voltages

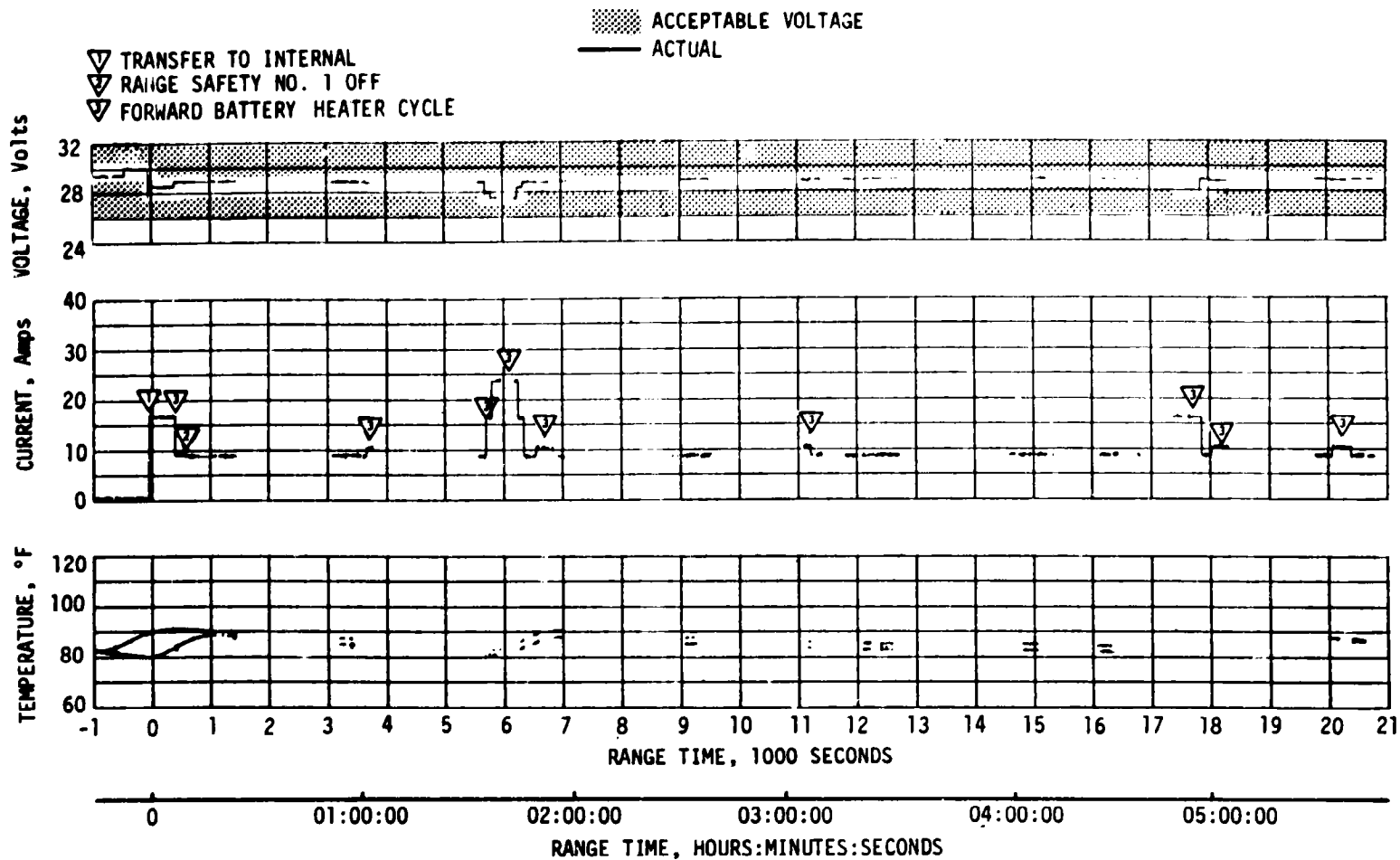


Figure 11-1. 5. 3 Stage Forward No. 1 Battery Voltage, Current, and Temperature

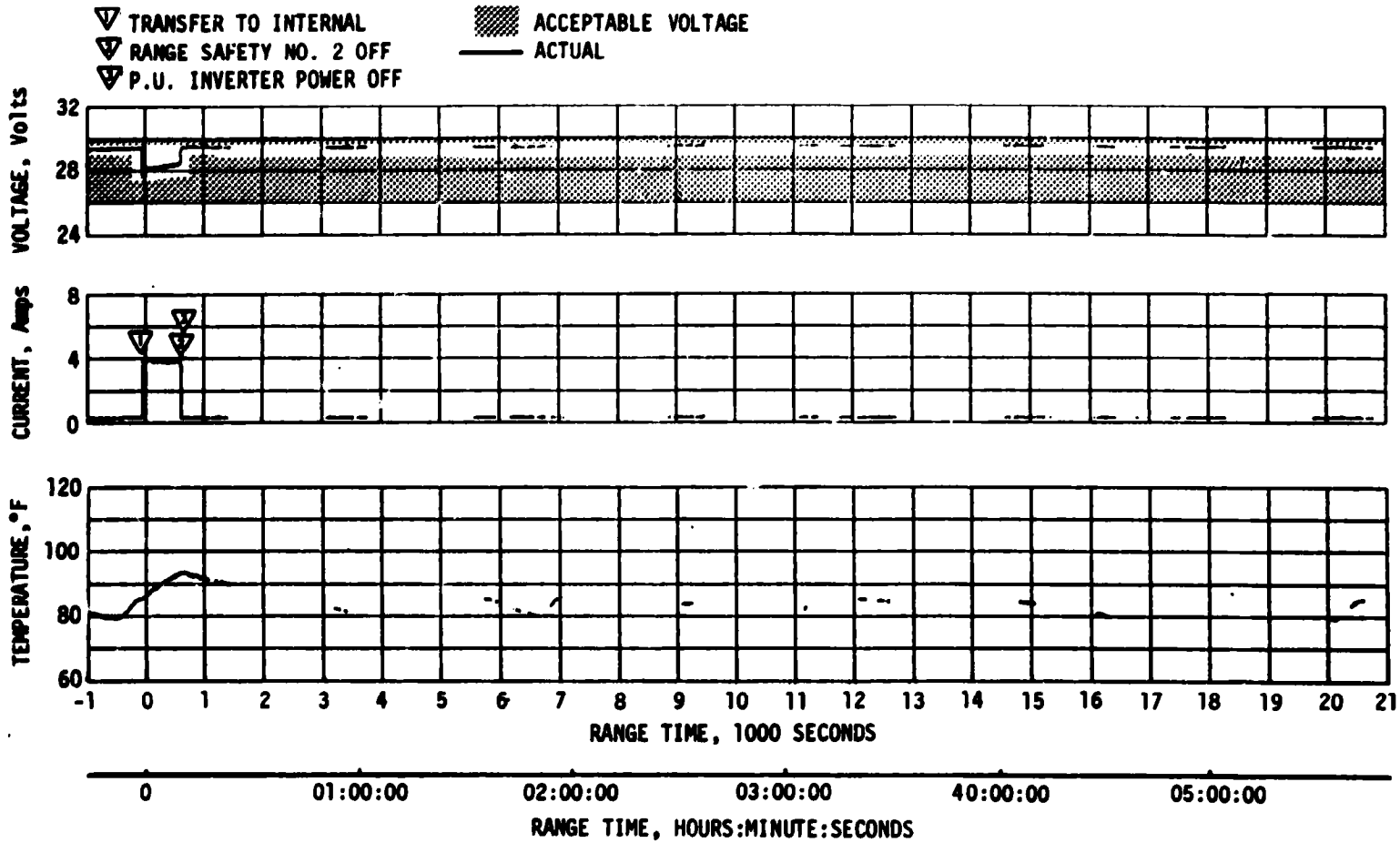


Figure 11-2. S-IVB Stage Forward No. 2 Battery Voltage, Current, and Temperature

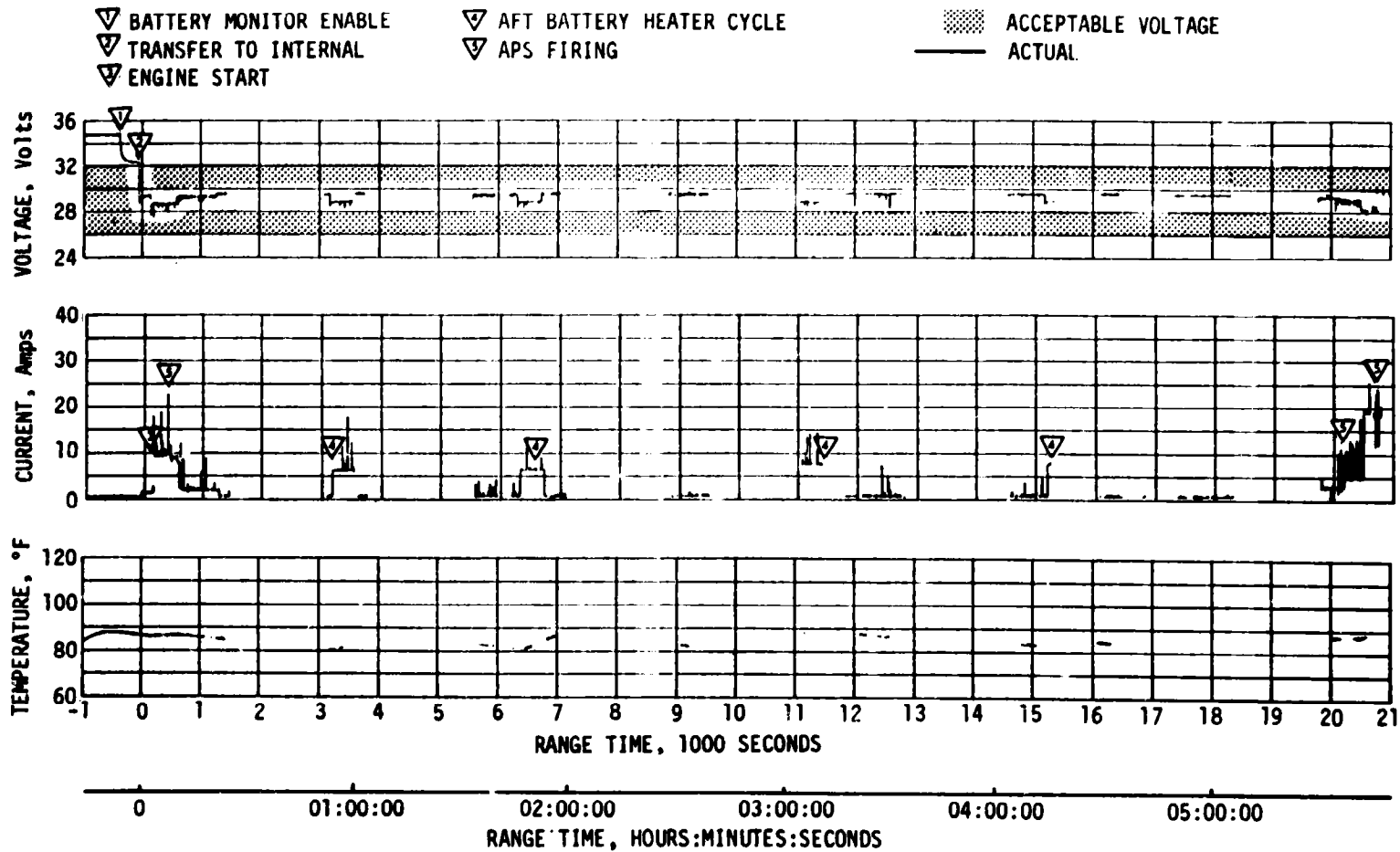


Figure 11-3. S-IVB Stage Aft No. 1 Battery Voltage, Current, and Temperature

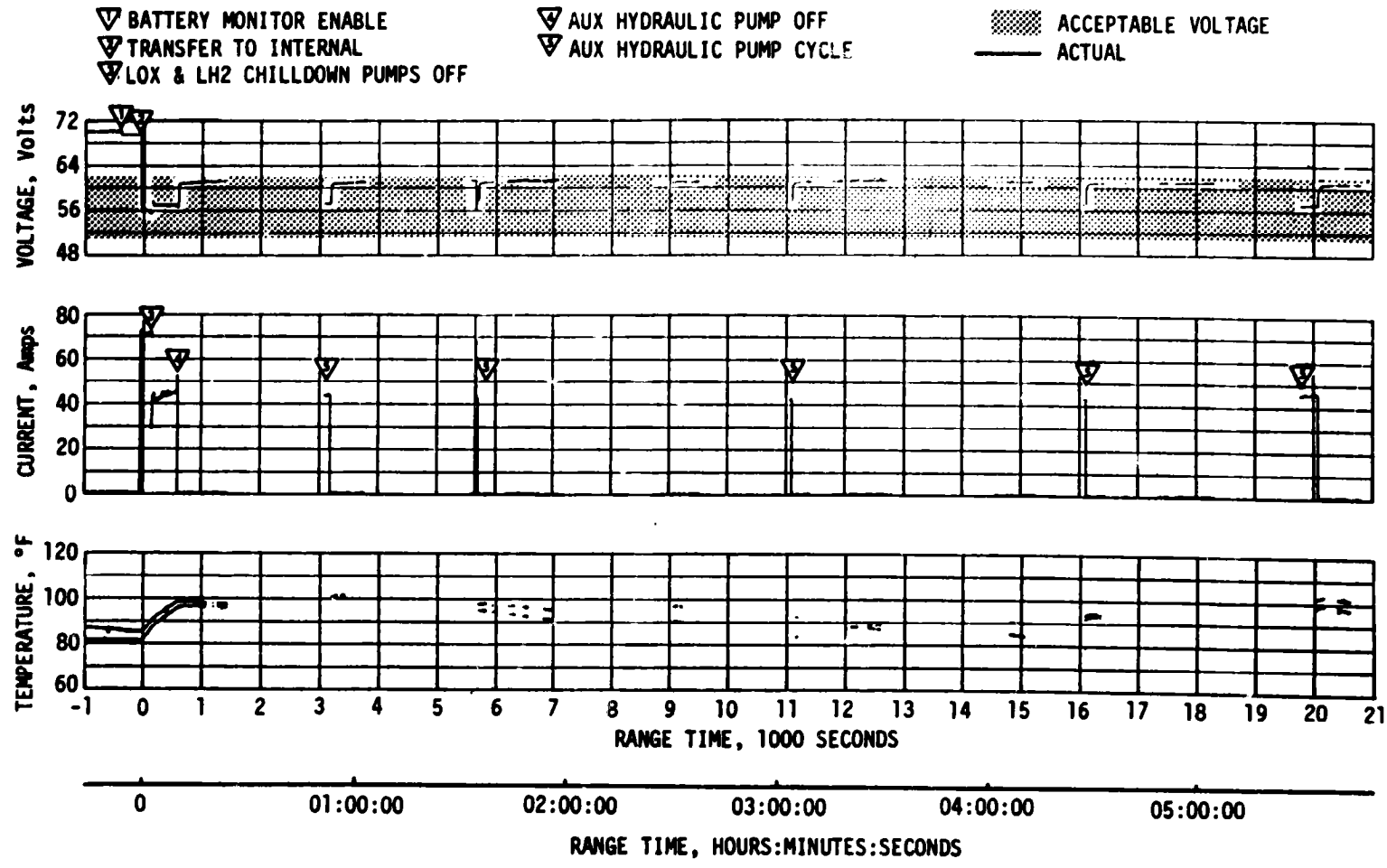


Figure 11-4. S-IVB Stage Aft No. 2 Battery Voltage, Current, and Temperature

Table 11-2. S-IVB Stage Battery Power Consumption

BATTERY	RATED CAPACITY (AMP-HR)	POWER CONSUMPTION*	
		AMP-HR	PERCENT OF CAPACITY
Forward No. 1 (4D30)	227.5	81.47	35.8
Forward No. 2 (4D20)	3.5	3.44	98.3
Aft No. 1 (4D10)	59.8	16.24	27.2
Aft No. 2 (4D40)	66.5	48.74	73.2

\*From Battery activation until end of telemetry (at 20,800 seconds)

remained within performance limits of 26 to 30 V. The battery temperature and current were nominal. Battery voltages, currents and temperatures are shown in Figures 11-5 through 11-7.

Battery power consumption and capacity for each battery are shown in Table 11-3.

The current sharing of the 6D10 and 6D30 batteries, to provide redundant power to the ST-124M-3 platform was satisfactory throughout the flight. During the S-IB burn, current sharing reached a maximum of 23 amperes and 24 amperes from the 6D10 and 6D30 battery, respectively, with an average of 19.5 amperes and 20 amperes (see Figure 11-5 and 11-6).

One of the possible causes of the gyro and accelerometer summation current shift (reference Section 9, Paragraph 9.4.1) was a voltage transient on the 6D31 and 6D11 bus. An analysis of the electrical sequencing for the period of the anomaly revealed no probable transient sources.

The 56 volt power supply maintained an output voltage of 55.5 to 56.5 V which is well within the required tolerance of 56  $\pm$ 2.5 V.

The 5 volt measuring power supply performed nominally, maintaining a constant voltage within specified tolerances.

The switch selector, electrical distributors and network cabling performed nominally.



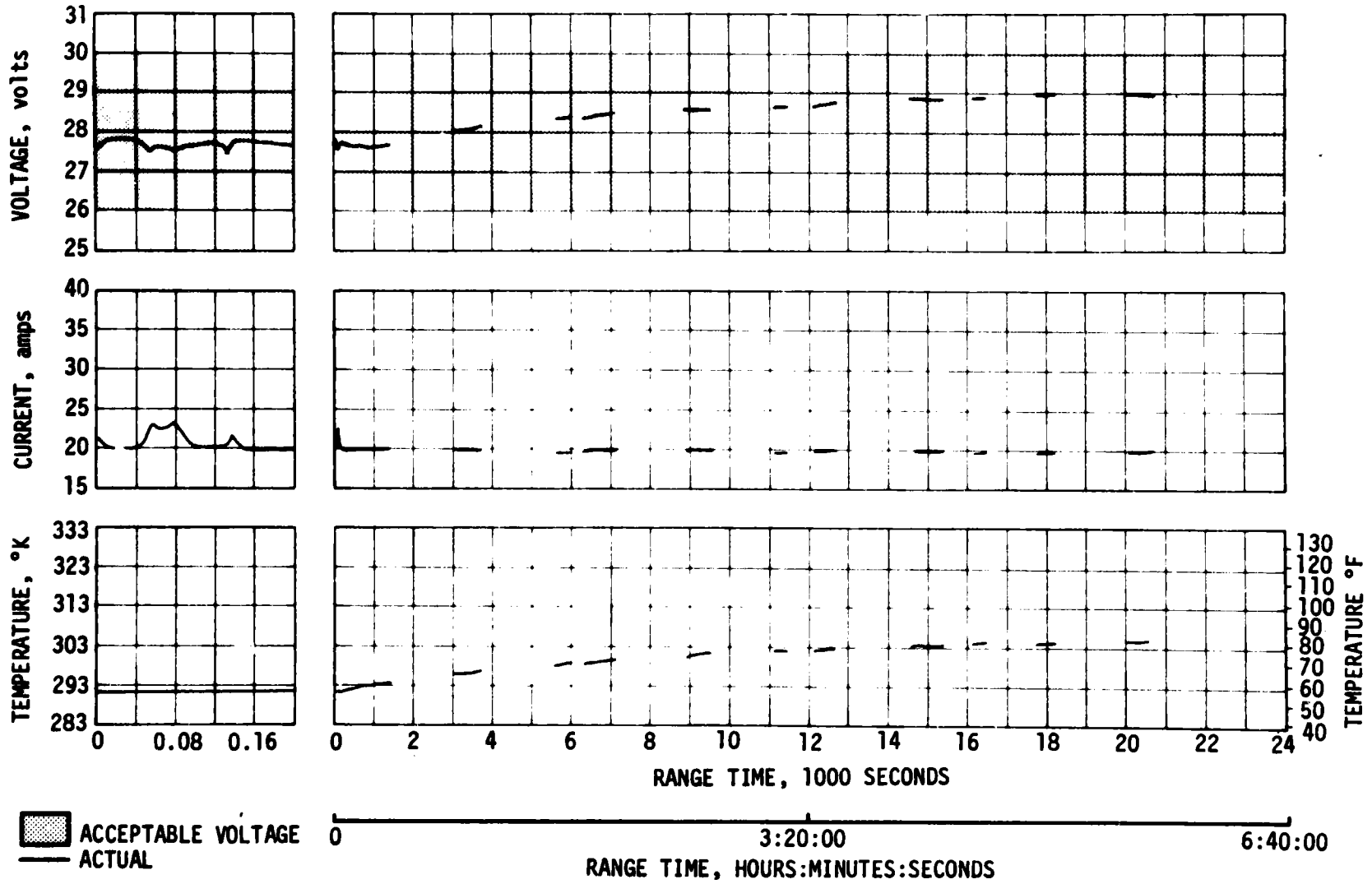


Figure 11-5. IU 6D10 Battery Parameters

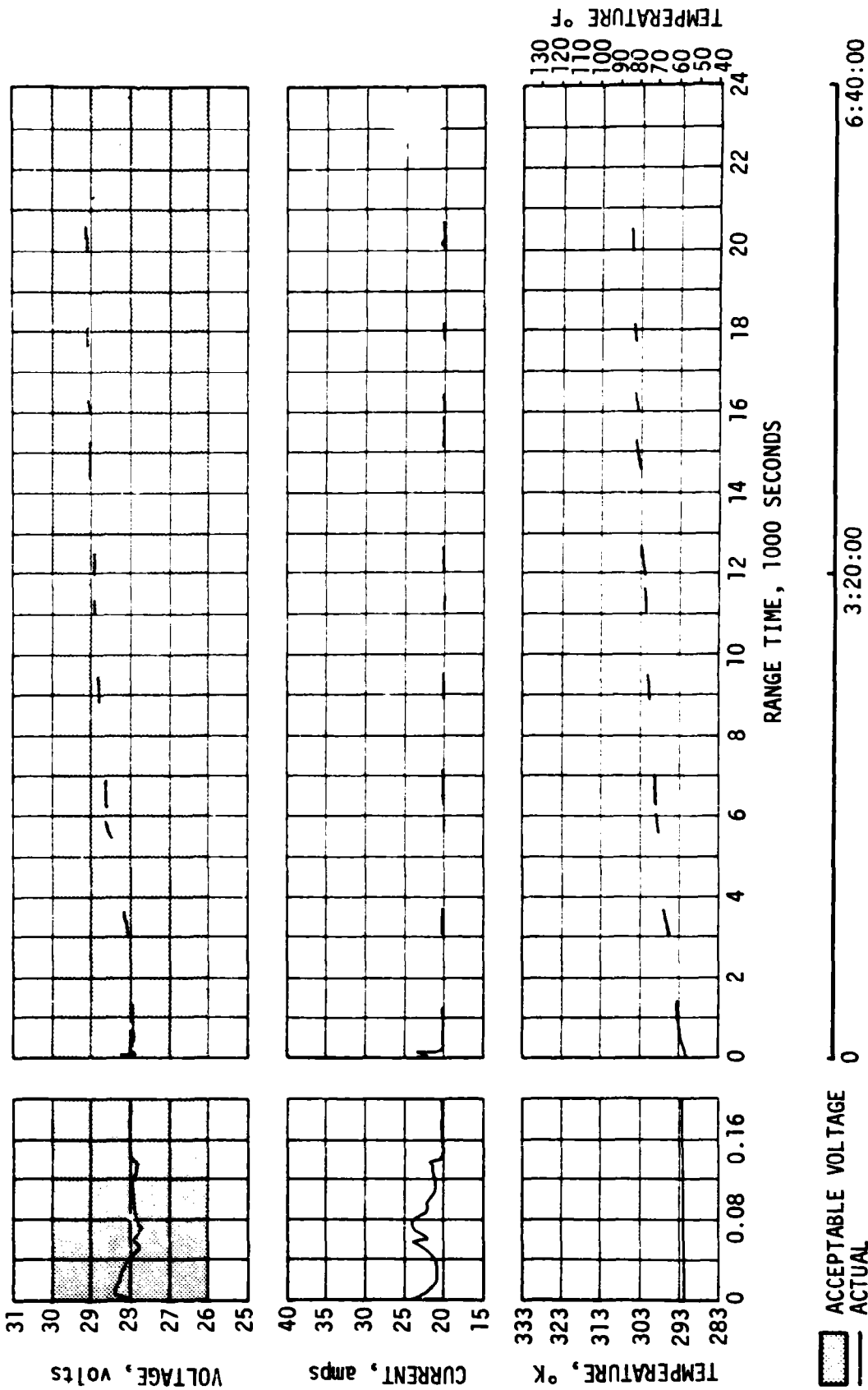


Figure 11-6. IU 6D30 Battery Parameters

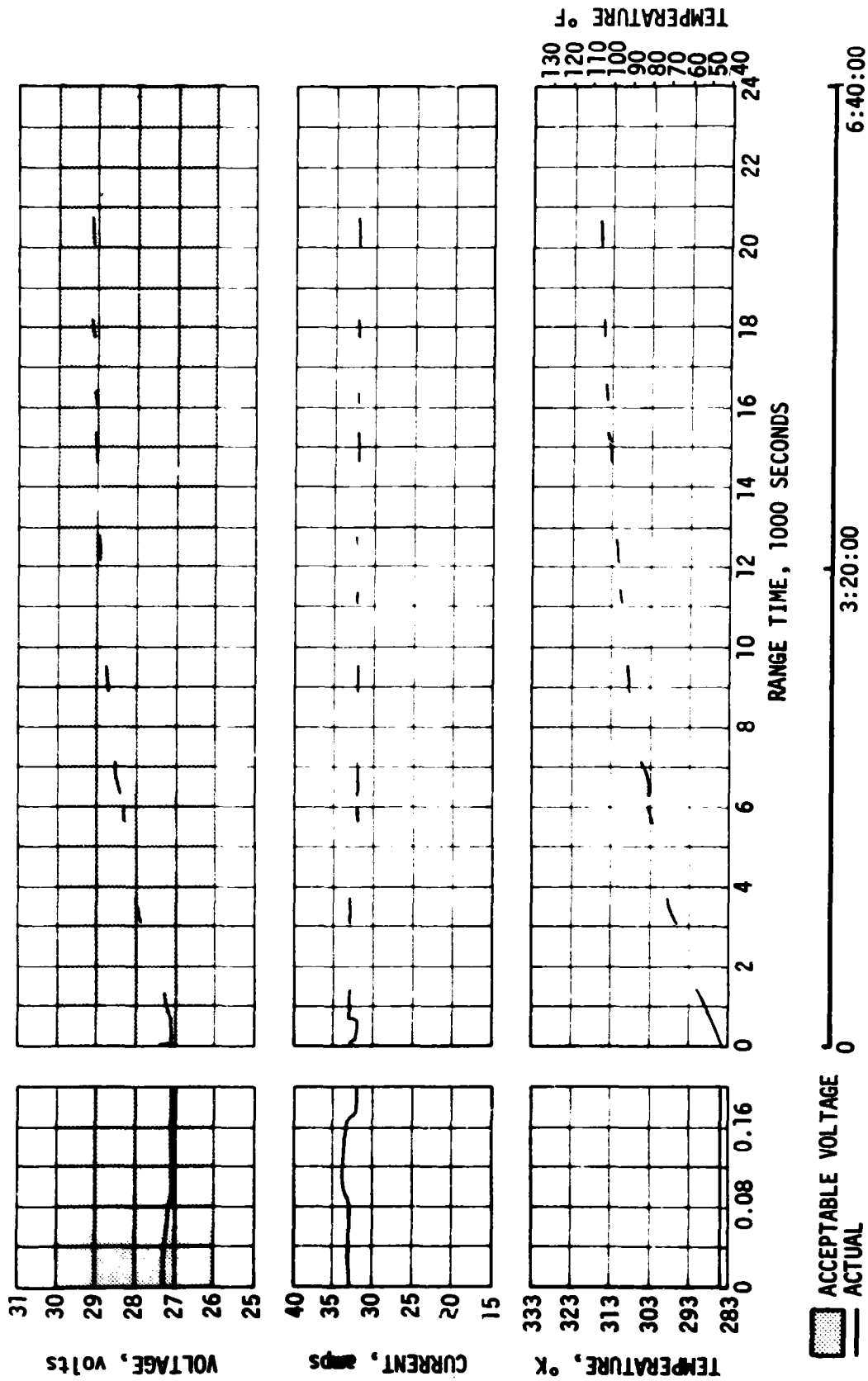


Figure 11-7. IU 6D40 Battery Parameters

Table 11-3. IU Battery Power Consumption

BATTERY	RATED CAPACITY (AMP-HR)	POWER CONSUMPTION*	
		AMP-HR	PERCENT OF CAPACITY
6D10	350	124.94	35.7
6D30	350	131.00	34.6
6D40	350	202.56	57.9

\*Battery Consumptions were calculated from battery activation until end of telemetry (at 20,628 seconds).

### 11.5 SATURN IB EMERGENCY DETECTION SYSTEM

The performance of the SA-206 EDS was normal and no abort limits were exceeded. All switch selector events associated with EDS for which data are available, were issued at the scheduled times. The discrete indications for EDS events also functioned normally. The performance of all thrust OK pressure switches and associated voting logic, which monitors engine status, was nominal insofar as EDS operation was concerned. S-IVB tank ullage pressures remained below the abort limits. EDS displays to the crew were normal.

The Q-Ball, which sensed the maximum dynamic pressure difference on previous flights, was electrically disconnected on this flight (see Appendix B).

As noted in Section 10, none of the rate gyros gave any indication of angular overrate in the pitch, yaw, or roll axis. The maximum angular rates were well below the abort limits.

The operation of the EDS Cutoff Inhibit Timer was nominal. The timer ran for 41.5 seconds which is within the specified limits of 40 to 42 seconds.

## SECTION 12

### VEHICLE PRESSURE ENVIRONMENT

#### 12.1 S-IB BASE PRESSURE

Base pressure data obtained from SA-206 have been compared with preflight predictions and/or previous flight data and show good agreement. Base drag coefficients were also calculated using the measured pressures and actual flight trajectory parameters.

There were three base pressure measurements made in the S-IB base region; two on the heat shield and one on the flame shield. One of the heat shield measurements was for differential pressure across the shield, and the other two measurements were for absolute pressures.

Results of the heat shield and flame shield absolute pressure measurements are shown in Figures 12-1 and 12-2, respectively. These data are presented as the difference between measured base pressures and ambient pressure and in coefficient form (measured-ambient/dynamic pressure). Values are compared with the band of data obtained from previous S-IB flights of similar vehicle base configuration and show good agreement. Considering the entire trajectory, the heat shield pressure remained close to the ambient pressure side ( $P_{\text{heat shield}} - P_{\text{ambient}} = 0$ ) of the data band from previous flights. The data indicate that during the first 70 seconds of flight and up to a corresponding altitude of 5.9 n. mi. the H-1 engine exhausts were aspirating the heat shield region, resulting in base pressures below ambient pressures. In the flame shield area, the aspirating effect was terminated at an altitude of 4.5 n. mi. Above these altitudes the reversal of engine exhaust products, due to plume expansion, resulted in base pressures above ambient as was expected.

Pressure loading measured near the outer perimeter of the SA-206 heat shield is compared with data from previous flights and predictions in Figure 12-3. The SA-206 values, although within the predicted band, are lower than previous S-IB flight data at altitudes below 5.9 n. mi. Part of this difference is due to heat shield pressures being near ambient during this time as mentioned earlier (Figure 12-1).

Base drag coefficients ( $P_{\text{ambient}} - P_{\text{base}}$ ) calculated from SA-206 flight data and the band formed by similar calculations for SA-203, SA-204, and SA-205 are shown in Figure 12-4. The measurements used in these calculations (three on SA-206) record localized pressure variations caused by engine aspiration and exhaust recirculation; however, they are representative of the average base pressures.

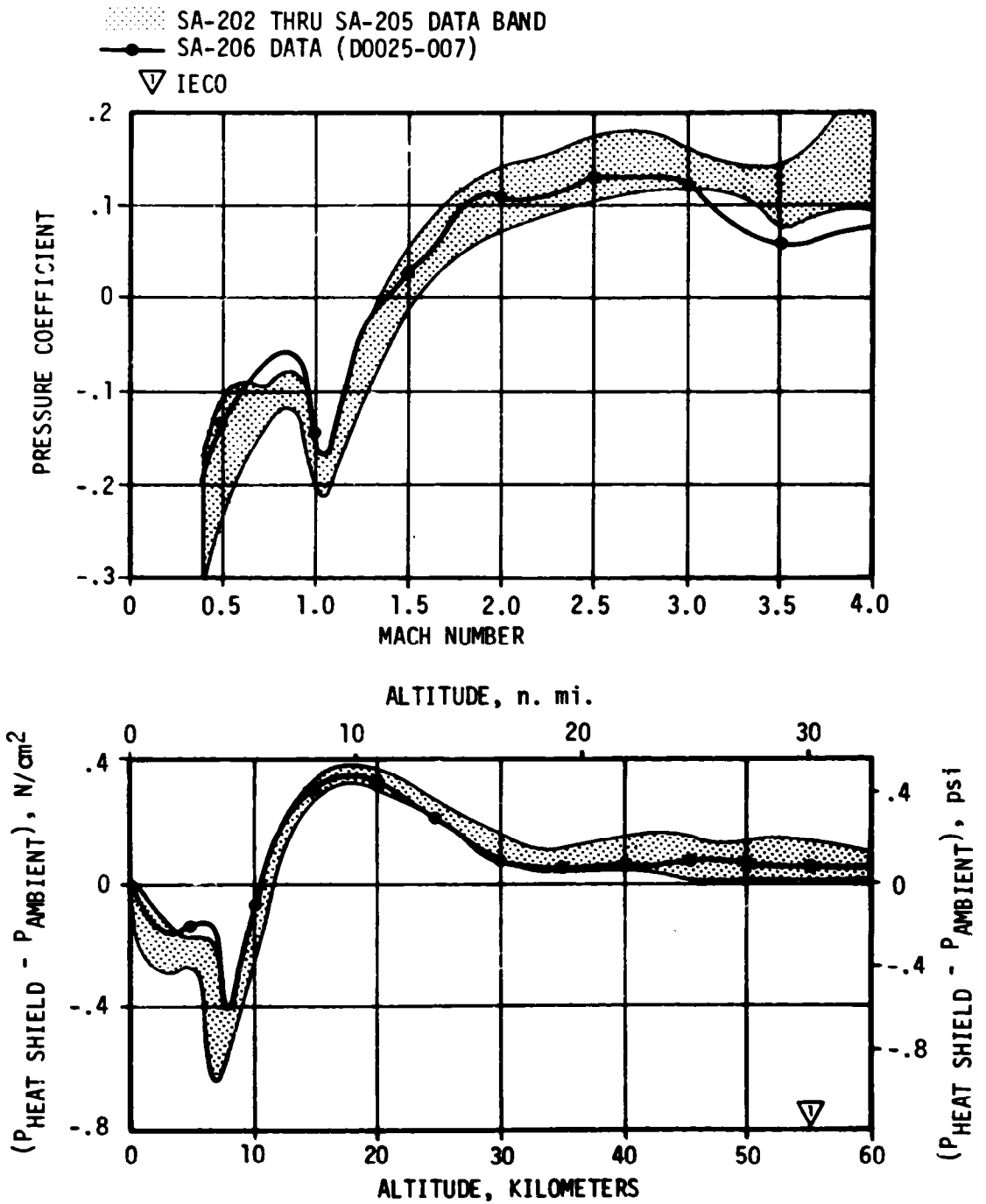


Figure 12-1. S-IB Stage Heat Shield Pressure

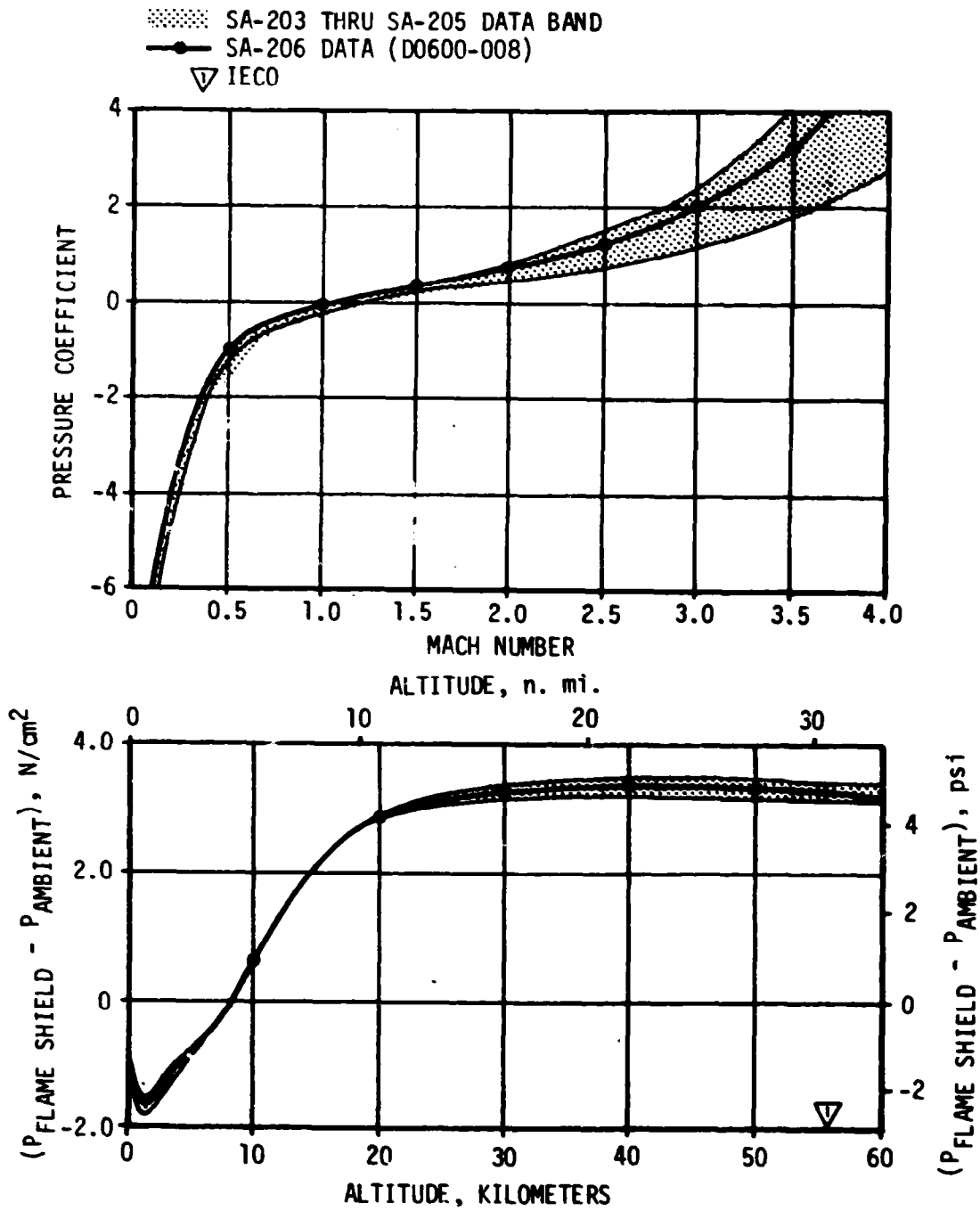


Figure 12-2. S-iB Stage Flame Shield Pressure

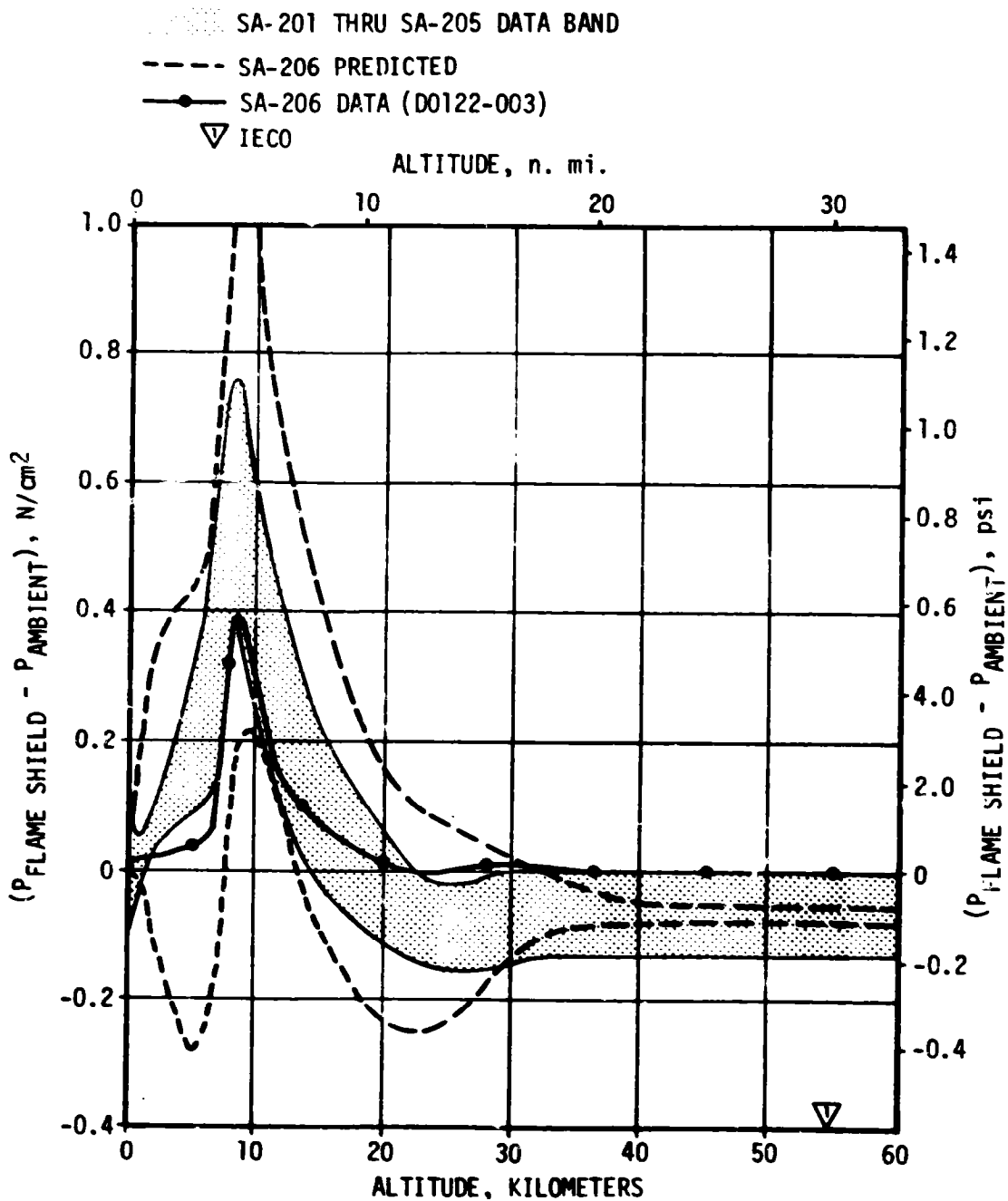


Figure 12-3. S-IB Stage Heat Shield Loading



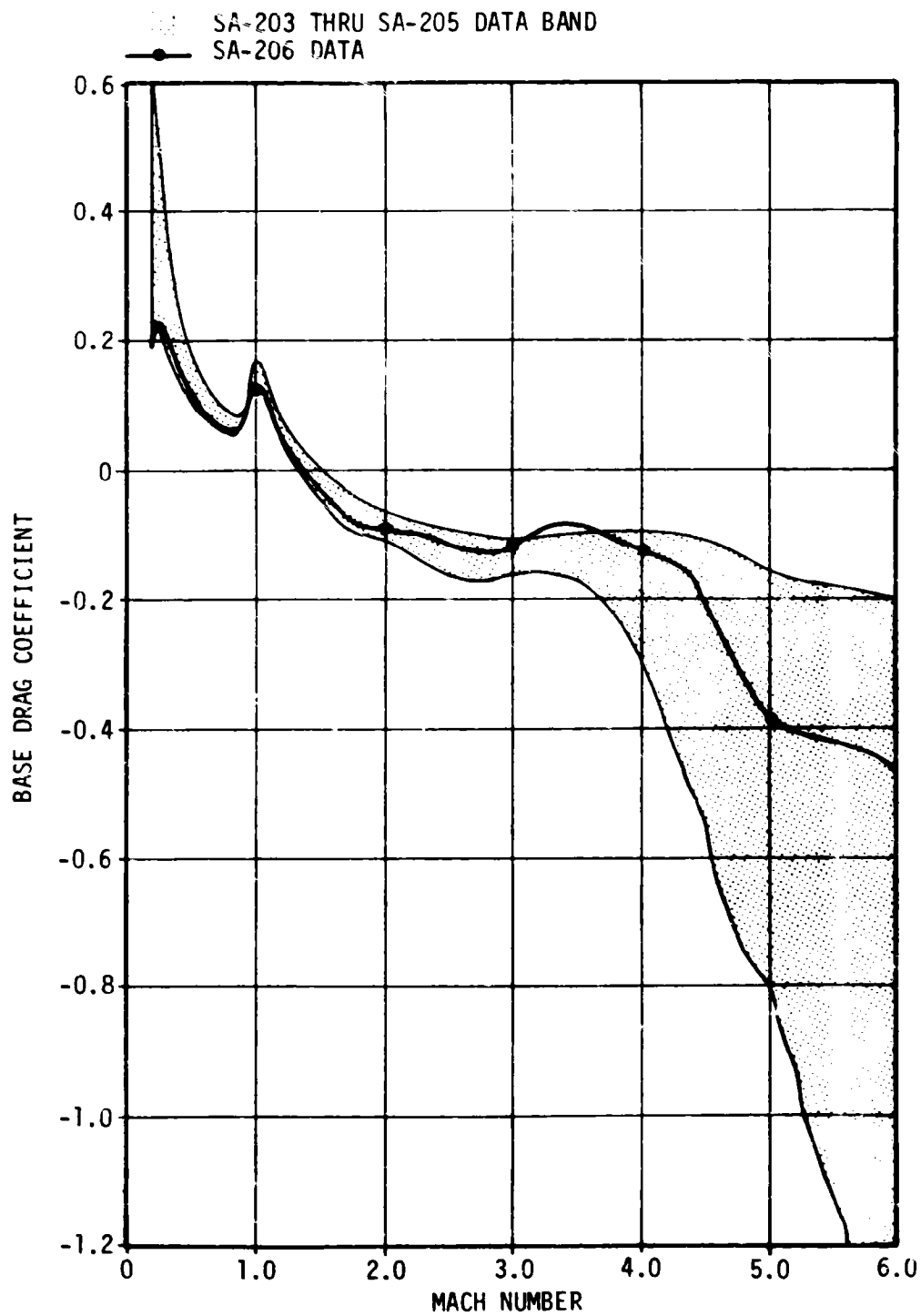


Figure 12-4. S-1B Stage Base Drag Coefficient

## SECTION 13

### VEHICLE THERMAL ENVIRONMENT

#### 13.1 S-IB BASE HEATING

Comparisons of SA-206 base region thermal data with corresponding data from SA-203, SA-204 and SA-205 show generally good agreement with slight differences being attributed to the H-1 engine uprating on the SA-206 vehicle. Measured heating rates in the base region were all below the S-IB stage design level.

There were seven thermal environment measurements taken in the base region; four on the heat shield and three on the flame shield. These consisted of a radiation and a total heat flux calorimeter in each of the two areas and three gas temperature thermocouples; two on the heat shield and one on the flame shield.

S-IB stage heat shield inner region thermal environment data are shown in Figure 13-1, 13-2 and 13-3. The trend of the SA-206 data traces is consistent with the bands formed by data from similar measurement locations on SA-203 through SA-205; also, these data are consistent with the base pressure data presented in Figure 12-1 showing the impact of exhaust gas reversal beginning at an altitude of approximately 5.4 n mi. Additionally, the data show that there is a sustained reversal of exhaust gases into the heat shield region at altitudes above 15.1 n mi.

Between approximately 20 and 60 seconds after liftoff, the heat shield inner region gas temperature data were noticeably higher than those recorded on previous flights as shown in Figure 13-3 for altitudes below 5.4 n mi. At least a portion of this increase was anticipated because of the increase in fuel-rich turbine exhaust discharge from the flame shield area associated with the SA-206, H-1 engine uprating. Since temperatures in this wake region are quite sensitive to small changes in turbine exhaust recirculation, and because of the instability of flow in the base region, actual gas temperature predictions are extremely difficult.

The higher gas temperature environment did not, however, result in a significant increase in total heating for the heat shield area. Measured SA-206 heat shield total heating rates (Figure 13-1) were generally within the previous data band with only a minor increase noted at altitudes between 0.6 and 1.6 n mi. This corresponds to the time from approximately 25 to 40 seconds.

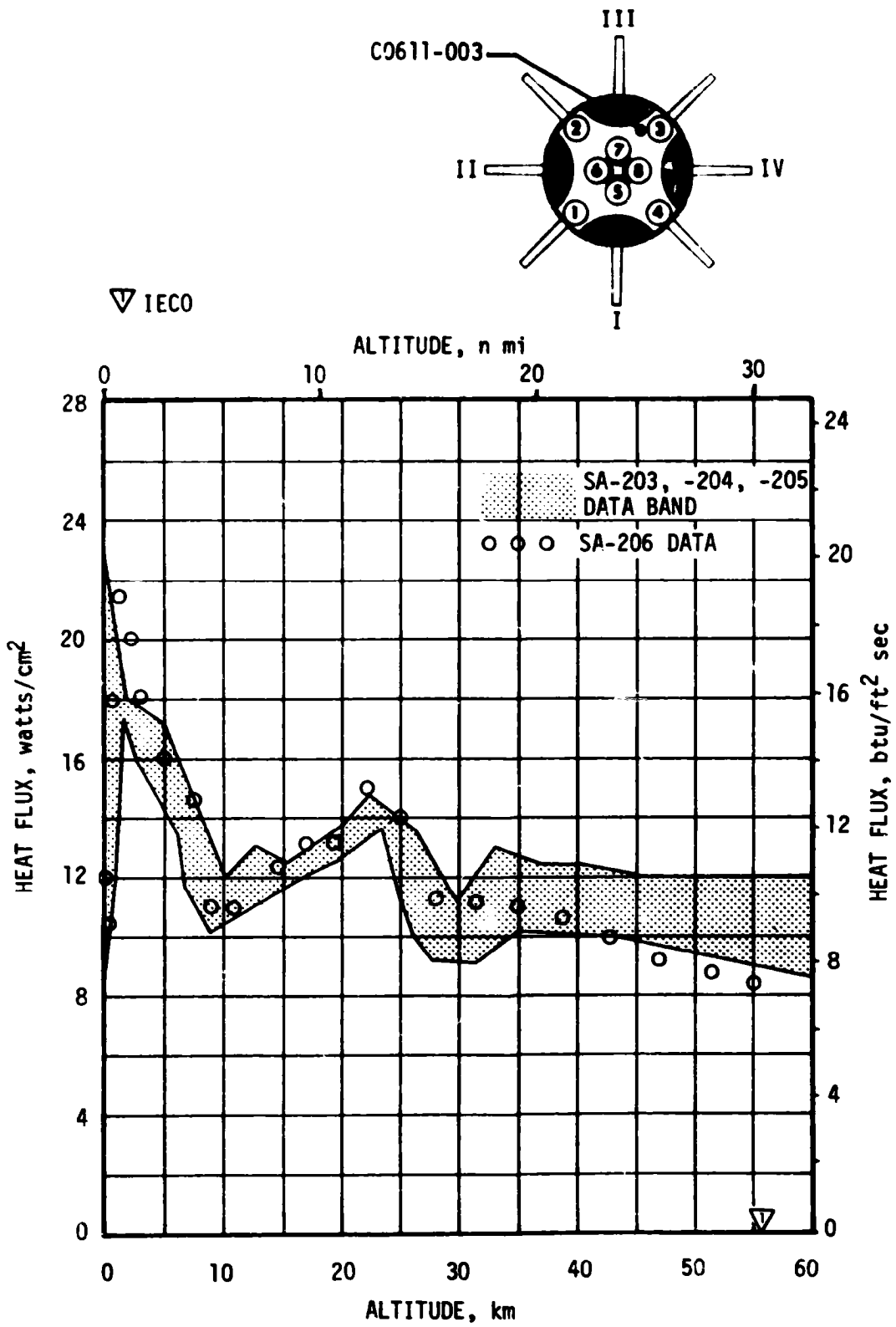


Figure 13-1. S-IB Stage Heat Shield Inner Region Total Heating Rates

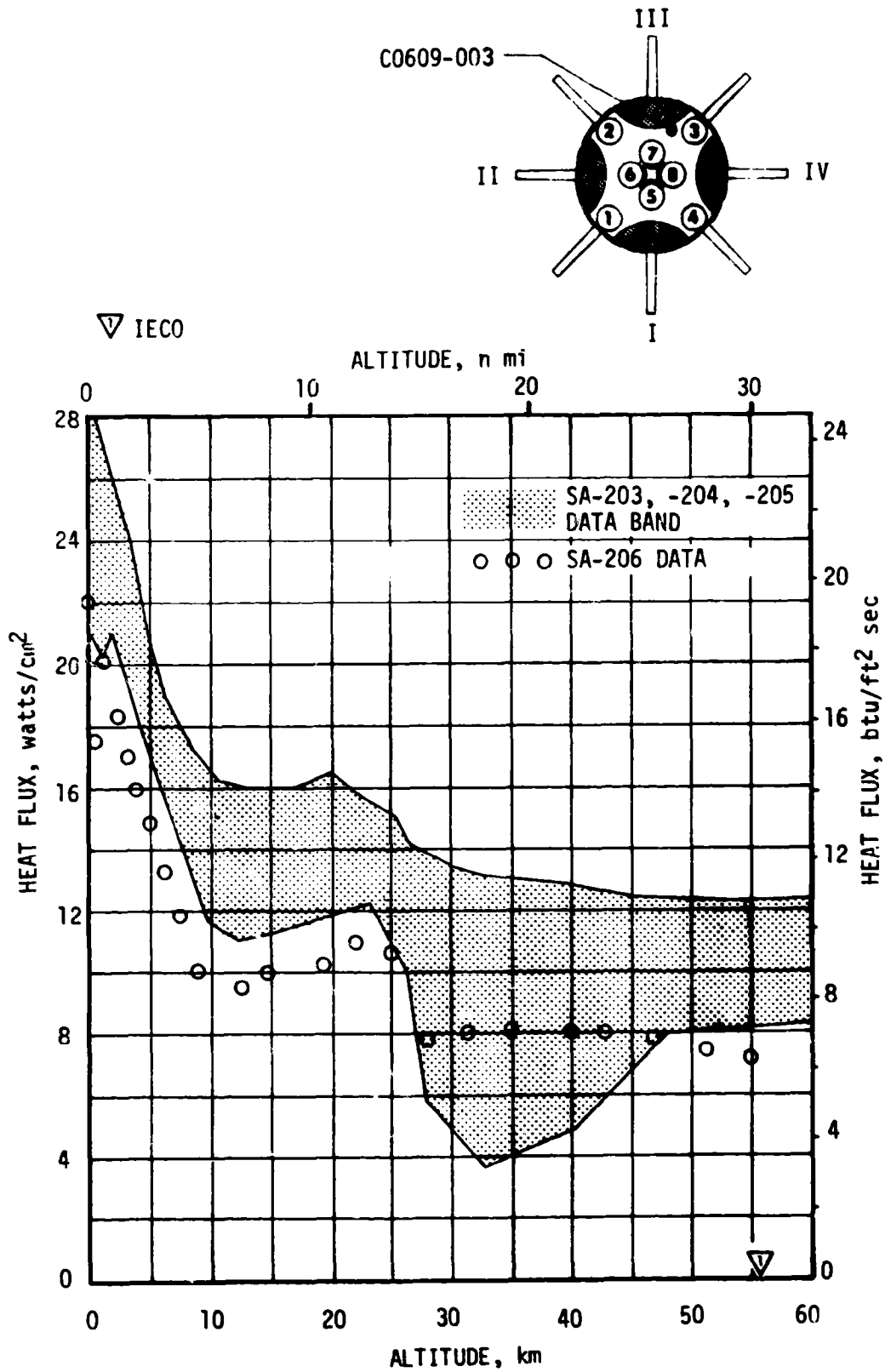


Figure 13-2. S-IB Stage Heat Shield Inner Region Radiation Heating Rate

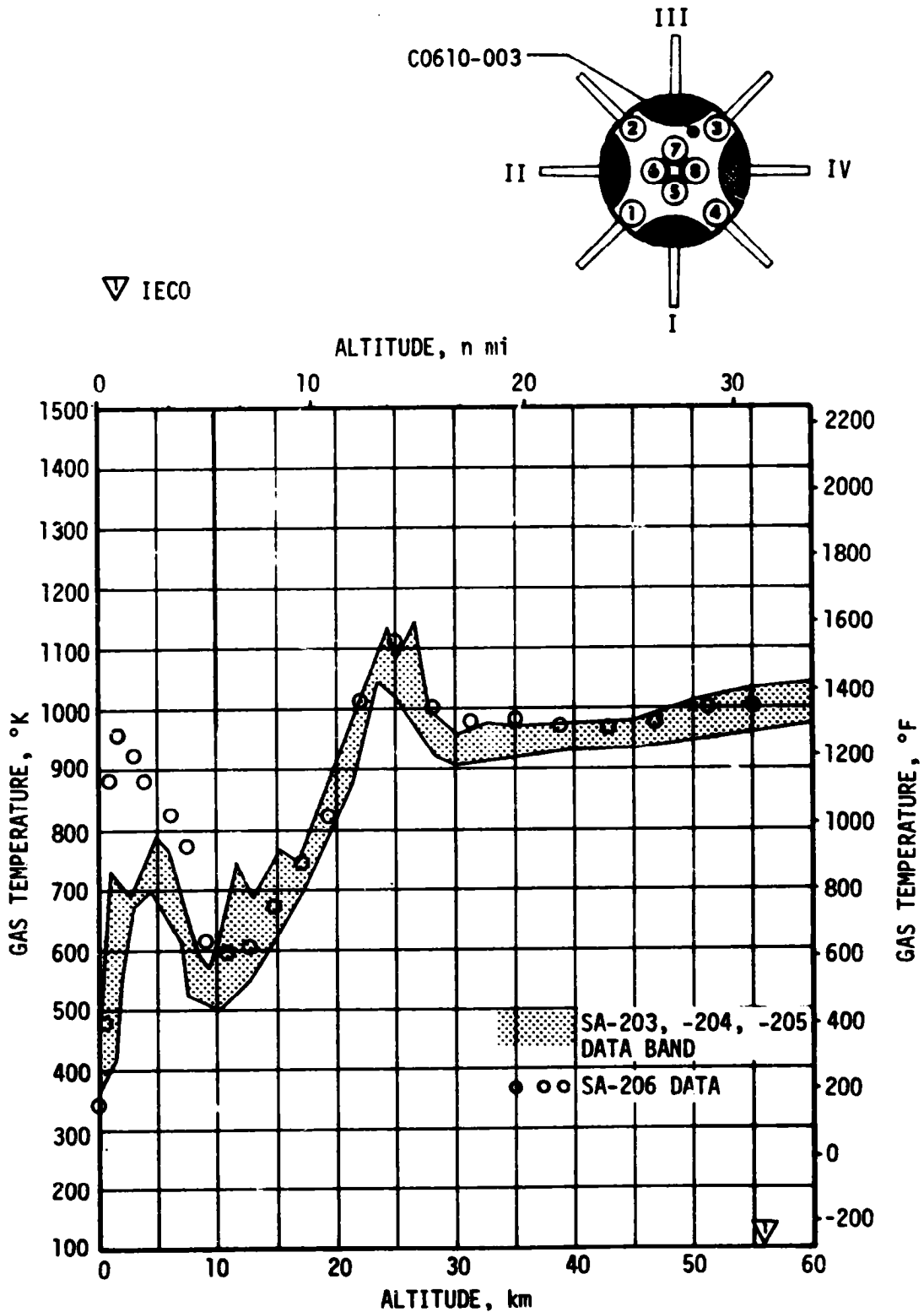


Figure 13-3. S-IB Stage Heat Shield Inner Region Gas Temperature

Radiation heating rates recorded for the S-IB stage heat shield of SA-206 (Figure 13-2) were generally 20 percent below the previous data band. This would imply that the view of the radiation calorimeter was partially occluded either by deposits on the window of the calorimeter or by increased quantities of opaque turbine exhaust gas between the instrument and the high-energy emitting source.

Gas temperature data from the single heat shield outer region thermal measurement are presented in Figure 13-4. There is good agreement between the SA-206 trace and the data recorded from previous flights. The higher gas temperature data point plotted at an altitude of 3 n mi represents a pulse of approximately 3 seconds in duration and is of little or no significance.

Data from the three flame shield thermal measurements are presented in Figure 13-5, 13-6 and 13-7. The data bands formed by the data extremes recorded on previous flights are also shown for comparison. As shown in Figures 13-5 and 13-6, both the total and radiation heating rates showed a slight increase over previous data at altitudes above 4.9 n mi. It is at this altitude (4.9 n mi) that the flame shield flow reversal becomes choked. The slight increase in heating is attributed to the uprated H-1 engine thrust on SA-206.

Flame shield gas temperature data (Figure 13-7) show excellent agreement with previous data. These data are relatively constant after 65 seconds (4.9 n mi altitude) at a value slightly above the turbine exhaust gas temperature. This indicates that the major portion of the gas reversal affecting the flame shield area was comprised of the fuel-rich inboard engine turbine exhaust. On a time plot of the flame shield data the first indication of this flame shield reversal was detected at approximately 25 seconds. This corresponds to a vehicle altitude of approximately 0.6 n mi.

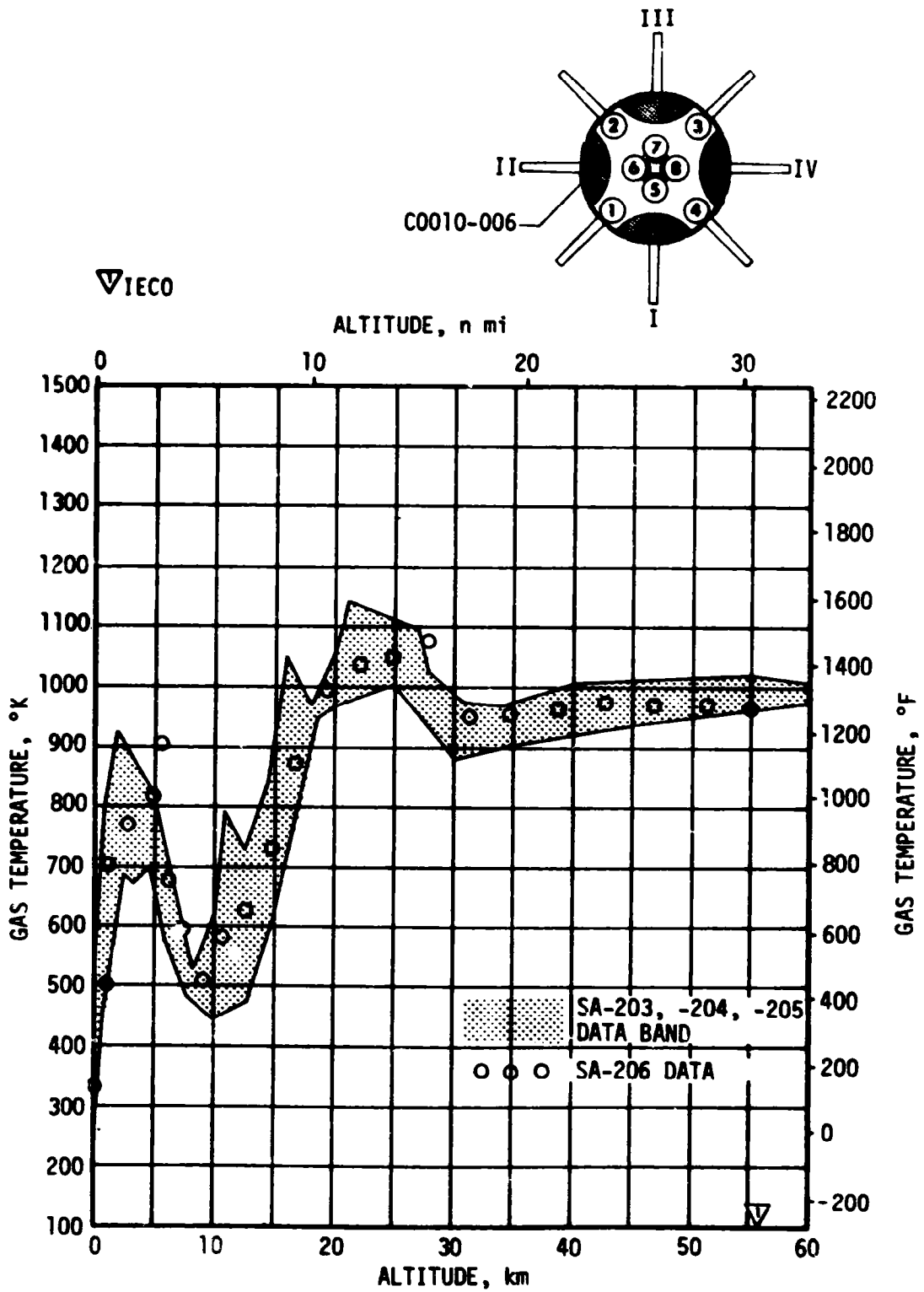


Figure 13-4. S-IB Stage Heat Shield Outer Region Gas Temperature

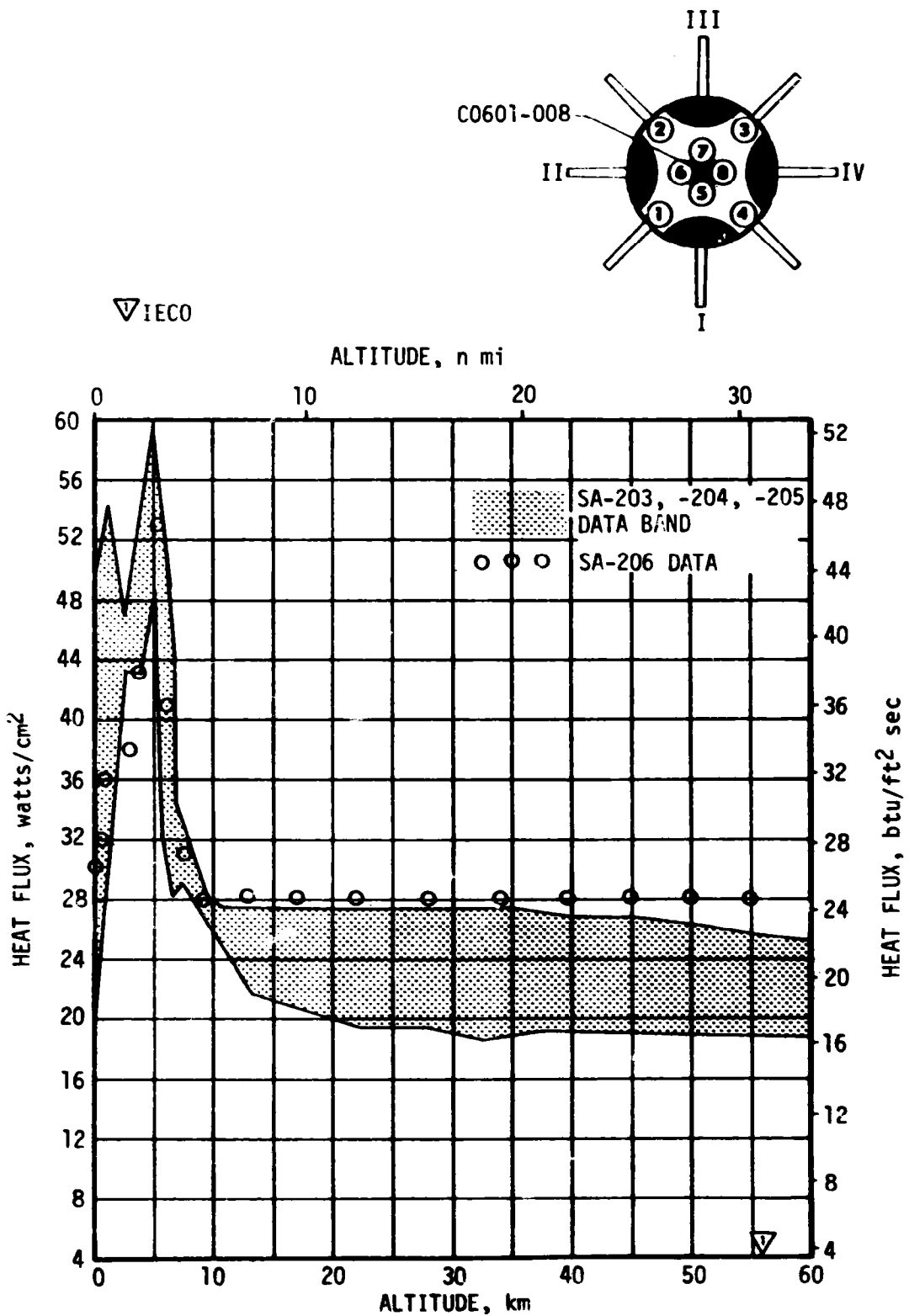


Figure 13-5. S-IB Stage Flame Shield Total Heating Rates



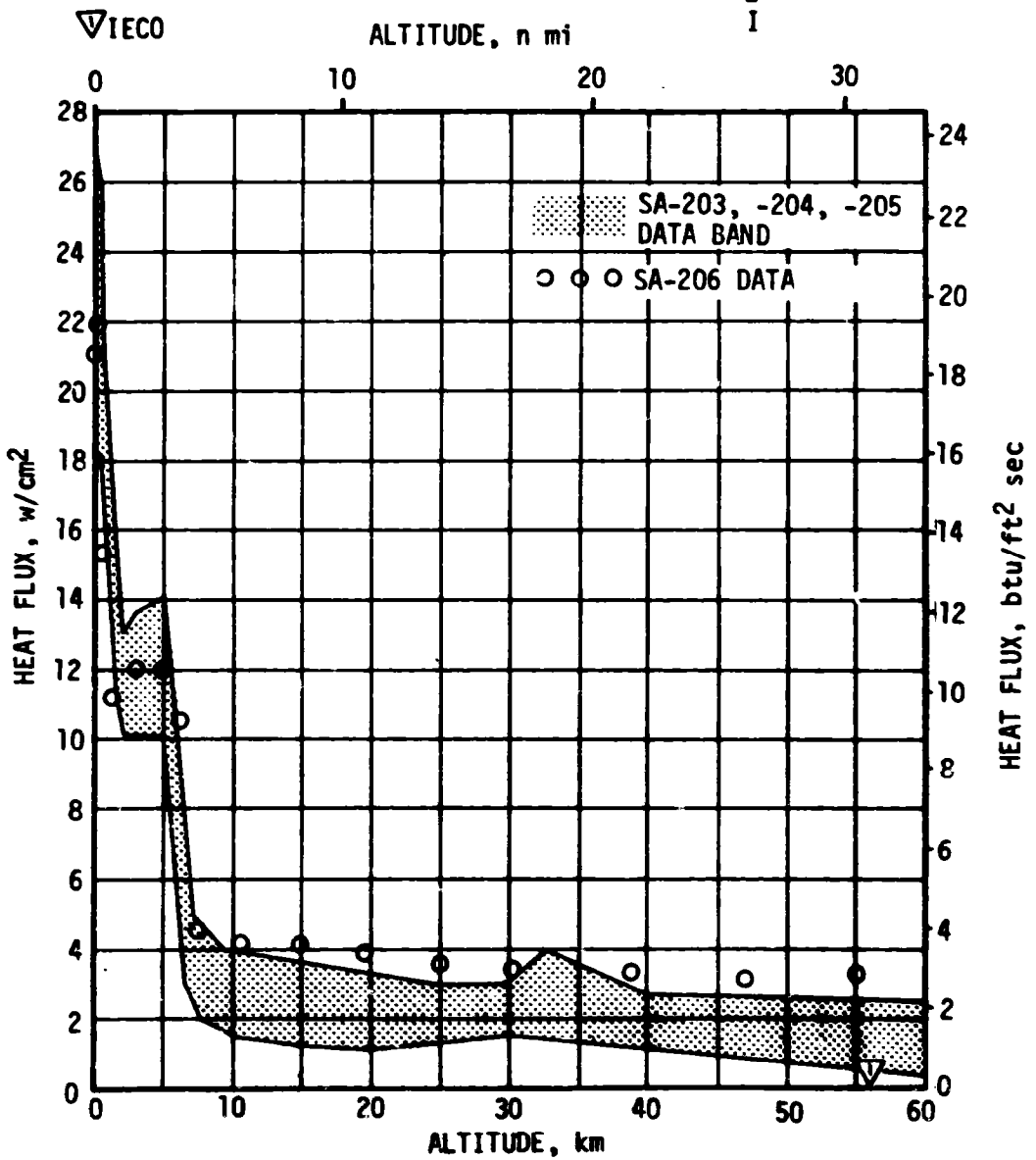
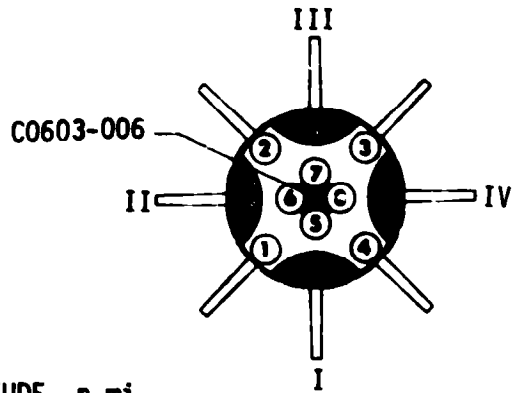


Figure 13-6. S-IB Stage Flame Shield Radiation Heating Rate

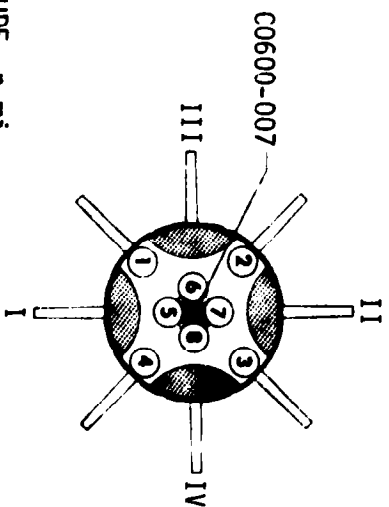
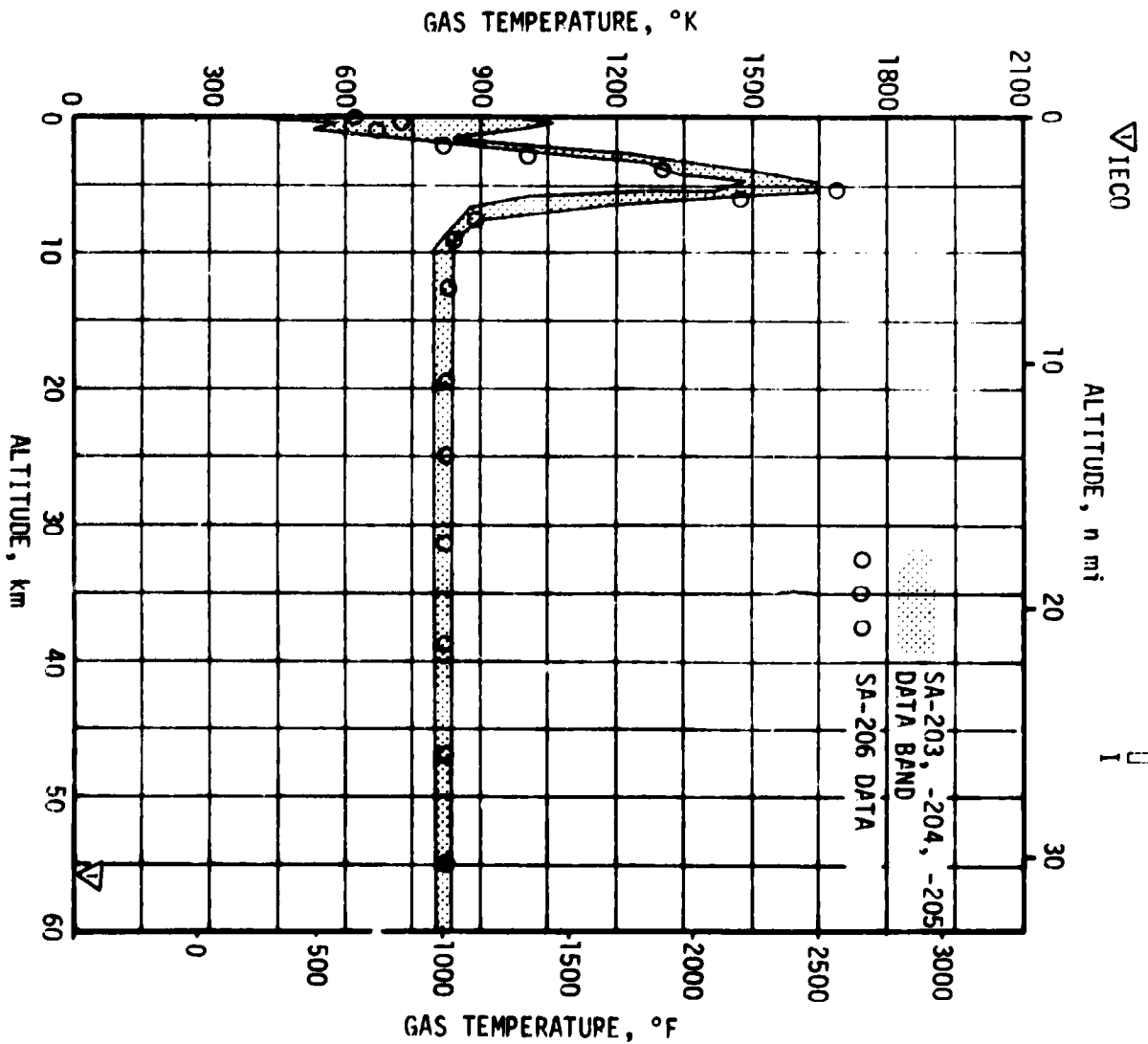


Figure 13-7. S-1B Stage Flame Shield Gas Temperature

## SECTION 14

### ENVIRONMENTAL CONTROL SYSTEM

#### 14.1 SUMMARY

The S-IB stage engine compartment and instrument compartment require environmental control during prelaunch operations, but are not actively controlled during S-IB boost. The desired temperatures were maintained at both areas during the prelaunch operations.

The IU stage Environmental Control System (ECS) exhibited satisfactory performance for the duration of the IU mission. Coolant temperatures, pressures, and flowrates were continuously maintained within the required ranges and design limits.

#### 14.2 S-IB ENVIRONMENTAL CONTROL

The S-IB engine compartment temperature, as recorded by the prelaunch compartment temperature measurement 12K22, was maintained at approximately 60°F for 10 hours prior to liftoff. Data from this measurement are monitored during prelaunch activities to assess ECS flow and supply temperature requirements for maintaining engine compartment temperature within the specified limits of 53 and 75°F. In maintaining the 60°F engine temperature, the ECS delivery was nominal with GN<sub>2</sub> being supplied to the S-IB stage aft compartment at the average rate of approximately 302 lbm/min, with an interface temperature (from measurement 12C39) of between 140 and 132°F.

Because of instrument positioning and/or data recording inaccuracy, the S-IB stage engine compartment thermocouples (measurement numbers C61-1 through C61-4) recorded prelaunch temperatures below the 60°F indicated by the 12K22 measurement. This is evidenced by the data traces shown in Figure 14-1. The positioning of these instruments is near the heat shield where the cooler gas settles. On the 12K22 measurement, the maximum error was 0.291 percent of a 31 to 100°F range.

The S-IB instrument compartment environmental conditioning system also performed satisfactorily during countdown. This was evidenced by measured temperatures of the D20 battery case by measurement WC 528-12. Recorded data from this measurement indicated the D20 battery temperature remained between 75 and 78°F throughout the countdown. This temperature range was maintained after LOX load by a GN<sub>2</sub> conditioning flow of 44 lbm/min at a temperature (recorded by facility measurement 12C43) of 79°F.

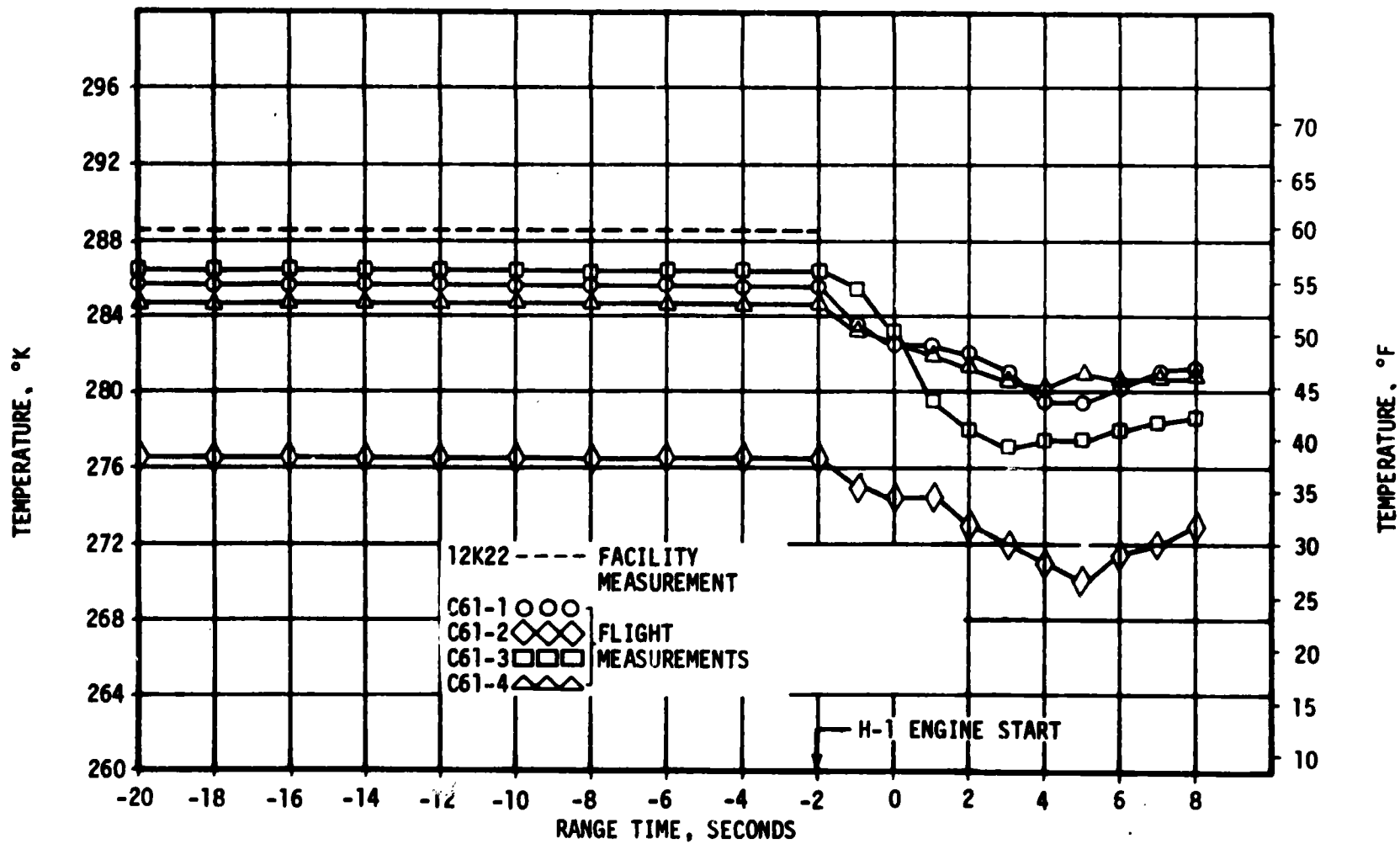


Figure 14-1. S-1B Engine Compartment Temperature

It was concluded that the critical components in the engine and instrument compartments were well within their qualification limits for the SA-206 launch.

### 14.3 IU ENVIRONMENTAL CONTROL

The IU ECS performance was satisfactory and maintained temperatures, pressures, and flowrates within the required limits for the duration of the IU mission.

#### 14.3.1 Thermal Conditioning System (TCS)

The TCS performance was satisfactory throughout the IU mission. The temperature of the coolant supplied to the IU thermal conditioning panels, IU internally cooled components and the S-IVB TCS was continuously maintained within the required limits of 45° to 68°F for the IU lifetime.

Sublimator performance parameters for the initial cycle are presented in Figure 14-2. The water supply valve opened as programmed at approximately 180 seconds, allowing water to flow to the sublimator. Significant cooling by the sublimator was evident at approximately 520 seconds at which time the temperature of the coolant began to rapidly decrease. At the first thermal switch sampling (780 seconds), the coolant temperature was below the thermal switch actuation point, thus the water valve was closed.

Figure 14-3 shows temperature control parameters over the total mission. Sublimator cooling was normal and the coolant control temperature was maintained within the required limits.

Hydraulic performance of the TCS was nominal as indicated by the parameters shown in Figure 14-4. System flowrates and pressures were relatively constant throughout the mission.

The TCS GN<sub>2</sub> supply sphere pressure decay, which is indicative of the GN<sub>2</sub> usage rate, was nominal as reflected by Figure 14-5.

#### 14.3.2 Gas Bearing Subsystem Performance

Gas Bearing Subsystem (GBS) performance was nominal throughout the IU mission. Figure 14-6 depicts the platform pressure differential (D11-603) and platform internal ambient pressure (D12-603).

The GBS GN<sub>2</sub> supply sphere pressure decay was nominal as shown in Figure 14-7.

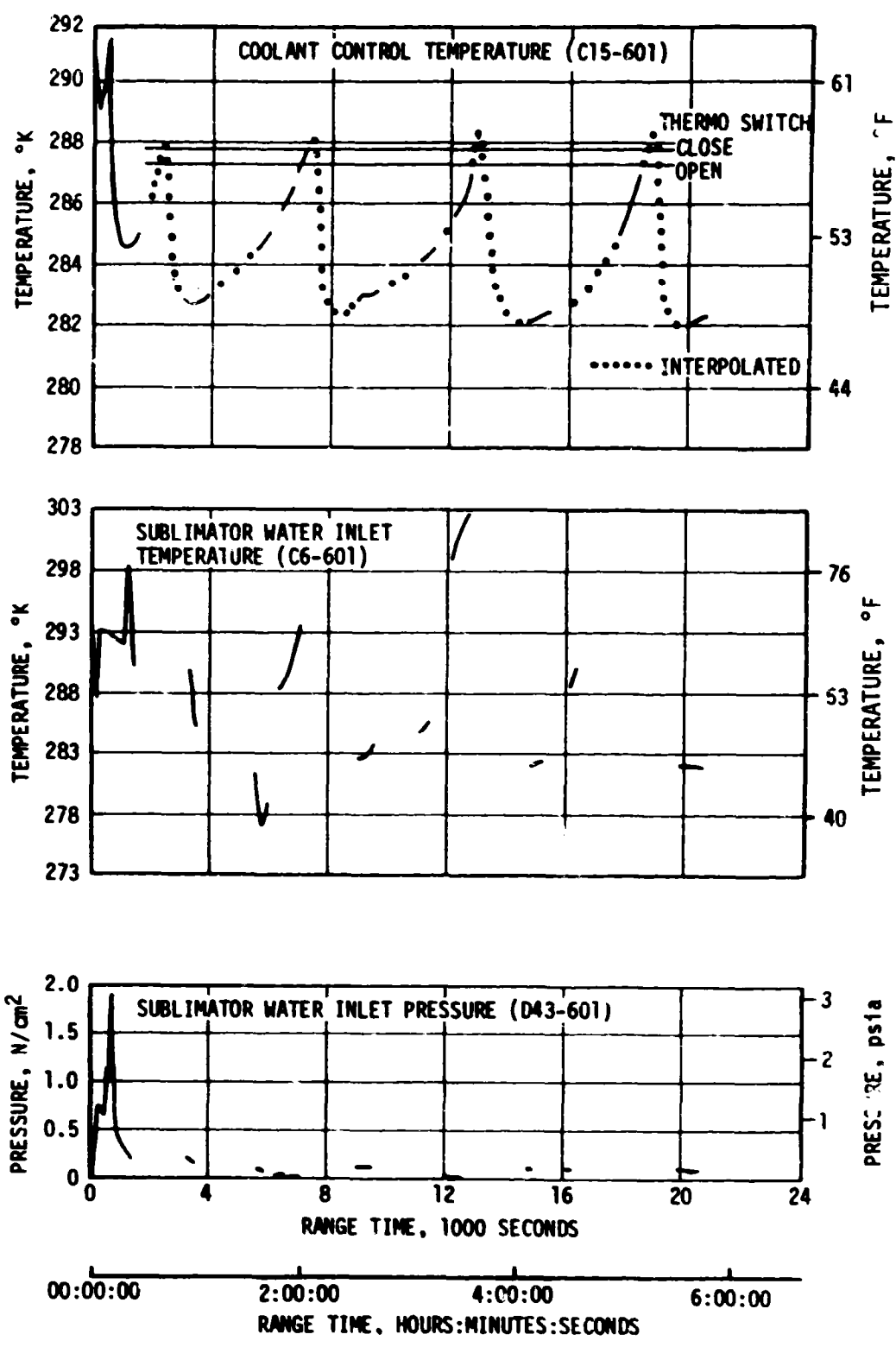


Figure 14-2. IU Sublimator Start Up Parameters for Initial Cycle

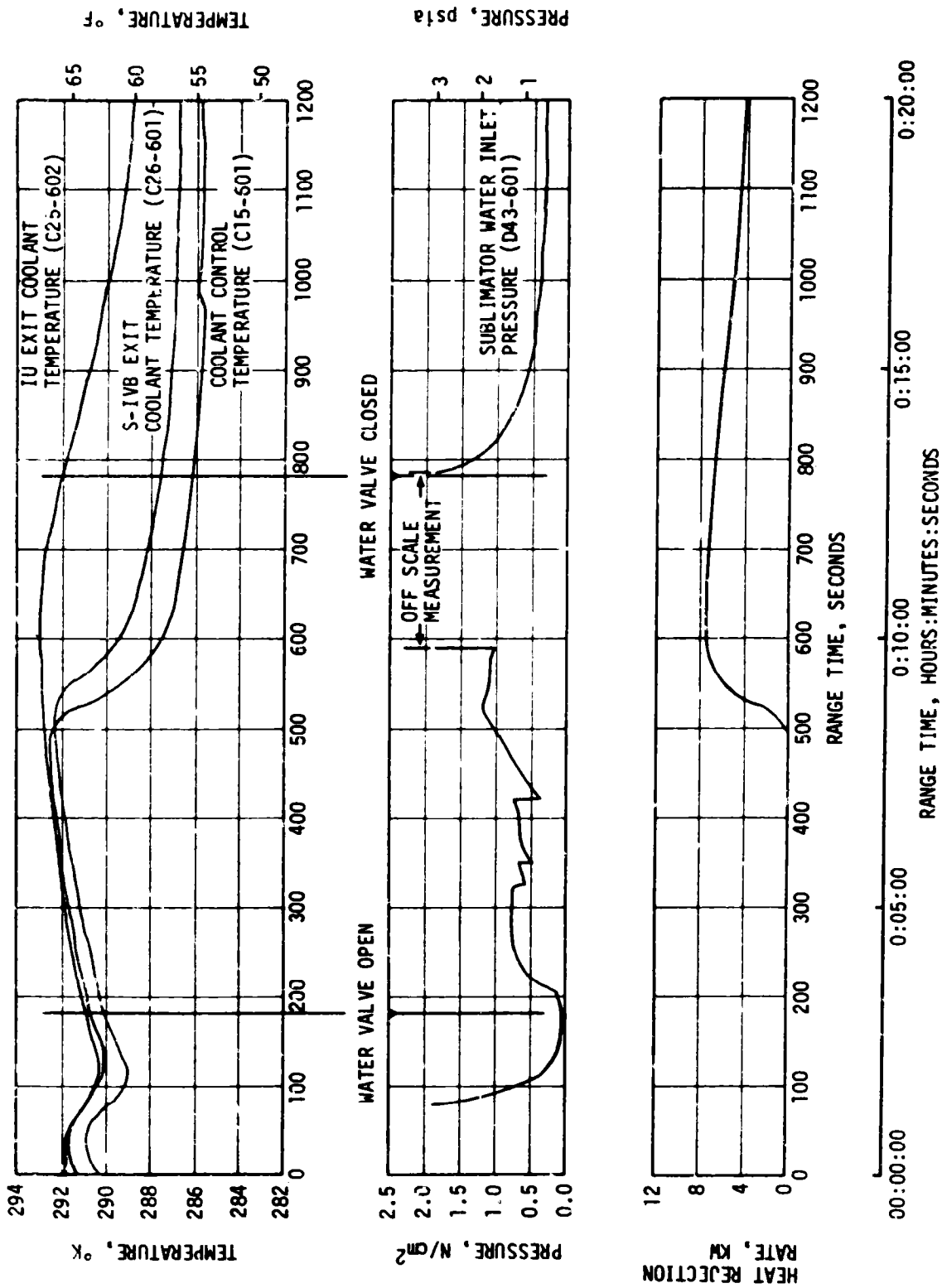


Figure 14-3. IU TCS Coolant Control Parameters

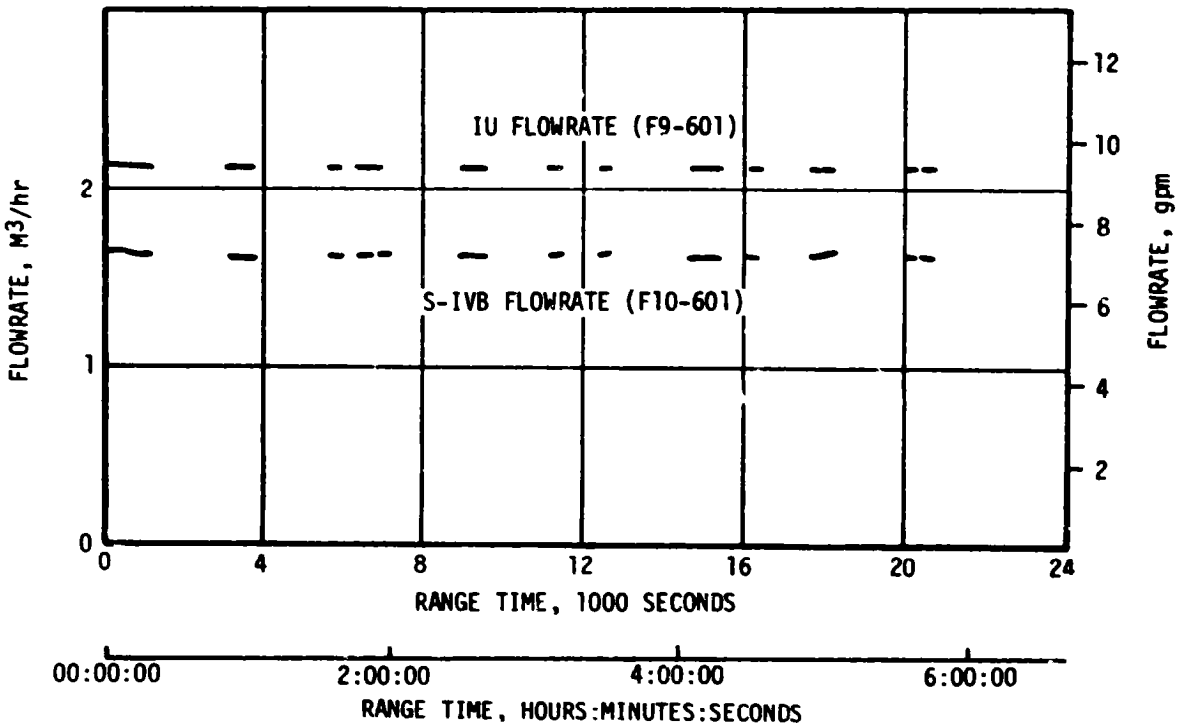
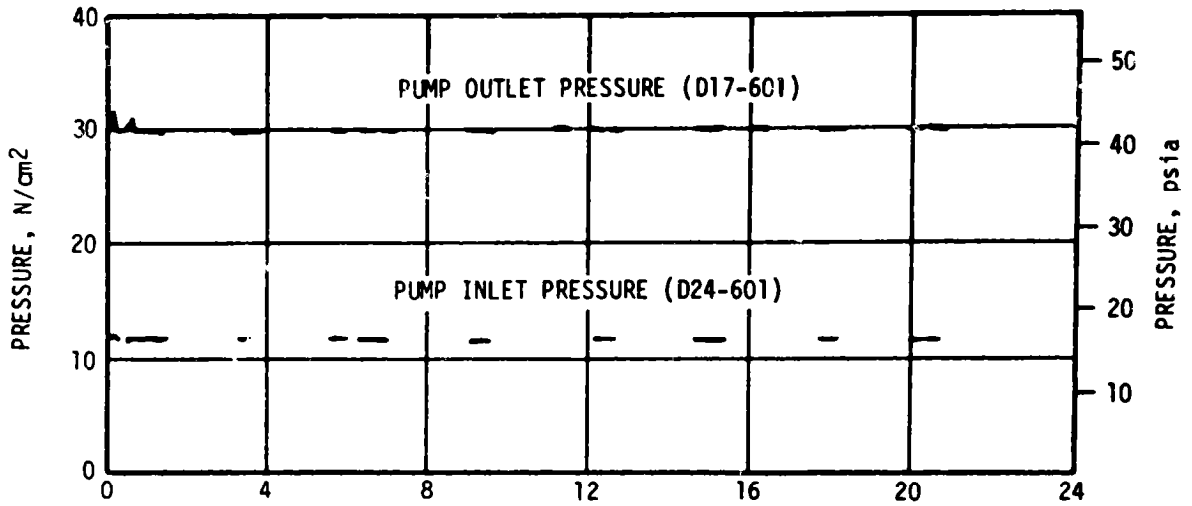


Figure 14-4. IU TCS Hydraulic Performance



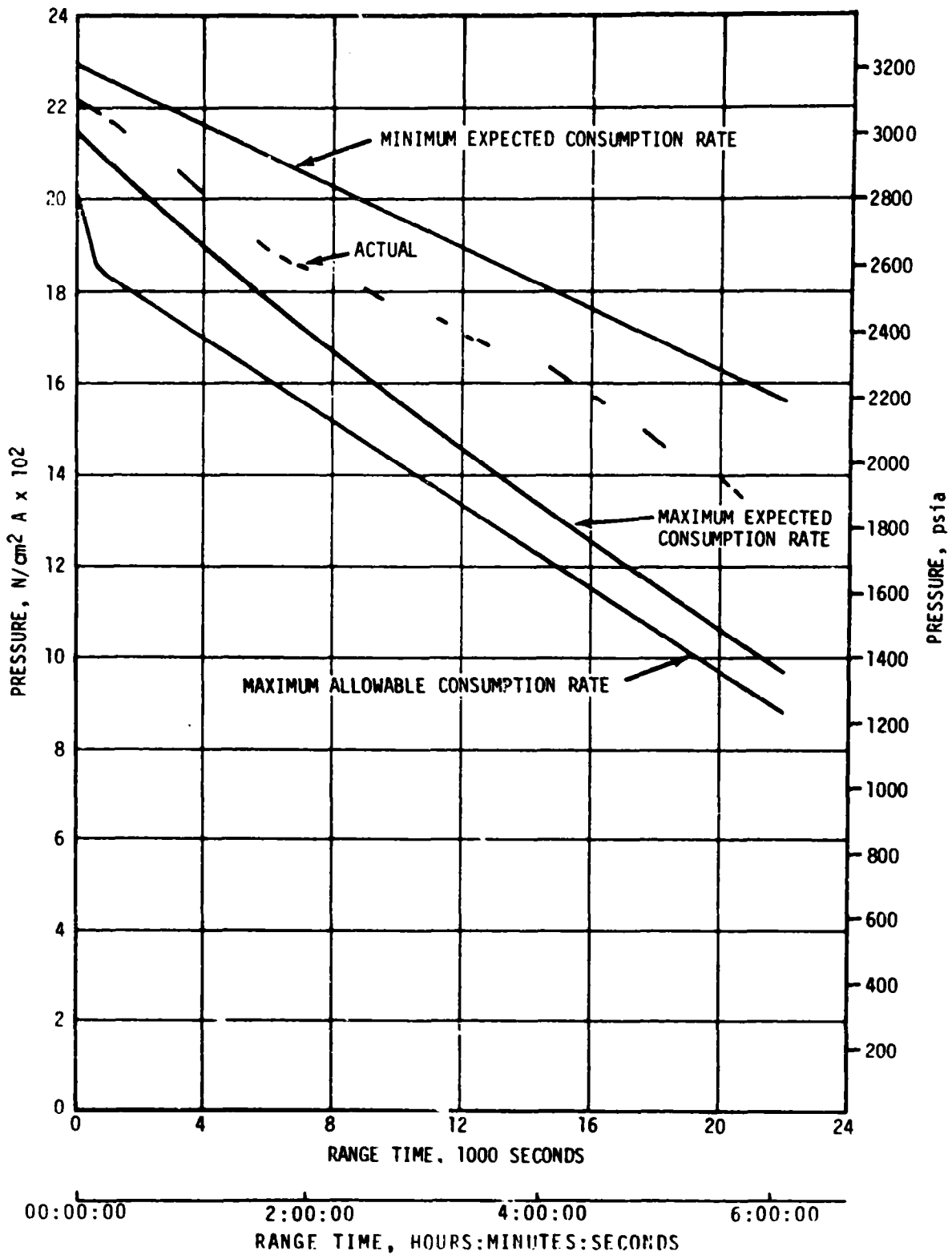


Figure 14-5. IU TCS GN<sub>2</sub> Sphere Pressure (D25-601)

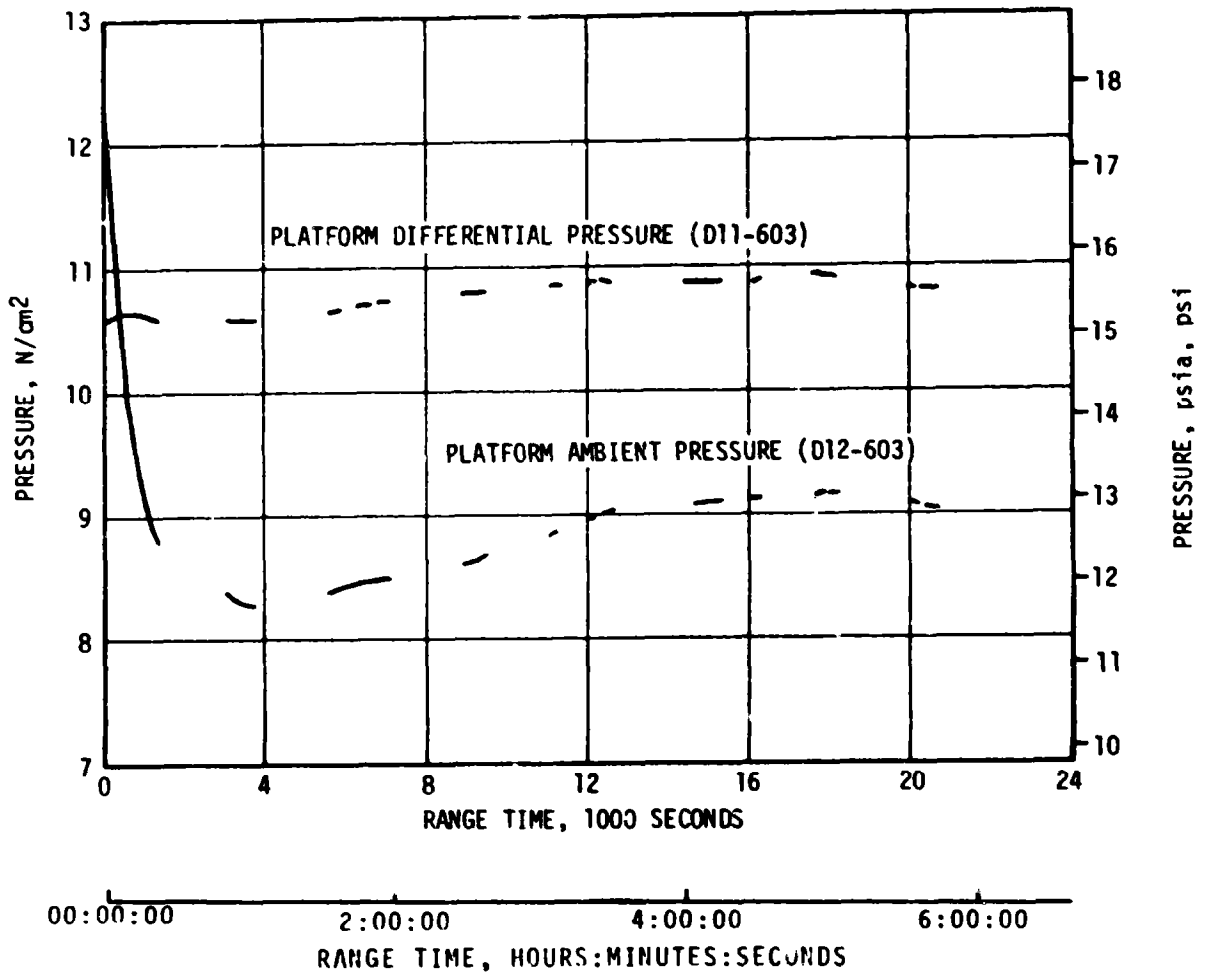


Figure 14-6. Inertial Platform GN2 Pressures

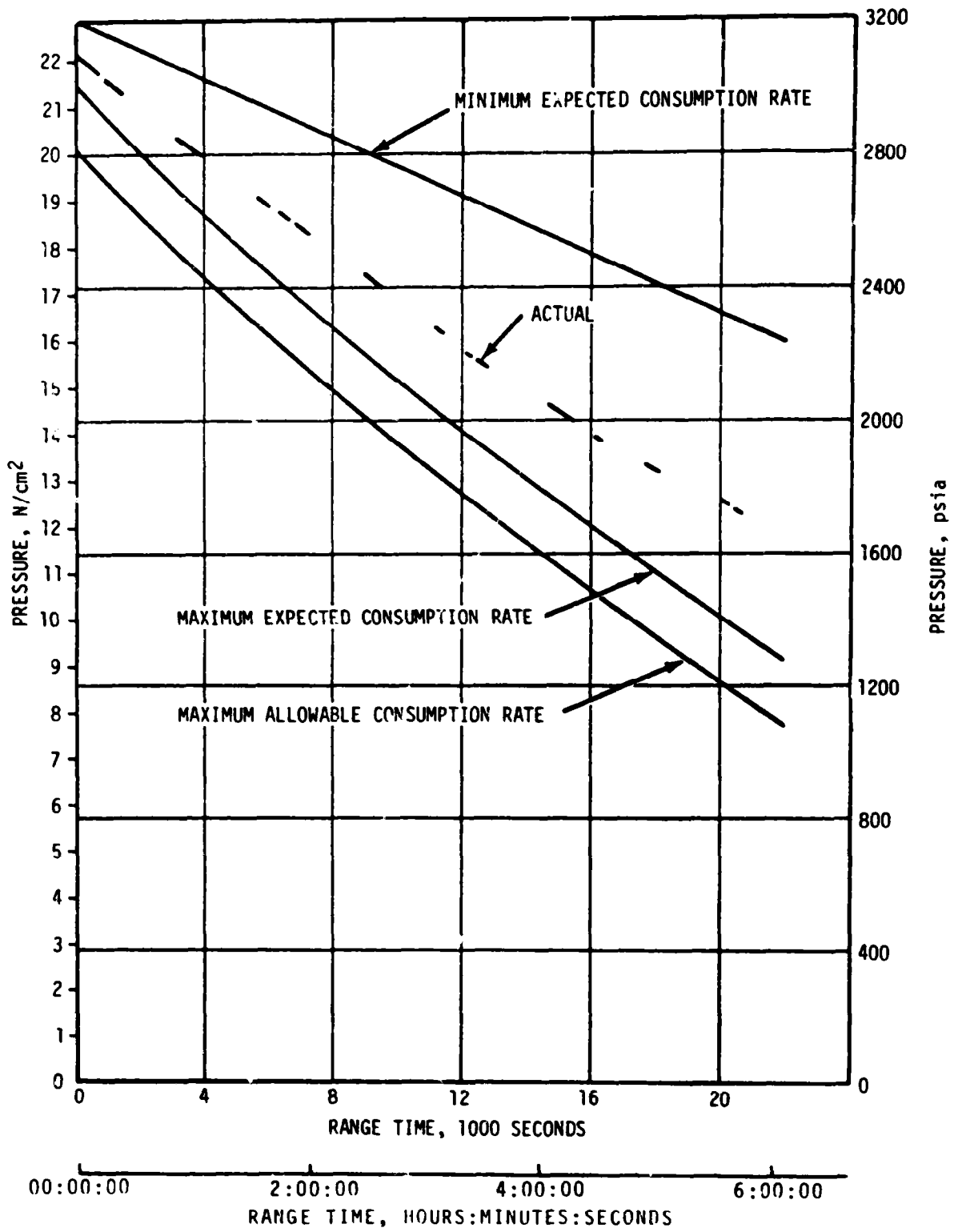


Figure 14-7. IU GBS GN<sub>2</sub> Sphere Pressure (D10-603)

### 14.3.3 Component Temperatures

All internally cooled component temperatures remained within expected ranges throughout the mission as shown in Figures 14-8 and 14-9.

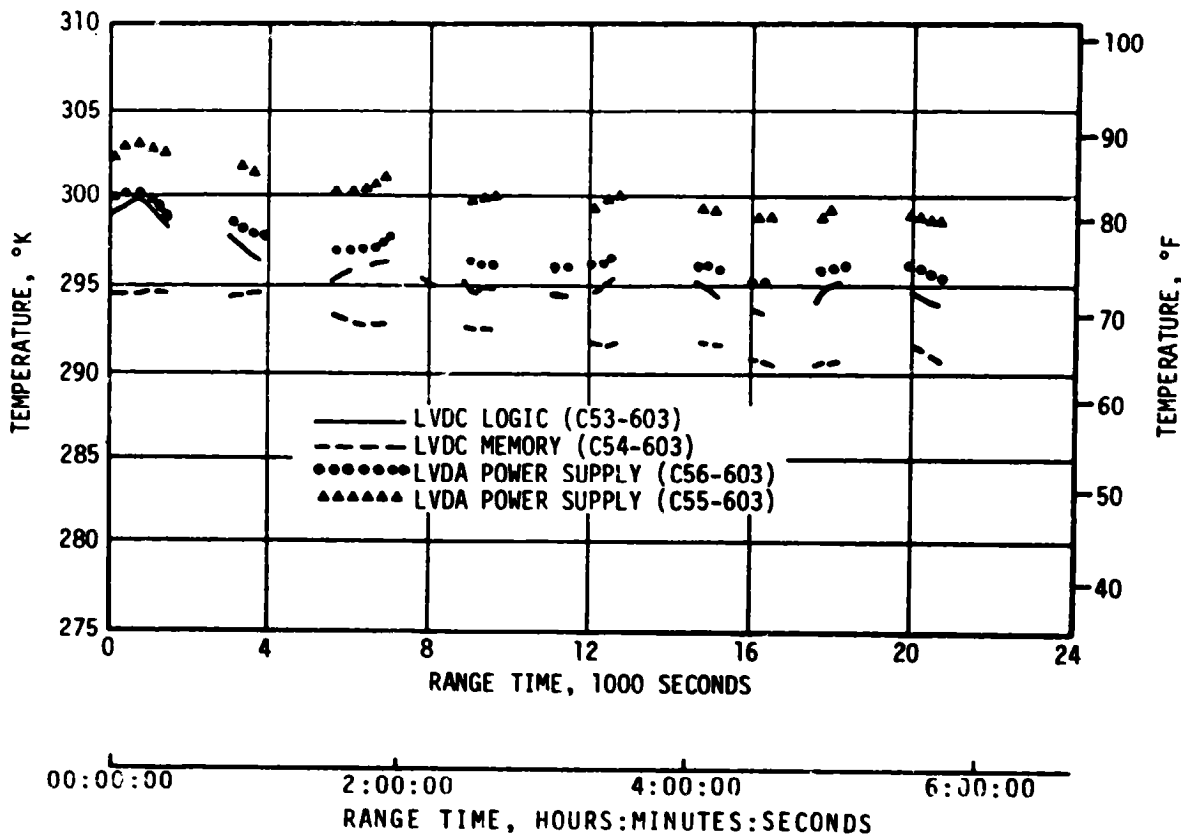


Figure 14-8. IU Selected Component Temperatures

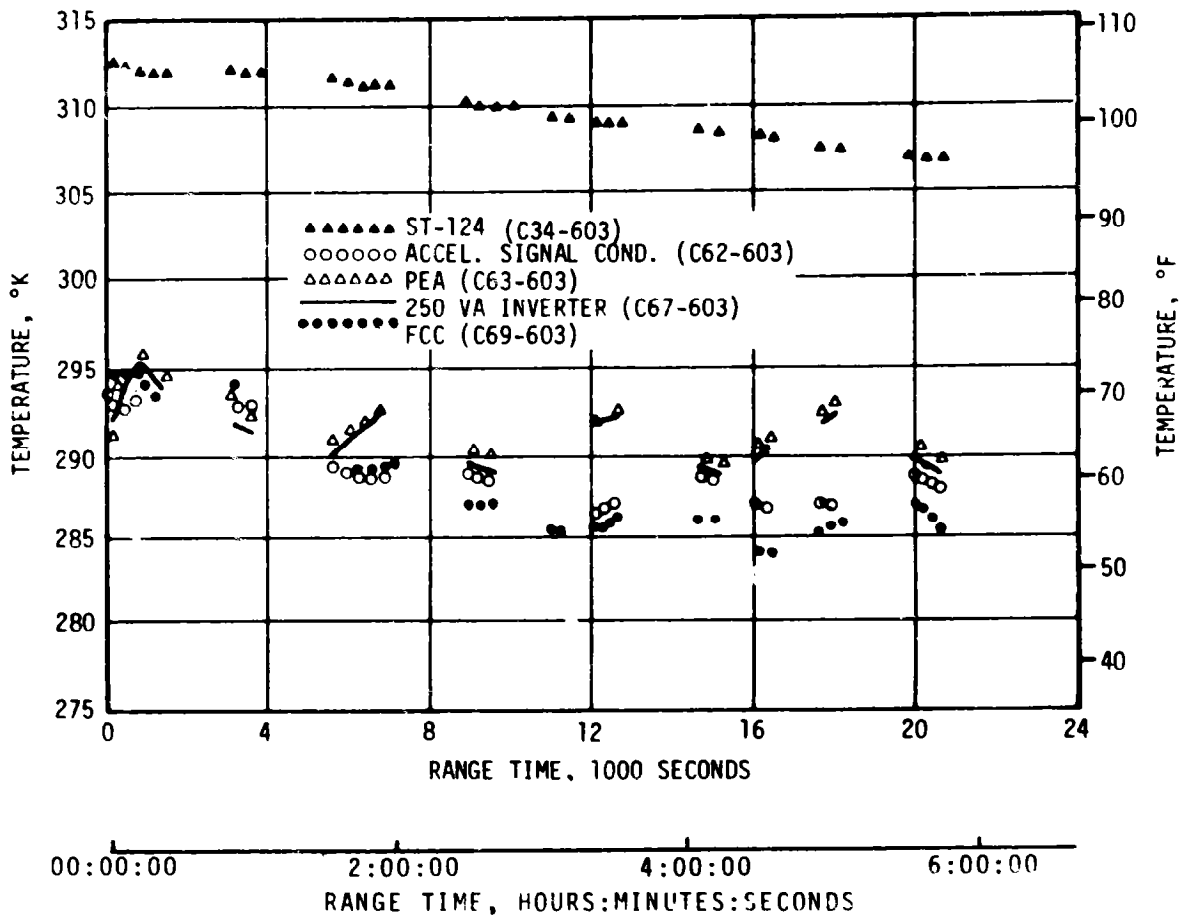


Figure 14-9. IU Selected Component Temperatures

SECTION 15  
DATA SYSTEMS

15.1 SUMMARY

All data systems performed satisfactorily with the exception of the Instrument Unit (IU) telemetry system during orbital operation. Flight measurements from onboard telemetry were 100 percent reliable.

Telemetry performance was normal except for noted problems, the most significant one being a momentary loss of synchronization of the S-IB telemetry signal at liftoff due to burst of electrical noise. A reduction in Radio Frequency (RF) radiated power from the IU telemetry links was experienced during the first orbital revolution. The usual interference due to flame effects and staging were experienced. Usable telemetry data were received until 20,800 seconds (5:46:40). Good tracking data were received from the C-Band radar, with Kwajalein (KWJ) indicating final Loss of Signal (LOS) at 21,475 seconds (5:57:55). The Secure Range Safety Command Systems (SRSCS) on the S-IB and S-IVB Stages were ready to perform their functions properly, on command, if flight conditions during launch phase had required destruct. The Digital Command System (DCS) performed satisfactorily from liftoff through deorbit. Although numerous real time reports of command difficulties were received, the problems have been isolated to ground station operational difficulties and/or onboard telemetry problems.

In general, ground engineering camera coverage was good.

15.2 VEHICLE MEASUREMENT EVALUATION

The SA-206 launch vehicle had 735 measurements scheduled for flight; two measurements were waived prior to start of the automatic countdown sequence leaving 733 measurements active for flight. No measurements failed during flight, resulting in an overall measurement system reliability of 100 percent.

A summary of measurement reliability is presented in Table 15-1 for the total vehicle and for each stage. The waived measurements and partially failed measurements are listed by stage in Tables 15-2 and 15-3. None of these measurement problems had any significant impact on postflight evaluation.

15.2.1 Gyro Summation Current and Accelerometer Summation Current  
Measurement Level Shift

Between Apollo Range Instrument Aircraft (ARIA-4) LOS at 3500 seconds and

Table 15-1. SA-206 Measurement Summary

MEASUREMENT CATEGORY	S-IB STAGE	S-IVB STAGE	INSTRUMENT UNIT	TOTAL VEHICLE
Scheduled	266	240	229	735
Waived	2	0	0	2
Failed	0	0	0	0
Partial Failed	0	1	0	1
Questionable	0	0	0	0
Reliability Percent	100%	100%	100%	100%

Table 15-2. SA-206 Flight Measurements Waived Prior to Flight

MEASUREMENT NUMBER	MEASUREMENT TITLE	NATURE OF FAILURE	REMARKS
S-IB STAGE			
S21-03	Strain Mounting Stud	Strain mounting stud measurement could not be balanced with signal conditioner. Measurement was out of tolerance (off scale) in both run and high modes.	Waiver CCSD-004-206
L500-03	LOX Level Discrete	Intermittent output from Probe No. 2.	Valid data received during flight.

Table 15-3. SA-206 Measurement Malfunctions

MEASUREMENT NUMBER	MEASUREMENT TITLE	NATURE OF FAILURE	TIME OF FAILURE (RANGE TIME)	DURATION OF SATISFACTORY OPERATION	REMARKS
MEASUREMENT PARTIAL FAILURES, S-IVB STAGE					
CO199-401	Temp-Thrust Chamber Jacket	Slow response to temperature changes during J2 Engine operation.	145 sec to 583 sec	0 to 145 sec; 583 sec thru remainder of data.	Probable inadequate thermal bond to thrust chamber jacket.

Corpus Christi (TEX) Acquisition of Signal (AOS) at 5600 seconds, both the Gyro Summation current and the accelerometer summation currents, (K61-603 and K62-603) exhibited level shifts from 3.69 amperes, down to 1.69 amperes and 1.165 amperes down to 1.125 amperes, respectively. Both measurements remained at the new value for the remainder of the flight.

Although initially the shifts in these measurements were thought to be questionable data, laboratory test results indicated that the measurements were reflecting actual current changes. Refer to paragraph 9.4.1 for a complete discussion of this anomaly.

### 15.3 AIRBORNE TELEMETRY SYSTEM EVALUATION

The S-IB and S-IVB stage telemetry systems provided good data from liftoff until each stage exceeded each subsystems' range limitations. The Instrument Unit data indicated nominal performance of the two telemetry subsystems until 970 seconds. After that time, telemetry data were degraded due to low signal strength received at the ground stations. This anomaly is discussed in detail in paragraph 15.3.2. Data degradation and dropouts, as indicated in Table 15-4, were experienced at various times due to the attenuation of RF signals as on previous flights. A dropout caused by S-IB/S-IVB separation (S-IB retro motors) occurred at Central Instrumentation Facility (CIF) and Merritt Island Launch Area (MILA) from 143.9 seconds to 145.9 seconds. The signal strength dropped approximately 60 db. All inflight calibrations occurred as programmed and were within specifications. The last telemetry signal was received at approximately 20,800 seconds (5:46:40) by ARIA-4. A summary of IU and S-IVB telemetry coverage showing AOS and LOS for each station is shown in Figures 15-1 and 15-2.

Table 15-4. SA-206 Launch Vehicle Telemetry Links Performance Summary

LINK	FREQUENCY (MHZ)	MODULATION	STAGE	FLIGHT PERIOD (RANGE TIME, SEC)	PERFORMANCE SUMMARY
GF-1	240.2	FM/FM	S-IB	0 to 380	Satisfactory
GP-1	256.2	PCM/FM	S-IB	0 to 380	Synchronization Loss Range Time (Sec)      Duration (Sec) 4.3                              .2
CP-1	258.5	PCM/FM	S-IVB	0 to 20,800	Satisfactory Data Dropouts Range Time (Sec)      Duration (Sec) 143.7                              2.2
DF-1	250.7	FM/FM	IU	0 to 20,628	Reduction in RF Radiated Power after 970 seconds
DP-1	255.1	PCM/FM	IU	0 to 20,628	Data Dropouts Range Time (Sec)      Duration (Sec) 143.9                              2



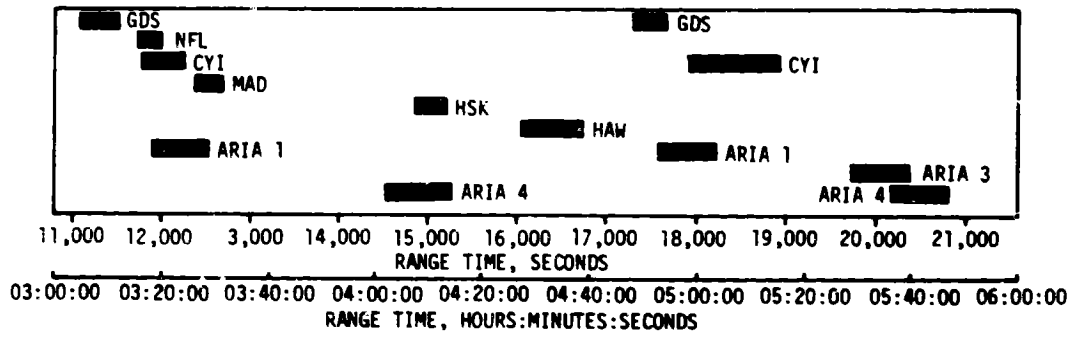
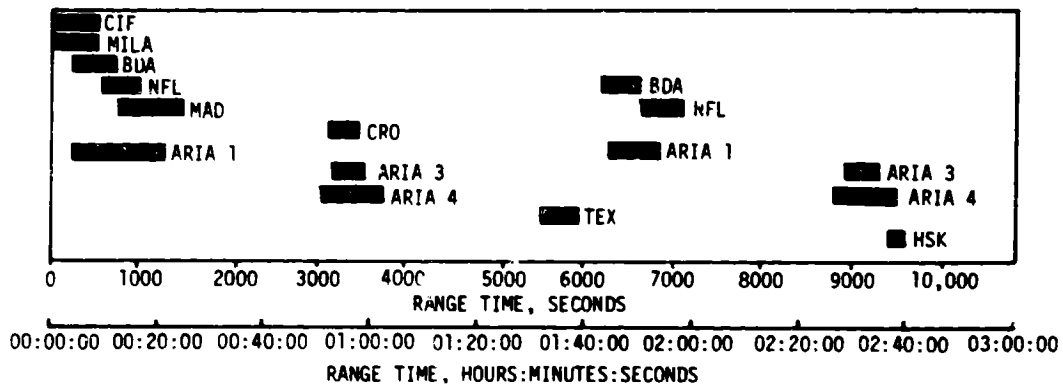


Figure 15-1. Instrument Unit Telemetry Ground Station Coverage

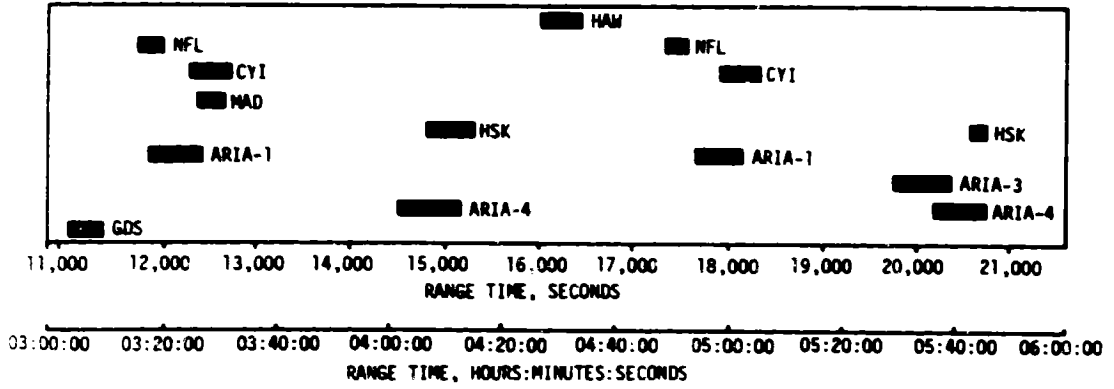
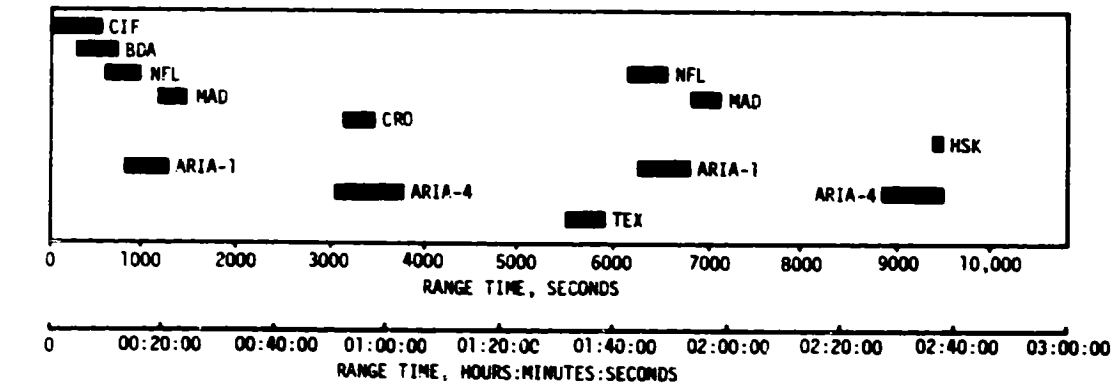


Figure 15-2. S-IVB Telemetry Ground Station Coverage

### 15.3.1 S-IB Telemetry System Loss of Synchronization

A loss of GP-1 Pulse Code Modulation (PCM) synchronization occurred in the ground stations at 4.282 seconds and recovered at 4.466 seconds (184 ms duration). This synchronization loss occurred during a period of widely varying RF signal strength and a high electrical noise environment. The noise environment and signal strength variations are normal for the first 10 seconds of flight. Analysis of the data indicates that the loss of synchronization in the ground station caused the AO multiplexer (MUX) data and the BO MUX data to interchange in the time frame for two wave trains. The AO MUX data appeared in the BO MUX time frame and the BO MUX data appeared in the AO MUX time frame. All the data during the 184 ms was recovered. Analysis of the CIF Predetection Magnetic Tape indicates a burst of electrical noise on the tape during the time of the varying RF signal strength and the synchronization loss.

### 15.3.2 IU Telemetry System Reduction in RF Radiated Power

At 970 seconds, 10 seconds after spacecraft separation, the DF1 and DP1 link signal strength levels at the receiving stations (Newfoundland [NFL] and ARIA-1) decreased abruptly. The DP1 link received signal level at ARIA-1 decreased 22 db from -97 dbm to -119 dbm (Figure 15-3). At NFL both the DP1 and DF1 signals dropped 23 db from -95 dbm to -118 dbm. No DF1 signal strength data was available from ARIA-1. A simultaneous abrupt decrease in indicated DP1 RF power output (J29-602) from 23.8 watts to 13.5 watts, was noted at the time of the decrease in downlink signal strength. The S-IVB CP1 downlink signal strength and forward and reflected power measurements were unaffected at this time.

At 1005 seconds, J29-602 increased abruptly from 13.5 watts to 15.2 watts and varied between 14.2 and 17.8 watts through the remainder of the flight (see Figure 15-4). An output power level of 13.5 watts is more than adequate for good PCM and FM data transmission in earth orbit. DP1 signal strength received at ground stations was much lower than 13.5 watt power output should provide. Therefore, the decrease in received signal strength cannot be attributed to the airborne RF transmitter. The DP1 and CP1 signal strength levels at ARIA-1 showed no significant change at 1005 seconds. DF1 and DP1 signal strengths remained lower than predicted for the remainder of the mission. The decreased DP1 signal strength level caused data dropout problems which to some degree affected the verification of commands transmitted to the IU command subsystem. The effect on command verification is discussed in paragraph 15.6.

A series of tests was conducted in the IBM Telemetry Engineering Laboratory in an effort to duplicate, or approximate, the flight failure signature. The telemetry subsystems flight configuration (Figure 15-5) was bread-boarded using lab models of telemetry RF hardware and cables built to IU requirements. Since both the DF1 and DP1 links were affected, the tests were concentrated on the areas where the two subsystems are common. Introducing open circuit and short circuit conditions at several points between the antennas and the power divider resulted in a maximum change

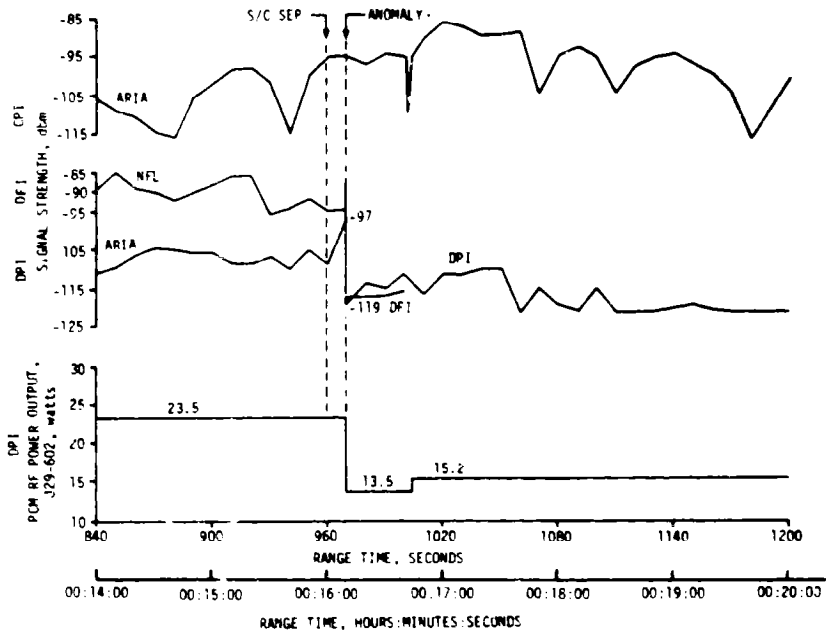


Figure 15-3. IU Telemetry Signal Strength and Power Output Plots Before and After Anomaly

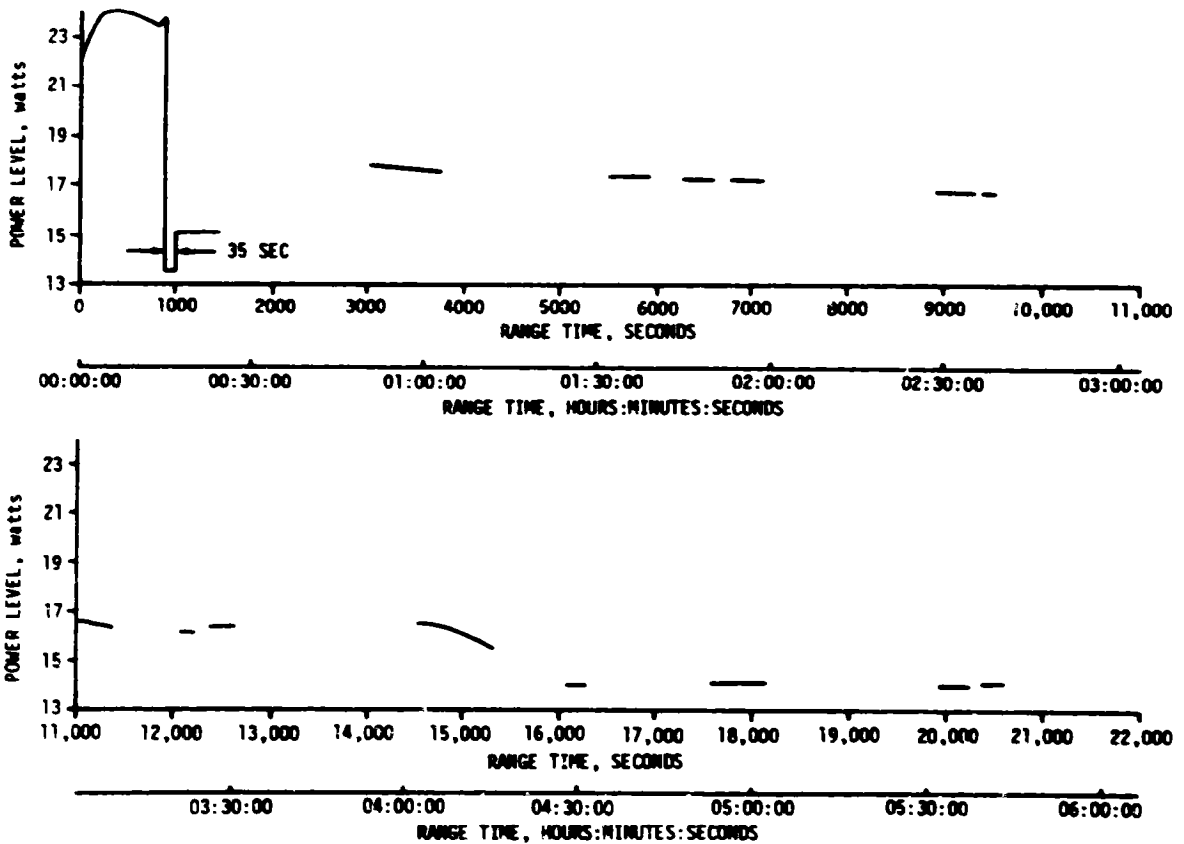


Figure 15-4. PCM Telemetry RF Power Output (Measurement J29-602)

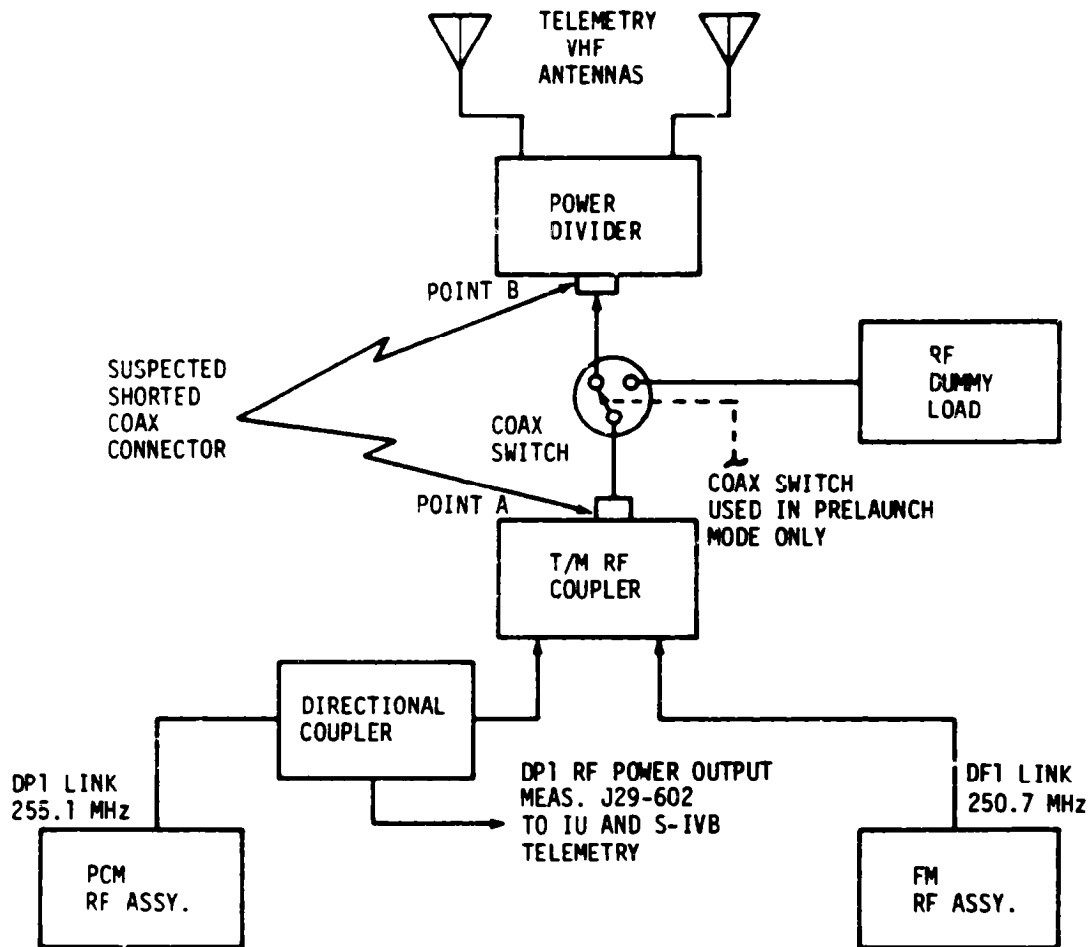


Figure 15-5. SA-206 IU Telemetry RF Subsystem

in J29-602 of only 5.5 watts. This is much less than the 10.3 watt decrease observed in the flight anomaly. Evacuating the telemetry RF coupler to simulate loss of pressurization resulted in much more severe RF signal degradation than observed in the flight anomaly. During vacuum tests the signal strength dropped 32 db and J29-602 dropped from 22 to 8 watts. The flight failure signature could only be approximated in the following two ways: a) shorting the output of the TM RF coupler (point A in Figure 15-5). J29 dropped from 20 watts to 12.5 watts. The DF1 and DP1 received signal levels each dropped 22 db, b) shorting the input to the TM power divider (point B in Figure 15-5). J29 dropped from 20 watts to 12.5 watts. The DF1 and DP1 received signal levels each dropped 25 db.

The short in each case was created by the insertion of a metal fragment in the female connector as shown in Figure 15-6.

The most likely source of a metal fragment in the Type-N coaxial connector

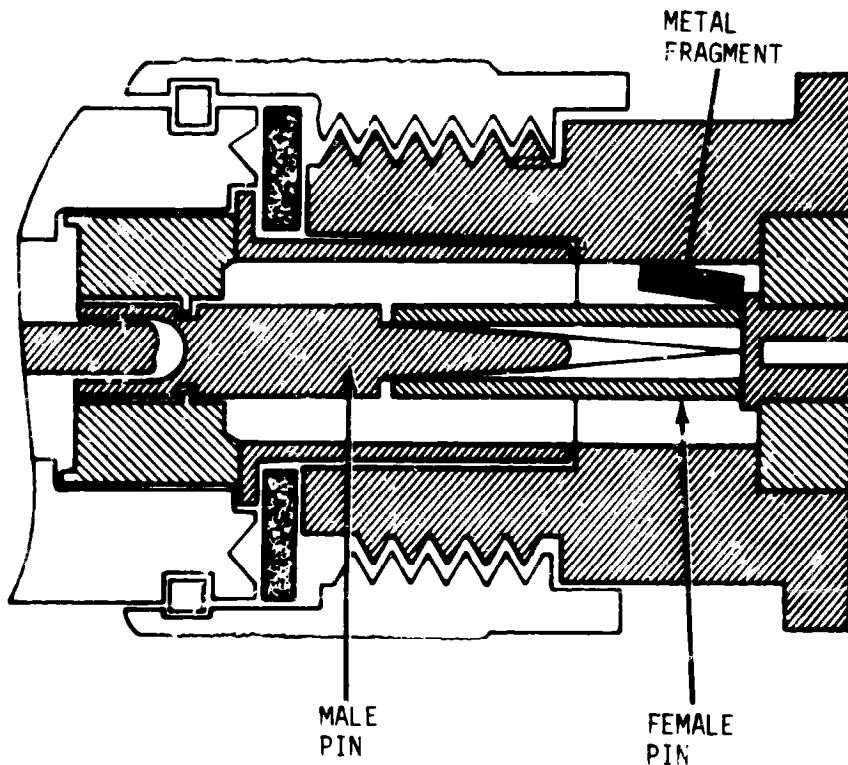
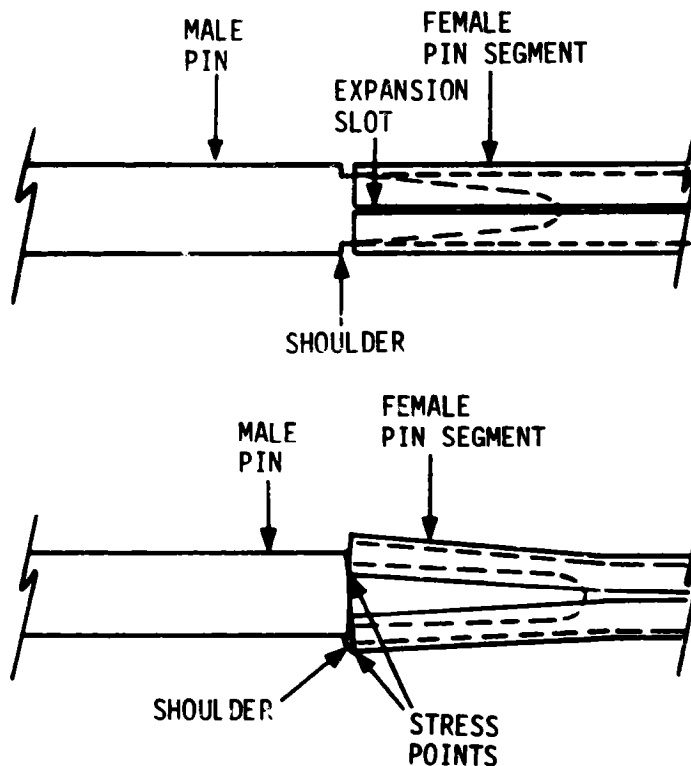


Figure 15-6. Mated RF Connectors

shell is one or more segments of the four segment female pin which could have been broken off by mating a defective or improperly fabricated male cable connector to the female connector. During the postflight tests this type breakage actually occurred when an acceptance test cable connector, with excessive protrusion of the male pin, was mated to an engineering model TM power divider connector. Figure 15-7 shows the connector mated, with the male connector pin protruding normally and excessively. Excessive pin protrusion stresses the segments of the female pin and can cause one or more segments of the female pin to break as was demonstrated in the case cited above. As illustrated in Figure 15-6, a metal fragment of approximately the same size as a broken female pin segment was capable of shorting the center pin to the connector shell when lodged in the correct position.

The results of this investigation indicate that degradation of telemetry signal strength observed during the S-1U-206 anomaly was most likely caused by a broken female pin segment lodged in the connector on the output of the TM RF coupler or the input to the TM power divider. The material was most likely lodged in such a manner that a normal shock or



NOTE:  
EXPANDED VIEW OF MATED RF CONNECTORS SHOWING  
MALE AND FEMALE PIN ONLY

Figure 15-7. RF Connector Pins

vibration in a weightless environment could jar the material into a shorting position.

Test cables from IBM Huntsville with Type-N coaxial connectors were inspected for excessive protrusion of the male pin. Fourteen of twenty-seven cables from the IBM Huntsville test area were found defective. About 90 percent of those inspected at Kennedy Space Center (KSC) were found defective. Only cables using uncaptivated center pin design connectors were found to be defective. Defective test cables will be scrapped or repaired.

An inspection of Type-N coaxial connectors with uncaptivated pins on IU's-207 through 212, 514, and 515 was conducted except that the command antenna connectors were excluded due to inaccessibility.

Two discrepancies were found on IU-210. The telemetry coaxial switch had a damaged J2 connector and the P1 plug of cable 603W121, which attaches to the J1 connector of the command directional coupler, had excessive protrusion of .023 inch (interference fit with the female pin of the component connector). These components were replaced and will be evaluated and dispositioned at a later date. Inspection of logistics spares at KSC revealed two out of four spare telemetry coaxial switches had damaged connectors. They were removed from spare status and will be evaluated and dispositioned at a later date. All other flight hardware logistics spares having Type-N coaxial connectors have been inspected and no defective ones found.

#### 15.4 C-BAND RADAR SYSTEM EVALUATION

The C-Band radar performed satisfactorily during flight. Phase front disturbances were experienced during boost as has occurred on previous missions. However, these disturbances produced only momentary increases in azimuth and elevation tracking angle errors. The onboard C-band measurements and ground tracking station data indicated no tracking problems during earth orbit.

A summary of C-band radar coverage time from AOS to LOS for each station is shown in Figure 15-8. One momentary phase front disturbance was reported by Cape Kennedy (CNV) at 100 seconds. Grand Bahama Island (GBI) experienced numerous phase front disturbances and several momentary dropouts during boost. Phase front disturbances result from severe antenna nulls or distorted beacon returns. All ground radars tracking during boost, except Patrick Air Force Base (PAFB), used beacon track for the entire boost period with the exception of momentary periods of skin track. PAFB skin tracked the vehicle from 20 to 545 seconds except for the period from 403 to 455 seconds when beacon tracking was used to track the vehicle through a weather system.

The last beacon tracking was by KWJ which acquired the C-band beacon near the ascending horizon. After initial beacon track, KWJ switched to skin track until LOS near the descending horizon. When skin track was lost, KWJ again acquired the C-band beacon and obtained a short track to a point slightly below the horizon. This confirmed C-band operation to approximately 6 hours after liftoff.

#### 15.5 SECURE RANGE SAFETY COMMAND SYSTEMS EVALUATION.

Telemetered data indicated that the command antennas, receivers/decoders,

 SKIN TRACKING  
 BEACON TRACKING

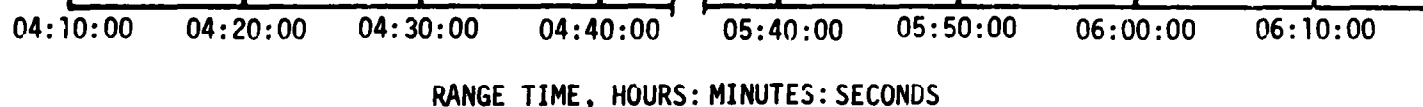
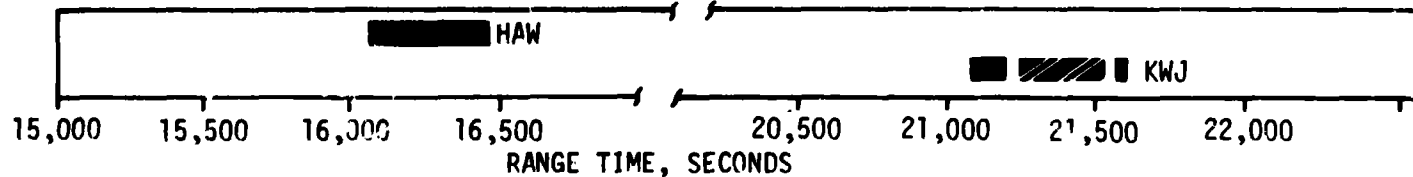
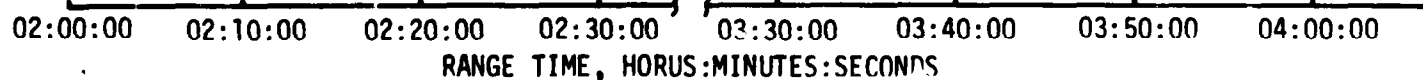
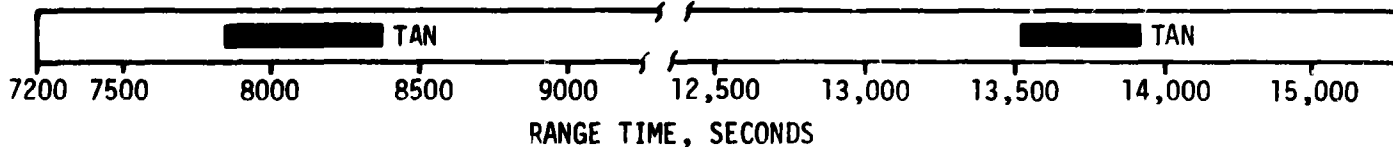
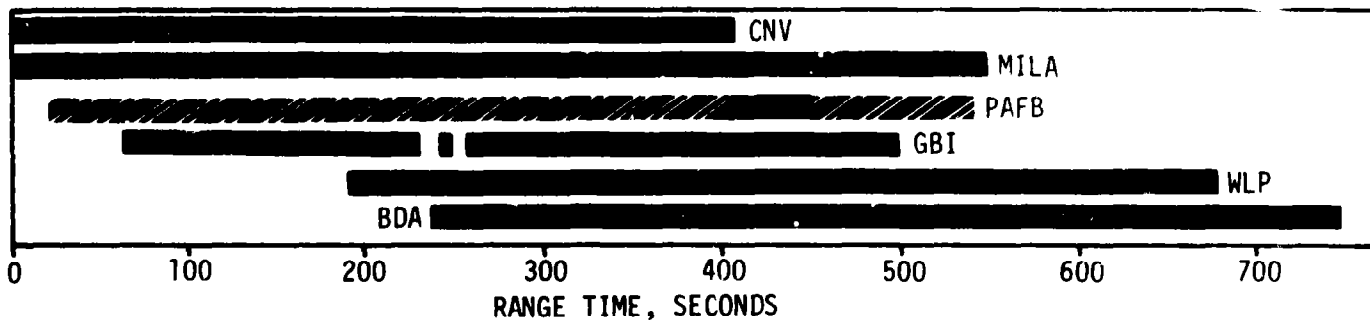


Figure 15-8. C-Band Acquisition and Loss Times



Exploding Bridge Wire (EBW) networks, and destruct controllers on each powered stage functioned properly during flight. They were in the required state-of-readiness if flight conditions during the launch had required vehicle destruct. Since no arm/cutoff or destruct commands were required, all data except receiver signal strength remained unchanged during the flight. Power to the S-IVB stage range safety command systems was cut off at 596.5 seconds by ground command, thereby deactivating (safing) the systems.

## 15.6 DIGITAL COMMAND SYSTEM EVALUATION

There were numerous real time reports of command difficulties in the Message Acceptance Pulse (MAP) and MAP override command modes. However, flight data analysis indicated flawless performance of the onboard DCS. Command difficulties have been isolated to ground station operational difficulties and/or onboard telemetry problems (see Paragraph 15.3.2).

Eighteen commands were initiated by Mission Control Center-Houston (MCC-H) and 183 command words were transmitted from various transmitting ground stations. A list of commands initiated by MCC-H is shown in Table 15-5.

The first three commands of the mission were successfully transmitted from NFL.

Madrid (MAD) experienced the first command problem during transmission of a general maneuver command at 7007 seconds (1:56:47) in the MAP mode. Data indicate there was a telemetry drop out, due to degraded DPL RF signal, immediately after onboard DCS generation of the Computer Reset Pulse (CRP) for the sixteenth word in the twenty-one word command. This resulted in failure of MAD to capture a CRP and generate a MAP for that word. Therefore, the automatic program sequence reacted normally by retransmitting the sixteenth word of the command three times. Each time, the onboard DCS rejected the word as out of sequence since it had already accepted the sixteenth word on the first transmission. The command was terminated normally after the third retransmission of the sixteenth word. No attempt was made to retransmit the command from MAD.

Goldstone (GDS) sent a terminate command to reset the DCS at 11,407 seconds (3:10:07) and then attempted to transmit the same general maneuver as MAD at 11,433 seconds (3:10:33) in the MAP mode. However, data indicate the command was sent after telemetry LCS at GDS. Since the command consists of 21 words and each word required verification via telemetry, the full command was not transmitted. The two terminate commands (one word commands) attempted at 11,440 seconds (3:10:40) and 11,451 seconds (3:10:51) could not be verified due to lack of telemetry data. It is most likely that all three commands were not received because the ground station was attempting to command the vehicle after it went over the horizon.

Table 15-5. SA-206 IU Commands

RANGE TIME		TRANS. STATION	COMMAND (NO. OF WORDS IN COMMAND)	NO. OF WORDS TRANS.	COMMAND MODE	REMARKS
SECONDS	HRS:MIN:SEC					
707	00:11:47	NFL	Memory Dump - 415 Exp. (7)	7	MAP	Accepted
749	00:12:29	NFL	Execute Gen. Man. Solar - Inertial Attitude (21)	21	MAP	Accepted
789	00:13:09	NFL	Memory Dump	7	MAP	Accepted
7,007	01:56:47	MAD	Execute Gen. Man. Local Horizontal Retrograde (21)	19	MAP	Not Accepted
11,407	03:10:07	GDS	Terminate (1)	1	MAP	Accepted
11,433	03:10:33	GDS	Same as 01:56:47 MAD Command	4	MAP	Not Accepted
11,440	03:10:40	GDS	Terminate (1)	4	MAP	Not Verified
11,451	03:10:51	GDS	Terminate (1)	1	MAP Override	Not Verified
11,869	03:17:49	BDA	Same as 01:56:47 MAD Command	4	MAP	Not Accepted
11,876	03:17:56	BDA	Terminate (1)	1	MAP Override	Not Accepted
11,880	03:18:00	BDA	Same as 01:56:47 MAD Command	21	MAP Override	Not Accepted
12,382	03:26:22	CYI	Terminate (1)	1	MAP Override	Accepted
12,389	03:26:29	CYI	Same as 01:56:47 MAD Command	21	MAP Override	Accepted
15,083	04:11:23	HSK	Execute Gen. Man. - 180° Roll (21)	21	MAP Override	Accepted
15,138	04:12:18	HSK	Terminate (1)	1	MAP Override	Accepted
15,167	04:12:47	HSK	Same as 04:11:23 HSK Command	21	MAP Override	Accepted
16,168	04:29:28	HAW	Deorbit Maneuver Load (21)	21	MAP	Accepted
16,192	04:29:52	HAW	Memory Dump for Deorbit (7)	7	MAP	Accepted

Two attempts were made to transmit a general maneuver (Local Horizontal Retrograde) command from Bermuda (BDA) at 11,869 seconds (3:17:49) and a 11,880 seconds (3:18:00). This was the same command previously attempted from MAD and GDS. No BDA telemetry is available during this pass, but NFL telemetry indicates no RF command signal at the onboard command receiver.

BDA analog tape voice annotation indicates BDA was tracking the Saturn Work Shop (SWS) during this pass when MCC-H initiated the command and had no antenna tracking the IU. This accounts for the lack of CPI, DPI, and DFI telemetry data from BDA and the absence of an uplink signal at the IU command receiver. Better coordination between MCC-H and the ground station could possibly have prevented this problem.

Grand Canary Island (CVI) was successful in transmitting a terminate command at 12,382 seconds (3:26:22) (to clear the onboard command circuitry) and the Execute General Maneuver - Local Horizontal Retrograde command at 12,389 seconds (3:26:29).

A roll command was sent from Honeysuckle Creek (HSK) twice, (in the MAP override mode) in an attempt to improve RF signal reception by allowing ground stations to command and receive telemetry data from the omni antennas on the opposite side of the vehicle. Data indicate the first (sent at 4:11:23) of the two commands was received and executed. The terminate command (sent at 4:12:18) was also received, and the second roll command (sent at 4:12:47) was received, but did not result in any activity since the roll had already been executed. There was no change in telemetry received signal strength level noted after the roll indicating that the telemetry problem was not antenna dependent. Command performance was also unaffected by the roll.

No problems were experienced during transmission of the last two commands from Hawaii (HAW). These commands were sent in the MAP mode and were verified in real time by generation of a MAP and execution of the maneuver.

#### 15.7 GROUND ENGINEERING CAMERAS

In general, ground camera coverage was good. Forty-eight items (43 from fixed cameras and 5 from tracking cameras) were received from KSC and evaluated. One item did not operate, one item did not have coded range time, four items were obscured due to frost and ice, and one item (vehicle vertical motion) had a misoriented field of view. As a result of these seven failures, system efficiency was 87 percent. The 500-inch focal length tracking camera followed the vehicle through S-IB/S-IVB separation. All separation events were timed.

## SECTION 16

### MASS CHARACTERISTICS

#### 16.1 SUMMARY

Total vehicle mass, determined from post-flight analysis, was within 1.15 percent of predicted from ground ignition through S-IVB stage cutoff signal with the exception of a longer than predicted S-IVB stage burn, resulting in a less than expected residual. Hardware weights, propellant loads and propellant utilization were close to predicted values during flight.

#### 16.2 MASS EVALUATION

Post-flight mass properties are compared with final predicted mass properties (MSFC Memorandum S&E-ASTN-SAE-73-8) and the operational trajectory (MSFC Memorandum S&E-AERO-MFP-9-73).

The post-flight mass properties were determined from an analysis of all available actual and reconstructed data from S-IB ignition through S-IVB cutoff. Dry weights of the launch vehicle are based on actual weighings and evaluation of the weight and balance log books (MSFC Form 998). Propellant loading and utilization was evaluated by stage contractors from propulsion system performance reconstructions. Spacecraft data were obtained from the Johnson Space Center (JSC).

Differences between predicted and actual dry weights of the inert stages and the loaded spacecraft were all within 0.87 percent of predicted, which is within acceptable limits.

During S-IB burn phase, the total vehicle mass was greater than predicted by 645 kilograms (1424 lbm) (0.11 percent) at ignition, and greater than predicted by 286 kilograms (629 lbm) (0.16 percent) at physical separation. These small differences may be attributed to a larger than predicted fuel loading and a larger than predicted upper stage weight.

S-IB burn phase total vehicle mass is shown in Tables 16-1 and 16-2.

During S-IVB burn phase, the total vehicle mass was more than predicted by 321 kilograms (709 lbm) (0.23 percent) at ignition, and less than predicted by 357 kilograms (787 lbm) (1.15 percent) at S-IVB stage cutoff signal. These differences are due primarily to a greater than predicted spacecraft weight and a less than expected residual. Total vehicle mass for the S-IVB burn phase is shown in Tables 16-3 and 16-4.

A summary of mass utilization and loss, both actual and predicted, from S-IB stage ignition through spacecraft separation is presented in Table 16-5. A comparison of actual and predicted mass, center of gravity, and moment of inertia is shown in Table 16-6.

Table 16-1. SA-206 Total Vehicle Masses (Kilograms)

EVENT	GROUND IGNITION		FIRST MOTION		INBOARD ENGINE CUTOFF SIGNAL		OUTBOARD ENGINE CUTOFF SIGNAL		SEPARATION SIGNAL	
	PRED	ACTUAL	PRED	ACTUAL	PRED	ACTUAL	PRED	ACTUAL	PRED	ACTUAL
RANGE TIME (SECT)	-3.10	-3.10	0.20	.20	137.90	136.7	140.90	142.20	142.20	143.90
S-IB STG DRY	38351.	38346.	38351.	38346.	38351.	38346.	38351.	38346.	38351.	38346.
LOX IN TANKS	283158.	283169.	277946.	277452.	1059.	1497.	0.	0.	0.	0.
LOX BELOW TANKS	3519.	3519.	3722.	3722.	3673.	3673.	1493.	1322.	1240.	1122.
LOX ULLAGE	13.	13.	35.	35.	1187.	1187.	1302.	1202.	1203.	1203.
RP1 IN TANKS	124663.	124949.	122759.	122808.	2071.	2420.	352.	418.	0.	35.
RP1 BELOW TANKS	2151.	2151.	2574.	2574.	2574.	2574.	2383.	2383.	2222.	2267.
RP1 ULLAGE	7.	7.	3.	3.	20.	20.	20.	20.	20.	20.
HELIUM SUPPLY	35.	35.	34.	34.	11.	11.	10.	10.	10.	10.
NITROGEN	6.	6.	6.	6.	6.	6.	6.	6.	6.	6.
HYDRAULIC OIL	12.	12.	12.	12.	12.	12.	12.	12.	12.	12.
ORONITE	14.	14.	14.	14.	2.	2.	2.	2.	2.	2.
FROST	453.	453.	453.	453.						
TOTAL S-IB STAGE	452383.	452056.	445913.	445465.	44975.	44957.	43822.	43707.	43074.	43032.
S-IB/S-IVB DRY	2567.	2571.	2567.	2571.	2567.	2571.	2567.	2571.	2567.	2571.
RETRO PROPELLANT	481.	482.	481.	482.	481.	482.	481.	482.	481.	482.
TOTAL FIRST STG	455432.	455711.	448965.	448920.	52024.	52811.	46671.	46702.	46123.	46086.
TOTAL S-IVB STG	115770.	115934.	115770.	115934.	115724.	115804.	115724.	115804.	115724.	115804.
INSTRUMENT UNIT	1919.	1930.	1919.	1930.	1919.	1930.	1919.	1930.	1919.	1930.
SPACECRAFT	19765.	19937.	19765.	19937.	19765.	19937.	19765.	19937.	19765.	19937.
TOTAL VEHICLE	592848.	593533.	586420.	586342.	189434.	193343.	184241.	184494.	183323.	183818.

Table 16-2. SA-206 Total Vehicle Masses (Pounds)

EVENT	GROUND IGNITION		FIRST MOTION		INBOARD ENGINE CUTOFF SIGNAL		OUTBOARD ENGINE CUTOFF SIGNAL		SEPARATION SIGNAL	
	PRED	ACTUAL	PRED	ACTUAL	PRED	ACTUAL	PRED	ACTUAL	PRED	ACTUAL
RANGE TIME (SECT)	-3.10	-3.10	0.20	.20	137.90	136.7	140.90	142.20	142.20	143.90
S-IB STG DRY	84550.	84529.	84550.	84529.	84550.	84529.	84550.	84529.	84550.	84529.
LOX IN TANKS	624257.	624283.	612768.	611678.	236.	3302.	0.	0.	0.	0.
LOX BELOW TANKS	759.	758.	8206.	8206.	8099.	8099.	3297.	2916.	2733.	2475.
LOX ULLAGE	30.	30.	79.	79.	2617.	2617.	2690.	2650.	2693.	2652.
RP1 IN TANKS	274833.	275423.	270637.	270744.	4566.	5335.	778.	917.	0.	77.
RP1 BELOW TANKS	4744.	4744.	5676.	5676.	5676.	5676.	5210.	5210.	4898.	4998.
RP1 ULLAGE	5.	5.	8.	8.	50.	50.	50.	50.	50.	50.
HELIUM SUPPLY	78.	78.	75.	75.	24.	24.	24.	24.	24.	24.
NITROGEN	13.	13.	13.	13.	9.	9.	9.	9.	9.	9.
HYDRAULIC OIL	28.	28.	28.	28.	28.	28.	28.	28.	28.	28.
ORONITE	33.	33.	33.	33.	6.	6.	6.	6.	6.	6.
FROST	1000.	1000.	1000.	1000.						
TOTAL S-IB STAGE	997333.	997937.	983078.	982084.	107972.	109096.	98611.	98359.	94962.	94809.
S-IB/S-IVB DRY	5661.	5670.	5661.	5670.	5661.	5670.	5661.	5670.	5661.	5670.
RETRO PROPELLANT	1062.	1064.	1062.	1064.	1062.	1064.	1062.	1064.	1062.	1064.
TOTAL FIRST STG	1004058.	1004671.	989799.	988818.	114695.	116430.	104334.	104093.	101685.	101682.
TOTAL S-IVB STG	255230.	255637.	255230.	255637.	495130.	495437.	282150.	282437.	282150.	282437.
INSTRUMENT UNIT	4231.	4290.	4231.	4290.	4231.	4290.	4231.	4290.	4231.	4290.
SPACECRAFT	43576.	43934.	43576.	43934.	43576.	43934.	43576.	43934.	43576.	43934.
TOTAL VEHICLE	1307099.	1308519.	1292437.	1292666.	417632.	420777.	406271.	406703.	404061.	403290.

Table 16-3. SA-206 Upper Stages and Payload Vehicle Masses (Kilograms)

	S-1B STAGE GROUND IGNITION		J-2 ENGINE START COMMAND		MAINSTAGE		J-2 ENGINE CUTOFF COMMAND		ORBITAL INSERTION	
	PRED	ACTUAL	PRED	ACTUAL	PRED	ACTUAL	PRED	ACTUAL	PRED	ACTUAL
RANGE TIME (SECI)	-3+10	-3+10	1+3+60	1+4+90	1+6+90	1+6+20	5+2+50	5+6+20	5+2+50	5+6+20
S-1VB STAGE DRY	9949.	10020.	9933.	10003.	9933.	10003.	9933.	10003.	9933.	10003.
ULL ROCKET CASES	97.	47.	97.	47.	97.	47.	97.	47.	97.	47.
ULL ROCKET GRAIN	79.	80.	79.	47.	79.	47.	79.	47.	79.	47.
LOR IN TANK	87830.	87765.	87830.	87765.	87729.	87698.	1754.	1136.	1766.	1109.
LOR BELOW TANK	180.	150.	180.	180.	180.	180.	180.	180.	180.	180.
LOR ULLAGE	11.	12.	11.	12.	14.	13.	164.	167.	159.	166.
LH2 IN TANK	17279.	17352.	17279.	17332.	17234.	17311.	993.	989.	993.	979.
LH2 BELOW TANK	26.	23.	26.	23.	26.	23.	26.	23.	21.	19.
H2 ULLAGE	72.	67.	72.	67.	72.	68.	206.	129.	203.	129.
HELIUM-LOR PRESS	114.	114.	114.	114.	114.	113.	43.	43.	43.	43.
APS PROPELLANT	59.	60.	59.	60.	59.	60.	59.	57.	57.	56.
GH2/START TANK	2.	2.	2.	2.	0.	0.	0.	0.	0.	0.
HYDRAULIC OIL	0.	0.	0.	0.	0.	0.	0.	0.	0.	0.
N2-HYD RESERVOIR	1.	1.	1.	1.	1.	1.	1.	1.	1.	1.
ENV1 CONT FLUID	6.	6.	6.	6.	6.	6.	6.	6.	6.	6.
HELIUM-APS	1.	1.	1.	1.	1.	1.	1.	1.	1.	1.
HELIUM-PNEUMATIC	5.	5.	5.	5.	5.	5.	5.	5.	5.	5.
FROST	45.	136.	0.	45.	0.	45.	0.	45.	0.	45.
TOTAL S-1VB STG	115770.	115954.	115676.	115615.	115664.	115619.	12379.	12812.	13225.	12756.
INSTRUMENT UNIT	1919.	1930.	1919.	1930.	1919.	1930.	1919.	1933.	1919.	1930.
SPACECRAFT	19765.	19937.	19765.	19937.	19765.	19937.	15374.	15777.	15374.	15777.
TOTAL VEHICLE	137655.	137822.	137561.	137664.	137169.	137506.	32877.	32520.	32823.	32469.

Table 16-4. SA-206 Upper Stages and Payload Vehicle Masses (Pounds)

	S-1B STAGE GROUND IGNITION		J-2 ENGINE START COMMAND		MAINSTAGE		J-2 ENGINE CUTOFF COMMAND		ORBITAL INSERTION	
	PRED	ACTUAL	PRED	ACTUAL	PRED	ACTUAL	PRED	ACTUAL	PRED	ACTUAL
RANGE TIME (SECI)	-3+10	-3+10	1+3+60	1+4+90	1+6+90	1+6+20	5+2+50	5+6+20	5+2+50	5+6+20
S-1VB STAGE DRY	21936.	22471.	21900.	22055.	21900.	22055.	21900.	22055.	21900.	22055.
ULL ROCKET CASES	214.	216.	214.	216.	214.	216.	214.	216.	214.	216.
ULL ROCKET GRAIN	176.	177.	169.	105.	176.	105.	176.	105.	176.	105.
LOR IN TANK	193633.	193534.	193633.	193534.	193610.	193542.	3067.	2506.	3067.	2446.
LOR BELOW TANK	397.	397.	397.	397.	397.	397.	397.	397.	367.	367.
LOR ULLAGE	29.	28.	29.	28.	32.	30.	363.	374.	364.	368.
LH2 IN TANK	38074.	38255.	38074.	38255.	37995.	38106.	2190.	2181.	2180.	2154.
LH2 BELOW TANK	58.	52.	58.	52.	58.	52.	58.	52.	48.	42.
H2 ULLAGE	160.	149.	160.	149.	180.	154.	450.	308.	452.	308.
HELIUM-LOR PRESS	253.	252.	253.	252.	252.	251.	96.	100.	95.	100.
APS PROPELLANT	132.	134.	132.	134.	132.	134.	126.	134.	126.	134.
GH2/START TANK	5.	5.	5.	5.	1.	1.	1.	1.	1.	1.
HYDRAULIC OIL	15.	15.	15.	15.	15.	15.	15.	15.	15.	15.
N2-HYD RESERVOIR	3.	3.	3.	3.	3.	3.	3.	3.	3.	3.
ENV1 CONT FLUID	14.	14.	14.	14.	14.	14.	14.	14.	14.	14.
HELIUM-APS	3.	3.	3.	3.	3.	3.	3.	3.	3.	3.
HELIUM-PNEUMATIC	12.	12.	12.	12.	12.	12.	12.	12.	12.	12.
FROST	100.	300.	0.	100.	0.	100.	0.	100.	0.	100.
TOTAL S-1VB STG	255230.	255337.	255223.	255229.	255299.	255241.	29990.	28447.	29376.	28123.
INSTRUMENT UNIT	4231.	4256.	4231.	4256.	4231.	4256.	4231.	4256.	4231.	4256.
SPACECRAFT	43576.	43934.	43576.	43934.	43576.	43934.	34366.	34784.	34366.	34766.
TOTAL VEHICLE	303037.	303627.	303020.	303529.	303006.	303121.	68874.	67237.	67954.	67103.

Table 16-5. SA-206 Flight Sequence Mass Summary

	ACTUAL		PREDICTED	
	KG	LBM	KG	LBM
S-IB STAGE AT GROUND IGNITION (G.I.)	452656.	977927.	452383.	977333.
S-IB/S-IVB INTERSTAGE AT G.I.	3054.	6734.	3049.	6723.
S-IVB STAGE AT G.I.	115954.	255637.	115770.	255230.
INSTRUMENT UNIT AT G.I.	1930.	4250.	1919.	4231.
CSY,SLA,LES	19937.	43954.	19763.	43576.
FIRST FLIGHT STAGE AT G.I.	593533.	1306519.	592366.	1307093.
THRUST BUILDUP PROP	-7190.	-15852.	-6467.	-14250.
FIRST FLIGHT STAGE AT FIRST MOTION	586342.	1292000.	585420.	1292837.
MAINSTAGE PROP	-399973.	-861750.	-400309.	-862331.
FROST	-653.	-1000.	-653.	-1000.
SEAL PURGE (N2)	-2.	-6.	-2.	-6.
GEAR BOX CONSUMPTION (RP-1)	-320.	-706.	-320.	-706.
FUEL ADDITIVE (KRONITE)	-12.	-27.	-12.	-27.
I.E.T.D. PROP	-495.	-2144.	-495.	-2144.
S-IVB FROST	-90.	-200.	-65.	-100.
FIRST FLIGHT STAGE AT O.E.C.O.S.	104494.	406740.	104231.	406271.
OETD TO SEP PROP	-691.	-1525.	-764.	-1664.
FIRST FLIGHT STAGE AT SEPARATION (PHYSICAL)	103802.	405215.	103517.	404567.
S-IB STAGE AT SEPARATION	-43015.	-94834.	-43057.	-94720.
S-IB/S-IVB INTERSTAGE	-3054.	-6734.	-3049.	-6723.
S-IVB AFT FRAME	-14.	-31.	-14.	-31.
S-IVB ULLAGE ROCKET PROPELLANT	-32.	-72.	-32.	-71.
S-IVB DETONATION PACKAGE	-2.	-5.	-2.	-5.
SECOND FLIGHT STAGE AT IGNITION (ESC)	137682.	303539.	137361.	302830.
THRUST BUILDUP PROP	-126.	-278.	-142.	-314.
ULLAGE ROCKET PROPELLANT	-47.	-103.	-47.	-105.
GH2 START TANK	-1.	-4.	-1.	-4.
SECOND FLIGHT STAGE AT 90 PERCENT THRUST	137506.	303151.	137169.	302406.



Table 16-5. SA-20E Flight Sequence Mass Summary (Continued)

	ACTUAL		PREDICTED	
	KG	LBW	KG	LBW
SECOND FLIGHT STAGE AT 90 PERCENT THRUST	137506.	303151.	137169.	302406.
AUX-PROP. POWER ROLL	-1.	-4.	-2.	-6.
MAINSTAGE	-102720.	-226474.	-102004.	-224886.
ULLAGE ROCKET CASES	-97.	-210.	-97.	-210.
LES	-4159.	-9170.	-4100.	-9030.
SECOND FLIGHT STAGE AT ECC	30520.	67257.	30077.	66074.
THRUST DECAY PROP	-35.	-84.	-36.	-80.
PROP BELOW VALVE	-18.	-40.	-10.	-20.
SECOND FLIGHT STAGE AT ETD	30404.	67103.	30023.	66704.
CSM	-13470.	-29817.	-13774.	-30374.
SLA PANELS ROTATED	0.	0.	0.	0.
VENT	-153.	-334.	-341.	-753.
CSM SEPARATED	16332.	36007.	16702.	36821.
S-IVB STAGE	-12602.	-27704.	-12480.	-27500.
V.I.U.	-1430.	-3256.	-1424.	-3151.
SLA	-1744.	-3867.	-1744.	-3987.

Table 16-6. SA-206 Mass Characteristics Comparison

EVENT	MASS		LONGITUDINAL C.G. (X STA.)		RADIAL C.G.		ROLL MOMENT OF INERTIA		PITCH MOMENT OF INERTIA		YAW MOMENT OF INERTIA	
	KILO POUNDS	O/O DEV.	METERS INCHES	DELTA	METERS INCHES	DELTA	KG-M2 O/O X10-6	DEV.	KG-M2 O/O X10-6	DEV.	KG-M2 O/O X10-6	DEV.
S-IB STAGE DRY	PRED	38351. 84550.	8.636 340.0		0.0160 0.6324		0.224		2.600		2.600	
	ACTUAL	38346. 84539.	8.643 340.3	0.007 0.29	0.0129 0.5099	-0.0031 -0.1245	0.224	-0.00	2.599	-0.00	2.599	-0.00
S-IB/S-IVB INTER-STAGE TOTAL	PRED	3050. 6723.	26.703 1051.3		0.0559 2.2022		0.033		0.023		0.024	
	ACTUAL	3054. 6734.	26.703 1051.3	0.000 0.00	0.0559 2.2022	0.0000 0.0000	0.033	0.16	0.023	0.16	0.024	0.16
S-IVB STAGE DRY AT G.I.	PRED	10047. 22150.	33.073 1302.1		0.2334 9.1923		0.074		0.269		0.269	
	ACTUAL	10118. 22307.	33.037 1300.7	-0.035 -1.39	0.2355 9.2720	0.0020 0.0796	0.075	0.90	0.272	0.81	0.271	0.81
INSTRUMENT UNIT TOTAL	PRED	1919. 4231.	42.796 1684.9		0.1481 5.8309		0.018		0.010		0.008	
	ACTUAL	1930. 4256.	42.796 1684.9	0.000 0.00	0.1481 5.8309	0.0000 0.0000	0.018	0.59	0.010	0.59	0.008	0.59
SPACECRAFT TOTAL	PRED	19766. 43576.	55.925 2201.8		0.0705 2.7786		0.038		0.532		0.533	
	ACTUAL	19837. 43954.	55.920 2201.6	-0.005 -0.20	0.0808 3.1827	0.0102 0.4042	0.038	0.13	0.529	-0.50	0.530	-0.60
1ST FLIGHT STAGE AT IGNITION	PRED	592888. 1307095.	18.933 745.4		0.0071 0.2807		2.155		75.981		75.981	
	ACTUAL	593534. 1308519.	18.948 746.0	0.015 0.59	0.0068 0.2701	-0.0002 -0.0105	2.156	0.05	76.235	0.33	76.234	0.33
1ST FLIGHT STAGE AT FIRST MOTION	PRED	586421. 1292836.	18.875 743.1		0.0073 0.2906		2.121		76.044		76.044	
	ACTUAL	586343. 1292666.	18.890 743.7	0.015 0.59	0.0071 0.2801	-0.0002 -0.0105	2.122	0.05	76.298	0.33	76.298	0.33

16-7

Table 16-6. SA-206 Mass Characteristics Comparison (Continued)

EVENT	MASS		LONGITUDINAL C.G. (Y, Z, A)		RADIAL C.G.		ROLL MOMENT OF INERTIA		PITCH MOMENT OF INERTIA		YAW MOMENT OF INERTIA	
	KILO POUNDS	O/O DEV.	METERS INCHES	DELTA	METERS INCHES	DELTA	KG-M <sup>2</sup> X10 <sup>-6</sup>	O/O DEV.	KG-M <sup>2</sup> X10 <sup>-6</sup>	O/O DEV.	KG-M <sup>2</sup> X10 <sup>-6</sup>	O/O DEV.
1ST FLIGHT STAGE AT OUTBOARD ENGINE CUTOFF SIGNAL	PRED	184281. 406270.	29.036 1143.1		0.0237 0.9334				38.547		38.547	
	ACTUAL	184494. 406741.	29.067 1144.3	0.030 1.20	0.0228 0.9013	-0.0008 -0.0320	0.426 0.427	0.24	38.652	0.27	38.652	0.27
1ST FLIGHT STAGE AT SEPARATION (PHYSICAL)	PRED	183917. 404586.	29.136 1147.0		0.0237 0.9334				38.105		38.105	
	ACTUAL	183803. 405215.	29.166 1148.3	0.030 1.20	0.0228 0.9013	-0.0008 -0.0320	0.423 0.423	0.25	38.209	0.27	38.209	0.27
2ND FLIGHT STAGE AT IGNITION (ESC)	PRED	137362. 302831.	35.684 1404.8		0.0264 1.0417				10.939		10.939	
	ACTUAL	137683. 303539.	35.707 1405.8	0.023 0.90	0.0259 1.0199	-0.0005 -0.0217	0.136 0.136	1.19	11.005	0.60	11.004	0.60
2ND FLIGHT STAGE AT 90 PERCENT THRUST	PRED	137169. 302407.	35.685 1404.9		0.0264 1.0417				10.936		10.935	
	ACTUAL	137507. 303151.	35.708 1405.8	0.023 0.90	0.0261 1.0299	-0.0002 -0.0117	0.135 0.135	1.19	11.002	0.60	11.001	0.60
2ND FLIGHT STAGE AT CUTOFF SIGNAL	PRED	30878. 68074.	43.951 1730.3		0.1120 4.4119				3.810		3.8090	
	ACTUAL	30521. 67287.	44.288 1743.6	0.337 13.28	0.1112 4.3800	-0.0008 -0.0319	0.132 0.132	1.25	3.724	-2.23	3.723	-0.21
2ND FLIGHT STAGE AT ETD	PRED	30823. 67954.	43.976 1731.3		0.1120 4.4119				3.798		3.7968	
	ACTUAL	30465. 67163.	44.316 1744.7	0.339 13.36	0.1115 4.3900	-0.0005 -0.0216	0.132 0.132	1.25	3.711	-2.26	3.710	-0.22
SPACECRAFT SEPARATED	PRED	16702. 36821.	35.216 1386.4		0.1911 5.9516				0.761		0.758	
	ACTUAL	16333. 36007.	35.365 1392.3	0.149 5.90	0.1984 6.2383	0.0072 0.2667	0.128 0.129	1.02	0.747	-1.79	0.744	-1.76

## SECTION 17

### SPACECRAFT SUMMARY

The SA-206/Skylab-2 space vehicle was launched at 9:00 a.m., EDT, on May 25, 1973, from Launch Complex 39B at the Kennedy Space Center, Florida. The spacecraft was manned by Captain Charles Conrad, Jr., Commander; Commander Joseph P. Kerwin, Science Pilot; and Commander Paul J. Weitz, Pilot.

The launch was originally scheduled for May 15, 1973. However, thermal problems encountered with the Saturn Work Shop (SWS) necessitated the rapid design and construction of supplemental hardware to be transported by the first manned vehicle. The interim period was also used for intensive crew training in new and modified procedures and to restow the command module with replacement and repair items for the Orbital Work Shop (OWS).

The spacecraft was inserted into earth orbit approximately 10 minutes after lift-off. The orbit achieved was 357 x 156 kilometers and, during a 6-hour period following insertion, four maneuvers were used to place the command and service module into a 424 x 415 kilometer orbit for rendezvous with the SWS. A fly-around inspection to evaluate the visible damage to the SWS was accomplished during the fifth revolution.

The crew provided a verbal assessment of the damage and the evaluation was supported by about 15 minutes of television coverage. Solar Array System (SAS) Wing No. 2 was completely missing. Solar Array System Wing No. 1 was only slightly deployed and was restrained by a part of the damaged meteoroid shield. Large sections of the meteoroid shield were missing and the exposed gold thermal material on the exterior of the OWS was badly discolored. Following the fly-around inspection, the command and service module was soft-docked with the SWS.

A standup extravehicular activity was initiated on May 25, 1973, to attempt the full deployment of SAS Wing No. 1. The activity was unsuccessful. Eight attempts were required to achieve a hard-docking configuration with the Orbital Work Shop. The first manned day terminated after a crew work period of 22 hours.

The crew activity for the second mission day was directed toward entry into the OWS. The crew removed and inspected the docking probe and drogue,

and then entered the Multiple Docking Adapter to activate the Airlock Module and the Multiple Docking Adapter systems. The OWS atmosphere was habitable, though hot, and the crew found no particular discomfort in working in the environment for 10 to 15 minute intervals.

The thermal parasol deployment was initiated through the solar scientific airlock about 5 hours into the second work day. Extension and positioning of the parasol was completed about 2 1/2 hours later and internal Saturn Work Shop temperatures began decreasing. The command module was then off-loaded and all systems were deactivated, except for those which were required to support the OWS requirements.

The crew established the OWS manning routine, and for the next 11 days performed scientific and medical experiments under a reduced power profile. On mission day 13, the Commander and Science Pilot exited the Work Shop and during a 3 1/2 hour extravehicular activity, successfully freed and deployed SAS Wing No. 1. Adequate power was then available in the OWS and crew activities approached the prelaunch planned procedures.

Another extravehicular activity was performed on the twenty-fifth manned day to recover Apollo Telescope Mount film cassettes, rearrange cameras, and obtain thermal coating samples. The Commander also performed inflight maintenance by tapping the SWS surface with a hammer to successfully reactivate a battery charger relay.

The command module was reactivated on the last mission day. The crew performed the final SWS closeout, entered the command module, and undocked. An SWS fly-around was performed to inspect and film the unmanned configuration.

The command module separated from the vicinity of the SWS at 05:40:00 EDT on June 22, 1973, and all entry events were normal. The command module landed in the Pacific Ocean approximately 1300 kilometers southwest of San Diego, California. Time of landing was 09:49:40 EDT on June 22, 1973. The spacecraft was within visual range of the recovery ship, the U. S. S. Ticonderoga. The command module remained in a Stable I attitude and the first manned Skylab visit terminated when the spacecraft and crew were aboard the recovery ship about 40 minutes after landing.

## SECTION 18

### MSFC INFLIGHT EXPERIMENT

Skylab Experiment M-415, a MSFC Thermal Control Coating (TCC) experiment was performed during the flight of SA-206. The object of the experiment was to determine the effects of preflight and flight environments on various thermal control coatings. The experiment contained 48 coatings that were uncovered and exposed to the environment at different times. Preliminary data indicates that:

- a. All 24 coatings were uncovered as planned.
- b. Temperature measurements were received as planned.
- c. Coatings which were exposed continuously from prelaunch exhibited no significant difference in absorptivity/emissivity (a/e) or temperature.
- d. Two of the three coatings sealed until first stage separation as planned, but exposed to retro motor plumes, indicated approximately the same a/e and temperatures but the third sample operated about 9°C cooler.
- e. At orbital insertion, all coatings which were exposed continuously from prelaunch were running 8 to 10°C hotter than the coatings which were sealed but exposed just prior to the retro motor firing.

## APPENDIX A

### ATMOSPHERE

#### A.1 SUMMARY

This appendix presents a summary of the atmospheric environment at launch time of the SA-206/SL-2. The format of these data is similar to that presented on previous launches of Saturn vehicles to permit comparisons. Surface and upper level winds, and thermodynamic data near launch time are given.

#### A.2 GENERAL ATMOSPHERIC CONDITIONS AT LAUNCH TIME

During the launch of Skylab 2, the Cape Kennedy launch area was experiencing cloudiness, high humidity, mild temperatures and gentle surface winds. These conditions resulted from a surface low pressure trough extending across northern Florida and into southern Georgia and Alabama. The axis of the trough (stationary front) was oriented from east-northeast to west-southwest. This trough produced broken cloudiness and widely scattered shower activity as far south as the central portion of Florida. See Figure A-1 for the surface synoptic weather map.

Surface winds in the Cape Kennedy area were light and southwesterly as shown in Table A-1. Wind flow aloft is shown in Figure A-2 (500 millibar level).

#### A.3 SURFACE OBSERVATIONS AT LAUNCH TIME

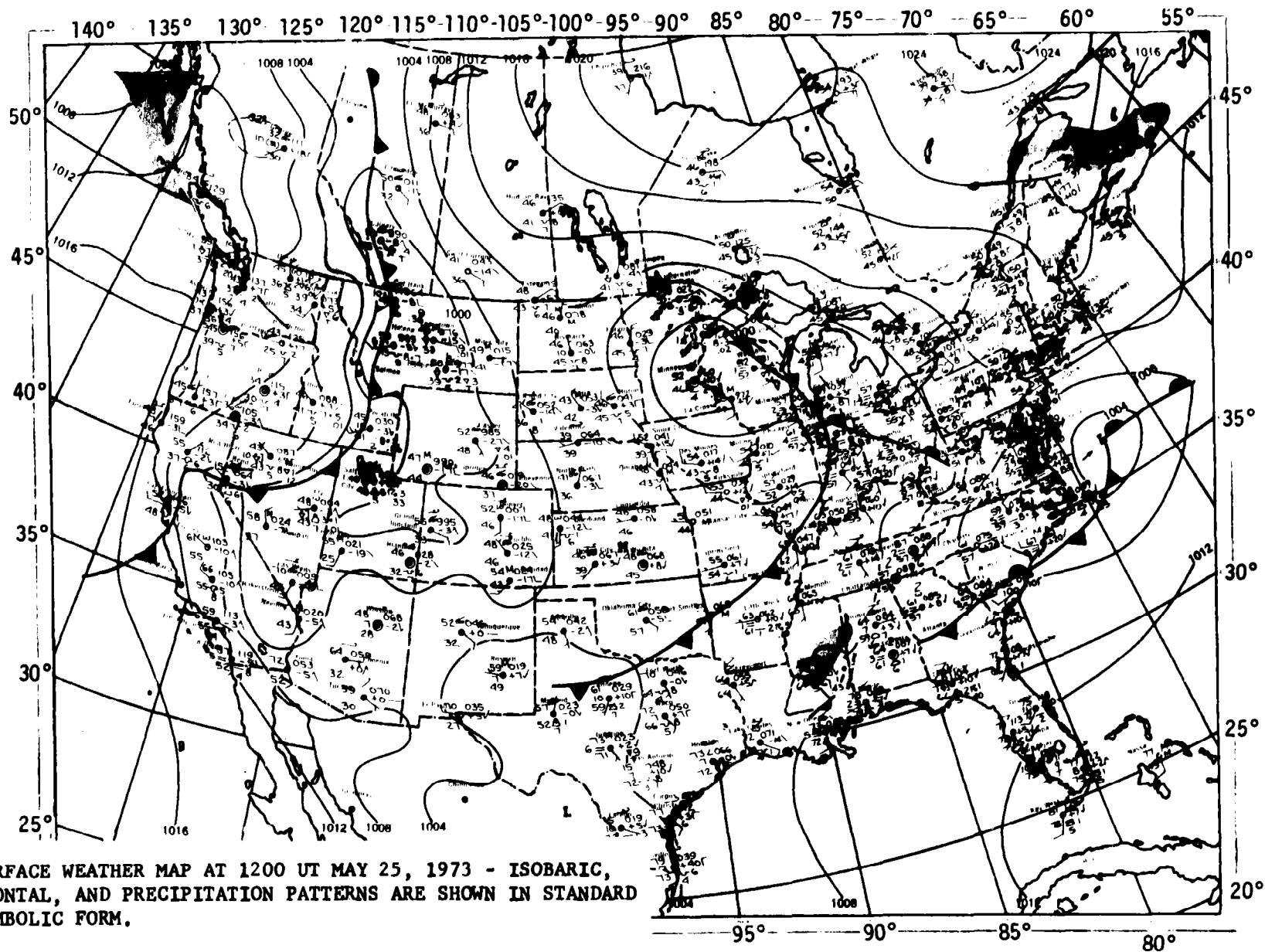
At launch time, total sky cover was 9/10, consisting of scattered fracto-cumulus at 0.2 kilometers (800 ft) with an altocumulus layer at 2.4 kilometers (8,000 ft). Cirrus clouds were observed at 9.1 kilometers (30,000 ft) altitude. Surface ambient temperature was 299°K (79.0°F). During ascent the vehicle did pass through the cloud layers. All surface observations at launch time are summarized in Table A-1. Solar radiation data for the day of launch is not available, due to miscalibration of the instruments. Lightning was not observed at launch time.

#### A.4 UPPER AIR MEASUREMENTS

Data were used from three of the upper air wind systems to compile the final meteorological tape. Table A-2 summarizes the wind data systems used. Only the Rawinsonde and the super Loki Dart meteorological rocket data were used in the upper level atmospheric thermodynamic analyses.

##### A.4.1 Wind Speed

Wind speeds were light, being 4.0 m/s (7.8 knots) at the surface and increasing to a peak of 42.0 m/s (81.7 knots) at 13.38 kilometers (43,881 ft). The winds began decreasing above this altitude, becoming relatively light



SURFACE WEATHER MAP AT 1200 UT MAY 25, 1973 - ISOBARIC, FRONTAL, AND PRECIPITATION PATTERNS ARE SHOWN IN STANDARD SYMBOLIC FORM.

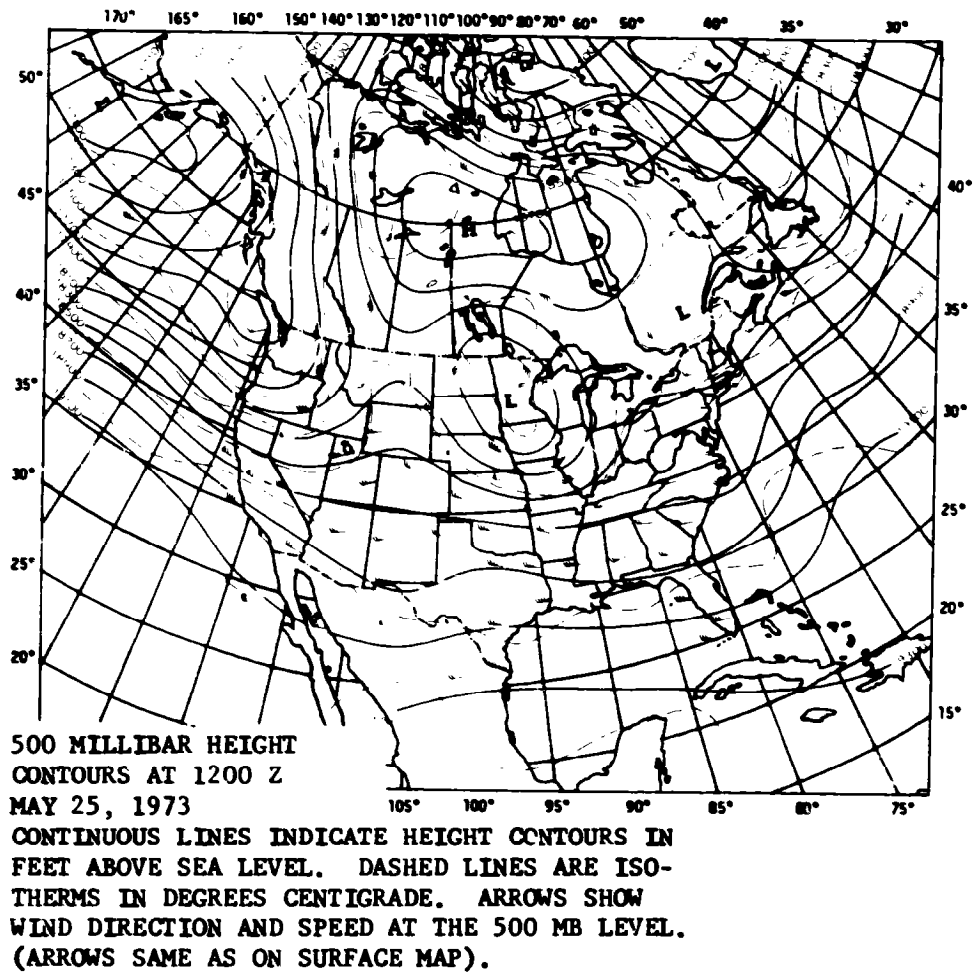
Figure A-1. Surface Weather Map Approximately 1 Hour Before Launch of SA-206/SL-2



Table A-1. Surface Observations at SA-206 Launch Time

LOCATION	TIME AFTER T-0 (MIN)	PRES-SURE N/CM <sup>2</sup> (PSIA)	TEM-PERATURE °K (°F)	DEW POINT °K (°F)	RELATIVE HUMIDITY (%)	VISI-BILITY KM (STAT MI)	SKY COVER			WIND*	
							CLOUD AMOUNT (TENTHS)	CLOUD TYPE	HEIGHT OF BASE METERS (FEET)	SPEED M/S (KNOTS)	DIR (DEG)
NASA 150 m Ground Wind Tower. Winds measured at 10 m (32.8 ft)**	0	10.105 (14.66)	299.3 (79.0)	296.5 (74.0)	85	10 GF (6)	5	Fracto-cumulus	244 (800)	3.0# (6.0)	260#
							5	Alto-cumulus	2,438 (8,000)		
							1	Cirrus	9,144 (30,000)		
							9###	--	--		
Cape Kennedy AFS*** Surface Measurements	10	10.112 (14.67)	297.4 (76.0)	295.9 (73.0)	91	--	--	--	4.0## (7.8)	210##	
Pad 39B Lightpole NW 18.3 m (60.0 ft)**	0	--	--	--	--	--	--	--	5.5 (10.7)	212	
Pad 39B LUT W 161.5 m (530 ft)**	0	--	--	--	--	--	--	--	6.1 (11.8)	224	

\* Instantaneous readings at T-0, unless otherwise noted.  
 \*\* Above natural grade.  
 # 10 minute average about T-0.  
 \*\*\* Balloon release site.  
 ## 1 minute average.  
 ### Total Sky cover.



**Figure A-2. 500 Millibar Map Approximately 1 Hour Before  
Launch of SA-206/SL-2**

Table A-2. Systems Used to Measure Upper Air Wind Data for SA-206

TYPE OF DATA	RELEASE TIME		PORTION OF DATA USED			
	TIME (UT)	TIME AFTER T-0 (MIN)	START		END	
			ALTITUDE M (ft)	TIME AFTER T-0 (MIN)	ALTITUDE M (ft)	TIME AFTER T-0 (MIN)
FPS-16 Jimsphere	1317	17	125 (410)	17	16,000 (52,493)	71
Rawinsonde	1310	10	16,250 (53,313)	63	24,750 (81,200)	91
Super Loki Dart	1330	30	66,000 (216,533)	30	25,000 (82,020)	56

at 19.25 kilometers (63,155 ft). Above this level, winds began increasing again as shown in Figure A-3. Maximum dynamic pressure occurred at 11.87 kilometers (38,942 ft). At max Q altitude, the wind speed and direction was 27.0 m/s (52.5 knots), from 291 degrees. SL-2 pad 39B wind data is available in MSFC memorandum, S&E-AERO-YT-21-73.

#### A.4.2 Wind Direction

At launch time, the surface wind direction was from 210 degrees. The wind directions were from the west and west-northwest throughout the troposphere and lower stratosphere, and became easterly above 20 kilometers (65,616 ft) altitude. Figure A-4 shows the complete wind direction versus altitude profile. As shown in Figure A-4, wind directions were quite variable at altitudes with low wind speeds.

#### A.4.3 Pitch Wind Component

The pitch wind velocity component (component parallel to the horizontal projection of the flight path) at the surface was a tailwind of 3.8 m/s (7.4 knots). The maximum tailwind, in the altitude range of 8 to 16 kilometers (26,247 to 52,493 ft), was 27.9 m/s (54.3 knots) observed at 14.93 kilometers (48,966 ft) altitude. See Figure A-5.

#### A.4.4 Yaw Wind Component

The yaw wind velocity component (component normal to the horizontal projection of the flight path) at the surface was a wind from the right of 1.2 m/s (2.3 knots). The peak yaw wind velocity in the high dynamic pressure region was from the left of 36.3 m/s (70.5 knots) at 13.35 kilometers (43,799 ft). See Figure A-6.

#### A.4.5 Component Wind Shears

The largest component wind shear ( $\Delta h = 1,000$  m) in the max Q region was a pitch shear of  $0.0145 \text{ sec}^{-1}$  at 14.93 kilometers (48,966 ft). The largest yaw wind shear, at these lower levels, was  $0.0141 \text{ sec}^{-1}$  at 14.38 kilometers (47,162 ft). See Figure A-7.

#### A.4.6 Extreme Wind Data in the High Dynamic Pressure Region

A summary of the maximum wind speeds and wind components is given in Table A-3. A summary of the extreme wind shear values ( $\Delta h = 1,000$  meters) is given in Table A-4.

### A.5 THERMODYNAMIC DATA

Comparisons of the thermodynamic data taken at SA-206 launch time with the annual Patrick Reference Atmosphere, 1963 (PRA-63) for temperature, pressure, density, and Optical Index of Refraction are shown in Figures A-8 and A-9, and are discussed in the following paragraphs.

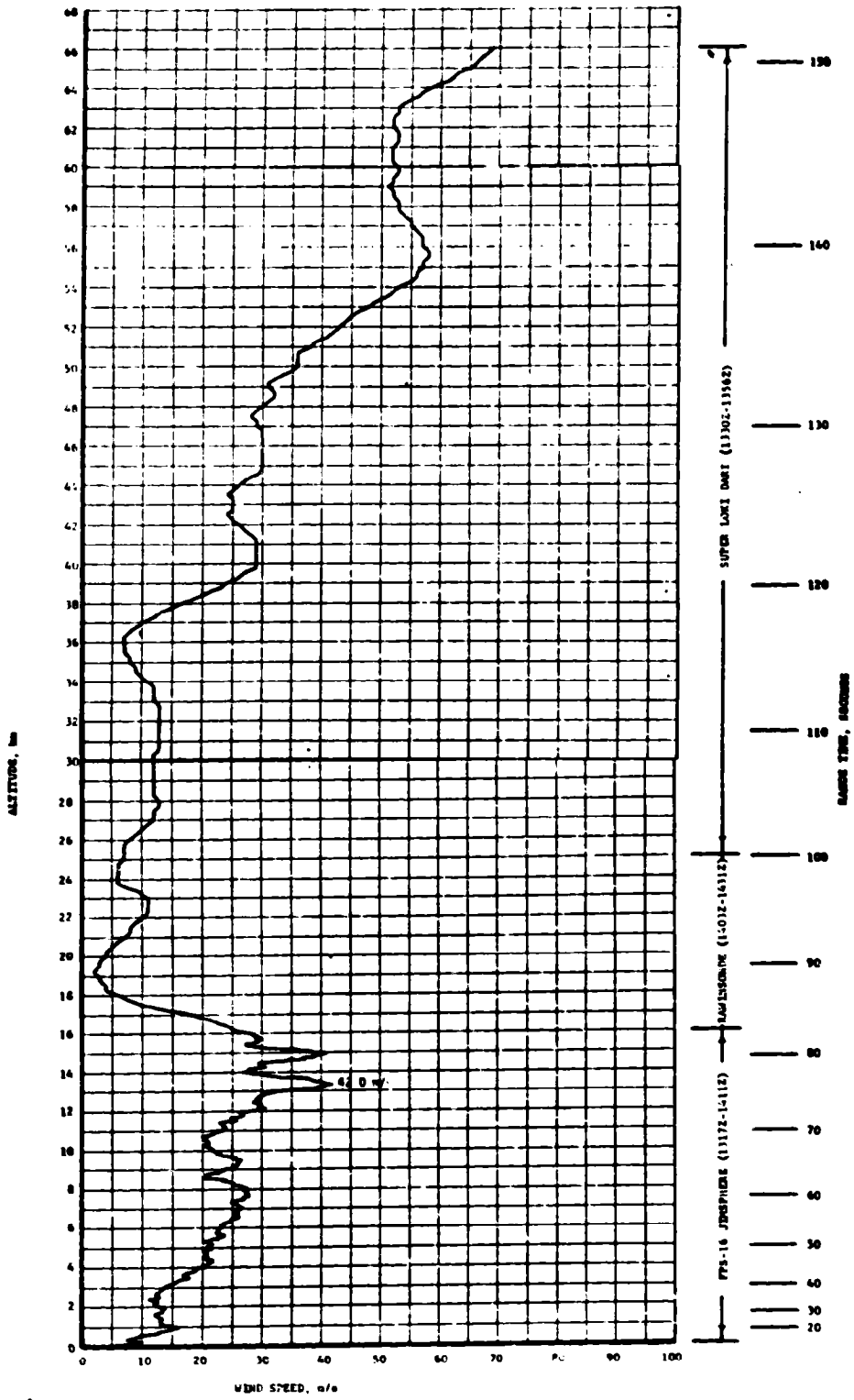


Figure A-3. Scalar Wind Speed at Launch Time of SA-206/SL-2

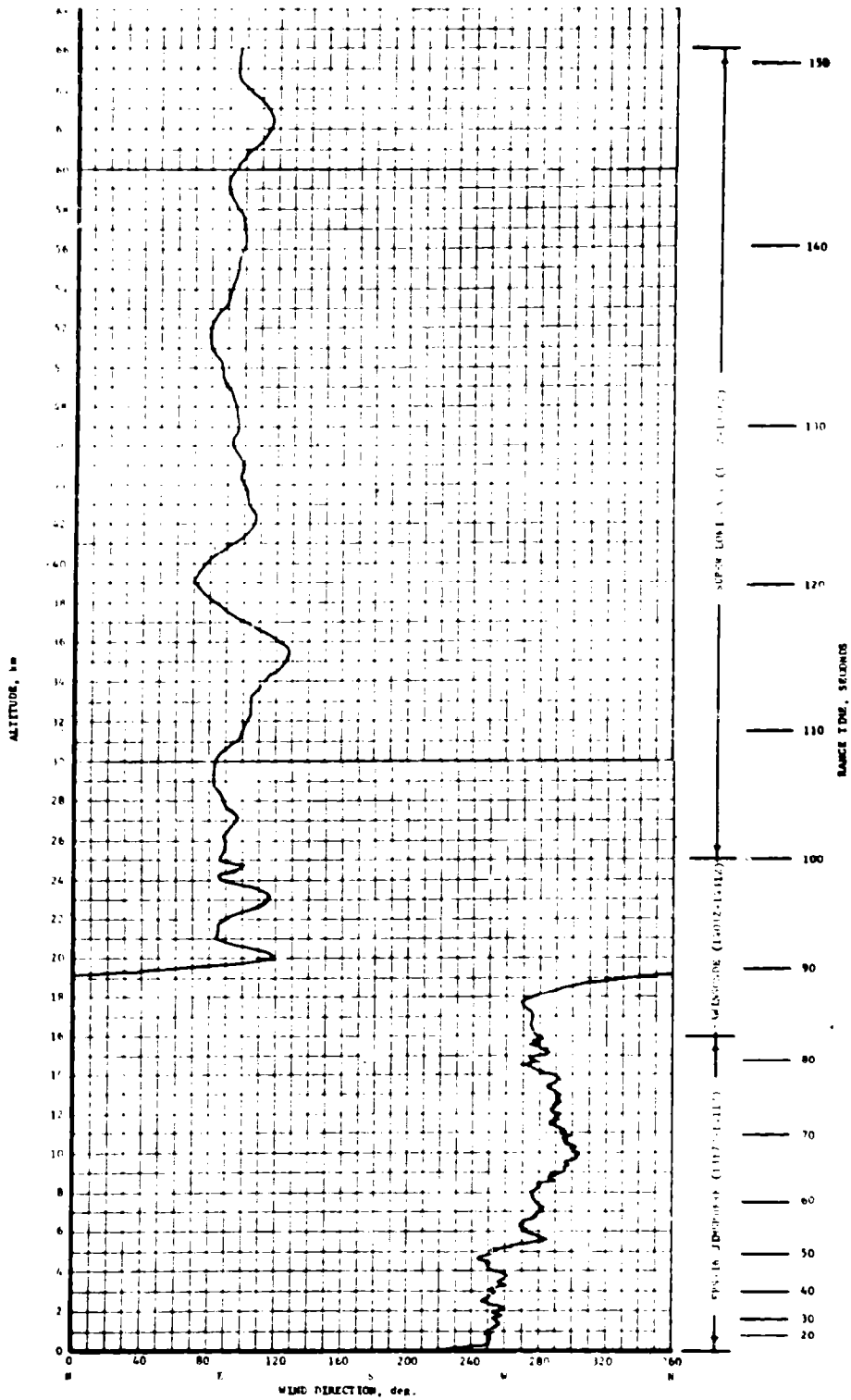


Figure A-4. Wind Direction at Launch Time of SA-206/SL-2

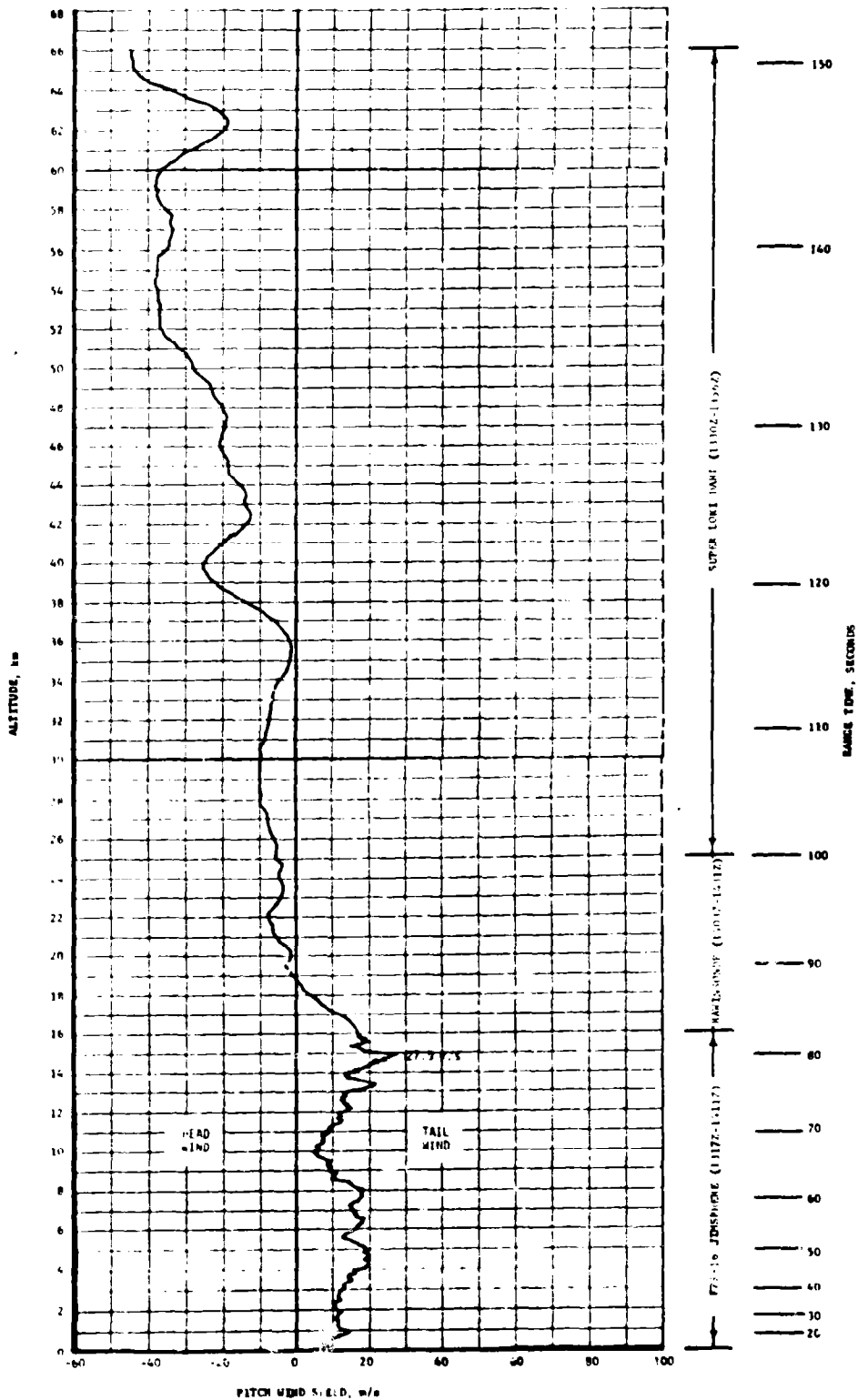


Figure A-5. Pitch Wind Velocity Component ( $W_x$ ) at Launch Time of SA-206/SL-2

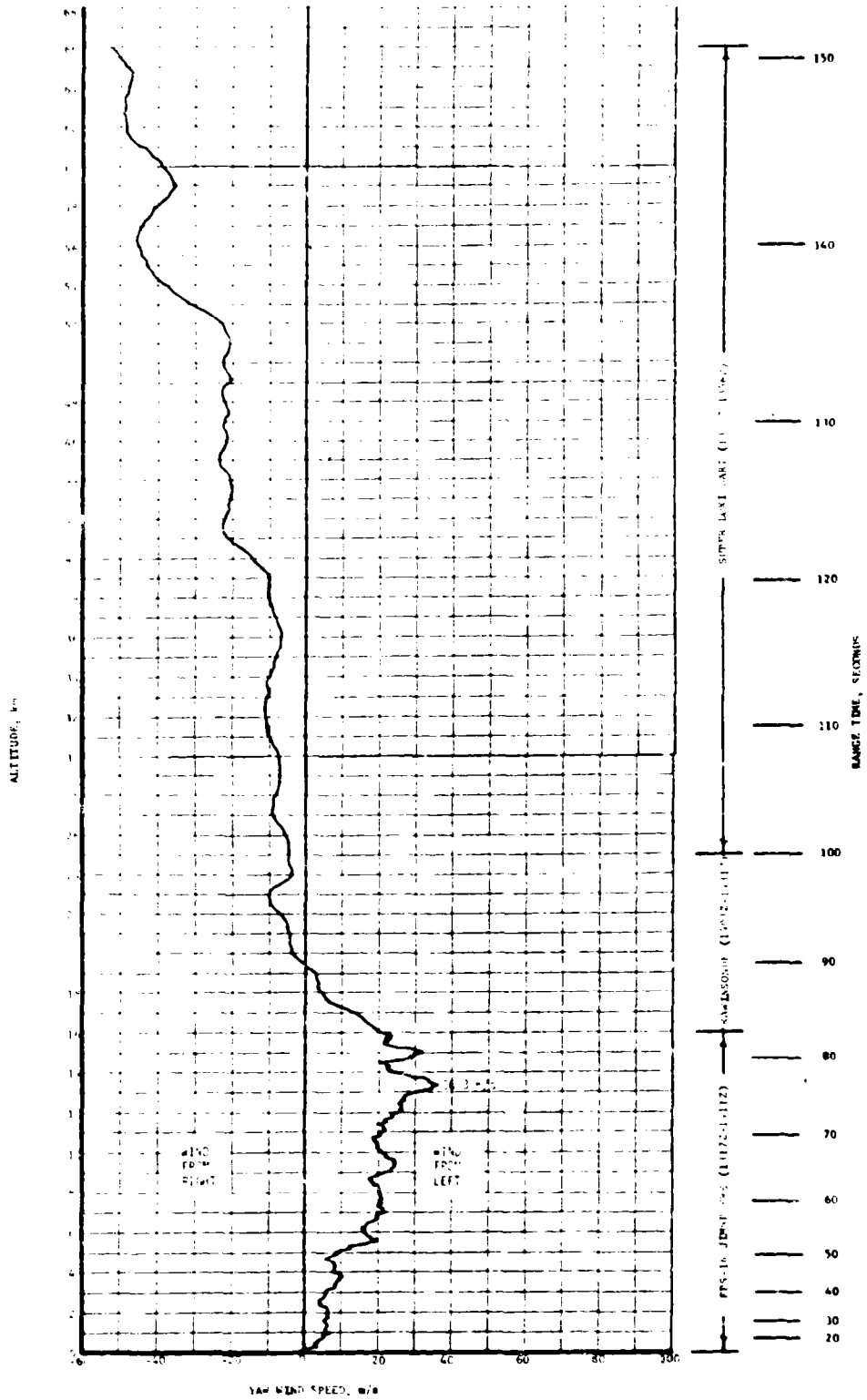


Figure A-6. Yaw Wind Velocity Component ( $W_z$ ) at Launch Time of SA-206/SL-2



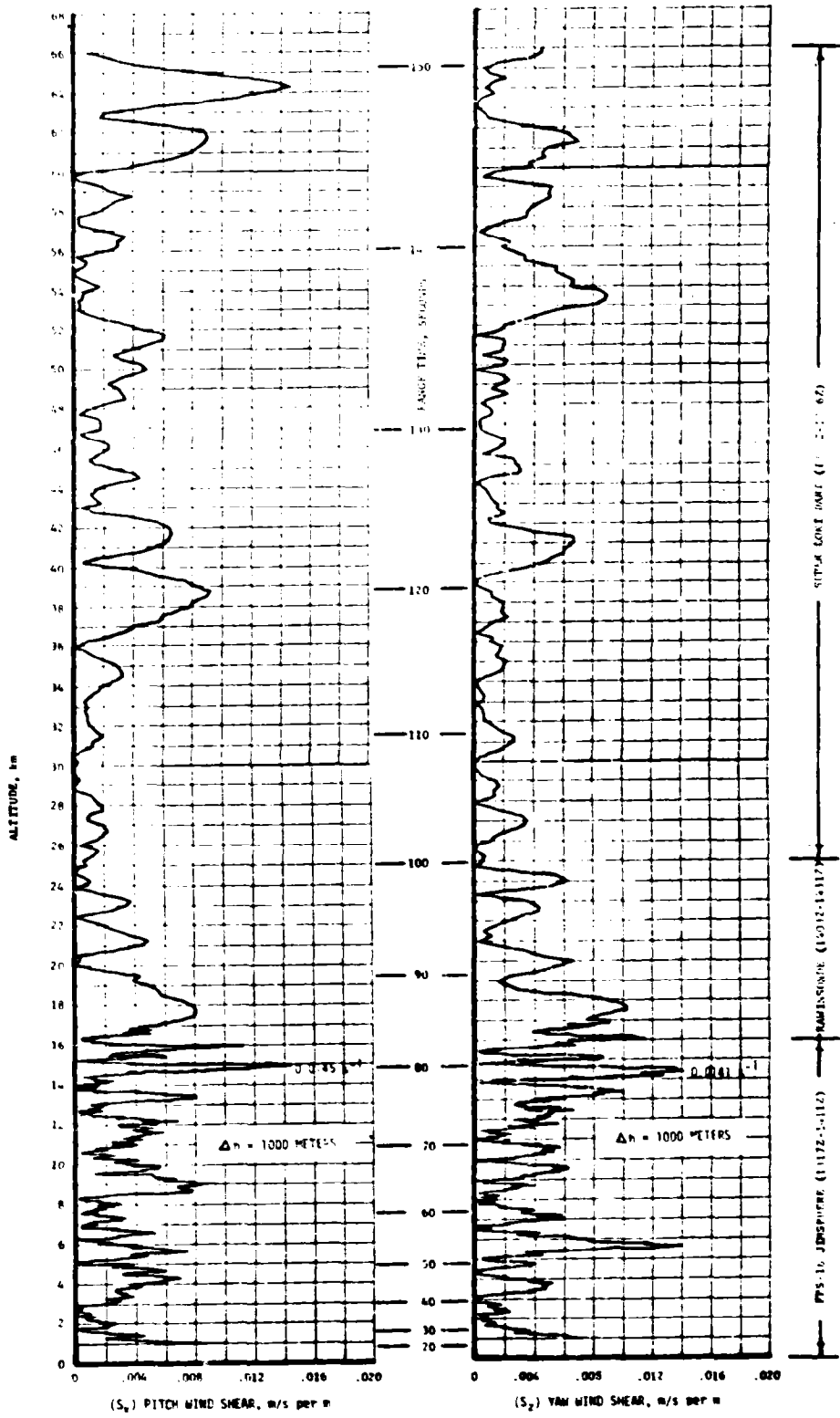


Figure A-7. Pitch ( $S_x$ ) and Yaw ( $S_z$ ) Component Wind Shears at Launch Time of SA-206/SL-2

Table A-3. Maximum Wind Speed in High Dynamic Pressure Region for Apollo/Saturn 201 through Saturn 206 Vehicles

VEHICLE NUMBER	MAXIMUM WIND			MAXIMUM WIND COMPONENTS			
	SPEED M/S (KNOTS)	DIR (DEG)	ALT KM (FT)	PITCH ( $W_x$ ) M/S (KNOTS)	ALT KM (FT)	YAW ( $W_y$ ) M/S (KNOTS)	ALT KM (FT)
AS-201	70.0 (136.1)	250	13.75 (45,100)	57.3 (111.4)	13.75 (45,100)	-43.3 (-84.2)	13.25 (43,500)
AS-203	18.0 (35.0)	312	13.00 (42,600)	11.1 (21.6)	12.50 (41,000)	16.6 (32.3)	13.25 (43,500)
AS-202	16.0 (31.1)	231	12.00 (39,400)	10.7 (20.8)	12.50 (41,000)	-15.4 (-29.9)	10.25 (33,600)
AS-204	35.0 (68.0)	288	12.00 (39,400)	32.7 (63.6)	15.25 (50,000)	20.6 (40.0)	12.00 (39,400)
AS-205	15.6 (30.3)	309	14.60 (44,500)	15.8 (30.7)	12.08 (36,800)	15.7 (30.5)	15.78 (47,500)
SA-206	42.0 (81.7)	286	13.38 (43,881)	27.9 (54.2)	14.93 (48,966)	36.3 (70.6)	13.35 (43,799)

Table A-4. Extreme Wind Shear Values in the High Dynamic Pressure Region for Apollo/Saturn 201 through Saturn 206 Vehicles

$(\Delta h = 1000 \text{ m})$				
VEHICLE NUMBER	PITCH PLANE		YAW PLANE	
	SHEAR ( $\text{SEC}^{-1}$ )	ALTITUDE KM (FT)	SHEAR ( $\text{SEC}^{-1}$ )	ALTITUDE KM (FT)
SA-201	0.0206	15.00 (52,500)	0.0205	12.00 (39,400)
SA-203	0.0104	14.75 (48,400)	0.0079	14.25 (46,800)
SA-202	0.0083	13.50 (44,300)	0.0054	13.25 (43,500)
SA-204	0.0118	16.75 (55,000)	0.0116	14.00 (45,900)
SA-205	0.0113	15.78 (48,100)	0.0085	15.25 (46,500)
SA-206	0.0145	14.93 (48,966)	0.0141	14.38 (47,162)

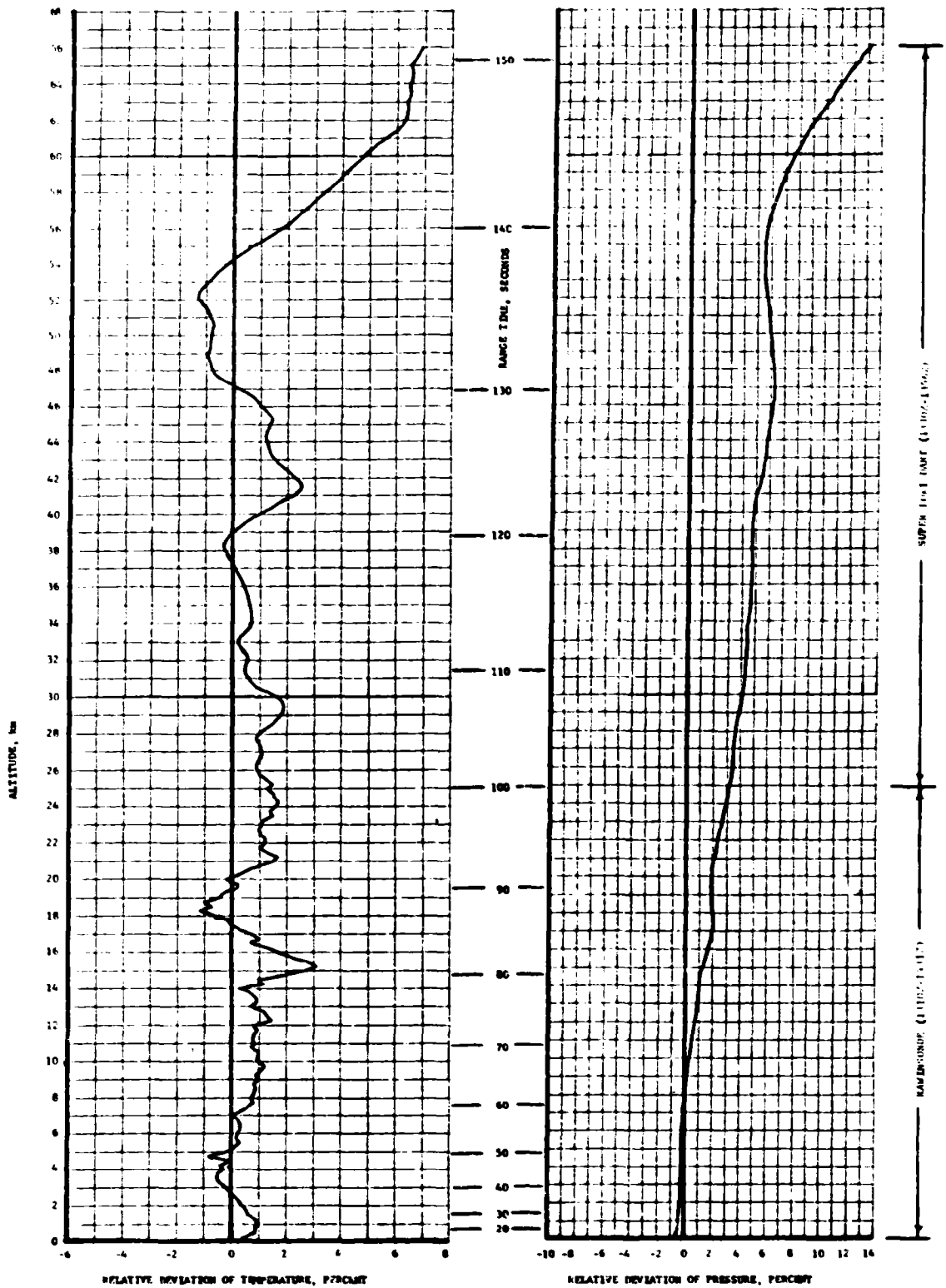


Figure A-8. Relative Deviation of Temperature and Pressure from the PRA-63 Reference Atmosphere, SA-206/SL-2

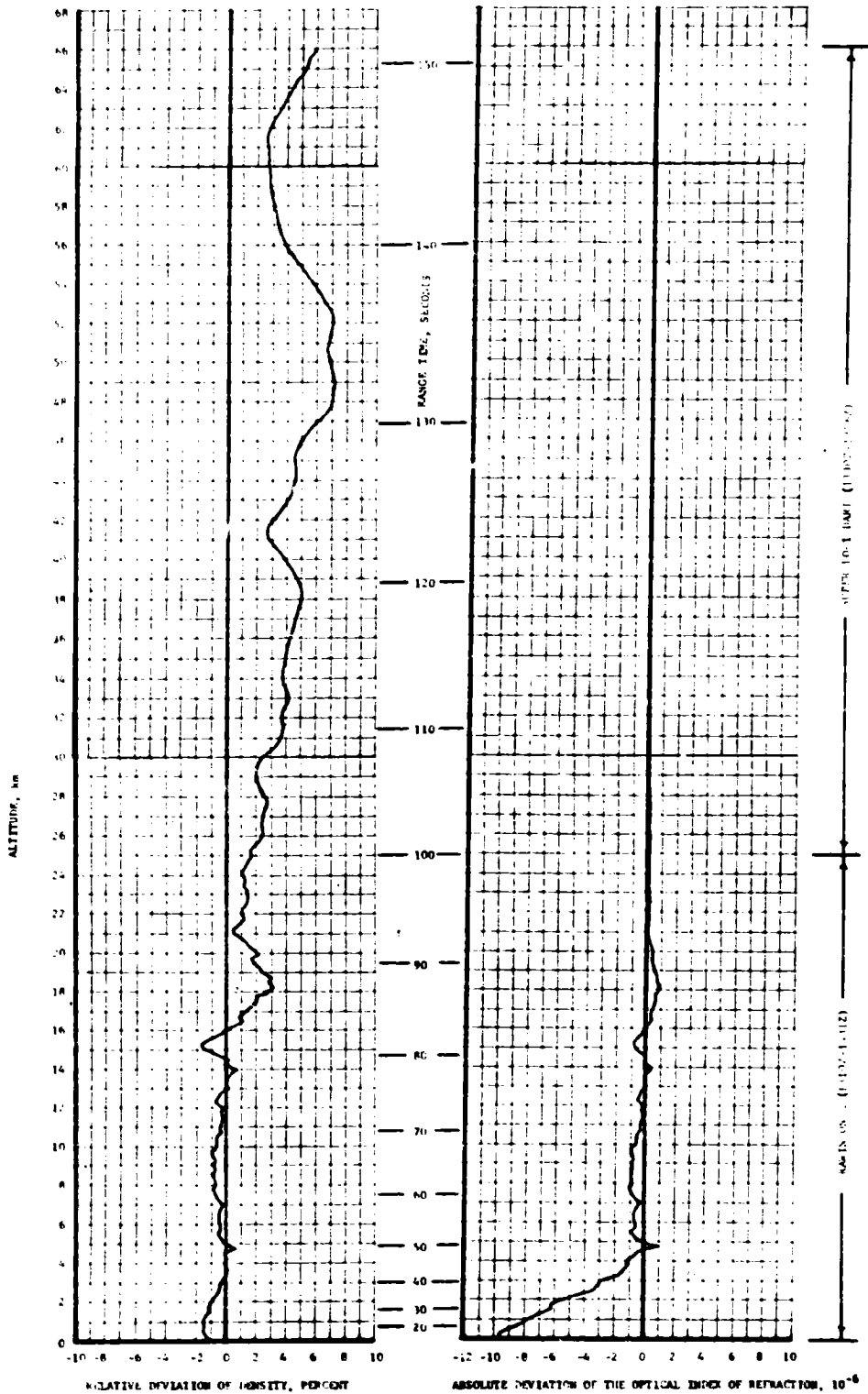


Figure A-9. Relative Deviation of Density and Absolute Deviation of the Index of Refraction from the PRA-63 Reference Atmosphere, SA-206/SL-2

### A.5.1 Atmospheric Temperature

Atmospheric temperature differences were small, generally deviating less than 3 percent from the PRA-63, below 57 kilometers (187,000 ft) altitude. Temperatures did deviate to +3.14 percent of the PRA-63 value at 15.25 km (50,032 ft). Air temperatures were generally warmer than the PRA-63, over the entire profile, as shown in Figure A-8.

### A.5.2 Atmospheric Pressure

Atmospheric pressure deviations were small in the lower levels of the atmosphere. Deviations were less than 3 percent of the PRA-63 below 24 kilometers (78,740 ft) altitude. See Figure A-8, which shows the entire pressure profile with altitude.

### A.5.3 Atmospheric Density

Atmospheric density deviations were small, generally being within 3 percent of the PRA-63 below 30 kilometers (98,424 ft) altitude. The density deviation reached a maximum of 3.24 percent greater than the PRA-63 value at 18.25 kilometers (59,875 ft) as shown in Figure A-9.

### A.5.4 Optical Index of Refraction

The Optical Index of Refraction at the surface was  $9.4 \times 10^{-6}$  units lower than the corresponding value of the PRA-63. The maximum negative deviation of  $-9.65 \times 10^{-6}$  occurred at 250 meters (820 ft). The deviation then became less negative with altitude, and approximated the PRA-63 at high altitudes, as is shown in Figure A-9. The maximum value of the Optical Index of Refraction was  $1.02 \times 10^{-6}$  units greater than the PRA-63 at 4.75 kilometers (15,584 ft).

## A.6 COMPARISON OF SELECTED ATMOSPHERIC DATA FOR SATURN IB LAUNCHES

A summary of the atmospheric data for each Saturn IB launch is shown in Table A-5.

Table A-5. Selected Atmospheric Observations for Apollo/Saturn 201 through Saturn 206 Vehicle Launches at Kennedy Space Center, Florida

VEHICLE NUMBER	VEHICLE DATA			SURFACE DATA						INFLIGHT CONDITION		
	DATE	TIME NEAREST MINUTE	LAUNCH COMPLEX	PRESSURE N/CM <sup>2</sup>	TEMPERATURE °C	RELATIVE HUMIDITY PERCENT	WIND*		CLOUDS	MAXIMUM WIND IN 8-16 KM LAYER		
							SPEED M/S	DIRECTION DEG		ALTITUDE KM	SPEED M/S	DIRECTION DEG
AS-201	26 Feb. 66	1112 EST	34	10.217	16.1	48	6.5	330	Clear	13.75	70.0	250
AS-203	5 Jul. 66	0953 EST	37B	10.166	30.2	69	6.3	242	1/10 Cumulus 1/10 Altocumulus 1/10 Cirrus	13.00	18.0	312
AS-202	25 Aug. 66	1216 EST	34	10.173	30.0	70	4.1	160	8/10 Cumulus 1/10 Cirrus	12.00	16.0	231
AS-204	22 Jan. 68	1748 EST	37B	10.186	16.1	93	4.2	45	3/10 Cumulus	12.00	35.0	288
AS-205	11 Oct. 68	1103 EDT	34	10.180	28.3	65	10.2	90	3/10 Cumulonimbus	14.60	15.6	309
SA-206	25 May 73	0900 EDT	39B	10.105	26.1	85	5.5 6.1	212 224	5/10 Fractocumulus 5/10 Altocumulus 1/10 Cirrus	13.38	42.0	286

\* Instantaneous readings from charts at T-0 (unless otherwise noted) from anemometers on launch pad light poles at the following levels: Pad 34 at 19.5 m (59.4 ft.), Pad 37B at 20.7 m (63.1 ft.), and Pad 39B at 18.3 m (60.0 ft.). Beginning with SA-206, wind measurements were required at the 161.5 m (530 ft) level from anemometer charts on the LUT. These instantaneous LUT winds are given directly under the listed pad light pole winds. Heights of anemometers are above natural grade.

## APPENDIX B

### SA-206 VEHICLE DESCRIPTION

#### B.1 INTRODUCTION

The Skylab-2 (SL-2) launch is the second of the Skylab series. The SL-2 vehicle as shown in Figure B-1 is comprised of a two stage Saturn IB launch vehicle with a manned, command and service module payload.

The Saturn IB (SA-206) launch vehicle is made up of three major stages; the S-IB-6 first stage booster, S-IVB-206 second stage booster, and IU-206 stage to provide launch vehicle guidance and sequencing commands during boost.

The payload for the SL-2 vehicle includes a manned Apollo Command Module (CM), an Apollo Service Module (SM), an Apollo Spacecraft/LM Adapter (SLA) and an Apollo Launch Escape System (LES).

The total vehicle is 223.5 feet long.

#### B.2. S-IB Configuration

The S-IB-6 stage major assemblies are shown in Figure B-2 and B-3. A summary of S-IB stage data is presented in Table B-1.

The main stage body is a cluster of nine propellant tanks. The cluster consists of four fuel tanks and four LOX tanks arranged alternately around a larger center LOX tank. Each tank has anti-slosh baffles to minimize propellant turbulence in flight. Stage electrical and instrumentation equipment is located in the forward and aft skirts of the fuel tanks.

A tail unit assembly supports the aft tank cluster and provides a mounting surface for the engines. Eight fin assemblies support the vehicle on the launcher and improve the aerodynamic characteristics of the vehicle. A stainless steel honeycomb heat shield encloses the aft tail unit for protection against the engine exhausts. A firewall above the engines separates the propellant tanks from the engine compartment. Eight H-1 engines boost the vehicle during the first phase of power flight. The four inboard engines are stationary and the four outboard engines gimbal for flight control. Two hydraulic actuators position each outboard engine on signal from the inertial guidance system.

A spider beam unit secures the forward tank cluster and attaches the S-IB stage to the S-IVB aft interstage. Seal plates cover the spider

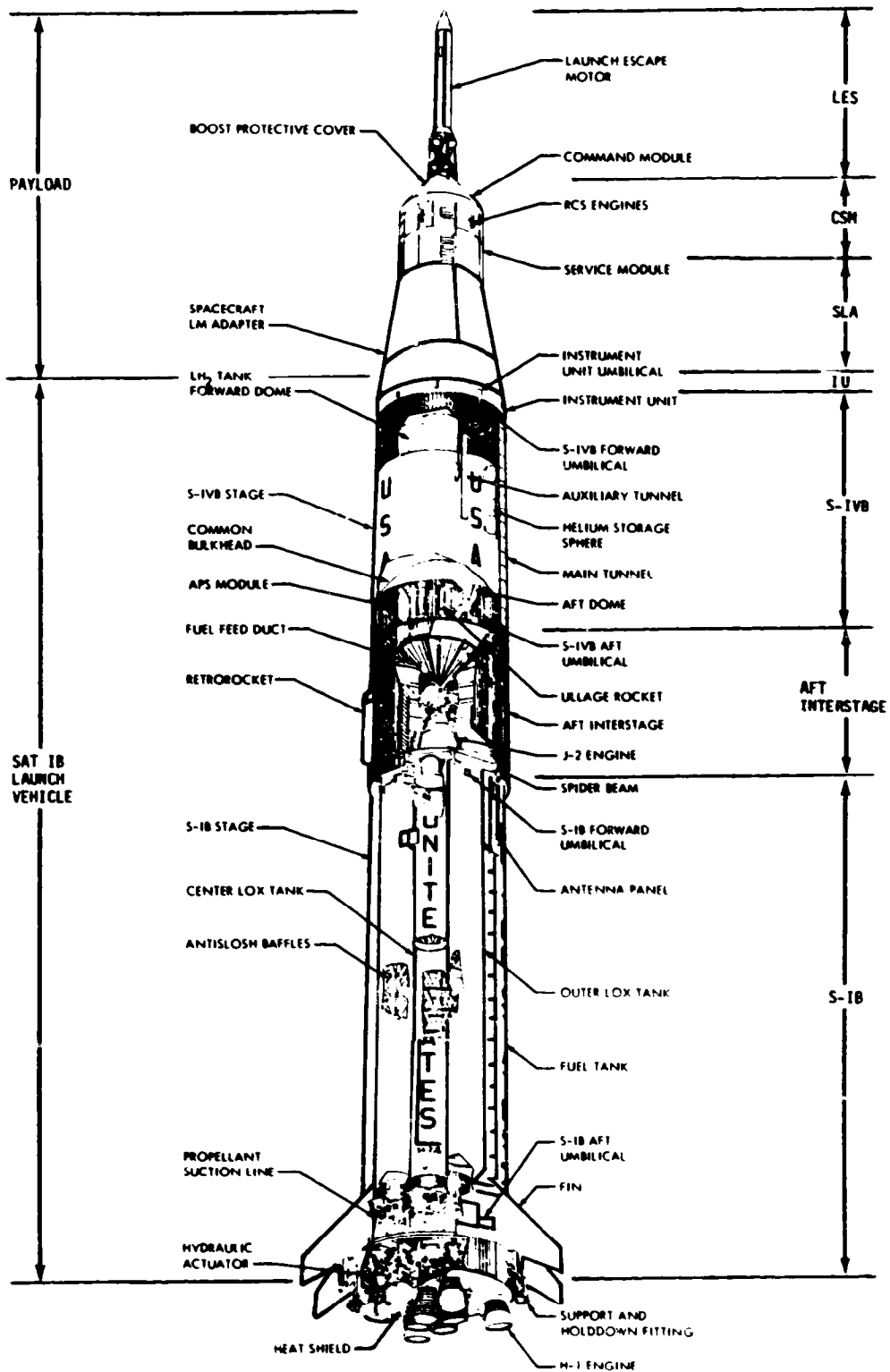


Figure B-1. SL-2 Space Vehicle



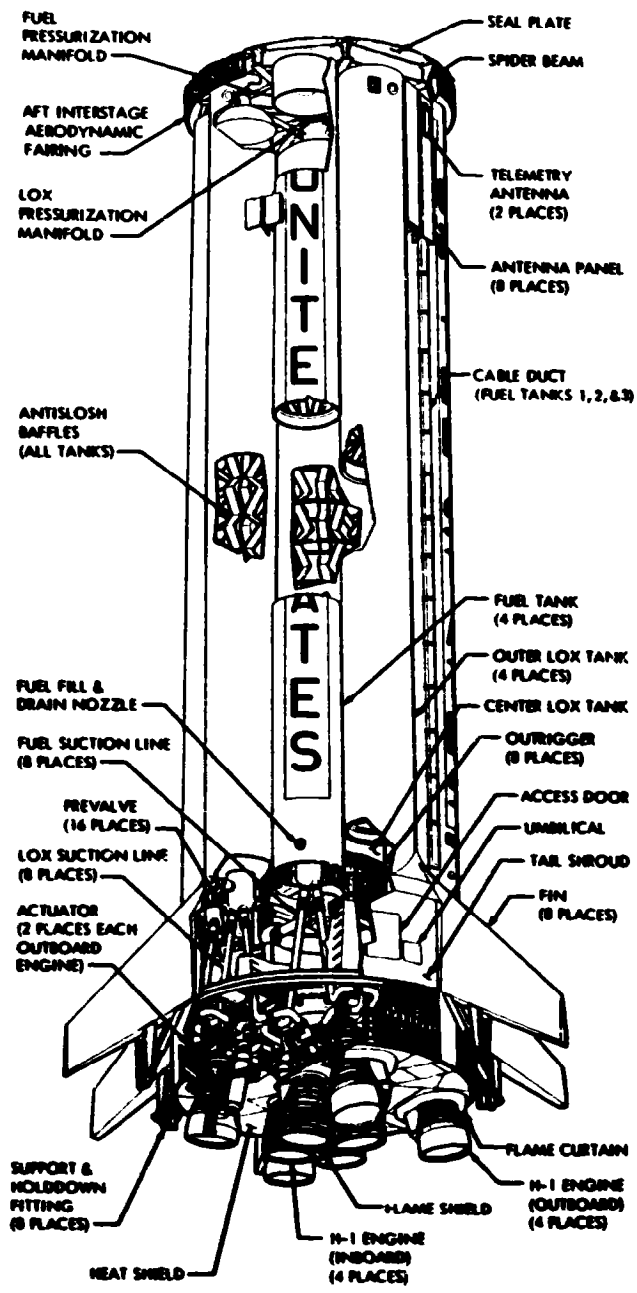


Figure B-2. S-IB Stage Configuration

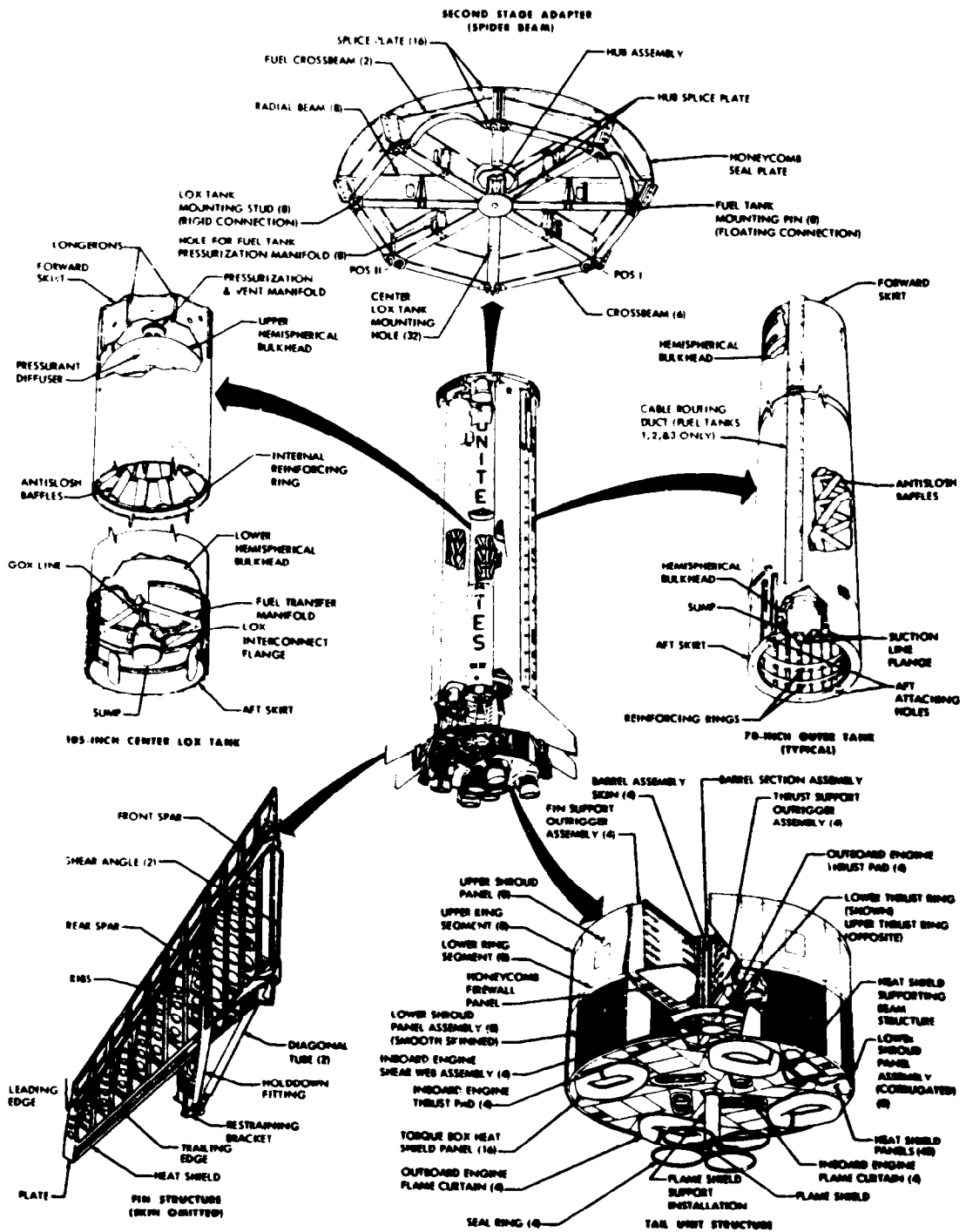


Figure B-3. S-IB Stage Structure

Table B-1. Summary of S-IB Stage Data

DIMENSIONS		HYDRAULIC SYSTEM	
Length	80.2 Feet	Actuators (Outboard only)	2 per engine
Diameter		Gimbal Angle	$\pm 6$ deg square pattern
At propellant tanks	21.4 Feet	Gimbal Rate	15 deg/sec in each plane
At tail unit assembly	22.8 Feet	Gimbal Acceleration	1776 deg/sec <sup>2</sup>
At fins	40.7 Feet		
Fin Area	53.3 FT <sup>2</sup> each of 8 fins	PRESSURIZATION SYSTEM	
MASS		Oxidizer Container	Initial helium from ground source; S-IB burn, GOX
Dry Stage	84,521 lbm	Fuel Container	Helium
Loaded Stage	997,127 lbm	Oxidizer Pressure	
At Separation	95,159 lbm	Preflight	58 psia
Engines, dry, less instrumentation		Inflight	50 psia
Inboard, plus Turbuckles	2,003 lbm each	Fuel Pressure	
Outboard, less hydraulics	1,980 lbm each	Preflight	17 psig
Propellant Load	912,606 lbm (408,000 KG)	Inflight	15 to 17 psig
ENGINES		Ullage	
Burn Time	141 seconds (approx)	Oxidizer	1.5%
Total thrust (sea level)	1.64 x 10 <sup>6</sup> lbf	Fuel	2.0%
Propellants	LOX and RP-1	ENVIRONMENTAL CONTROL SYSTEM	
Mixture Ratio	2.23:1 $\pm 2\%$	Preflight Air Conditioning	Aft compartment & instrument compartments F1 and F2
Expansion Ratio	8:1	Preflight GN <sub>2</sub> Purge	Aft compartment & instrument compartments F1 and F2
Chamber Pressure	702 psia	ASTRONICS SYSTEM	
Oxidizer NPSP (Minimum)	35 Feet of LOX or 65 psia	Guidance	Pitch, roll, and yaw program thru the IU during S-IB burn.
Fuel NPSP (Minimum)	35 Feet of RP-1 or 57 psia	Telemetry	FM/FM, 240.2 MHz; PCM/FM, 256.2 MHz
Gas Turbine Propellants	LOX and RP-1	Electrical	Batteries, 28 Vdc (2 zinc-silver oxide); master measuring voltage supply, 28 Vdc to 5 Vdc.
Turbopump Speed	6680 RPM	Range Safety System	Parallel electronics, redundant ordnance connections.
Engine Mounting			
Inboard	32 in. radius, 3 deg cant angle		
Outboard	95 in. radius, 6 deg cant angle		

beam to provide an aft closure for the S-IVB stage engine compartment.

The significant configuration differences between S-IB-6 and S-IB-5 are listed in Table B.2.

### B.3 S-IVB Stage Configuration

The S-IVB-206 stage is shown in Figure B-4. The S-IVB stage has nominal dimensions of 59 feet in length and 21.6 feet in diameter. The basic airframe consists of the aft interstage, thrust structure, aft skirt, propellant tanks, and forward skirt. The aft interstage assembly provides the load supporting structure between the S-IVB stage and the S-IB stage. The thrust structure provides support for engines, piping, wiring and interface panels, ambient helium sphere, and some of the LOX tank and engine instrumentation. The aft skirt assembly is the load bearing structure between the LH<sub>2</sub> tank and aft interstage. The propellant tank assembly consists of a cylindrical tank with a hemispherical shaped dome at each end. Contained within this assembly is a common bulkhead which separates the LOX and LH<sub>2</sub>.

The forward skirt assembly extends forward from the intersection of the LH<sub>2</sub> tank sidewall and the forward dome providing a hard attach point for the IU.

The S-IVB is powered by one J-2 engine with a nominal thrust of 225,000 lbf at the 5.5 mixture ratio which is employed for the greater portion of the burn. LOX is supplied to the engine by a 6 inch low pressure duct from the LOX tank. LH<sub>2</sub> is supplied by a vacuum jacketed low pressure 10 inch duct emanating from the LH<sub>2</sub> tank. Prior to liftoff LH<sub>2</sub> tank pressurization is provided by ground supplied helium. After S-IVB engine start, GH<sub>2</sub> for LH<sub>2</sub> tank pressurization is bled from the thrust chamber hydrogen injector manifold. Prior to launch, LOX tank pressurization is also accomplished by a ground helium supply. During S-IVB engine burn, GHe from storage spheres, located in the LH<sub>2</sub> tank, is warmed by a heat exchanger to supply tank pressurization.

Pitch and yaw control of the S-IVB is accomplished during powered flight by gimbaling the J-2 engine and roll control is provided by operating the Auxiliary Propulsion System (APS).

The APS provides three axis stage attitude control. The APS modules are located on opposite sides of the S-IVB aft skirt at Positions I and III. Each module contains its own oxidizer system, fuel system, and pressurization system. Nitrogen Tetroxide (N<sub>2</sub>O<sub>4</sub>) is used as the oxidizer and Mono-methyl Hydrazine (MMH) is the fuel for these engines.

Additional systems on the S-IVB are:

- a. The hydraulic system which gimbals the J-2 engine.

Table B-2. Significant S-IB Stage Configuration Changes

SYSTEM	CHANGE	REASON
Structures	Repair of F-1 Fuel Tank.	In the interest of economy, fuel tank F-1 was salvaged from S-IB-1 and utilized on S-IB-6.
Propulsion and Mechanical	Control LOX vent and relief valve from GSE.  Change bolt material in prelaves to eliminate stress corrosion.  Route sensing lines to fuel vent valve.  Change Fuel Pressurization Nozzle and LOX Pressurization Orifice.  Revise R-Seal Coating Material.  Delete LOX Replenish System  Replacement of Quick-Disconnect Coupling.	Improve flight reliability by eliminating two single-point failure modes.  Bolt material was changed to A-286 steel, an alloy not susceptible to stress corrosion, to improve system reliability and safety.  Eliminate the possibility of fuel entrapment to enhance system safety and launch-on-time probability.  Provide an increased flowrate of the propellants to accommodate the 205 F engine.  Eliminate the possibility of a valve failure caused by the use of materials that are not LOX compatible.  On LC-39, LOX replenishing will be done through the main fill system; therefore, stage LOX replenishing was removed, eliminating a single-point failure mode and reducing stage weight.  Quick-disconnect seal dislodged during plug-out test on S-IB-1 through S-IB-5.
Flight Control	Eliminate Accumulator Sleeve and Static Seal  Repair Actuator Potentiometer Roll Pin.  Change hydraulic actuator piston cap seal.	Eliminate O <sub>2</sub> leakage into the hydraulic oil.  Add a safety lock to the actuator Beta feedback potentiometer to preclude a single-point failure.  To preclude seal bypass leakage.
Instrumentation	Revise POGO measurements.  Incorporate Class 1 Telemetry Documentation  Add redundant measurement to monitor regulator control pressure.	Added vibration and pressure measurements to monitor any existence of POGO.  Provide telemetry drawing sets in accordance with MSFC requirements for use on all Saturn stages.  To preclude a launch delay due to a measurement failure.
Electrical	Eliminate single-point relay contact failures.  New battery with improved regulation.  Redundant wiring for critical interface functions.  Revise criteria for acceptance of level sensors and depletion sensors.  Prevalve inhibit modification.	To enhance overall stage reliability.  Provide better voltage regulation for low current loads.  To eliminate single-point failures by providing redundant paths for critical interface functions.  Additional test criteria provides assurance of operation at inherent reliability level.  Electrical circuit incorporated to inhibit operation of prevalves during EDS and range safety tests.
Environmental Control	Close holes in boattail.  Add boattail water level sensors.	To prevent entrance of outside air.  To provide ground observer with an indication of water level.
H-1 Engine System	Incorporation of 205 F engine.	H-1 engine increased from 200 k to provide higher first stage thrust and higher vehicle performance.

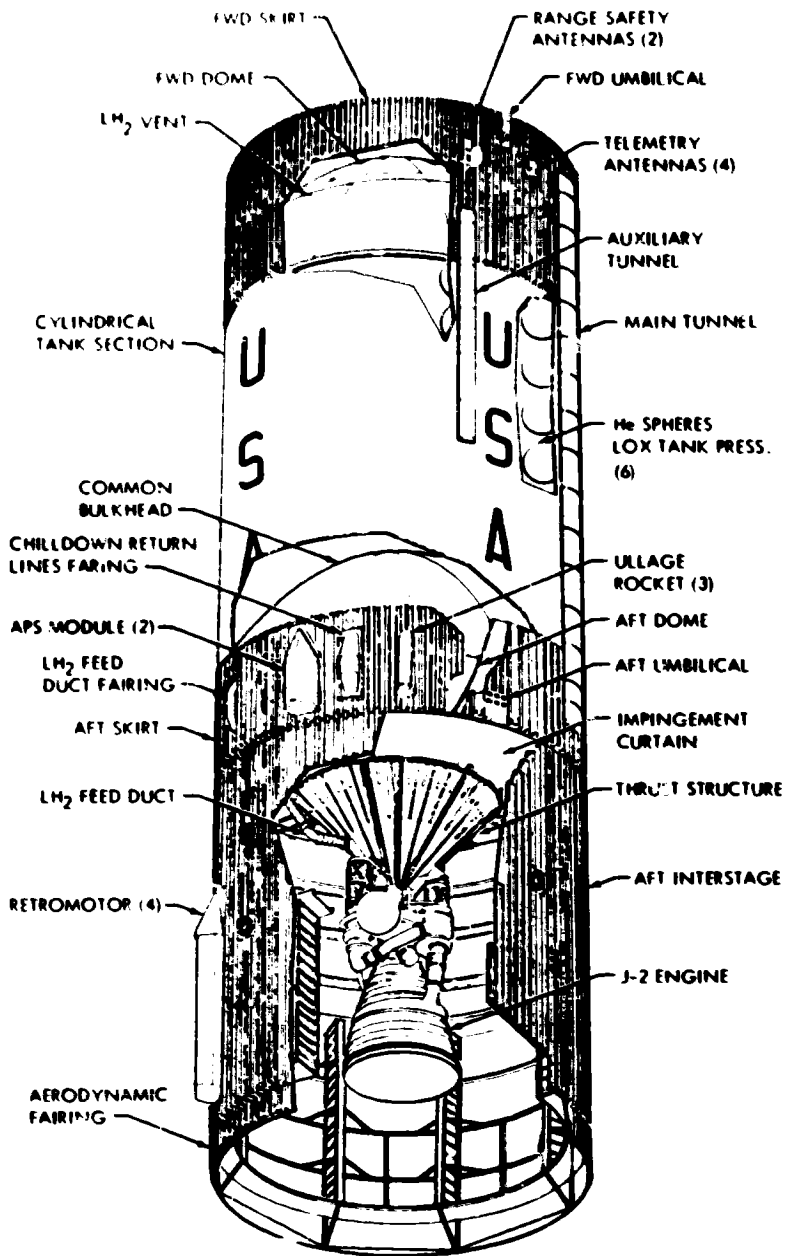


Figure B-4. S-IVB Stage Configuration

- b. Electrical system which supplies and distributes power to the various electrical components.
- c. Thermoconditioning system which thermally conditions the electrical/electronic modules in the forward skirt area.
- d. Data acquisition and telemetry system which acquires and transmits data for stage evaluation.
- e. A set of ordnance systems used for rocket ignition, stage separation, ullage motor jettison and range safety.

The more significant configuration changes between SA-205 S-IVB and SA-206 S-IVB are shown in Table B-3.

#### B.4 IU Configuration

The IU, as shown in Figure B-5, is a short cylinder fabricated from an aluminum alloy honeycomb sandwich material. The IU cylinder has a diameter of 21.6 feet and a length of 3 feet. The cylinder is manufactured in three 120 degree segments which are joined by splice plates into an integral load bearing unit. The top and bottom edges of the cylinder are made from extruded aluminum channels bonded to the honeycomb sandwich material. Cold plates are attached to the interior of the cylinder which serve both as mounting structure and thermal conditioning units for the electrical/electronic equipment.

Other systems included in the IU are:

- a. The Environmental Control System (ECS) which maintains an acceptable environment for the IU equipment and S-IVB forward skirt.
- b. The electrical system which supplies and distributes electrical power to the various systems.
- c. The EDS which senses onboard emergency situation.
- d. The navigation, guidance, and control system.
- e. The measurements and telemetry system which monitors and transmits signals to ground monitoring stations.
- f. The flight program which controls the LVDC from seconds before liftoff until the end of the launch vehicle mission.

The more significant changes between IU-206 and previous Instrument Units are shown in Table B-4.

Table B-3. S-IVB Significant Configuration Changes

SYSTEM	CHANGE	REASON
Propulsion	<p>Addition of LOX tank non-propulsion vent system</p> <p>*Add thermal control coatings on tank domes, components, etc</p> <p>Adds redundant vent and relief valve with latch open capability</p> <p>Rework LOX vent and relief valves to assure RPV valve crack pressure is always lower than the vent and relief valve relief pressure</p> <p>Utilize dual (Apollo type) regulator for the pneumatic control module</p> <p>Variable position P<sub>1</sub> valve replaced with two position (4 P and 5.5 IMP) valve</p> <p>Change LOX and L<sub>2</sub> low pressure feed ducts from one ply bellows to two ply bellows</p> <p>*Added redundant LH<sub>2</sub> fast fall sensor to provide a backup for the existing calibrated sensor</p> <p>Modified AP's incorporating a redesigned high/low pressure transducer mounting adaptor, replacement of bulkhead fitting with IC adapters, replacement of Inlon O-rings with seals and the addition of a helium recharge system capable of supplying helium from the LH<sub>2</sub> ambient repress system</p> <p>Interconnect the stage pneumatic supply bottle with the J-2 engine helium control bottle</p>	<p>Improved altitude control during coast mode</p> <p>To extend the stage coast capability from 4.5 to 7.5 hours</p> <p>To provide tank safety operations while conserving pneumatics and battery power</p> <p>To assure the RPV system is the primary mode of LOX tank pressure relief</p> <p>Provide regulator with improved regulation characteristics</p> <p>Increased flight reliability by removing PU Electronics Assembly control over IMP valve</p> <p>To provide increased safety margin in case of flow resonance</p> <p>Implementation of S-IVB/IB alternate propellant loading capability</p> <p>To provide greater reliability by eliminating possible leak sources and providing a helium recharge system</p> <p>Utilization of stage helium to backup the J-2 engine pneumatic system during boost minimizes a potential leak problem</p>
J-2 Engine	<p>Installation of an improved J-2 engine redesigned Electrical Control Assembly (ECA) package incorporating new timers with redundant micro-circuits</p> <p>Replace start tank vent and relief valve</p>	<p>To eliminate single failure points and improve reliability</p> <p>Relief requirements revised to permit longer hold time on pad</p>
Electrical	<p>Elimination of the LOX depletion cutoff function</p> <p>Add redundant battery heater control thermostat to switch heater power "on" at 50°F, and "off" at 70°F</p> <p>Modification of the LH<sub>2</sub> depletion sensor system electrical circuitry to utilize the existing (spare) fourth depletion sensor in a 3 out of 4 voting logic. The system was formerly a 2 out of 3 voting system</p> <p>*Modify stage system to aid increased battery capacity and provide capability to re-enable engine control power in the event of an early FUS cutoff</p>	<p>Eliminates single point failure which could cause premature engine shutdown</p> <p>Failure of heater control sensor could cause launch delay or loss of secondary mission if batteries should exceed redline requirements</p> <p>To protect against a single point flight failure</p> <p>To provide for 7-1/2 hour coast and de-orbit capability</p>
Instrumentation	<p>Addition of measurements A0012-403, U0265-403 and D0266-401 to the stage telemetry</p>	<p>Provide parameters for analysis of S-IVB/IB low frequency vibration</p>
Hydraulics	<p>Replace the AVCO Hydraulic Accumulator Charging Valve with a valve manufactured by Schrader</p>	<p>Improve reliability by eliminating a single point leak path</p>
Structures	<p>Replace electrical bonding strap on LOX tank vent line</p>	<p>To provide a LOX compatible material for the bonding strap</p>

NOTE: All items shown have flown on previous Saturn/Apollo launch vehicles except for the items with an asterisk (\*) which have a first effectivity on SL-2.



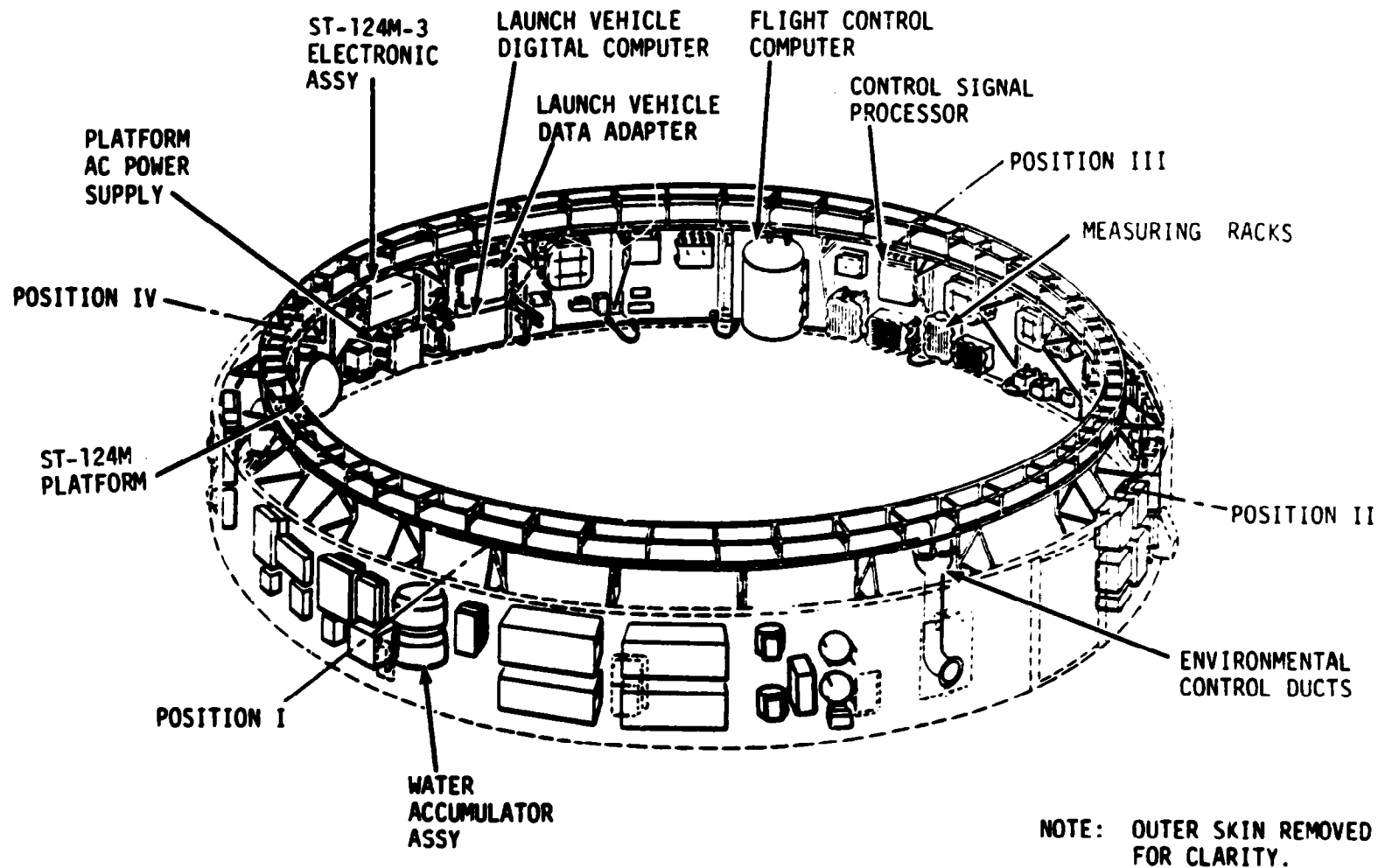


Figure B-5. Instrument Unit Configuration

Table B-4. IU Significant Configuration Changes

SYSTEM	CHANGE	REASON
Network	<p>Provide redundancy for time base 2 and 3 initiate.</p> <p>Provide redundant interrupt for low level sensors dry.</p> <p>Add third S-IR engine cutoff signal.</p> <p>Deactivate O-Ball and delete associated measurements.</p> <p>6D20 battery deleted.</p>	<p>Critical time bases not hardware redundant.</p> <p>Existing discrete operated too slowly which could result in loss of mission.</p> <p>Eliminate simplex cutoff signal failure.</p> <p>O-Ball no longer used as abort cue.</p> <p>No requirement.</p>
Navigation, Guidance & Control	<p>Modify control gain and sharing networks in Flight Control Computer (FCC) to provide a greater gain margin at Max 0.</p>	<p>SL-2 control system analysis showed that increased gains are required for off-nominal conditions.</p>
Instrumentation and Communications	<p>Add "A12", "00265" and "00266" Measurements.</p>	<p>Evaluate POGO and load responses.</p>
Experiment	<p>Install thermal control coating experiment R-415.</p>	<p>Directed by ECR 66-0109.</p>
Special	<p>The following is a list of changes originally flown on Saturn V's:</p> <ul style="list-style-type: none"> <li>o Incorporate CSR backup guidance scheme</li> <li>o Add FCC rate gyro filters</li> <li>o Add battery temperature measurements</li> <li>o Provide redundant ST-120R power supply</li> <li>o Provide redundant critical power</li> <li>o Add lightning detection devices</li> <li>o Add thrust OK lights circuitry</li> <li>o Modify guidance failure indication</li> <li>o Relocate gas bearing heat exchanger</li> <li>o Add 20-micron gas bearing regulator filter</li> <li>o Install redundant coolant pump</li> <li>o Add coolant pump switchback capability</li> <li>o Change coolant to organic floccul 100</li> <li>o Relocate modulating flow control valve</li> <li>o Incorporate 165 in<sup>3</sup> G<sub>2</sub> sphere</li> <li>o Incorporate improved water accumulator diaphragm</li> <li>o Install thermal shrouds</li> <li>o Modify ST-120R mechanical configuration</li> <li>o Larger volume coolant accumulator</li> </ul>	<p>Increase reliability and capabilities of S-IR IUs.</p>
Digital Command System Capability	<p>Additional Commands</p> <ul style="list-style-type: none"> <li>o Ladder Magnitude Limit Command - Provides the capability to change the ladder magnitude limits for the pitch, yaw, and roll channels (maximum value of 15.3 degrees).</li> <li>o S-1WB/IU Deorbit Command - Provides the capability to start time base 5 and subsequent sequences for LOI and hydrogen dumps.</li> </ul>	<p>To support attitude control capability.</p> <p>To support de-orbit capability.</p>
S-1WB/IU Deorbit	<p>Utilize S-1WB propellant dump in time base 5:</p> <ul style="list-style-type: none"> <li>o LOI dump</li> <li>o Hydrogen dump</li> </ul> <p>Time Base 5 initiation specified by S-1WB/IU Deorbit BC command:</p> <ul style="list-style-type: none"> <li>o TB55 (Time of Dump Sequence Start referenced to T0)</li> <li>o TLBD (Time of LOI Dump Duration)</li> <li>o THBD (Time of Hydrogen Dump Duration)</li> </ul> <p>Switch selector sequence controls dumps</p>	<p>To support deorbit requirement.</p>
R-415 Experiment	<p>Provide switch selector sequencing</p> <ul style="list-style-type: none"> <li>o Jettison experiment covers during nominal switch selector sequencing (panels 1 and 2 cover 4 at T3 + 0.6; panels 1 and 2 cover 2 at T3 + 1R.0, and panels 1 and 3 cover 3 at T4 + 2752).</li> </ul> <p>Provide a specified inertial attitude so that experiment samples experience constant solar illumination</p> <ul style="list-style-type: none"> <li>o Calculate pitch and yaw guidance commands to orient Xg axis parallel to Sun.</li> <li>o Calculate roll orientation to align R-415 experiment with solar vector.</li> </ul>	<p>To support R-415 experiment requirement.</p>

## B.5 Spacecraft Configuration

The spacecraft, as shown in Figure B-6 includes a Launch Escape System (LES), a Command Module (CM), a Service Module (SM), and a Spacecraft Lunar Module Adapter (SLA). From the bottom of the SLA to the top of the LES, the spacecraft measures approximately 81.8 feet.

The Launch Escape Tower (LET) is the forward most part of the Saturn IB space vehicle. Basic configuration of the LET consists of a nose cone, three rocket motors, a canard assembly, a structural skirt, a titanium-tube tower, and a boost protective cover. The purpose of the three rocket motors is tower jettison, escape, and pitch control. The LET is jettisoned shortly after S-IVB stage ignition.

The CM is designed to accommodate three astronauts. The CM is a conically shaped structure consisting of an inner pressure vessel (crew compartment) and an outer heat shield. The CM is approximately 11.15 feet long. Aluminum honeycomb panels and aluminum longerons are used to form the pressure tight crew compartment. Stainless steel honeycomb covered with an ablative material is used to construct the outer heat shield.

The SM is a cylindrical aluminum honeycomb shell with fore and aft aluminum honeycomb bulkheads. Six aluminum radial beams divide the SM into sectors. These beams have a triangular truss between the CM and SM with pads at the apex to support the CM. The SM also houses the Service Propulsion System (SPS) which includes an engine and propellant tanks.

The SLA is 28.0 feet long and the forward and aft diameters are 12.83 feet and 21.6 feet, respectively. The SLA is constructed in two sets of four panels, the panels being made from aluminum honeycomb.

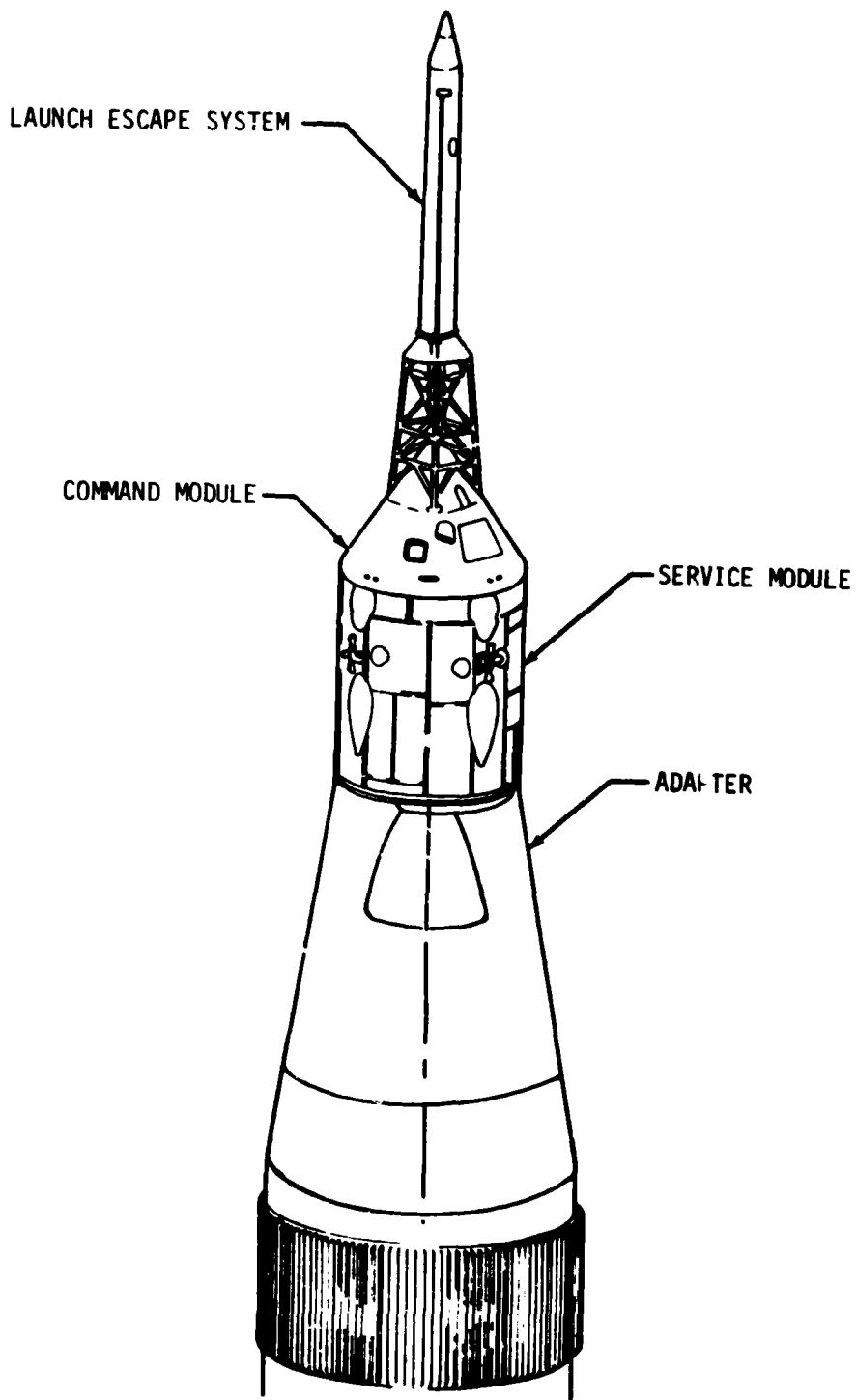


Figure B-6. Apollo Spacecraft

**APPROVAL**

**SATURN IB LAUNCH VEHICLE FLIGHT EVALUATION REPORT**

**SA-206, SKYLAB-2**

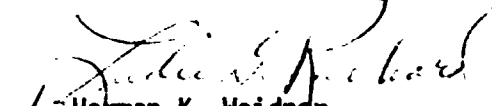
**By Saturn Flight Evaluation Working Group**

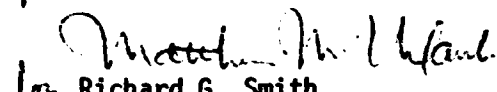
The information in this report has been reviewed for security classification. Review of any information concerning Department of Defense or Atomic Energy Commission programs has been made by the MSFC Security Classification Officer. The highest classification has been determined to be unclassified.

  
Stanley L. Fragge  
Security Classification Officer

This report has been reviewed and approved for technical accuracy.

  
George H. McKay, Jr.  
Chairman, Saturn Flight Evaluation Working Group

  
Herman K. Weidner  
Director, Science and Engineering

  
Richard G. Smith  
Saturn Program Manager

**END**

**DATE**

**FILMED**

**DEC 14 1973**